



Project N. 037110

Project Acronym: NEAREST

*Project title: Integrated observations from NEAR shore sourcES
of Tsunamis: towards an early warning system*

Instrument: STREP

Thematic priority: 1.1.6.3 GOCE (GIObal Change and Ecosystems)

Deliverable n 34a2 “Project information materials (updates)”

Due date of deliverable: September 2008
Actual submission date: September 2008

Start date of the project: 01/10/2006

Duration 36 months

Organisation name of the lead contractor for this deliverable: ISMAR

Final release

Project Co founded By the European Commission within the Sixth Framework Programme (2002-2006)		
Dissemination level		
PU	Public	X
PP	Restricted to other programme participants (including Commission Services)	
RE	Restricted to a group specified by the Consortium (including Commission Services)	
CO	Confidential, only for members of the Consortium (including Commission Services)	

Published papers



Seismic anisotropy beneath southern Iberia from SKS splitting

L. Buontempo ^{a,*}, G.H.R. Bokelmann ^b, G. Barruol ^b, J. Morales ^a

^a Instituto Andaluz de Geofísica, Universidad de Granada, Campus Cartuja, Spain

^b Université Montpellier II, CNRS, Géosciences Montpellier, CC060, F-34095 Montpellier cedex 5, France

ARTICLE INFO

Article history:

Received 19 January 2008

Received in revised form 16 May 2008

Accepted 11 June 2008

Available online 26 June 2008

Editor: R.D. van der Hilst

Keywords:

seismic anisotropy

lithosphere

asthenosphere

subduction

delamination

Gibraltar arc

ABSTRACT

Seismic anisotropy of the south Iberian upper mantle is investigated using shear-wave splitting of SKS phases. We analyzed teleseismic events recorded by sixteen permanent broadband stations installed on the southern Iberian Peninsula and in northern Africa, and we determined fast polarization directions ϕ , and delay times δt between fast and slow components. The area of investigation extends across two important geological structures in the Variscan Iberian Peninsula: the Variscan Iberian Massif in its center, and the Gibraltar arc in the Southeast, that represents the most westerly Alpine belt in the western Mediterranean. Shear-wave splitting measurements from stations in the Betic domain show homogeneous ENE–WSW fast directions nearly parallel to the trend of the mountain belt, and smooth spatial variations. Stations in the North, toward the southern part of the Variscan Iberian Massif show homogeneous fast directions however trending NS to NE–SW, different from those recorded in the Betic. These observations may reflect a post-Hercynian (Variscan) deformation of the Ossa-Morena zone, related to the main stages in the tectonic evolution of this part, namely transpressional stage, transtensional stage and shortening episode, or a deformation related to the posterior Alpine orogeny. Along the Gibraltar arc, we observe a smoothly varying ϕ trend changing from ENE–WSW in the Eastern Betics to NS in the area of Gibraltar and Ceuta, following more or less the general trend of the mountain belt around the Alboran Sea, and the coastline. Since a similar rotation is also visible in results from Pn anisotropy, this suggests that the anisotropy is vertically coherent starting from just below the Moho. Comparing the anisotropy pattern expected from various geodynamic models with the observed SKS splitting suggests that the anisotropy is best explained by a model of slab rollback, rather than by delamination models.

© 2008 Elsevier B.V. All rights reserved.

1. Introduction

During the last decades, seismological techniques have been developed to analyze the deep deformation of the Earth, and particularly the relation between plate tectonics and mantle flow as well as the internal deformation of the plate (e.g., Silver and Chan, 1988). The most popular technique uses the birefringence in anisotropic media that induces the splitting of shear waves and allows one to obtain quantitative information about seismic anisotropy in the upper mantle below a seismic station. Seismic anisotropy in the upper mantle is dominated by elastic anisotropy of rock-forming minerals which develop lattice-preferred orientations (LPO) or fabrics in response to strain (e.g. Nicolas and Christensen, 1987; Mainprice et al., 2000). The primary constituent of the upper mantle is olivine which is more anisotropic than most other minerals. Olivine deforms by dislocation-creep at upper mantle conditions (Nicolas and Christensen, 1987), and it generally aligns the main crystallographic

axes with respect to the structural directions (lineation, pole of the foliation), therefore producing a large-scale anisotropy that is detectable by seismic waves. The anisotropy is thus correlated with the strain in the upper mantle, and it therefore allows constraining deformation at that depth within the Earth remotely from the surface.

The most useful seismological phase for studying shear-wave splitting is the SKS phase. It travels through the mantle as an S wave, through the liquid outer core as a P wave after a S to P conversion at the core–mantle boundary, and is converted back into a radially polarized S wave when passing back in the mantle. On its way to the Earth's surface, this SKS phase is split into two mutually orthogonally polarized shear waves as it propagates through an anisotropic medium. From three-component seismic records, two parameters can be measured to quantify the anisotropy: 1) the difference in arrival time (δt) between the two split waves that depends on thickness and the intrinsic anisotropy of the medium, and 2) the polarization plane azimuth ϕ of the faster split shear wave that is related to the orientation of the anisotropic structure. Shear-wave splitting measurements can therefore characterize the orientation and to a lesser degree the depth extent of the mantle strain field (see review by Savage, 1999).

Determining the vertical location of the anisotropic layer(s) is always challenging since the splitting of SKS phases may occur somewhere between the core–mantle boundary and the station.

* Corresponding author. Tel.: +34 958 249554; fax: +34 958160907.

E-mail addresses: luisa@iag.ugr.es (L. Buontempo), Bokelmann@gm.univ-montp2.fr (G.H.R. Bokelmann), barruol@gm.univ-montp2.fr (G. Barruol), morales@iag.ugr.es (J. Morales).

Other phases such as local S (e.g. Bowman and Ando, 1987), may help to constrain the anisotropy distribution beneath a station, but they require the presence of nearby seismogenic zones. Petrophysical analyses of mantle minerals and rocks (Mainprice et al., 2000; Mainprice et al., 2005) suggest that anisotropy lies in the uppermost 400 km of the Earth. Recent theoretical studies using finite-frequency sensitivity kernels provide similar conclusions since SKS splitting are shown to be more sensitive to the upper mantle above the transition zone than to the lower mantle (Sieminski et al., 2007). If one assumes that the crust may contribute only a few tenths of a second to the total SKS splitting (Barruol and Mainprice, 1993; Godfrey et al., 2000), these arguments suggest that the anisotropy lies primarily in the subcrustal upper mantle. It is however not clear whether the anisotropy lies within the lithosphere and is related to a ‘frozen’ deformation (Silver and Chan, 1988), or within the asthenosphere and is thus related to present-day plate motion (Vinnik et al., 1992). This question can be addressed by SKS splitting only indirectly since these observations constrain only weakly the depth of anisotropy within the upper

mantle. On the other hand, this question can in principle be resolved combining SKS observations with surface wave anisotropy and Pn observations. We will in fact use Pn in this study to compare with SKS splitting results.

The area of interest of this paper, in southern Iberia and around the Gibraltar arc, represents a key area of geodynamic interest for the Africa–Eurasia collision and for the various stages of opening and closure of the Mediterranean basins. Various geodynamic models and mechanisms have been proposed to explain the large-scale structures and timing constraints, based on regional-scale recycling of lithosphere into the mantle, such as active continental subduction (Morales et al., 1999), delamination (Seber et al., 1996a) or active oceanic subduction (Lonergan and White, 1997; Gutscher et al., 2002).

In this study, we present new shear-wave splitting measurements obtained at permanent stations located in the Betic and Rif Cordillera and in the southern part of the Variscan Iberian Massif. We compare these new results with previous ones from Iberia (Díaz et al., 1998; Schmid et al., 2004), as well as from Pn phase anisotropy (Calvert et al.,

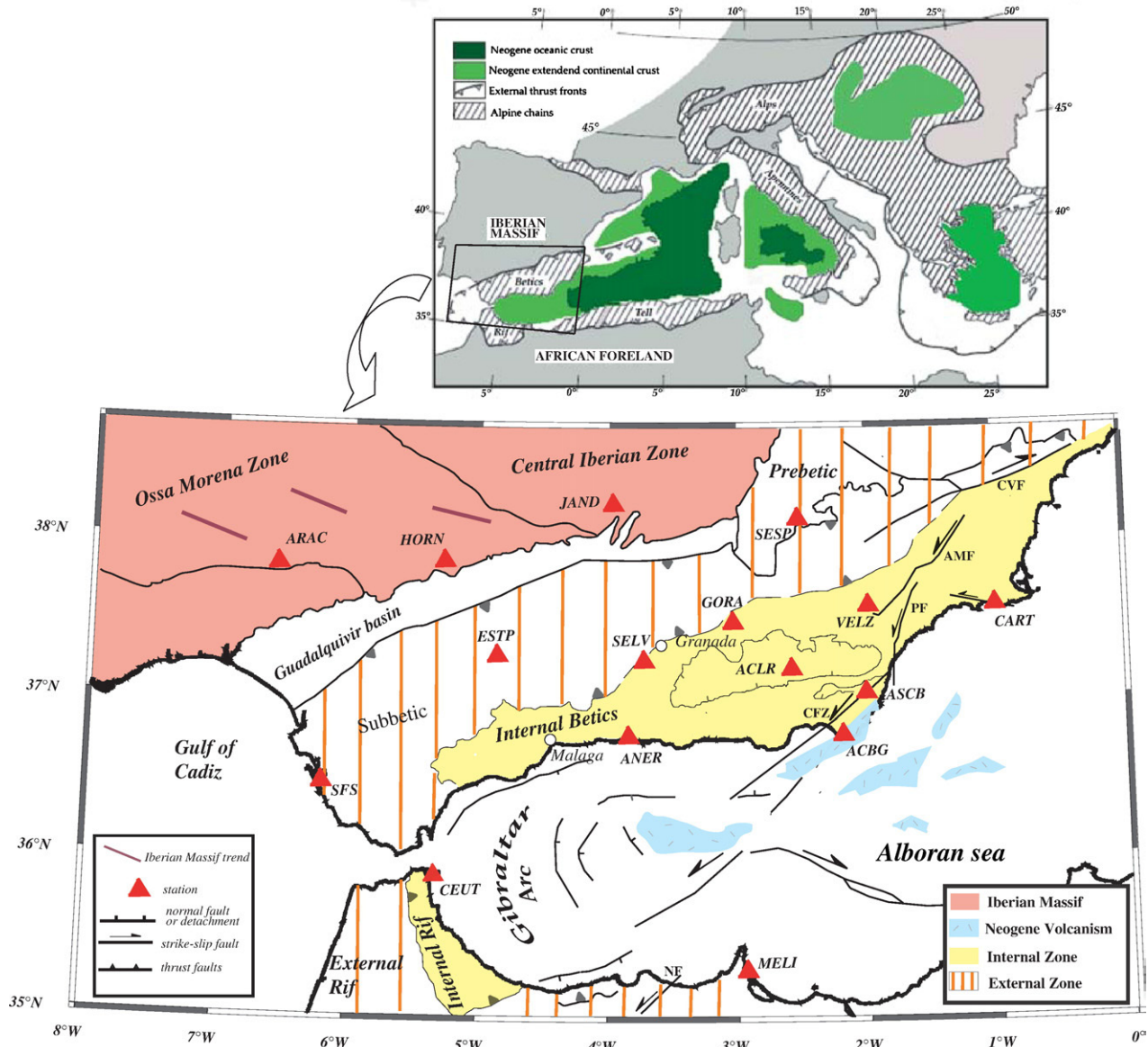


Fig. 1. Tectonic sketch of the Mediterranean area showing the Neogene basins and Alpine chains (top, redrawn from Comas et al., 1999) and geological setting of South of Iberia and North of Africa (bottom, redrawn from Lonergan and White, 1997; Platt et al., 2003). Main faults are shown in the External and Internal Zones and in the Alboran Domain (CVF: Crevillente fault, AMF: Alhama de Murcia fault, PF: Palomares fault, CFZ: Carboneras fault, NF: Nekor fault). Locations of seismological stations used in this study are also shown by triangles.

2000b). In the light of tomographic models for this region we propose that all these anisotropy observations may help to constrain and to better understand the geodynamic setting of this complex area.

2. Geodynamic setting

The Betic and Rif belts, connected through the Gibraltar arc, represent the most westerly Alpine range in southern Europe (Fig. 1). Together with the Alboran basin, these belts constitute one of the most complex and most debated geological regions in the western Mediterranean. A major characteristic of the Alboran basin is that it is an extensional regime (Comas et al., 1999) within a general collision regime, induced by the convergence of Africa and Eurasia from the Cretaceous to Paleogene (Dewey et al., 1989). The geological records and geophysical observations shed some light on the evolution of the region. Formally, the Gibraltar arc is divided into three pre-Neogene crustal domains: the first consists of Mesozoic and Tertiary sedimentary rocks deformed during the Neogene as a thrust-and-fold belt mainly directed to the NW and WNW (e.g., García-Dueñas, 1969; García-Hernández et al., 1980), which covered the South-Iberian and Maghrebian continental paleo-margins and constitute the External Zones of the Betics and Rif. The second corresponds to the sediments deposited on oceanic troughs or thin continental crust (Luján et al., 2006) and belongs to the so-called Flysch Trough that is well-represented in the Rif and Tell regions. The last one, the Alboran crustal domain, represents the internal zones of the orogen, composed mainly of Paleozoic to Mesozoic rocks affected by low to very high-grade metamorphism that were deformed mainly during the late Cretaceous to Paleogene and thrust onto the south Iberian and north African margins during the Early Miocene (Balanyá and García-Dueñas, 1988). Three tectono-metamorphic complexes are recognized in this zone, the Nevado-Filabride, the Alpujarride and the Malaguide in the Betics. The Alboran domain shows N-S continuity below the sea and constitutes the metamorphic basement of the Alboran basin (Platt et al., 1996). That basin represents a post-orogenic back arc basin (Lonergan and White, 1997), similar to the Calabrian arc (Faccenna et al., 2004; Rosenbaum and Lister, 2004), formed during the westward migration of the orogenic wedge. The main extension occurred during the Early Miocene (Comas et al., 1999), coeval with shortening in the orogen. The extension was associated with subsidence during the Miocene and accompanied by tholeitic and calcoalkaline magmatism (Turner et al., 1999; Duggen et al., 2005). Since the Upper Miocene–Pliocene until present, a contractive episode with a roughly NW–SE direction, although varying from the Upper Miocene to the Pliocene (Ott D'Estevou and Montenat, 1985; De Larouzière et al., 1988; Galindo-Zaldívar et al., 1997) manifests itself by strike-slip tectonics, mainly in the eastern Betics and

Alboran basin. This contractive episode was accompanied by magmatism of mainly shoshonitic, lamproitic and alkaline basalts (Lonergan and White, 1997; Zeck et al., 1998; Duggen et al., 2005).

At present, the kinematics of the Gibraltar arc as defined by GPS and seismic moment tensor observations shows different deformation styles that are characterized by NNW-directed thrust faulting near the Algerian coast and the SW of Iberia and an E–W extensional regime in the Alboran Sea (Stich et al., 2003, 2006). A crucial role is played by the so-called Trans-Alboran shear zone, a major structure formed by NE–SW sinistral strike-slip faults, and NW–SE conjugates in the partitioning of the strain in the region (Fernández-Ibáñez et al., 2007) that allow coeval shortening and extensional structures in a oblique convergent plate margin between Africa and Europe.

Several models have been proposed to explain the formation of the Gibraltar arc. These models may be compared by considering the style of recycling of lithospheric material back into the mantle that may occur in the form of lithospheric delamination (e.g. Seber et al., 1996a; Platt et al., 1998; Calvert et al., 2000b), convective removal (Platt and Vissers, 1989), or subduction (Lonergan and White, 1997; Gutscher et al., 2002).

Platt and Vissers (1989) proposed that a lithospheric thickening as a result of convergence created a collisional ridge of thick crust underlain by a thick root of cold lithospheric mantle, during late Eocene to Oligocene time. Such a gravitationally unstable root could have been removed by convection and replaced by an asthenospheric mantle during the late Oligocene, resulting in the uplift and extension of the region and in the exhumation of metamorphic rocks and high-temperature peridotites from the base of the crust. The continuous convergence between Africa and Eurasia is then proposed to be accommodated by shortening in the external zones of the belts (Subbetic and External Rif).

The model proposed by Seber et al. (1996a) is also based on delamination, and is somewhat similar to the model of Platt and Vissers (1989). The difference is the style of removal of the thickened lithosphere. Seber et al. (1996a) proposed indeed that, as a consequence of compression, a thickened lithosphere was underlying the (thickened) crust, and that gravitationally unstable lithospheric root was progressively replaced by hot asthenosphere by convective removal from the crust toward W and NW. A consequence of the resulting asthenospheric inflow is the heating of the crust inducing an uplift and the extension in the Alboran area.

The slab rollback model of Royden (1993) and Lonergan and White (1997) is very different from the above models, since it focuses primarily on subduction of oceanic lithosphere under the Alboran Sea. As the rate of subduction exceeds the rate of convergence, the subduction zone began migrating to the west while the crust of the

Table 1

Station locations and mean splitting parameters, given as mean values (m), median values (md) and weighted-mean values (w) with 2σ errors

Station name	Latitude (°)	Longitude (°)	ϕ_m (°)	$\sigma\phi_m$ (°)	δf_m	$\sigma\delta f_m$	ϕ_{md} (°)	δf_{md}	ϕ_w	$\sigma\phi_w$	δf_w	$\sigma\delta f_w$	Number of observations
ACBG	36.7686	-2.1939	59.42	7.94	1.70	0.64	59.59	1.88	67.09	1.59	1.86	0.08	5
ACLR	37.1897	-2.5822	77.16	8.49	1.74	0.69	77.20	2.00	82.60	4.26	1.72	0.18	6
ANER	36.7623	-3.8453	31.12	21.11	1.54	0.8	36.82	1.18	35.91	1.29	1.29	0.06	16
ARAC	37.8800	-6.5800	63.65	12.51	0.99	0.35	67.81	1.00	65.00	6.95	0.79	0.12	8
ASCB	37.0394	-2.0056	54.26	14.76	1.46	0.73	63.46	1.52	65.73	2.51	1.62	0.16	6
CART	37.5868	-1.0012	68.86	7.97	1.56	0.31	69.74	1.50	72.93	1.27	1.46	0.07	11
CEUT	35.8831	-5.3263	-3.61	22.27	2.06	0.88	-3.61	2.06	-15.01	3.76	1.71	0.44	2
ESTP	37.2713	-4.8662	81.14	13.05	1.56	0.59	83.16	1.34	63.44	3.12	1.45	0.18	9
GORA	37.4805	-3.0398	72.71	6.85	1.30	0.38	74.46	1.12	73.28	5.36	1.18	0.14	5
HORN	37.8200	-5.2800	58.06	21.19	1.07	0.4	57.56	0.94	40.15	2.28	0.92	0.1	14
JAND	38.22	-3.97	6.49	48.64	1.72	0.33	31.52	1.80	1.03	3.75	1.61	0.32	3
MELI	35.2899	-2.9392	66.87	8.24	1.43	0.6	63.11	1.50	67.51	3.27	0.95	0.09	3
SELV	37.2383	-3.7277	59.01	14.65	1.04	0.56	52.48	0.81	48.33	4.56	0.86	0.12	6
SESP	38.1208	-2.5452	66.28	28.69	1.68	0.63	72.26	1.70	47.35	1.38	1.77	0.11	14
SFS	36.4656	-6.2055	-1.27	28.41	1.10	0.99	-1.27	1.10	17.03	7.91	0.87	0.41	2
VELZ	37.5838	-1.9880	69.66	12.87	1.45	0.48	66.45	1.40	64.94	2.64	1.39	0.08	8

For (m) errors give two times the standard deviation of individual values; for (w) they give the error of the weighted mean.

former collision ridge (Internal Zone) was broken up and dispersed, and the crust behind this region was thinned by extension. In the northern and southern portions of the subduction zone, the westward movement slowed down as Iberian and African lithosphere was encountered and the emplacement of the Internal Zone was accommodated by shortening in the continental margins. The central portion of the subducting trench continued its westward migration and the continued subduction-zone rollback induced extension beneath the Alboran Sea. On the other hand, several other models consider different geometries and dip direction for the subducting slab: the above models invoke eastward subduction of oceanic lithosphere rolling back to the west (Lonergan and White, 1997; Gutscher et al., 2002); others consider an extinct subduction oriented northwards (e.g., Zeck, 1996). Recent analyses of body-wave dispersion at Ceuta (Bokelmann and Maufroy, 2007) indicate very different dispersion characteristics of events arriving from the West from those arriving from the East, which suggests the presence of an oceanic slab beneath the Alboran Sea.

3. Data and method

In this study, we used seismic data recorded by 13 permanent broadband stations of the Instituto Andaluz de Geofísica (IAG), and by 3 broadband seismic stations of the ROA-UCM-GEOFON (Real Observatorio de la Armada in San Fernando—Universidad Computense Madrid-Geofon). The station locations are reported in Fig. 1 and Table 1.

Locations and centroid times of teleseismic events used to extract the data from the continuous record were taken from the Harvard

catalogue, <http://www.seismologyharvard.edu/CMTsearch.html> and arrival times of theoretical SKS phases at the stations were calculated using the theoretical Earth model IASP91 (Kennett, 1995) with the IASP91TTIM software (Buland and Chapman, 1983; Kennett and Engdahl, 1991). From the teleseismic events covering the period 2001–2006, we selected events occurring at distances larger than 85° and of magnitude (M_w) larger than 5.7. The selected events are shown in Fig. 2, with a global projection centered on southern Spain and preserving the azimuths. For the distance range between 130 and 165° we also selected SKKS phases. A careful visual inspection of the data allowed us to keep about 207 seismograms from 67 teleseismic events.

For each selected event, we calculated the two splitting parameters, that is, the azimuth of the fast axis ϕ and the delay time δt between the fast and slow component of the shear waves. We performed these measurements using SplitLab (Wüstenfeld and Bokelmann, 2007; Wüstenfeld et al., 2008), which utilizes three different techniques simultaneously: the rotation-correlation method (e.g. Bowman and Ando, 1987), that is maximizing the cross-correlation between the radial and transverse component of the SKS phase, the minimum energy method (Silver and Chan, 1991), that is minimizing the energy on the transverse component, and the minimum eigenvalue method (Silver and Chan, 1991). Fig. 3 shows an example of the application of these techniques for an event that arrives from the North at station ACBG. Under good measurement conditions, i.e. good signal-to-noise ratio and a favorable backazimuth, these methodologies give similar splitting parameters. The comparison between the different methods is helpful for characterizing cases of small δt where seismograms do not show clear SKS splitting, the so-called Null measurements, and for

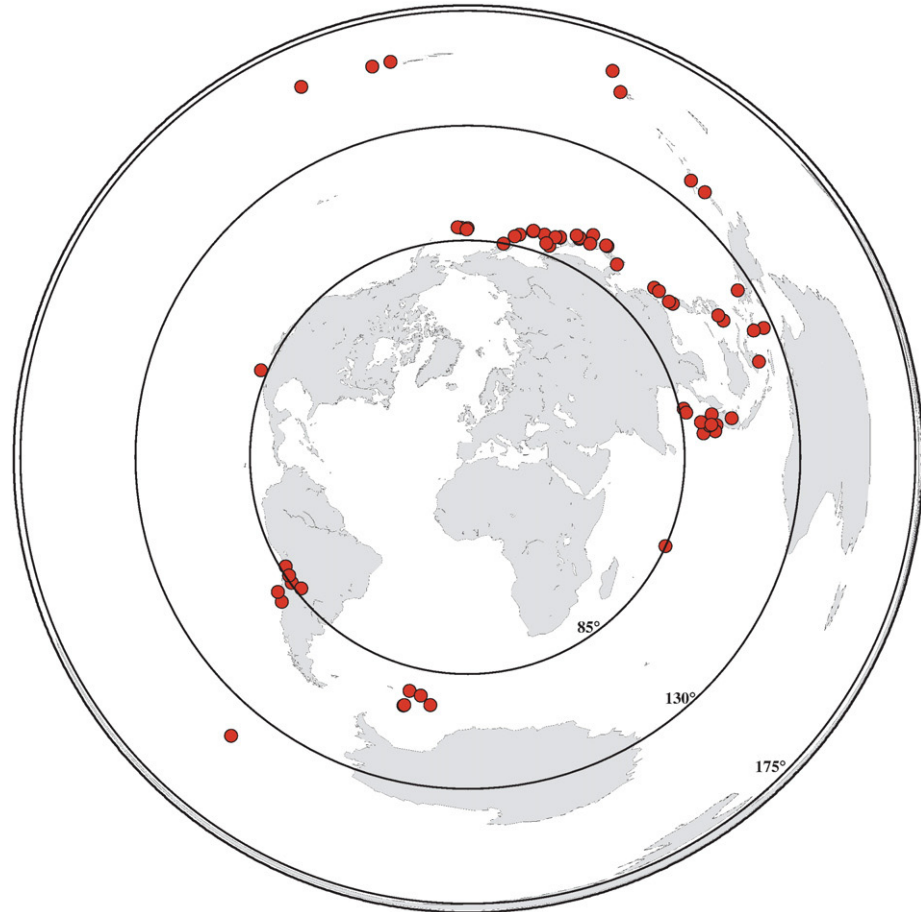


Fig. 2. Spatial distribution of earthquakes used in this study in a projection that preserves backazimuths, centered on the Alboran. The 85° (minimum distance for SKS splitting measurement) and 130° of epicentral distance are also shown.

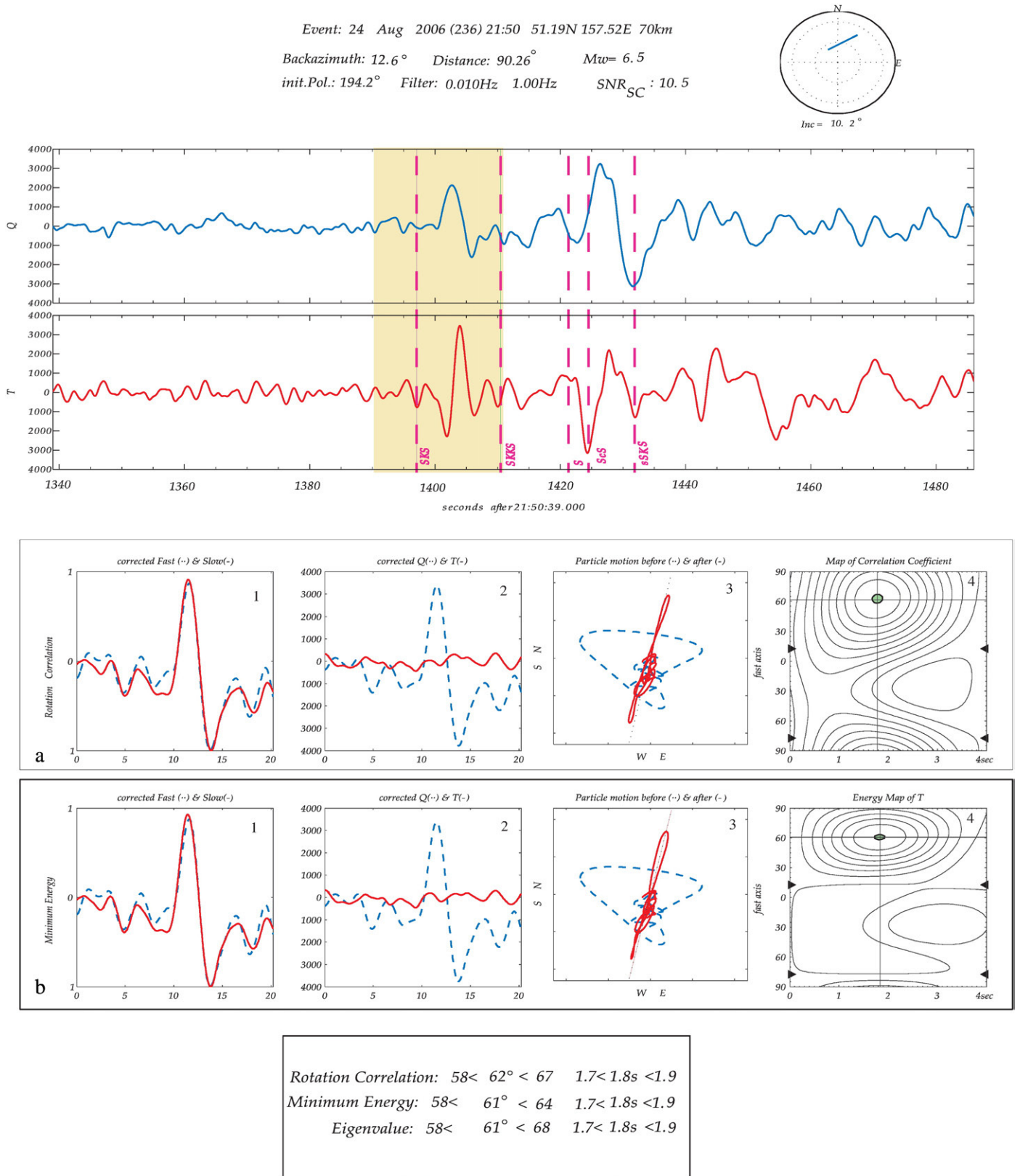


Fig. 3. Example of data processing using SplitLab software (Wüstefeld et al., 2008) at ACBG station. (top) The upper panel shows the event information and the initial radial and transverse components. Dashed lines are the predicted phase arrival times from IASP91; the shaded area is the selected window for the shear-wave splitting processing. (middle) Figures for inspecting the performance are shown with four plots for the rotation-correlation method in panel a) and four plots for the minimum energy method in panel b). From left to right: 1) fast and slow components (dashed and continuous lines, respectively), corrected for the calculated splitting delay time; 2) corrected radial and transverse components (dashed and continuous lines, respectively), note that the energy on the transverse component is well removed after anisotropy correction; 3) the particle motion in the horizontal plane (dashed) becomes linear after the correction for anisotropy (solid); 4) contour plot for the maximum value of correlation coefficient and for the energy on transverse component as function of delay time and fast polarization angle. The shaded area marks the 95% confidence interval. (bottom) Numerical values that summarize the results for the three methodologies are given at the bottom, with their respective error ranges.

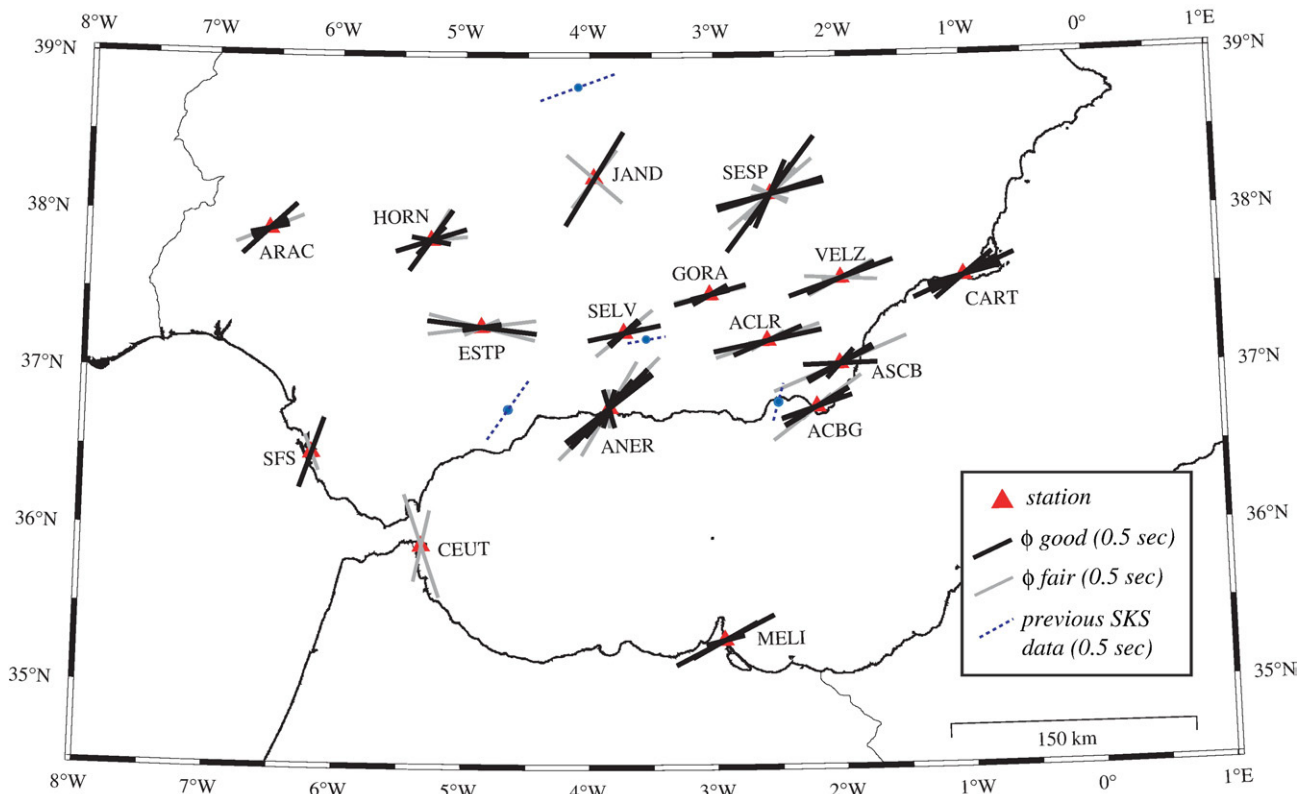


Fig. 4. Splitting results shown at the seismic stations used in the present study. Each measurement is characterized by a fast azimuth ϕ , and the length of the segment is proportional to the delay time δt . Good (thick dark lines) and fair (thin lines) are represented.

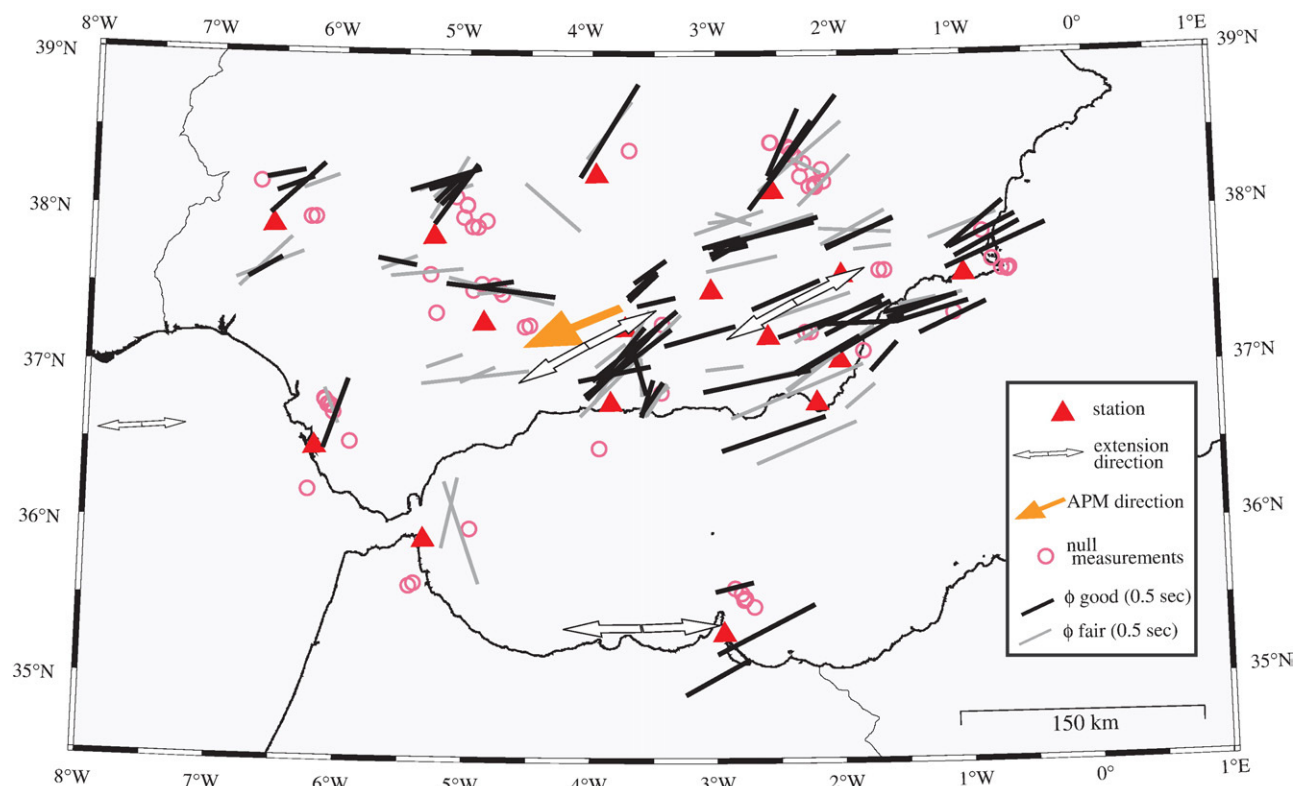


Fig. 5. Individual splitting measurements projected at 150 km depth along the ray paths. Good measurements are shown by thick lines, fair measurements by thin lines. Null measurements (events with no apparent splitting) are shown by circles. White arrows are average stress extension directions calculated by Stich et al. (2006), the dark arrow shows absolute plate motion direction for the model HS3-Nuvel-IA (Gripp and Gordon, 2002).

discriminating them from cases of existent but weak splitting. Null measurements occur when the SKS phase is not split. This may happen when the medium is isotropic or when the backazimuth of the incoming SKS wave is parallel to either the slow or the fast directions in the anisotropic layer. In the case of a simple anisotropic medium, Null and non-Null measurements have to be consistent with each other. For simplicity in the discussion and pictures we present only measurements obtained with the minimum energy method. Table 1 gives resulting splitting parameters (ϕ and δt) for each seismogram.

We qualified the splitting results as “good”, “fair”, and “poor” as proposed by Barrool et al. (1997), i.e., depending on the quality of the seismograms, on the signal-to-noise ratio of the initial phase, on the

amount of energy on the transverse component, on the correlation of the two split waveforms, and on the elliptical particle motion before anisotropy correction and its linearization after correction. Waveforms with good or fair quality generally provide similar results with and without filtering, indicating that results do not overly depend on the filter parameters. We generally choose to not filter the data unless required to remove high frequencies and/or long-period noise.

We will initially assume that the anisotropy is characterized by layer (s) with horizontal symmetry axes. Dipping axes of symmetry (or some orthorhombic symmetry systems) can cause systematic variations of splitting parameters as functions of backazimuth. However the small number of observations at each station precludes testing such cases.

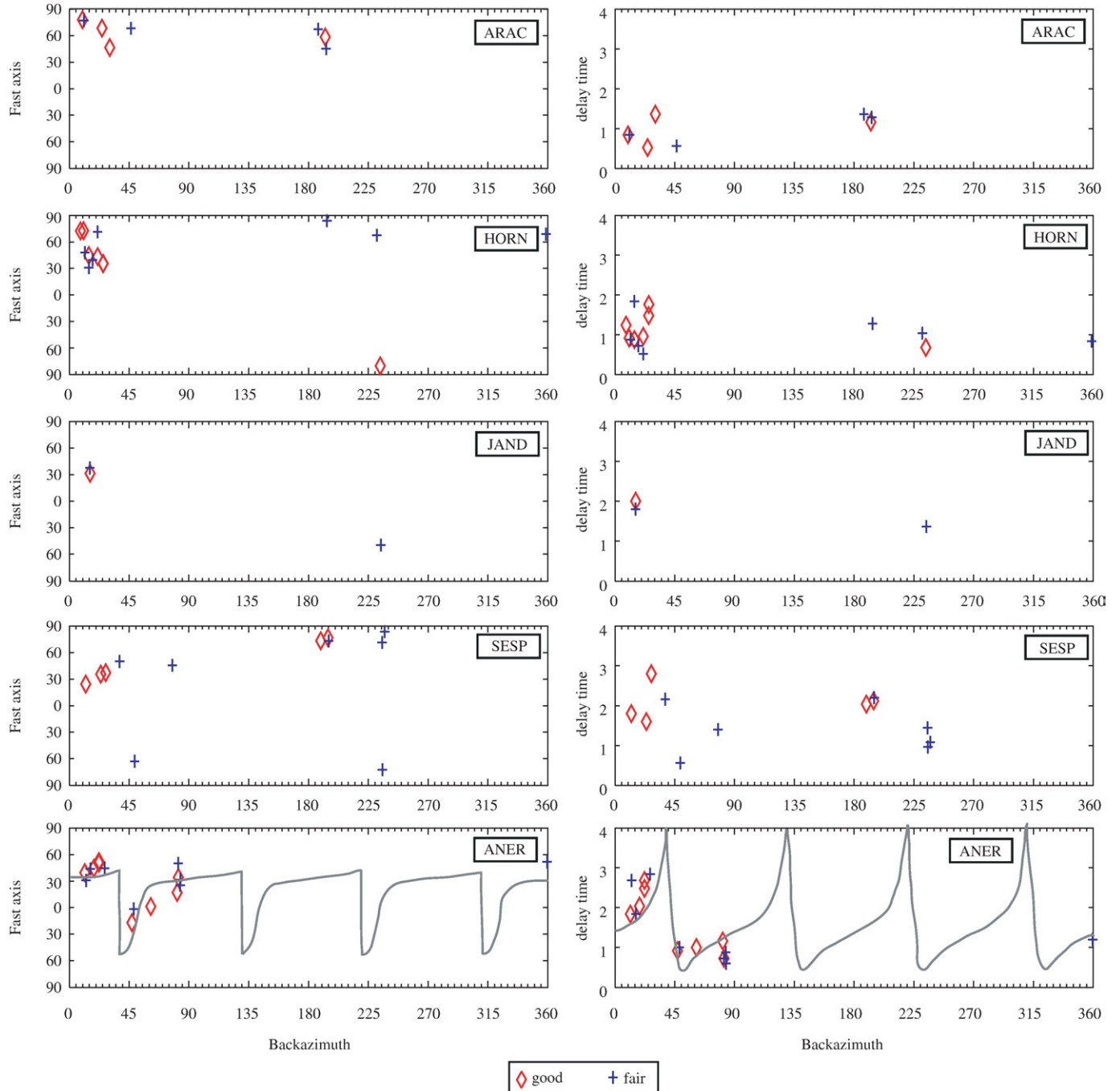


Fig. 6. Backazimuthal distribution of SKS splitting for stations SESP, JAND, HORN, ARAC, and ANER that are not easily explained by a single anisotropic layer. The panels for ANER also show the prediction for the best-fitting two-layer model. See text for explanation.

4. Results of SKS splitting

The individual splitting measurements (see Table 2, given in the Electronic supplement) are plotted in Fig. 4 at the various stations to evaluate the coherence of the results. Lines show the fast anisotropy directions ϕ , obtained from the minimum energy method, and their lengths are proportional to the splitting delay time δt . “Good” data are shown by thick dark lines, and “fair” data by thin lines; “poor” data are not plotted. Most stations in the Eastern Betics, CART, VELZ, ACBG, GORA, ACLR and ASCB show a homogeneous ϕ trending roughly N70°E and high delay times of around 1.5 s. Given the weak spreading of fast direction measurements ϕ at stations in that region, and the spatial coherence, the splitting observed at those stations is likely originating within a single anisotropic layer that is well-constrained by a suitable number of measurements. We record a similar trend for the station MEI in Northern Africa, where the fast direction is N68°E with a delay time of roughly 0.95 s. Interestingly, ϕ is nearly North-South at stations SFS and CEUT, i.e., parallel to the trend of the Gibraltar arc. At each of these two stations unfortunately, measurement conditions were relatively difficult, and there are only two measurements available at CEUT from 3 yr of data analyzed, (N12°E, $\delta t=1.44$ s and N19°W $\delta t=2.68$ s), and two non-Null measurements at SFS (N19°E, $\delta t=1.80$ s and N21°W $\delta t=0.4$ s).

Díaz et al. (1998) used data from temporary stations and found a fast direction oriented N80°E at a station in the southern part of the Variscan Iberian Massif. In the Betics, they observed a NNE-SSW trend in the eastern part that changes to E-W in the central part, near Granada, and again NNE-SSW near the coast of Malaga interpreted in terms of their particular lithospheric geodynamic settings. Schmid et al. (2004) studied the station CART, in the eastern part of Betic, and MEI in the north of Africa, finding fast directions in the Betic trend, oriented N70°E and N56°E respectively.

At a number of stations, there is a clear backazimuthal dependence of the splitting parameters, like at stations ARAC, HORN, JAND, SESP, and ANER. Such a backazimuthal dependence of splitting parameters may be explained either by invoking vertical variation of anisotropy, e.g. by the presence of two (or more) anisotropic layers, or by lateral variations of anisotropy. First, we address the case of lateral heterogeneity. In order to better visualize the lateral sampling of the anisotropy measurements and the regional-scale stability of the anisotropy parameters beneath the stations, we choose to project the individual splitting measurements of good and fair quality along their incoming rays to a depth of 150 km (Fig. 5). Although the splitting of the SKS waves is not well-located vertically, this representation is helpful since it plots the splitting parameters closer to the location where they were acquired. The measurements with well-constrained anisotropy (“good”) are presented as thick dark lines while measurements of lower quality (“fair”) are shown by thin lines. In addition, Fig. 5 presents the Null measurements by open circles. In the eastern and internal Betics, this figure clearly indicates smooth spatial variation of the anisotropic structures beneath most stations (with the exception of ANER, see discussion below). Such a pattern was less clear in Fig. 4. It suggests that the variation is not caused by noise in the observations. It is apparently due to real anisotropic variations at depth. This suggests that the upper mantle beneath the Internal Betics is dominated by a single anisotropic layer, with smoothly varying fast directions. Station ESTP located in the Subbetic domain shows a homogeneous distribution of the fast directions that led us to conclude that this part is characterized by a single layer. We will address the nature of this anisotropy and its smooth spatial variation in detail below.

The splitting parameters observed at stations ARAC, HORN and JAND near the transition to the Variscan Iberian Massif, SESP in the Prebetic units, and ANER in the Internal Betics, are not fully explained by lateral variation of splitting. These 5 stations are characterized by an apparent backazimuthal variation of the splitting parameters as shown in Fig. 4. The projection at depth of the individual splitting

measurements (Fig. 5) suggests strong lateral variations at small scale-length. Such a rapid variation is not easily explained by lateral variation since the Fresnel zone of SKS phases in the upper mantle that quantifies the width of the zone over which the SKS ‘average’ the structure, is 100 to 200 km wide for SKS waves with 10 s period. For these 5 stations, we show the detailed ϕ and δt backazimuthal variation in Fig. 6. A single anisotropic layer would produce a constant fast direction ϕ , independent of backazimuth, as well as a constant splitting delay δt . With the possible exception of station ARAC, such a simple single layer does not explain the observations at these stations. However, the stations are characterized by varying amounts of data, partly due to the different running periods of the stations. Data at station JAND were available only from July 2006 and therefore provide only few SKS measurements. Nevertheless, the station exhibits a general NE trend except for the event on day 237 (year 2006, see Table 2 Electronic supplement) with backazimuth of 234° that shows a different ϕ . The small number of data cannot constrain the results for that station. For ANER, there is a nearly North-South trend for such events that arrive from ENE, but data with NNE backazimuth show NE-SW fast directions. The stations HORN, SESP and ARAC exhibit a good number of data which will allow the discussion of a possible two-layer case that we will present below.

5. Discussion

A striking feature in the anisotropy pattern observed in this study is that the Eastern Betics seems to be well-described by a single and rather homogeneous anisotropic layer, whereas a more complex anisotropic model likely involving lateral and vertical variations of anisotropy seems to be present in the upper mantle beneath stations in the North, and perhaps the West and the South. The Eastern Betics show indeed a smooth lateral variation of anisotropy, whereas stations in the Western and Southern part of this region indicate much stronger lateral variations in the splitting parameters. There are also strong lateral variations associated with the transition from the Betic to Variscan Iberia, in addition to two-layer anisotropy as we will show below, as is required at some of the stations at least.

5.1. Eastern Betics

Fast directions are oriented ENE-WSW in the Eastern Betics, and there is a smooth spatial variation clearly visible in Fig. 5 that is more or less parallel to the mountain belt. The anisotropy in that region is easily explained by a single anisotropic layer. The average splitting delay time in that region is about 1.5 s, which is consistent with a layer that is 150 km thick assuming the typically used value of 4% anisotropy in the upper mantle (Mainprice and Silver, 1993; Mainprice et al., 2000). Tomographic models for the region, (e.g. Blanco and Spakman, 1993), show a pronounced low-velocity anomaly in the upper mantle under the Betics between 30 and 100 km depth that is also apparent and even more pronounced in the Pn tomographic model of Calvert et al. (2000a). This area is also the locus of a pronounced high attenuation anomaly of Sn waves (Calvert et al., 2000b). This may suggest that continental mantle material under the Betics has been replaced by asthenospheric material. Geochemical studies favor such a hypothesis by suggesting an edge delamination that could have occurred under the Betics (Duggen et al., 2005). If the lithosphere has indeed been removed, this should suggest that the deformation recorded by the seismic anisotropy under the Betics is associated rather with hot and thus relatively low-viscosity material. At larger depths, however, velocities are again relatively high in tomographic models (e.g., Blanco and Spakman, 1993) down to the transition zone, including the zone of very deep seismicity around 600 km depth (Buorn et al., 1997).

The ENE-WSW fast directions observed in the Eastern Betics are nearly parallel to the absolute plate motion direction, which is 239°

and 2 cm/yr for the motion model Nuvel1A relative to the hotspot reference system HS3 (Gripp and Gordon, 2002). Although the Eurasian plate motion vector is slow and therefore still matter of debate, a simple deformation model related to plate motion of the Iberian/Eurasian plate over the deeper mantle might thus explain the anisotropy. In this context, the gradual rotation of fast direction along the coast might be explained reasonably by invoking a deviation of mantle flow around the Iberian lithosphere, following similar suggestions of Bormann et al. (1996) for central Europe and of Barruol et al. (1997) and Fouch et al. (2000) for North America. This might also explain the minor difference of 10° between the average fast direction in the Eastern Betics and the absolute plate motion direction.

On the other hand, the observed fast directions in the Eastern Betics also show an interesting correlation with crustal features which is not expected in the case of plate motion induced asthenospheric anisotropy. The convergence direction between the African and the Iberian/Eurasian plate is NNW–SSE, and the current style of deformation in the crust is predominately left-lateral strike-slip faults with a NE–SW trend (e.g. Alhama de Murcia, Palomares and Carboneras faults). Vauchez and Nicolas (1991) suggested that in many collisional belts the dominant motion is strike-slip parallel to the main trend of the belt. In this case, both crustal and mantle fabrics may reflect these movements, and the entire lithosphere develops a fabric and becomes anisotropic. They attribute this anisotropy to a dominant mantle flow parallel to the mountain belt during orogeny. Such a structure is well illustrated in the Ronda peridotite massif where pervasive structures and fabric in the lithospheric and asthenospheric mantle are well preserved (Vauchez and Garrido, 2001). The present-day extension direction inferred by Stich et al. (2006), using moment tensors of crustal earthquakes, is N240°E, which is indeed parallel to the inferred fast polarization directions. The anisotropy is thus also consistent with a notion of vertically coherent deformation of crust and mantle as initially proposed by Silver and Chan (1988, 1991), except that we are dealing with hot deformed mantle in this region, and thus probably with current deformation, rather than fossil deformation remaining from the creation of continental lithosphere. For the close-by Gulf of Cadiz region, Stich et al. (2005) have shown that the stresses imposed by the Africa–Iberia plate convergence have the same geometry in the crust and the mantle. The convergence thus imposes a similar lateral boundary condition over a considerable depth range. Crust and mantle in the Betics may thus both be constrained to deform in a similar fashion. The observed anisotropy under the Eastern Betics could be thus caused by a combination of this kind of vertically coherent deformation, and absolute-motion-related deformation, both producing a seismic anisotropy such as the observed one. The relative importance of each is not constrained though. Interestingly, a model of slab rollback is also consistent with such coherence between crustal and upper mantle deformation. The retreat to the WSW of the Alboran slab may have induced a large transcurrent deformation in the mantle beneath the eastern Betics but also in its crust.

5.2. Variscan belt

The northernmost stations of our study area are situated on or near the Variscan Iberian Massif. The fast anisotropy directions we observe at these stations are trending more NE–SW than those recorded by stations in the Betics that trend more ENE–WSW. These directions do not appear to correspond to orientations of geological structures in the Variscan basement, since the latter trend more or less NW–SE in the Northwest portion of Iberia and East–West in eastern Spain. While we do not obtain those “Variscan” directions for our northernmost stations that are near the southern end of the Variscan belt, they are in fact observed further North, in the center of Variscan Iberia (Silver and Chan, 1988; Schmid et al., 2004), where they are roughly E–W. Three of our northernmost stations show a wide range of fast orientations (Figs. 5 and 6). Different anisotropy parameters are obtained for

measurements arriving from the North and South. This is not easily explained by lateral heterogeneity, unless all these stations are located above a geological suture zone so that events arriving from the North and the South could experience a different medium. Since these stations are indeed near the Betics deformation front, we wish to further test both hypotheses for the northernmost stations, namely the ‘lateral heterogeneity hypothesis’ and the ‘two-layer anisotropy hypothesis’. Fig. 5 illustrates the ‘lateral variation hypothesis’, where splitting results were projected along the incoming rays to 150 km depth. In this view, fast directions that show up to the North of the stations, within the Iberian Variscan Massif, are generally associated with NE–SW fast direction, while results generally show more East–West trending fast directions, for southern backazimuth i.e., close to the general Betics trend. This is particularly clear at station SESP, and it may indicate that the events arriving from the south are experiencing the same anisotropic structure as the stations located further south in the Internal Betics. This would suggest that SESP may lie close to an important boundary between lithospheric blocks. Among the northern stations of our study area, ARAC shows little backazimuthal dependence of the anisotropy parameters: NE–SW fast directions are visible both to the North and to the South of the station.

On the other hand, we may assume a two-layer model for each of these four northern stations, to try to explain the observed variation of the splitting parameters apparent in Fig. 6. Constraining the four parameters of a two-layer model requires a relatively good backazimuthal coverage (see Walker et al., 2007), which we do not have. We therefore decided to apply a similar approach as Fontaine et al. (2007) for the SKS splitting obtained at oceanic island stations, by considering the area as homogeneous enough to group the individual splitting measurements together into a single “virtual” station. We processed measurements obtained from the four stations together, since they have similar backazimuthal coverages. Different from the other three stations, SESP is located within the Betic Cordillera, in the so-called Pre-Betic. Nevertheless splitting parameters are more like those of the stations at the limit, e.g. HORN, rather than the other station on the Betics.

If there were several anisotropic layers present at depth, mantle deformation would not necessarily mimic crustal deformation. A tectonic decoupling somewhere within the lithosphere might explain why anisotropic directions in the area are different from the trend of the mountain belt. Seismic reflection profiles in the south-western portion of the Iberian Massif show that the Moho is discontinuous (Simancas et al., 2003), particularly under the Ossa-Morena and Central Iberian Massif. In fact, the Moho is probably a decoupling zone between the mantle and the crust in the area.

Following the approach defined by Silver and Savage (1994), we therefore tested two-layer models by varying ϕ and δt in the upper and lower layer by increments of 2° and 0.2 s, respectively, and compared the expected backazimuthal variations with our observations. We use the statistical technique presented in Walker et al. (2005) to judge the significance of the variance reduction over the best-fitting one-layer model. Testing all possible two-layer models (Fig. 7), we find that the best-fitting models belong to three groups of models, 1) those having NE–SW fast directions in both layers, 2) those having NE–SW for the upper layer and NW–SE for the lower layer, and 3) vice-versa. While the best model formally falls into the second category, we cannot rule out the other two cases, including the one of a shallower layer with NW–SE fast azimuths, that would indeed correspond to the trend of the Variscan basement in its southern portion. This ambiguity is in part due to the backazimuthal distribution of the events being rather limited, but more fundamentally since a second layer with exactly perpendicular orientation to the first one only varies the splitting delay but does not produce a backazimuthal variation of fast direction and splitting delay. We note that the splitting delay associated with the lower layer is quite small (0.2 s). While the additional variance reduction (39%) associated with this weak second layer is slightly statistically significant, we choose to

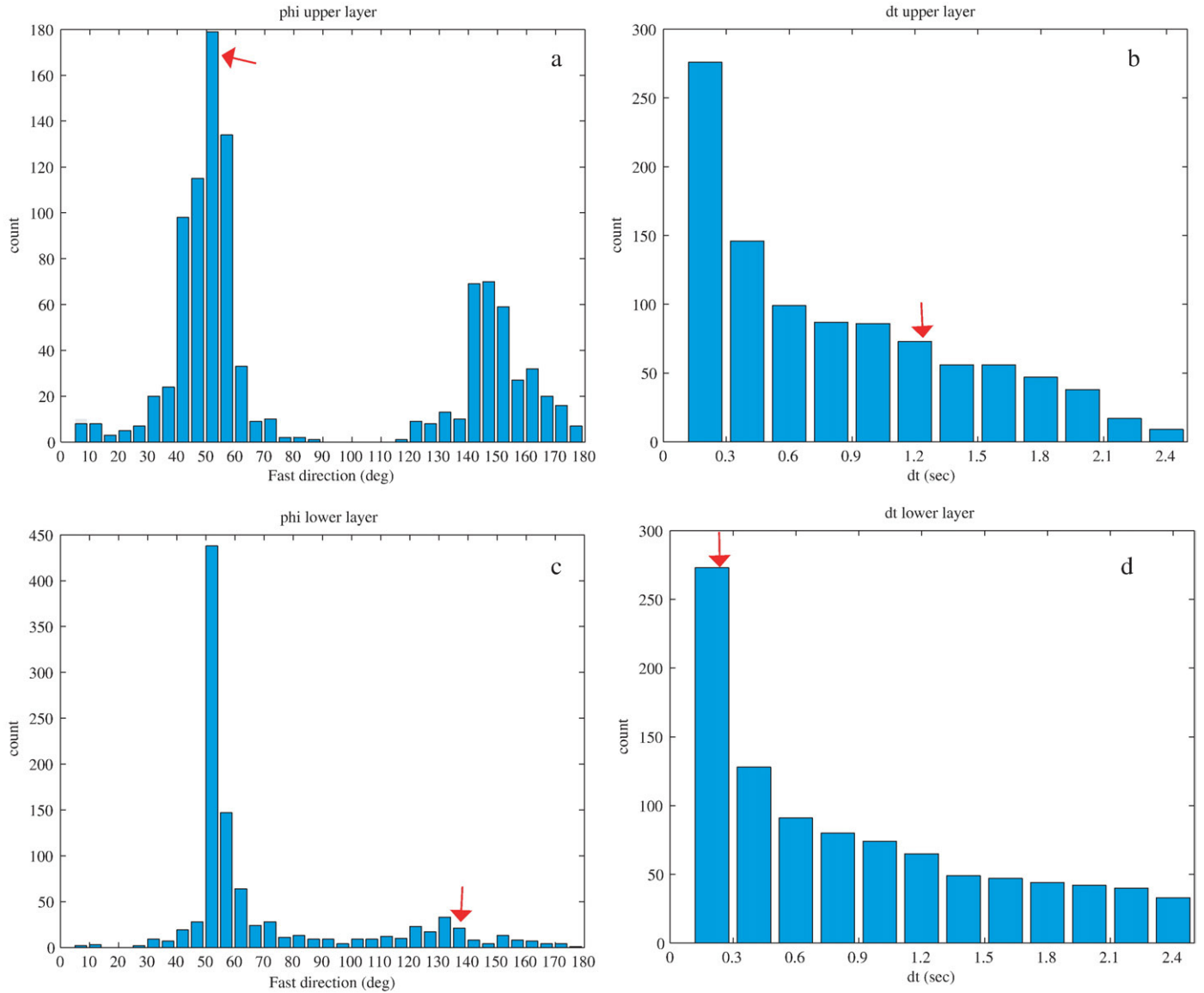


Fig. 7. Statistical analysis of two-layer modelling for the joint data set of 4 stations in the north (ARAC + HORN + JAND + SESP): parameters for the 1000 best-fitting models are shown as histograms for a) fast direction in upper layer; b) delay time in the upper layer c) fast direction in the lower layer; d) delay time in the lower layer. The arrows show the optimum values for each model, $\phi = N52^\circ E$ and $\phi = N136^\circ E$ for a) and c) respectively, and $\delta t = 1.2$ s and $\delta t = 0.2$ s for b) and d) respectively.

not attribute much significance to this. The backazimuthal variation that is present in the data may likely represent a complexity that is perhaps better characterized by an anisotropy that varies laterally.

5.3. Gibraltar arc: constraints on geodynamic models

Fast directions in Southernmost Spain, close to Gibraltar show rather distinct orientations from those in the Internal or External Betics: ϕ trends more or less North–South at the two stations CEUT and SFS. Station ANER near Malaga provides evidence for higher complexity and perhaps multi-layer anisotropy. We have therefore performed a two-layer modeling as detailed above but consider only the results obtained at this station. The thousand best two-layer models obtained for ANER give a best-fitting model with fast direction ϕ for the upper layer of $N28^\circ E$ and for the lower layer of $N68^\circ E$ (Fig. 8), and splitting delays 1.0 and 0.6 s. This result suggests that this station lies in a region of transition between the eastern Betics where ϕ trend ENE (i.e., close to the ANER lower layer ϕ) and the Gibraltar arc where ϕ trend close to NS (i.e., close to the ANER upper layer ϕ). Interestingly, the close NS trend of the upper layer seems also to coincide with the

N–S line of intermediate-depth earthquakes (Morales et al., 1999; Calvert et al., 2000b). Nevertheless, we note that for the fast directions in the two layers, the maxima of the histograms in Fig. 8 are only 20° apart. Even though the statistical improvement is slightly significant, we defer a deeper discussion of a possible two-layer anisotropy until data from more stations around ANER become available.

We consider both Pn and SKS anisotropy measurements, which provide different and complementary depth sampling (e.g., Pera et al., 2003). SKS waves travel almost vertically and are not able to localize the precise depth range of the anisotropy, except that a layer of more than 100 km thickness is required to explain the observed splitting delay times (Mainprice and Silver, 1993; Ben Ismail and Mainprice, 1998), and that it should be in the upper mantle. On the other hand, Pn travels horizontally just below the Moho, and thus constrains anisotropy at that depth level. Pn models for the area have been produced by Calvert et al. (2000b) and by Serrano et al. (2005) which give rather similar results in the area of interest. In each case, arrival times of regional events have been used to determine isotropic and anisotropic velocity variations. The agreement of anisotropic fast directions from Pn and SKS are in fact remarkable on the Spanish side

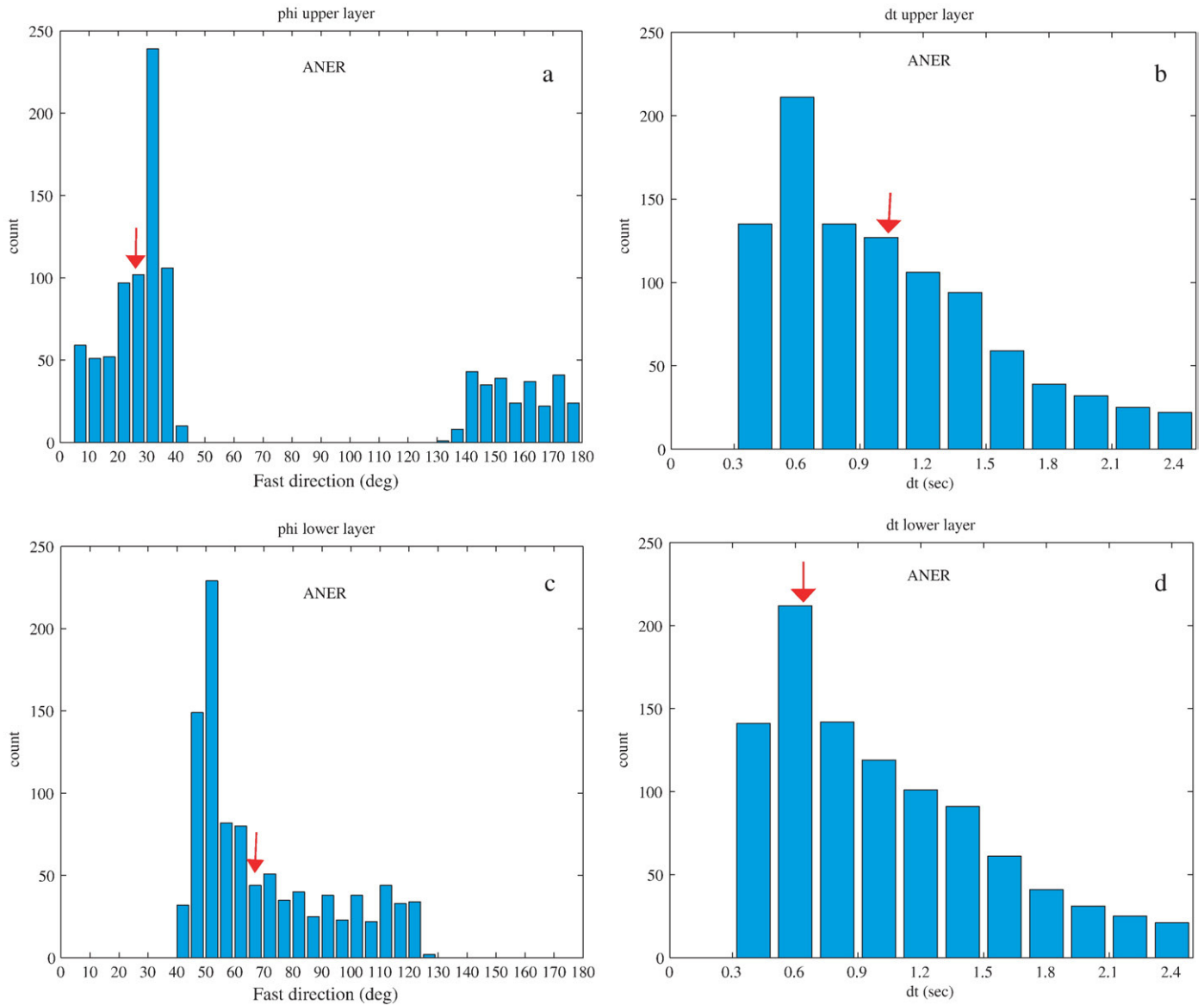


Fig. 8. Statistical analysis of two-layer modelling for station ANER: parameters for the 1000 best-fitting models are shown as histograms for a) fast direction in upper layer; b) delay time in the upper layer; c) fast direction in the lower layer; d) delay time in the lower layer. The arrows show the optimum values for each model, $\phi = N28^\circ E$ and $\phi = N68^\circ E$ for a) and c) respectively, and $\delta t = 1.0$ s and $\delta t = 0.6$ s for b) and d) respectively.

of the Alboran arc (Fig. 9). Not only are these fast directions parallel in the eastern Betics, but they seem to rotate together with the large-scale geological structures of the Alboran arc, and parallel with the coast, in a similar fashion for the shallowest and somewhat deeper mantle. The model may perhaps suggest that this parallelism is not present on the African side of the Gibraltar arc where fast Pn trend NS to NNW–SSW and fast split SKS trend NE–SW. The model is less well-constrained in that area, but if the feature is real, this may suggest a complete decoupling between the sub-Moho and the deeper anisotropy. However, the similarity between Pn and SKS fast directions may reflect different tectonic processes at depth, particularly in the vicinity of a subduction zone. Indeed, if there is subduction in the area, as has often been argued (e.g., Gutscher et al., 2002), Pn may be affected by the anisotropy above the slab, whereas SKS might be sensitive to the anisotropy below, above, and possibly within the slab. Fast split directions parallel to the slab is a rather common feature in subduction zones, both above and below the slab. This has been found for instance in New Zealand (Marson-Pidgeon and Savage,

2004) and in Northern Italy (Mele et al., 1998). Trench-parallel fast directions, may be explained either by invoking trench-parallel flow (e.g., Russo and Silver, 1994), or by invoking a hydrated mantle wedge above the slab (Jung and Karato, 2001). The degree of hydration of the mantle wedge and of magnitude of the applied stress above a subduction zone appears to have a strong influence on the style of seismic anisotropy (e.g., Jung and Karato, 2001; Kaminski and Ribe 2002): Slab-parallel seismic fast axes from SKS can in principle be explained either by slab-parallel flow in an anhydrous mantle wedge or by slab-normal compression in a hydrous mantle wedge. Such a pattern of anisotropy may show apparently erratic behaviour in some places; this may perhaps help to explain the complexity that we find at station ANER.

Deep structure and dynamics beneath the Alboran area has been widely debated throughout the last decades and a wide variety of geodynamic models has been proposed for the area. These models can be categorized by the way material is recycled into the mantle. If mantle lithosphere has been removed as has been proposed in the

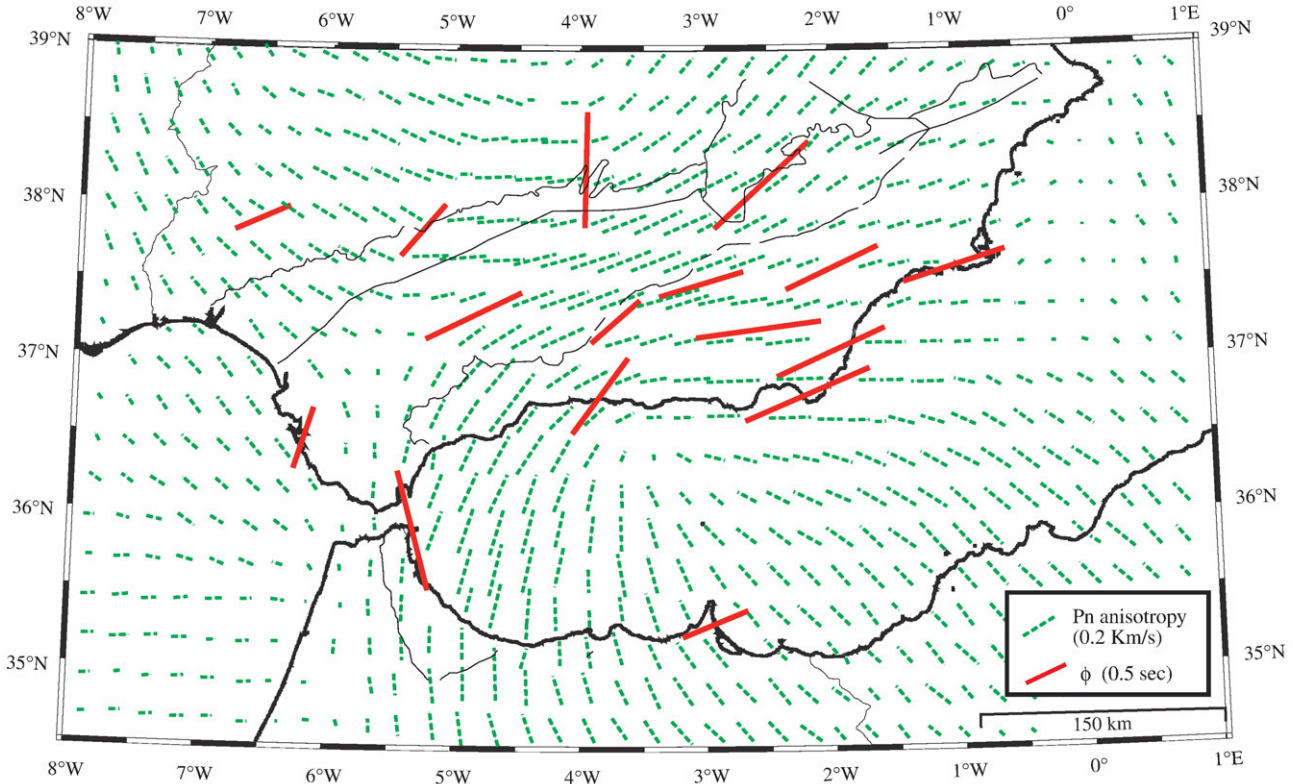


Fig. 9. Comparison of SKS fast directions (weighted-mean values from this study) with Pn-fast directions (redrawn from Calvert et al., 2000b). See text for explanations.

convection-removal hypothesis (Platt and Vissers, 1989) and the delamination model (e.g., Seber et al., 1996a), this would require the removed material to be replaced by asthenospheric material. This replacement would correspond to a flow that is directed radially inwards. An idealized convective-removal model would in fact imply that such a flow would be acting radially inwards from all directions. One should not expect to observe a radial flow from all directions though, since any asymmetry or heterogeneity would easily lead to an asymmetric flow, more like that to be expected in a delamination model. However, a radial flow would necessarily exist somewhere, to replace the material that has been recycled into the mantle. This flow would produce anisotropic fast directions that are oriented radially. Fig. 5 shows however, that the flow is oriented more or less tangentially to the Alboran Sea region. The required radial flow is thus not observed. This suggests that convective-removal and delamination models are unlikely to explain the anisotropy observations. On the other hand, subduction to the Northwest, as proposed by Zeck (1996), would require a rollback to the South to produce trench-parallel flow. Focal mechanisms of intermediate-depth seismicity are consistent with this, but hypocenters do not show a dip toward the North. In fact, they do not show a clear Benioff zone at all, but a line of seismicity dipping steeply to the South. For that same area, teleseismic and regional tomographic studies indicate a pronounced high-velocity anomaly located beneath the Alboran Sea (e.g. Blanco and Spakman, 1993; Calvert et al., 2000b; Seber et al., 1996a). Calvert et al. (2000b) produced a tomographic model that showed a robust high-velocity anomaly beneath the west Alboran Sea and west and central Betics between 100 and 150 km. Assuming that these positive velocity anomalies indicate a region of cooler mantle, the most likely interpretation is that it indicates the presence of lithospheric mantle in view of the coherent continuation of the anomaly at depth. The positive anomaly extends from lithospheric depths beneath the Strait of Gibraltar and southern Spain to depths of about 350–400 km

beneath the Alboran Sea, and it is interpreted as a lithospheric body that has descended into the upper mantle. More recently, waveform studies (Bokelmann and Maufroy, 2007) have indicated dispersed body-wave arrivals propagating through the mantle under the Alboran Sea, that favor the presence of a subducted slab under the Alboran Sea, still containing a continuous low-velocity crustal layer. Wortel and Spakman (2000) also proposed a slab structure isolated in the mantle below the Betic-Alboran region at 200 km depth and that seems to be connected with deep seismicity at depths of about 640 km. Lonergan and White (1997) proposed that there was a subduction zone beneath the Alboran Sea that is now extinct. They suggested that the ancient subducting slab in the Western Mediterranean was split into two fragments, the eastern one of which has continued to roll back toward the south-east, generating the Tyrrhenian Sea and forming the present-day Calabrian arc. The other slab fragment rolled back to the west, generating the Alboran Sea and the Betic-Rif orocline. Our SKS splitting observations, together with the previously published Pn results, show a spectacular rotation following the curvature of the roll back and of the mountain chain. If the SKS fast directions are to be explained by a rotation similar to that shown by the Pn observations, this would be explained most easily by a toroidal mantle flow under the subducting lithosphere that shows rollback toward the west. There is an interesting similarity with the Calabrian arc in Southern Italy, for which shear-wave splitting results have been presented by Civello and Margheriti (2004) and more recently by Baccheschi et al. (2007). The asthenospheric toroidal flow induced by the Tyrrhenian slab roll back is presently beneath Calabria (Civello and Margheriti, 2004; Baccheschi et al., 2007) but may have left some imprint in the mantle all along its Neogene travel path from southern France (Barruol et al., 2004) to Sicily (Lucente et al., 2006). Seismic anisotropy beneath the Betics is likely related to a similar phenomenon, and thus to the large-scale dynamics of ocean opening in the Southwestern Mediterranean.

6. Conclusions

We have studied upper mantle seismic anisotropy in Southern Spain and around the Gibraltar arc. Our observations suggest a consistent splitting direction parallel to the mountain belt in the Internal Betics, a more northerly direction at stations located further north in the transition with the Variscan Iberia, and a rotation of fast split directions toward NS azimuths around the Gibraltar arc.

The Eastern Betics anisotropy observations are well explained by a single layer of anisotropy with a fast anisotropic direction trending ENE, with smooth and small variations in space. In the transition region between the Variscan and the Betics, the anisotropy shows backazimuthal variations of splitting parameters. Models of two-layer anisotropy and lateral heterogeneous anisotropy have been tested, and a strong lateral change in anisotropy is likely for the transition region toward the Variscan Iberian Massif. Close to Gibraltar, fast directions are oriented close to N-S at CEUT and SFS and this suggests a gradual rotation around the arc. Combining Pn and SKS anisotropy, geological features and tomographic images allow us to discuss the various families of geodynamic models. Our SKS measurements are difficult to reconcile with geodynamic models based on delamination or convective removal. The observations instead favor models of subduction and rollback of the western Mediterranean slab.

Acknowledgements

We warmly thank Andreas Wüstefeld for his useful help in the use of SplitLab software, and Alain Vauchez, Daniel Stich, Carlos Garrido and Francisco Vidal for fruitful discussions. We also thank Martha Savage and an anonymous reviewer for their comments and corrections. SplitLab is available at <http://www.gm.univ-montp2.fr/splitting/> together with its user guide, the related publications and the SKS World splitting database. Figures are created using the GMT software of Wessel and Smith (1995). This study was possible thanks to the effort of collecting high-quality broadband seismic data of the IAG-UGR and ROA-UCM-Geofon networks. We received support through Spanish project CGL2005-04541-C03-01-BTE, European Commission project NEAREST (GoCE-03710) and Junta de Andalucía RNM104 and through the project Topo-Iberia CSD2006.

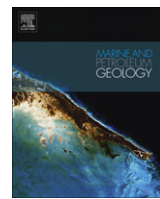
Appendix A. Supplementary data

Supplementary data associated with this article can be found, in the online version, at doi:[10.1016/j.epsl.2008.06.024](https://doi.org/10.1016/j.epsl.2008.06.024).

References

- Baccheschi, P., Margheriti, L., Steckler, M.S., 2007. Seismic anisotropy reveals focused mantle flow around the Calabrian slab (Southern Italy). *Geophys. Res. Lett.* 34, L05302. doi:[10.1029/2006GL028999](https://doi.org/10.1029/2006GL028999).
- Balanyá, J.C., García-Dueñas, V., 1988. El Cabalgamiento cortical de Gibraltar y la tectónica de Béticas y Rif. presentado en II Congreso Geológico de España. Simposium sobre Cinturones Orogénicos.
- Barruol, G., Mainprice, D., 1993. A quantitative evaluation of the contribution of crustal rocks to the shear wave splitting of teleseismic SKS waves. *Phys. Earth Planet. Inter.* 78 (3–4), 281–300. doi:[10.1016/0031-9201\(93\)90161-2](https://doi.org/10.1016/0031-9201(93)90161-2).
- Barruol, G., Silver, P.G., Vauchez, A., 1997. Seismic anisotropy in the eastern US: deep structure of a complex continental plate. *J. Geophys. Res.* 102 (B4), 8329–8348.
- Barruol, G., Deschamps, A., Coutant, O., 2004. Mapping Upper mantle anisotropy beneath SE France by SKS splitting indicates a Neogene asthenospheric flow induced by the Apenninic slab rollback and deflected by the deep Alpine roots. *Tectonophysics* 394, 125–138. doi:[10.1016/j.tecto.2004.08.002](https://doi.org/10.1016/j.tecto.2004.08.002).
- Ben Ismaïl, W., Mainprice, D., 1998. An olivine fabric database: an overview of upper mantle fabrics and seismic anisotropy. *Tectonophysics* 296 (1–2), 145–157.
- Blanco, M.J., Spakman, W., 1993. The P-wave velocity structure of the mantle below the Iberian Peninsula: evidence for subducted lithosphere below southern Spain. *Tectonophysics* 221, 13–34.
- Bokelmann, G.H.R., Maufroy, E., 2007. Mantle structure under Gibraltar constrained by dispersion of body waves. *Geophys. Res. Lett.* 34, L22305. doi:[10.1029/2007GL030964](https://doi.org/10.1029/2007GL030964).
- Bormann, P., Grünthal, G., Kind, R., Montag, H., 1996. Upper mantle anisotropy beneath Central Europe from SKS wave splitting: effects of absolute plate motion and lithosphere asthenosphere boundary topography? *J. Geodynamics* 22 (1–2), 11–32.
- Bowman, J.R., Ando, M., 1987. Shear-wave splitting in the upper-mantle wedge above the Tonga subduction zone. *Geophys. J. R. Astron. Soc.* 88, 25–41.
- Buñor, E., Coca, P., Urdías, A., Lasa, C., 1997. Source mechanism of intermediate and deep earthquakes in southern Spain. *J. Seismol.* 1, 113–130.
- Buland, R., Chapman, C.H., 1983. The computation of seismic travel times. *Bull. Seismol. Soc. Am.* 73, 1,271–1,302.
- Calvert, A., Sandvol, E., Seber, D., Barazangi, M., Roecker, S., Mourabit, T., Vidal, F., Alguacil, G., Jabour, N., 2000a. Geodynamic evolution of the lithosphere and upper-mantle beneath the Alboran Region of the western Mediterranean—constraints from travel-time tomography. *J. Geophys. Res.* 105, 10871–10898.
- Calvert, A., Sandvol, E., Seber, D., Barazangi, M., Vidal, F., Alguacil, G., Jabour, N., 2000b. Propagation of regional seismic phases (Lg and Sm) and Pn velocity structure along the Africa–Iberia plate boundary zone: tectonic implications. *Geophys. J. Int.* 142, 384–408.
- Civello, S., Margheriti, L., 2004. Toroidal mantle flow around the Calabrian slab (Italy) from SKS splitting. *Geophys. Res. Lett.* 31, L10601. doi:[10.1029/2004GL019607](https://doi.org/10.1029/2004GL019607).
- Comas, M.C., Platt, J.P., Soto, J.I., Watts, A.B., 1999. The origin and tectonic history of the Alboran Basin: insights from Leg 161 results. In: Zahn, R., Comas, M.C., Klaus, A. (Eds.), Proc. ODP, Sci. Results. Ocean Drilling Program, College Station, TX, pp. 555–579.
- De Larouzière, F.D., Bolze, J., Bordet, P., Hernández, J., Montenat, C., Ott d'Estevou, P., 1988. The Betic segment of the lithospheric Trans-Alboran shear zone during the Late Miocene. *Tectonophysics* 152, 41–52.
- Dewey, J.F., Helman, M.L., Turco, E., Hutton, D.H.W., Knott, S.D., 1989. Kinematics of the western Mediterranean, in: Conference on Alpine tectonics. In: Coward, M.P., Dietrich, D., Park, R.G. (Eds.), Geological Society of London Special Publications, London, pp. 265–283.
- Díaz, J., Gallart, J., Hirn, A., Paulissen, H., 1998. Anisotropy beneath the Iberian Peninsula: the contribution of the ILIHA-NARS broad-band experiment. *Pure Appl. Geophys.* 151, 395–405.
- Duggen, S., Hoernle, K., Van den Bogaard, P., Garbe-Schonberg, D., 2005. Post-collisional transition from subduction- to intraplate-type magmatism in the westernmost Mediterranean: evidence for continental-edge delamination of subcontinental lithosphere. *J. Petrol.* 46, 1155–1201.
- Faccenna, C., Piromallo, C., Crespo-Blanc, A., Jolivet, L., Rossetti, F., 2004. Lateral slab deformation and the origin of the western Mediterranean arcs. *Tectonics* 23, TC1012. doi:[10.1029/2002TC001488](https://doi.org/10.1029/2002TC001488).
- Fernández-Ibáñez, F., Soto, J.I., Zoback, M.D., Morales, J., 2007. Present-day stress field in the Gibraltar Arc (western Mediterranean). *J. Geophys. Res.* 112, B08404. doi:[10.1029/2006JB004683](https://doi.org/10.1029/2006JB004683).
- Fontaine, F.R., Barruol, G., Tommasi, A., Bokelmann, G.H.R., 2007. Upper-mantle flow beneath French Polynesia from shear wave splitting. *Geophys. J. Int.* 223. doi:[10.1111/j.1365-246X.2007.03475.x](https://doi.org/10.1111/j.1365-246X.2007.03475.x).
- Fouch, M.J., Fischer, K.M., Parmentier, E.M., Wysession, M.E., Clarke, T.J., 2000. Shear wave splitting, continental keels, and patterns of mantle flow. *J. Geophys. Res.* 105 (B3), 6255–6275.
- Galindo-Zaldívar, J., Jabaloy, A., González-Lodeiro, F., Aldaya, F., 1997. Crustal structure of the central sector of the Betic Cordillera (SE Spain). *Tectonics* 16, 18–37.
- García-Dueñas, V., 1969. Les unités allochtones de la zone Subbétique, dans la transversale de Grenade (Cordillères Bétiques, Espagne). *Rev. Geogr. Phys. Geol. Dyn.* 2, 211–222.
- García-Hernández, M., López-Garrido, A.C., Rivas, P., Sanz de Galdeano, C., Vera, J.A., 1980. Mesozoic paleogeographic evolution of the External Zones of the Betic Cordillera. *Geol. Mijnb.* 59, 155–168.
- Godfrey, N.J., Christensen, N.I., Okaya, D.A., 2000. Anisotropy of schists: contribution of crustal anisotropy to active source seismic experiments and shear wave splitting observations. *J. Geophys. Res.* 105, 27991–28007.
- Gripp, A.E., Gordon, R.G., 2002. Young tracks of hotspots and current plate velocities. *Geophys. J. Int.* 150, 321–361.
- Gutscher, M.A., Malod, J., Rehault, J.P., Contrucci, I., Klingelhofer, F., Mendes, V.L., Spakman, W., 2002. Evidence for active subduction beneath Gibraltar. *Geology* 30, 1071–1074.
- Jung, H., Karato, S., 2001. Water-induced fabric transitions in olivine. *Science* 293, 1460–1463. doi:[10.1126/science.1062235](https://doi.org/10.1126/science.1062235).
- Kaminski, E., Ribe, N.M., 2002. Timescales for the evolution of seismic anisotropy in mantle flow. *Geochem. Geophys. Geosystem* 3, 1051. doi:[10.1029/2001GC000222](https://doi.org/10.1029/2001GC000222).
- Kennett, B.L.N., 1995. Seismic traveltimes table. In: Ahrens, T.J. (Ed.), Global Earth Physics. A Handbook of Physical Constants. AGU Ref. Shelf. AGU, Washington, DC, pp. 126–143.
- Kennett, B.L.N., Engdahl, E.R., 1991. Travel times for global earthquake location and phase identification. *Geophys. J. Int.* 105, 429–465.
- Lonergan, L., White, N., 1997. Origin of the Betic-Rif mountain belt. *Tectonics* 16, 504–522.
- Lucente, F.P., Margheriti, L., Piromallo, C., Barruol, G., 2006. Seismic anisotropy reveals the long route of the slab through the western-central Mediterranean mantle. *Earth Planet. Sci. Lett.* 241, 517–529. doi:[10.1016/j.epsl.2005.10.041](https://doi.org/10.1016/j.epsl.2005.10.041).
- Luján, M., Crespo-Blanc, A., Balanyá, J.C., 2006. The Flysch Trough thrust imbricate (Betic Cordillera): a key element of the Gibraltar Arc orogenic wedge. *Tectonics* 25, TC6001. doi:[10.1029/2005TC001910](https://doi.org/10.1029/2005TC001910).
- Mainprice, D., Silver, P.G., 1993. Interpretation of SKS-waves using samples from the subcontinental lithosphere. *Phys. Earth Planet. Inter.* 78, 257–280. doi:[10.1016/0031-9201\(93\)90160-B](https://doi.org/10.1016/0031-9201(93)90160-B).
- Mainprice, D., Barruol, G., Ben Ismail, W., 2000. The seismic anisotropy of the Earth's mantle: from single crystal to polycrystal. In: Karato, S.I. (Ed.), Earth's Deep Interior: Mineral Physics and Tomography from the Atomic to the Global Scale.. Geodyn. Ser. AGU, Washington, D.C., pp. 237–264.
- Mainprice, D., Tommasi, A., Couvy, H., Cordier, P., Frost, D.J., 2005. Pressure sensitivity of olivine slip systems: implications for the interpretation of seismic anisotropy of the Earth's upper mantle. *Nature* 433, 731–733.

- Marson-Pidgeon, K., Savage, M., 2004. Shear-wave splitting variations across an array in the southern North Island, New Zealand. *Geophys. Res. Lett.* 31, 21602. doi:10.1029/2004GL021190.
- Mele, G., Rovelli, A., Seber, D., Hearn, T., Barazangi, M., 1998. Compressional velocity structure and anisotropy in the uppermost mantle beneath Italy and surrounding regions. *J. Geophys. Res.* 103 (B6). doi:10.1029/98JB00596.
- Morales, J., Serrano, I., Jabajoy, A., Galindo-Zaldívar, J., Zhao, D., Torcal, F., Vidal, F., González Lodeiro, F., 1999. Active continental subduction beneath the Betic Cordillera and the Alborán Sea. *Geology* 27, 735–738.
- Nicolas, A., Christensen, N.I., 1987. Formation of anisotropy in upper mantle peridotites—A review. In: Fuchs, K., Froideveaux, C. (Eds.), *Composition Structure and Dynamics of the Lithosphere Asthenosphere System*. AGU, Washington D.C., pp. 111–123.
- Ott D'Estevou, P., Montenat, C., 1985. Evolution structurale de la zone bétique orientale (Espagne) du Tortonian à l'Holocene. *C. R. Acad. Sci. Paris* 300, 363–368.
- Pera, E., Mainprice, D., Burlini, L., 2003. Petrophysical properties of the upper mantle beneath the Torre Alfina area (Northern Apennines, Central Italy). *Tectonophysics* 370, 11–30.
- Platt, J.P., Vissers, R.L.M., 1989. Extensional collapse of thickened continental lithosphere: a working hypothesis for the Alboran Sea and Gibraltar Arc. *Geology* 17, 540–543.
- Platt, J.P., Soto, J.I., Comas, M.C., Leg 161 Shipboard Scientific Party, 1996. Decompression and high-temperature-low-pressure metamorphism in the exhumed floor of an extensional basin, Alboran Sea, western Mediterranean. *Geology* 24 (5), 447–450.
- Platt, J.P., Soto, J.I., Whitehouse, M.J., Hurford, A.J., Kelley, S.P., 1998. Thermal evolution, rate of exhumation, and tectonic significance of metamorphic rocks from the floor of the Alboran extensional basin, western Mediterranean. *Tectonics* 17, 671–689.
- Platt, J.P., Whitehouse, M.J., Kelley, S.P., Carter, A., Hollick, L., 2003. Simultaneous extensional exhumation across the Alborán Basin: implications for the causes of late orogenic extension. *Geology* 31, 251–254.
- Rosenbaum, G., Lister, G.S., 2004. Neogene and Quaternary rollback evolution of the Tyrrhenian Sea, the Apennines and the Sicilian Maghrebides. *Tectonics* 23, TC1013. doi:10.1029/2003TC001518.
- Royden, L.H., 1993. Evolution of retreating subduction boundaries formed during continental collision. *Tectonics* 12, 629–638.
- Russo, R., Silver, P., 1994. Trench-parallel flow beneath the Nazca Plate from seismic anisotropy. *Science* 263, 1105–1111.
- Savage, M.K., 1999. Seismic anisotropy and mantle deformation: what have we learned from shear wave splitting? *Rev. Geophys.* 37, 69–106.
- Schmid, C., Van der Lee, S., Giardini, D., 2004. Delay times and shear wave splitting in the Mediterranean region. *Geophys. J. Int.* 159, 275–290.
- Seber, D., Barazangi, M., Ibenbrahim, A., Demnati, A., 1996a. Geophysical evidence for lithospheric delamination beneath the Alboran Sea and Rif-Betics mountains. *Nature* 379, 785–790.
- Serrano, I., Hearn, T.M., Morales, J., Torcal, F., 2005. Seismic anisotropy and velocity structure beneath the southern half of the Iberian peninsula. *Phys. Earth Planet. Inter.* 150 (4), 317–330.
- Sieminski, A., Liu, Q., Trampert, J., Tromp, J., 2007. Finite-frequency sensitivity of body waves to anisotropy based upon adjoint methods. *Geophys. J. Int.* 171, 368–389. doi:10.1111/j.1363-246X.2007.03528.x.
- Silver, P.G., Chan, W.W., 1988. Implications for continental structure and evolution from seismic anisotropy. *Nature* 335, 34–39.
- Silver, P.G., Chan, W.W., 1991. Shear wave splitting and subcontinental mantle deformation. *J. Geophys. Res.* 96, 16429–16454.
- Silver, P.G., Savage, M., 1994. The interpretation of shear-wave splitting parameters in the presence of two anisotropic layers. *Geophys. J. Int.* 119, 949–963.
- Simancas, J.F., Carbonell, R., González Lodeiro, F., Pérez Estaún, A., Juñllin, C., Ayarza, P., Kashubin, A., Azor, A., Martínez Poyatos, D., Almodóvar, G.R., Pascual, E., Saez, R., Exposito, I., 2003. Crustal structure of the transpressional Variscan orogen of SW Iberia: SW Iberia deep seismic reflection profile (IBERSEIS). *Tectonics* 22 (6), 1062.
- Stich, D., Ammon, C.J., Morales, J., 2003. Moment tensor solutions for small and moderate earthquakes in the Ibero-Maghreb region. *J. Geophys. Res.* 108, 2148. doi:10.1029/2002JB002057.
- Stich, D., Mancilla, F., Morales, J., 2005. Crust–mantle coupling in the Gulf of Cadiz (SW-Iberia). *Geophys. Res. Lett.* 2, L13306. doi:10.1029/2005GL023098.
- Stich, D., Serpelloni, E., Mancilla, F., Morales, J., 2006. Kinematics of the Iberia-Maghreb plate contact from seismic moment tensors and GPS observations. *Tectonophysics* 426, 295–317.
- Turner, S.P., Platt, J.P., George, R.M.M., Kelley, S.P., Pearson, D.G., Nowell, G.M., 1999. Magmatism associated with orogenic collapse of the Betic-Alboran Domain. *SE Spain*. *J. Petrol.* 40, 1011–1036.
- Vauchez, A., Nicolas, A., 1991. Mountain building: strike parallel motion and mantle anisotropy. *Tectonophysics* 185, 183–201.
- Vauchez, A., Garrido, C., 2001. Seismic properties of an asthenosperherized lithospheric mantle: constraints from lattice preferred orientations in peridotite from the Ronda Massif. *Earth Planet. Sci. Lett.* 192, 245–259.
- Vinnik, L.P., Makeyeva, L.I., Milev, A., Usenko, A.Yu., 1992. Global patterns of azimuthal anisotropy and deformations in the continental mantle. *Geophys. J. Int.* 111, 433–447.
- Walker, K.T., Bokelmann, G.H.R., Klemperer, S.L., Bock, G., 2005. Shear-wave splitting around the Eifel hotspot: evidence for a mantle upwelling. *Geophys. J. Int.* 163, 962–980.
- Walker, K.T., Bokelmann, G.H.R., Klemperer, S.L., Bock, G., the Eifel plume team, 2007. Seismic anisotropy in the asthenosphere beneath the Eifel region. In: Ritter, J.R.R., Christensen, U.R. (Eds.), *Mantle plumes – a multidisciplinary approach*. Springer-Verlag, VIII, pp. 439–464.
- Wessel, P., Smith, H.F., 1995. New version of the Generic Mapping Tools released. *EOS, Trans. Am. Geophys. Un.* 76, 329.
- Wortel, M.J.R., Spakman, W., 2000. Subduction and slab detachment in the Mediterranean-Carpathian region. *Science* 290, 1910–1917.
- Wüstefeld, A., Bokelmann, G.H.R., 2007. Null detection in shear-wave splitting measurements. *Bull. Seismol. Soc. Am.* 97 (4), 1204–1211.
- Wüstefeld, A., Bokelmann, G.H.R., Zaroli, C., Barruol, G., 2008. SplitLab: a shear-wave splitting environment in Matlab. *Comput. Geosci.* doi:10.1016/j.cageo.2007.1008.1002.
- Zeck, H.P., 1996. Betic-Rif orogeny: subduction of Mesozoic Tethys lithosphere under eastward drifting Iberia, slab detachment shortly before 22 Ma, and subsequent uplift and extensional tectonics. *Tectonophysics* 254, 1–16.
- Zeck, H.P., Kristensen, A.B., Williams, I.S., 1998. Post-collisional volcanism in a sinking slab setting-crustal anatexis origin of pyroxene-andesite magma, Caldear Volcanic Group, Neogene Alborán volcanic Province, southeastern Spain. *Lithos* 45, 499–522.



Marine and Petroleum Geology

journal homepage: www.elsevier.com/locate/marpetgeo

Tectonic shortening and gravitational spreading in the Gulf of Cadiz accretionary wedge: Observations from multi-beam bathymetry and seismic profiling

Marc-André Gutscher^{a,b,*}, Stephane Dominguez^c, Graham K. Westbrook^d, Pascal Gente^{a,b}, Nathalie Babonneau^{a,b}, Thierry Mulder^e, Eliane Gonthier^e, Raphael Bartolome^f, Joaquim Luis^g, Filipe Rosas^h, Pedro Terrinhaⁱ, The Delila and Delsis Scientific Teams^{1,2,3,4,5}

^a Université Européenne de Bretagne, France^b Université de Brest, CNRS, UMR 6538 Domaines Océaniques, Institut Universitaire Européen de la Mer, Place Nicolas Copernic, 29280 Plouzane, France^c GM, UMR5243, University of Montpellier, France^d University of Birmingham, United Kingdom^e EPOC, UMR5805, University of Bordeaux, France^f CMIMA, Barcelona, Spain^g University of Algarve, Portugal^h University of Lisbon, Portugalⁱ INETI, Department of Marine Geology, Lisbon, Portugal

ARTICLE INFO

Article history:

Received 20 October 2006

Received in revised form 18 September 2007

Accepted 23 November 2007

Available online xxx

Keywords:

Iberia

Morocco

Accretionary wedge

Decollement

Gravitational spreading

ABSTRACT

The Gulf of Cadiz lies astride the complex plate boundary between Africa and Eurasia west of the Betic-Rif mountain belt. We report on the results of recent bathymetric swathmapping and multi-channel seismic surveys carried out here. The seafloor is marked by contrasting morphological provinces, spanning the SW Iberian and NW Moroccan continental margins, abyssal plains and an elongate, arcuate, accretionary wedge. A wide variety of tectonic and gravitational processes appear to have shaped these structures. Active compressional deformation of the wedge is suggesting by folding and thrusting of the frontal sedimentary layers as well as basal duplexing in deeper internal units. There is evidence for simultaneous gravitational spreading occurring upslope. The very shallow mean surface and basal slopes of the accretionary wedge (1° each) indicate a very weak decollement layer, geometrically similar to the Mediterranean Ridge accretionary complex. Locally steep slopes (up to 10°) indicate strongly focused, active deformation and potential gravitational instabilities. The unusual surface morphology of the upper accretionary wedge includes "raft-tectonics" type fissures and abundant sub-circular depressions. Dissolution and/or diapiric processes are proposed to be involved in the formation of these depressions.

© 2008 Elsevier Ltd. All rights reserved.

1. Introduction

The Gulf of Cadiz lies off the coasts of Southwest Iberia and Northwest Morocco at the eastern edge of the so-called Azores-Gibraltar transform and west of the Betic-Rif mountain belt (Fig. 1). Here the plate boundary between Africa and Eurasia is complex, marked by a broad region of deformation spanning about 200 km in

a north-south direction (Sartori et al., 1994; Tortella et al., 1997; Jimenez-Munt et al., 2001). Tectonic models proposed for the Gibraltar – Gulf of Cadiz region can be divided into two main groups; those invoking delamination of continental lithosphere beneath the Betic-Rif Alboran Sea region (Platt and Vissers, 1989; Calvert et al., 2000), and those favoring subduction of oceanic lithosphere, with associated roll-back (Lonergan and White, 1997; Gutscher et al., 2002; Duggen et al., 2004). Available tomographic data show the presence of an east-dipping slab of cold, dense lithosphere extending continuously from the Atlantic domain of the Gulf of Cadiz to the 660 km discontinuity beneath the Alboran Sea. This, together with marine seismic studies that showed eastward dipping crust was interpreted to indicate active east-dipping subduction beneath Gibraltar (Gutscher et al., 2002). GPS data indicate an independent west-moving tectonic block in the Betic-Rif Alboran region, which has been alternatively interpreted as being related to subduction roll-back (Fernandes et al., 2007) or as roll-back linked to delamination (Fadil et al., 2006).

* Corresponding author. Université de Brest, CNRS, UMR 6538 Domaines Océaniques, Institut Universitaire Européen de la Mer, Place Nicolas Copernic, 29280 Plouzane, France. Tel.: +33 (0) 2 98 49 87 27; fax: +33 (0) 2 98 49 87 60.

E-mail address: gutscher@univ-brest.fr (M.-A. Gutscher).

¹ Joao Ferreira, Jorge Marques, Henrique Duarte, Vasco Valadares, University of Lisbon, Portugal.

² Francesca Camurri, University of Parma, Italy.

³ Emmanuelle Thiebot, University of Brest, France.

⁴ Jose Vicente, University of Lisbon, Portugal.

⁵ Caterina Basile, University of Bologna, Italy.

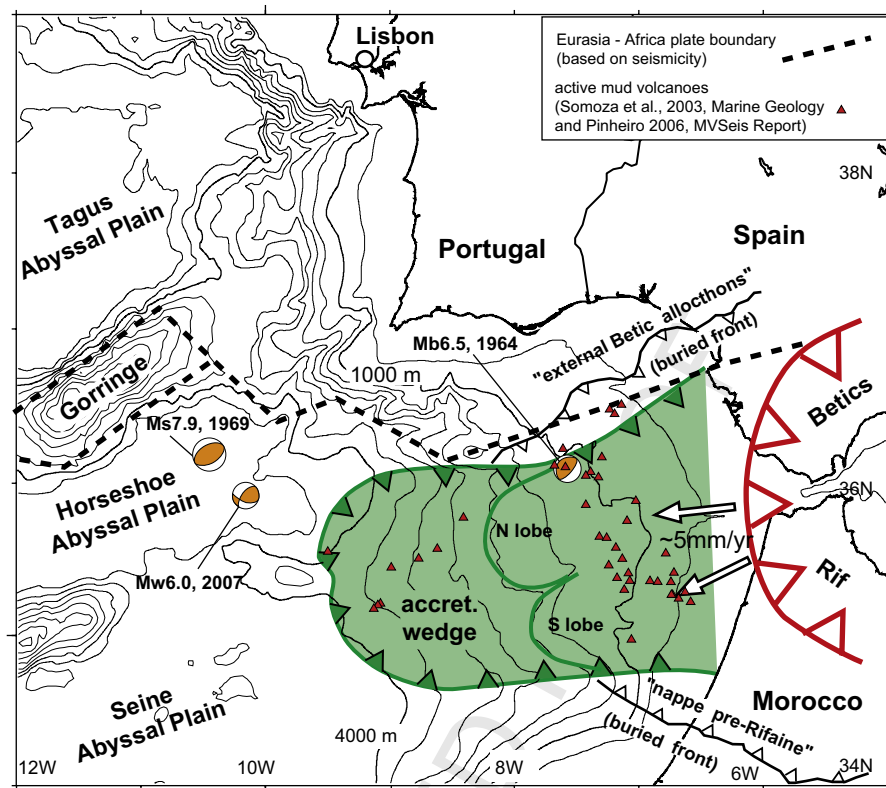


Fig. 1. General location map and geodynamic setting of the Gulf of Cadiz – Gibraltar region. Gor = Gorringe Bank, HAP = Horseshoe Abyssal Plain, SAP = Seine Abyssal Plain, GoC = Gulf of Cadiz, WAS = West Alboran Sea, EAS = East Alboran Sea. Note the abandoned Miocene deformation front on the SW Spanish and NW Moroccan platforms, and the more internal position of the current deformation front here.

The Gulf of Cadiz region is also the site of strong instrumental and historical earthquakes like the 1969 M7.9 Cape St. Vincent earthquake (Fukao, 1973), 1964 M6.5 Huelva earthquake and the 1755 M8.7 Great Lisbon earthquake (Martinez-Solares et al., 1979; Johnston, 1996), though the exact source of the latter remains a matter of debate (Zitellini et al., 2001; Terrinha et al., 2003; Gracia et al., 2003a,b; Gutscher, 2004). The search for the source region of the 1755 earthquake has, in large part, stimulated numerous marine geophysical surveys in the region. An accurate inventory of the active faults in the area can make a significant contribution to improving long-term seismic hazard assessments for the region. We report here on multi-beam bathymetric data acquired in 2004 Q2 during the Delila Cruise on the NRV Portuguese vessel Dom Carlos, as well as other available multi-beam bathymetric data in the central Gulf of Cadiz. We present an analysis of distinct morphological provinces observed on the seafloor, as well as the boundaries separating them. Marine seismic reflection data are also presented, in order to provide constraints on the geometry of the lithologic layers at depth.

2. Data

2.1. Delila bathymetric data

Bathymetric data were acquired during the Delila cruise by the NRV Dom Carlos using the Simrad EM120 multi-beam system, which has 191 beams. The system consists of 12 kHz projector array along the ship's keel and hydrophone array across the projector. The Simrad EM120 generates $1^\circ \times 2^\circ$ narrow beams at a regular aperture spacing. The swath width used during this cruise was 130° . The ping interval increased with water depth, for example about 15 s at 3000 m. The accuracy of the depth measurement is

reported as 0.5% of the depth. The raw data files obtained include the data record (bathymetry, intensity, beam position), the side-scan record (binary side scan image), nautical information, and correction parameters such as water and velocity structure. The average speed of the ship during the bathymetric survey was 8–10 knots. This allowed us to obtain bathymetric data with a horizontal spatial resolution of ~50–80 m (in 3000 m water depth). Track lines are displayed in the inset in Fig. 2. Significant overlap commonly exists between two adjacent profiles.

Four Sound Velocity Profiles (SVP) between sea-level and 2000 m depth were performed over the geographic region mapped (Fig. 2, inset). From 2000 to 4000 m depth, data from published oceanographic profiles were used for each region corrected for the season using data provided by the Portuguese Instituto Hidrográfico (IH), and these were extrapolated to depths below 4000 m where required.

The IH Team processed the multi-beam data using CARIS-HIPS software. In general, the processing sequence consisted of conversion of the raw data from native format to the application format, quality control on the raw data, automatic removal of outliers by customized filters/procedures, manual/semiautomatic removal of outliers, generation of cruise grids, integration with other data sets available.

The Delila bathymetric data (Fig. 2) reveal several distinct morphological provinces: the southeastern edge of the Horseshoe Abyssal Plain and the NW deformation front of a high rugosity sedimentary slope, Coral Patch ridge, an ESE trending basement high (rising 1000 m above the adjacent seafloor) which indents the high rugosity sedimentary slope, the eastern Seine abyssal plain with several fields of salt diapirs, an E–W escarpment, which forms the northern limit of the Rharb submarine valley and bounds the high rugosity sedimentary slope on the south, and finally, the

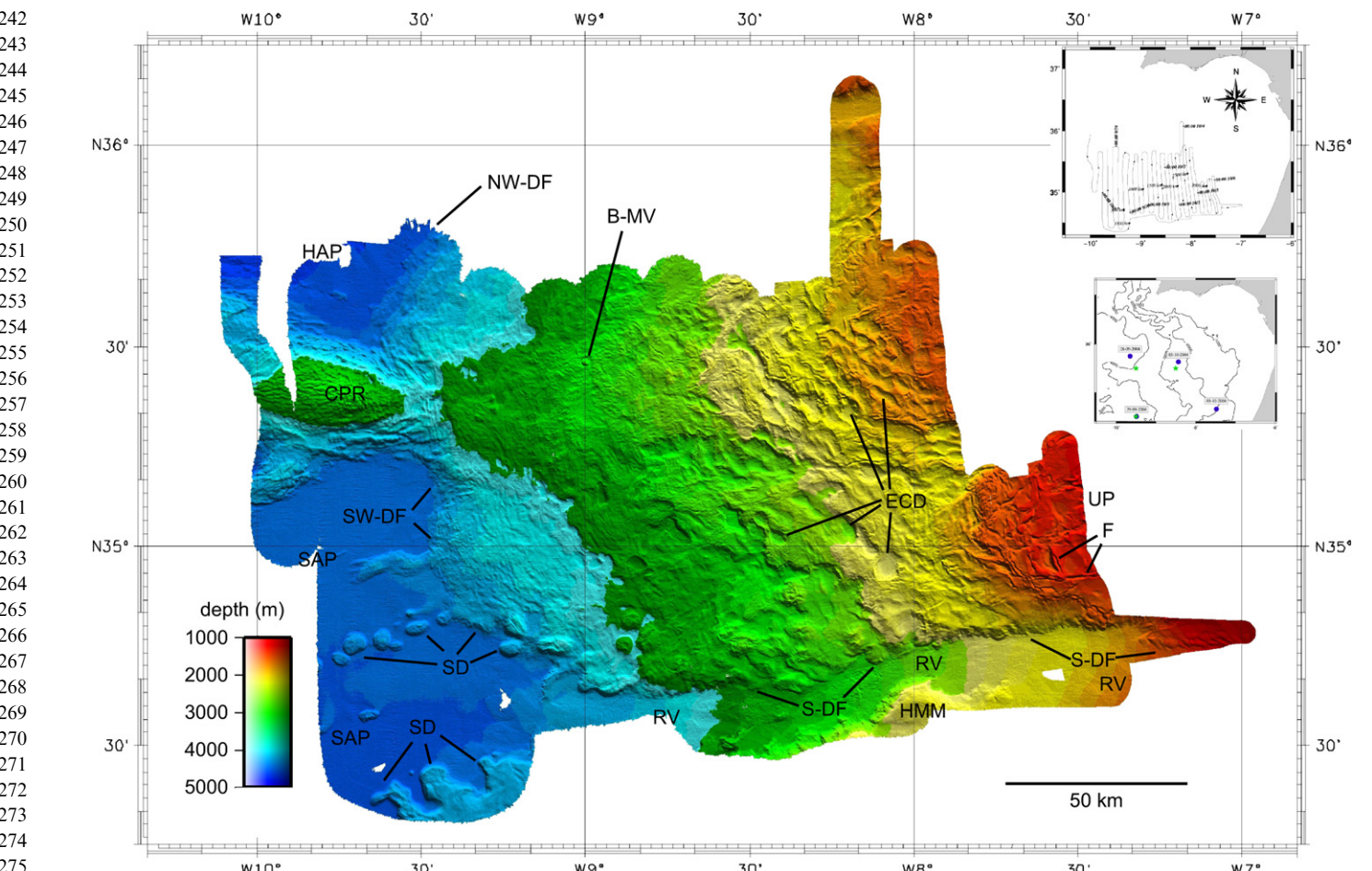


Fig. 2. Bathymetric map of multibeam (EM120) data acquired during Delila cruise (Sept./Oct. 2004). Inset shows tracklines and the position of SVP's (sonic velocity profiles) acquired. Geographic and morphologic features here and in Fig. 3: HAP = Horseshoe Abyssal Plain, SAP = Seine Abyssal Plain, SD = salt diapirs, CPR = Coral Patch Ridge, B-MV = Bonjardim mud volcano, NW-DF = northwestern deformation front, SW-DF = southwestern deformation front, S-DF = southern deformation front, ECD = elongate and circular depressions, RV = Rharb submarine valley, UP = Upper plateau, F = fissures.

internal portions of this latter domain, marked by abundant curvilinear ridges and troughs. This high rugosity sedimentary slope, with an undulating surface morphology is an accretionary wedge as imaged in seismic profiles (Gutscher et al., 2002). The lower portion of the accretionary wedge (4200–3500 m water depth) has a roughly arcuate boundary and is dominated by short wavelength (2–5 km) curvilinear ridges, arrayed sub-parallel to the deformation front. Overall the surface of the wedge consists of a hummocky slope, dipping gently to the west (about 0.8–1.2° to the west, northwest or southwest). The seafloor of the mid to upper wedge (3500–1000 m water depth) has a higher rugosity and is dominated by troughs and sub-circular to lobe-shaped, enclosed depressions that are commonly elongated parallel to the arcuate boundary of the accretionary wedge. The troughs and depressions reach several kilometers in width and have a typical vertical drop of 200 m. The uppermost portion of the accretionary wedge (<1000 m water depth) closest to the Moroccan coast shows a relatively smooth, plateau-like surface, broken up by elongate sub-linear fissures, consisting typically of two parallel ridges, separated by a deep, narrow trough.

2.2. Bathymetric compilation

The bathymetric compilation presented here (Fig. 3) includes data from several other cruises, notably the Cadisar, Cadisar2, TV-GIB and DelSis cruises (RV Suroit EM300 system), MatesPro cruise

(NRP Dom Carlos EM120 system) and the GAP cruise (RV Sonne EM120 system). The R/V Suroit data from the Cadisar (Mulder et al., 2003) and Cadisar2 (Mulder et al., 2006) cruises were processed with Caraïbes software (developed by Ifremer) and typically have a spatial resolution better than 30 m (in water depths < 2000 m). The MatesPro data (Terrinha et al., in press) were processed by the IH Team. The GAP bathymetric data (Kopf et al., 2003) in the SE portion of the Gulf of Cadiz were processed using Caraïbes software and integrated into this compilation to close the gap between the regions covered by the Cadisar and Delila data.

The compilation reveals the continuity of the morphological provinces documented by the Delila data, in the neighboring regions as well as other morphologically diverse provinces. In particular the northern and north-eastern portions of the accretionary wedge and the limits of the SW Iberian margin can be seen more clearly. These include, deeply incised canyons of the Algarve margin (off southern Portugal), and the sedimentary structures of the contourite levee formed by the Mediterranean Outflow Water as described in previous publications (Mulder et al., 2003, 2006). The compilation also shows a widespread region of sub-circular depressions, most strongly expressed in the depth interval 1400–3000 m and marked by ECD (=enclosed circular depressions) on Fig. 3. Most of these depressions are closed. Their shape and distribution suggest they are not simply elongate basins “trapped” between two anticlinal ridges, nor slump scars formed by submarine slides or normal faulting. Instead their morphology is reminiscent of a “karst” type

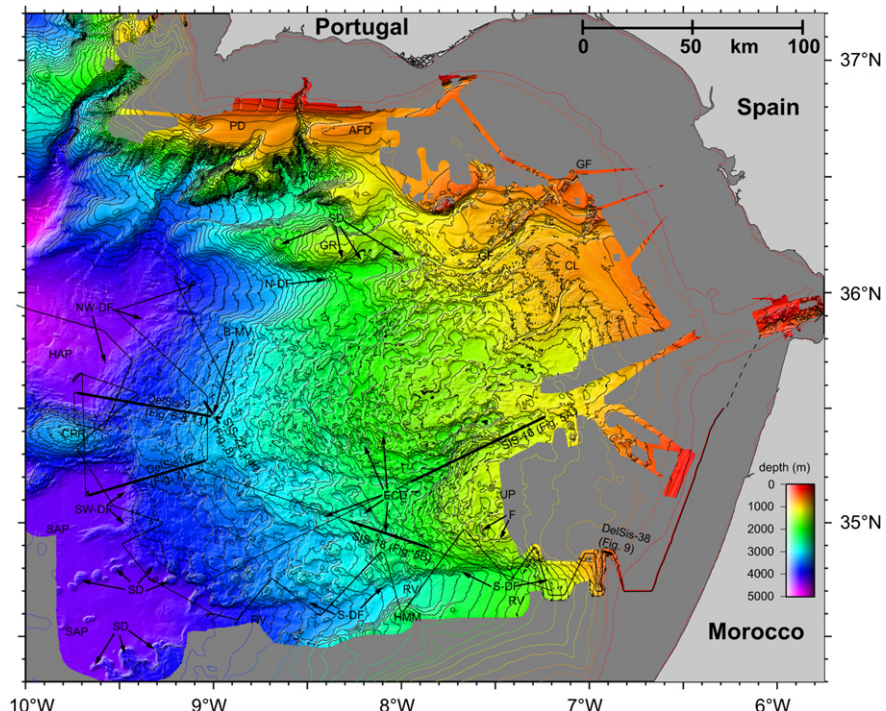


Fig. 3. Compilation of multibeam bathymetric data in the Gulf of Cadiz acquired during the following cruises: GAP (Kopf et al., 2003); Cadisar (Mulder et al., 2003); Cadisar2 (Mulder et al., 2006); MatesPro (Terrinha et al., in press); TV-GIB (Gutscher et al., 2006); Delila (this paper); Delsis (April 2005). In regions without multi-beam coverage colored contour lines are shown every 200 m from the GEBCO 1 min grid (IOC et al., 2003). Additional features (not listed in Caption to Fig. 2) include GR = Guadalquivir Ridge, PC = Portimao canyon, AFD = Albufeira – Faro Drift, CL = Contouritic levee, N-DF = northern deformation front, GF = Guadalquivir Fault, MV = mud volcanoes. The thin black lines indicate seismic reflection profiles discussed in the text. The thick lines are the portions shown in Figs. 5–11.

topography, i.e. depressions formed by some sort of mass removal process.

2.3. Structural interpretation of bathymetric data

A seafloor slope map (Fig. 4A), calculated from the bathymetric compilation, shows the distribution of the maximum and minimum slopes of the study area. The maximum slope provides an estimate of the mechanical properties of the sea-floor strata (e.g. coefficient of internal friction, which is related to slope stability). It also provides clues as to which portions of the seafloor are being shaped by active processes (tectonic, sedimentary, gravitational). The steepest slopes in the region ($10\text{--}15^\circ$) are found along the incised southern Portuguese canyons, bounding the basement highs in the deep abyssal domains, on the flanks of salt diapirs, and locally along the southern edge and some internal boundaries of the accretionary wedge. All slopes greater than $10\text{--}15^\circ$ can be considered to be potentially unstable, since they exceed the angle of internal friction of unconsolidated marine sediments and are thus exposed to active non-aggradation shaping processes (e.g. erosion). Indeed evidence of slide scars is found on both the northern and southern flanks of the Guadalquivir Ridge, an uplifted basement high (roughly 1000 m in height) just south of the Portuguese margin (Fig. 4A,B). Overall, the accretionary wedge is characterized by very gentle surface slopes ($<2^\circ$ in general). However, along its external and internal boundaries the seafloor can locally reach slopes of up to 10° , surprisingly steep for young, high porosity, unconsolidated sediments.

A structural interpretation (Fig. 4B) summarizes the morphological provinces described above. The internal portions of the accretionary wedge can be sub-divided into two a northern and southern lobe, with a N-S width of about 100 and 70 km, respectively. The lower boundaries of these lobes are defined roughly by the 2000 m depth contour and are marked by arcuate bands of high

slopes ($\sim 10^\circ$) in the slope gradient map (Fig. 4A). The southern lobe, (identified as the “upper plateau” in Figs. 2 and 3), is marked by elongate fissures, suggesting active gravitational spreading. Here a series of linear structures is observed, consisting of approximately 0.5 km wide narrow valleys bounded by 0.3 km wide ridges on both sides. These linear structures are at high angles to each other and connect to defining a mosaic fabric of polygons that resemble the patterns of mud-cracks or hydraulic fracturing. The shorter lineaments trend at a high angle to the slope of lobe surface and are parallel to the longest lineaments that are organized in an echelon geometry sub-parallel to the contour of the southern slope. These lineaments are intersected by E-W trending ones sub-parallel to the dip of the lobe surface. These lineaments are interpreted here as tensile fractures due to the stretching of the unconsolidated plastic cover of the accretionary wedge while it is sliding downslope. Similar patterns of “raft tectonics” fissures have been described on the Angola margin (Duval et al., 1992; Hudec and Jackson, 2002) or the Nile deep-sea cone (Gaullier et al., 2000).

2.4. Seismic data

Seismic data presented here, are of two types: 360-channel seismic data acquired by the RV Nadir in April 2001 during the SISMAR project (with 4.5 km long streamer and a 4805 cu in tuned airgun array) and 24-channel seismic data acquired by the RV Suroit in April 2005 during the Delsis cruise. Additional information on acquisition and processing of SISMAR MCS data are also available for profile SIS-4 further SW along the Moroccan continental margin (Contrucci et al., 2004), which was pre-stack depth migrated at the Geomar Seismic Processing Center, as were lines SIS-16 and SIS-22 (Thiebot and Gutscher, 2006).

The 24-channel seismic system consists of a 300 m long digital seismic streamer with a 12.5 m group spacing, towed roughly 200 m behind the ship. The acoustic source is provided by two GI

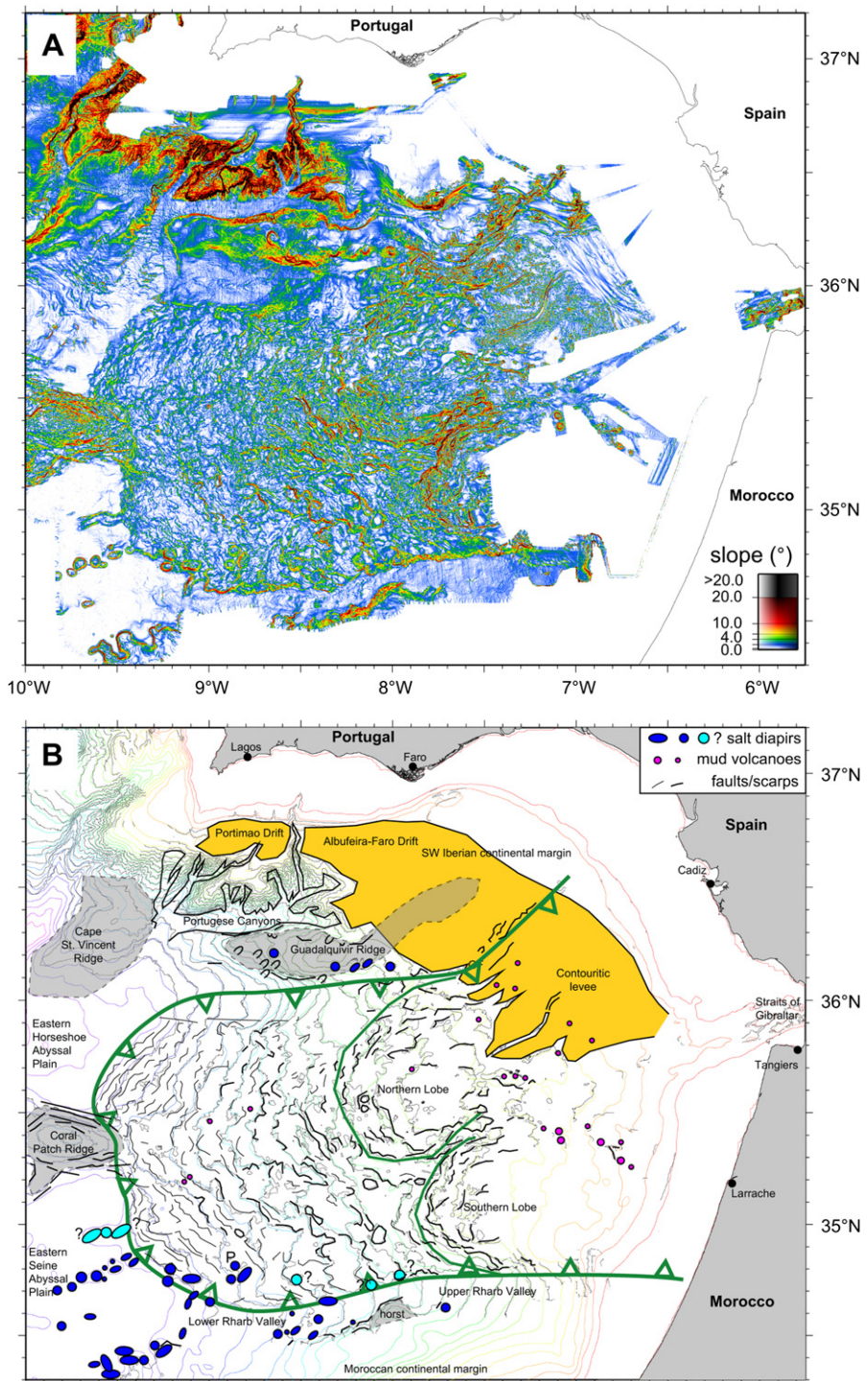


Fig. 4. A) Slope map of seafloor relief in the Gulf of Cadiz (from compilation of Fig. 3). Note the steepest slopes (10–15°) are observed locally in the following domains: the Portuguese canyons (e.g. Faro and Portimao), along the flanks of salt domes, along active thrust faults, along fissures in the arcuate upslope boundaries of the accretionary wedge. (B) Structural interpretation of the morphological domains in the Gulf of Cadiz. The deformation front of the west-vergent accretionary wedge is marked by thrust teeth. The black lines indicate lineaments observed on the slope map, which may be faults or scarps. Thick lines are 8–15° slopes, thin lines 2–8° slopes. Colored bathymetric contour lines are shown every 200 m from the GEBCO 1 min grid (IOC et al., 2003).

air-guns (105 and 45 cu in), fired every 10 s. Seismic processing included band-pass filtering, stacking and migration at water velocity (1500 m/s).

SISMAR profile SIS-16 images the internal structure of the southern lobe (Fig. 5A). A band of sub-horizontal to gently westward dipping reflectors can be observed underlying a small fore-arc basin (about 1–2 km thick). The steep scarp at the front of this lobe

coincides with an east dipping thrust, which appears to break through to the sea-floor. If this thrust soles out to the subhorizontal to slightly W dipping band of reflectivity, then the upper plateau/southern lobe is undergoing gravitational spreading above this detachment. At greater depth an east dipping thrust fault can be seen, which may sole out to the boundary between a more competent backstop further east, and underplated partially

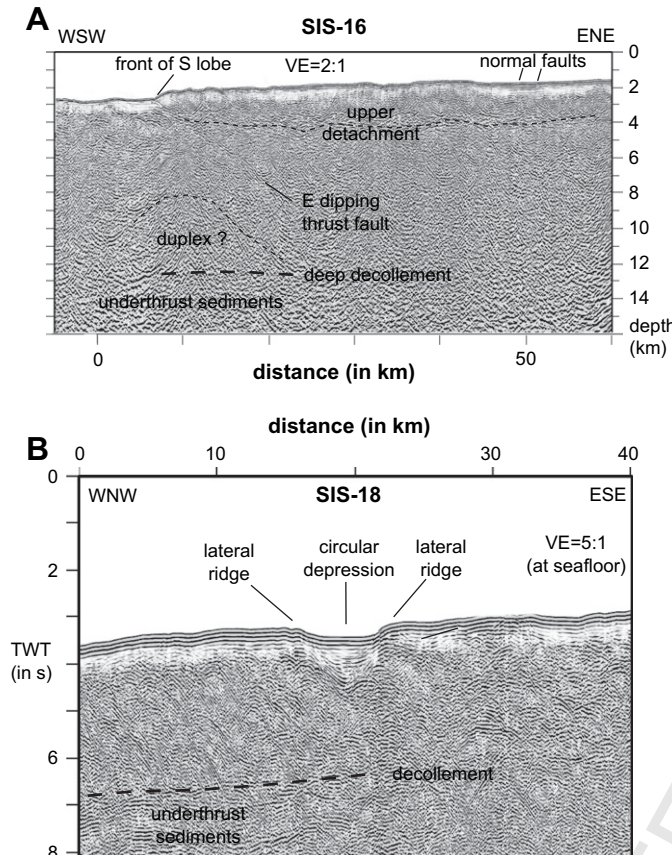


Fig. 5. (A)Upper portion of 360-channel seismic profile SIS-16 (pre-stack depth migrated section) showing a steep tectonic front and a region of sub-horizontal reflectivity. This front marks the boundary of the southern lobe which appears to be a gravitationally spreading unit above an extremely weak upper detachment. (B) Portion of 360-channel seismic profile SIS-18 (time migrated section) across a sub-circular depression, note the basin in cross-section shows evidence of subsidence and relative uplift of the ridge to the east, possibly due to the effects of diapirism.

consolidated sediments in the deepest portion of the accretionary wedge (Fig. 5A). This limit coincides with a change in the seismic velocity (Gutscher et al., 2002) as well as a lateral density change as obtained by gravity modeling (Thiebot and Gutscher, 2006). At the rear of the shallow basin of profile SIS-16, two normal faults are seen cutting through the uppermost sediments.

SISMAR profile SIS-18 crosses one of the sub-circular depressions in the central portion of the accretionary wedge (Fig. 5B). The depression shows a thicker than usual section of "transparent" drape sediments (750 mS TWT, rather than the 550 mS), and indicates a roughly symmetrical pattern of subsidence. The basin is surrounded by gentle outer ridges (like lips), which have steep internal scarps ($\geq 10^\circ$) and show some signs of folding (i.e. – on the NW ridge) (Fig. 5B). The uplift of the ridges and subsidence of the basin appear to be recent and linked by a common process.

DelSis lines 9 and 17 cross the deformation front and the outer part of the accretionary wedge, which is characterized by gentle surface slopes of $1\text{--}3^\circ$ (Figs. 3, 6, and 7). Line 9 crosses from the easternmost Horseshoe abyssal plain, across a fairly uniform portion of the wedge, as far as the Bonjardim mud volcano (Fig. 6). Line 17 starts just south of Coral Patch Ridge in the easternmost Seine abyssal plain and samples a somewhat steeper lower slope (about 3° slope), which seems to have been affected by the interaction of the accretionary wedge with the Coral Patch Ridge indenter (Fig. 7). Indeed, the top of basement, as imaged in line 17, seems to show a local high in the prolongation of the southern flank of Coral Patch Ridge, which uplifts and steepens the overlying

accretionary wedge, a process well known from analog modeling and seismic studies (Dominguez et al., 1998; Westbrook, 1982). A transparent sedimentary unit (with generally low seismic reflectivity), 200–300 m thick, lies above the recognisably deformed sediments of the upper part of the accretionary wedge. This layer shows gentle undulations suggestive of modest compressive and distributed deformation, but no thrust faults are imaged that clearly penetrate this section.

The upper part of the accretionary wedge is composed of units with no organised internal layering but with high reflectivity of a chaotic character. Beneath the abyssal plains (on both lines), the 200–300 m thick layer of "chaotic facies" sediment lies beneath the 300–600 m thick, surface sequence of low reflectivity, well stratified sediments (Figs. 6 and 7). The chaotic facies has been interpreted as a Tortonian "olistostrome" by numerous authors (Bonin et al., 1975; Sartori et al., 1994; Torelli et al., 1997; Medialdea et al., 2004). In the western part of the Gulf of Cadiz, Medialdea et al. (2004) consider that the allochthonous units of their central domain, equivalent to the lower part of the accretionary wedge, were formed between the late Miocene and the Present and so, here the chaotic facies may have an age of 5 Ma or younger. The primary origin of the chaotic facies as a submarine mass transport deposit is supported by observations on the seismic lines in the Seine abyssal plain of the thin distal member of this series of slides pinching out to the southwest. The eastward thickening of chaotic unit in the accretionary wedge is shown in the seismic sections to be a consequence of progressive imbrication by east-dipping ramp thrusts, which sole out to a decollement beneath this layer (Figs. 6 and 7). Further beneath the wedge, the upper parts of the sequence beneath the chaotic layer are thrust into duplexes, adding material to the base of the wedge and thickening it further. This interpretation is supported by the section from the more deeply penetrating seismic profile SIS-22 (shown in part in Fig. 8), which shows layered sequences above, as well as beneath, the active decollement, with the chaotic facies occupying only the upper half or less of the accretionary wedge in the vicinity of the Bonjardim mud volcano.

Thus, these new high-resolution seismic profiles clearly show that (1) the thick wedge of deformed sediments occupying the central Gulf of Cadiz, is not composed entirely of chaotic facies sediments, (2) the chaotic facies is a relatively thin (<300 m) unit within a continuous, undeformed stratigraphic sequence beneath the abyssal plains, (3) the chaotic facies is substantially thickened within the accretionary wedge through imbrication by thrust faults and possibly through internal deformation.

In the uppermost part of the southern lobe, extension with an E-W component is indicated by the presence of normal faults (Fig. 11). This may be the consequence of gravitational spreading of the southern lobe causing tension in the upper slope. Unfortunately, the multi-beam bathymetric coverage here is incomplete, and we do not have a clear image of the morphology created by gravitationally induced extension.

3. Discussion

3.1. Active processes and weak layers

A schematic cross-section (Fig. 10), based on the bathymetry and seismic profiles presented above illustrates the location of the different active processes shaping the accretionary wedge. Tectonic thickening occurs at the front through imbricate thrusting and internal shortening within and below the chaotic units. The undulations in the layer overlying the wedge appear to reflect this internal shortening. Basal duplexes are observed towards the front of the wedge, beneath the chaotic facies layer and absorb some shortening well. The deeper internal portions of the wedge show

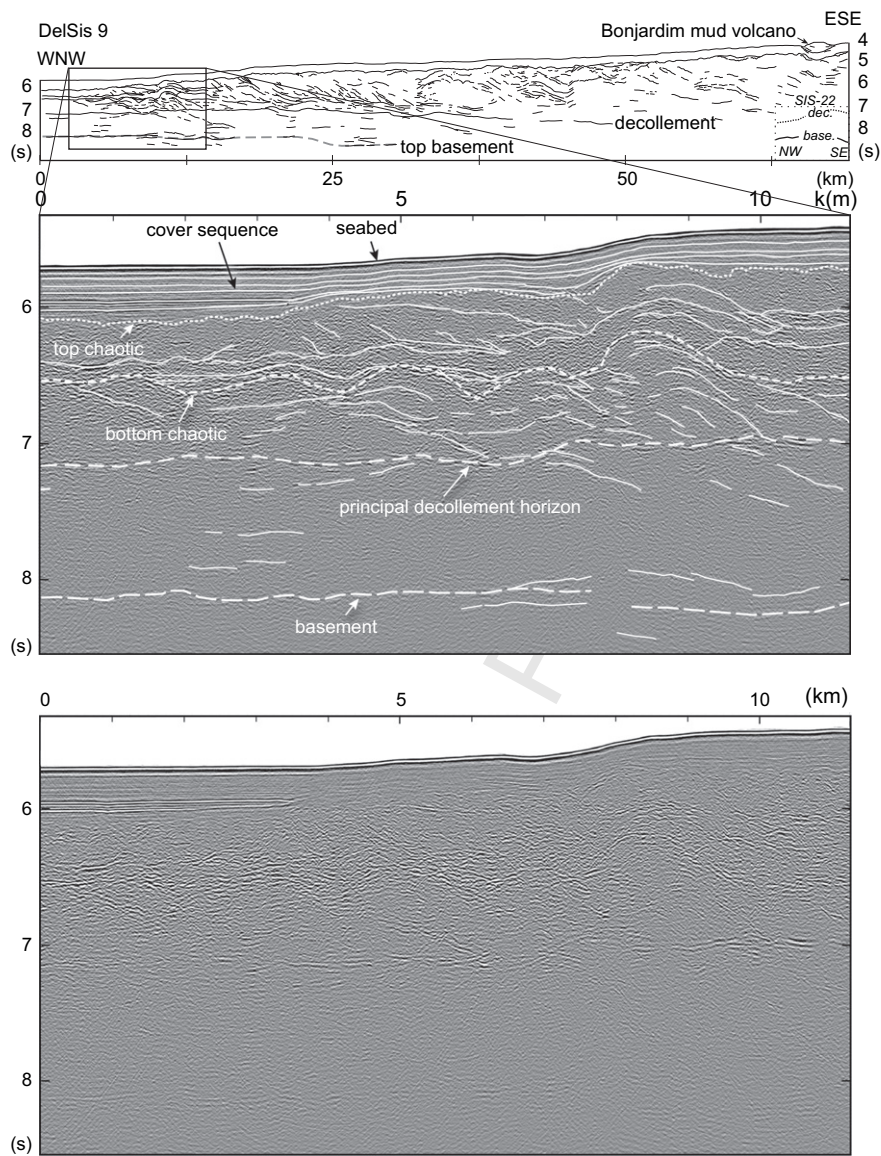


Fig. 6. Seismic section from Delsis Line 9. Top: Line drawing of seismic section, which was migrated with a velocity of 1500 m/s, showing the major reflectors and other reflectors illustrative of the structure. The position of the top of basement (oceanic crust), which is derived from nearby SISMAR lines in addition to this section, is shown as a dashed grey line. At the southeastern end of the line in the vicinity of the Bonjardim mud volcano, the positions of reflections from the principal decollement and the basement seen in SISMAR seismic section 22 (shown in Fig. 8), which crosses Delsis 9 at an angle of 47° at Bonjardim, are indicated by the thick dashed and solid lines, respectively. Middle: The part of the seismic section shown by the box in the line drawing. The interpretation, depicted in the line drawing, is shown in white. Vertical exaggeration at the seafloor is 2.5. Bottom: The part of the seismic section shown by the box in the line drawing, without interpretation.

abundant dipping reflectors, predominantly East dipping, including some fairly coherent bands of reflections at depth, suggesting this is not the same lithologic unit as the chaotic facies. The majority of the tectonic thickening within the internal wedge (2–12 km below the sea-floor) appears to occur through underplating of the sediment section below the frontal decollement, though this is not clearly imaged by our seismic data and the exact geometry remains speculative (Fig. 10). Indeed, mass balance considerations would require unreasonable amounts of shortening, to create the entire accretionary wedge, solely through accretion/thickening of the chaotic facies layer.

The deepest coherently bedded section of the wedge generally exhibits a ramp-flat geometry (labeled duplexes in Fig. 10) with strain concentrated at widely spaced ramp thrusts. By comparison the spacing of thrusts in the chaotic unit is much closer and it appears much more intensely deformed. Localized bedding present in the chaotic unit where it lies beneath the abyssal plain cannot be recognized when it occurs in the accretionary wedge.

This suggests that it forms a weak layer within the wedge, absorbing large amounts of strain. A weak layer appears to exist higher up, beneath the upper lobes of the accretionary wedge, and may represent a thin deformed layer of the chaotic unit. The sub-horizontal to gently west-dipping reflective layer beneath the upper wedge seems to serve as a basal detachment for gravity sliding towards the west within the upper lobes. Thus, the surface morphology and structures observed on the seismic profiles suggest the presence of multiple weak internal layers within the wedge.

3.2. Comparison with other accretionary wedges

The extremely low surface angle (1°) and shallow dip (1°) of the basal decollement for the Gulf of Cadiz accretionary wedge, result in a wedge taper of 2°, which is diagnostic of an extremely low effective friction along the base of the wedge (Westbrook et al., 1982; Davis et al., 1983; Westbrook and Smith, 1983; Lallemand et al., 1994). An examination of other accretionary wedges reveals

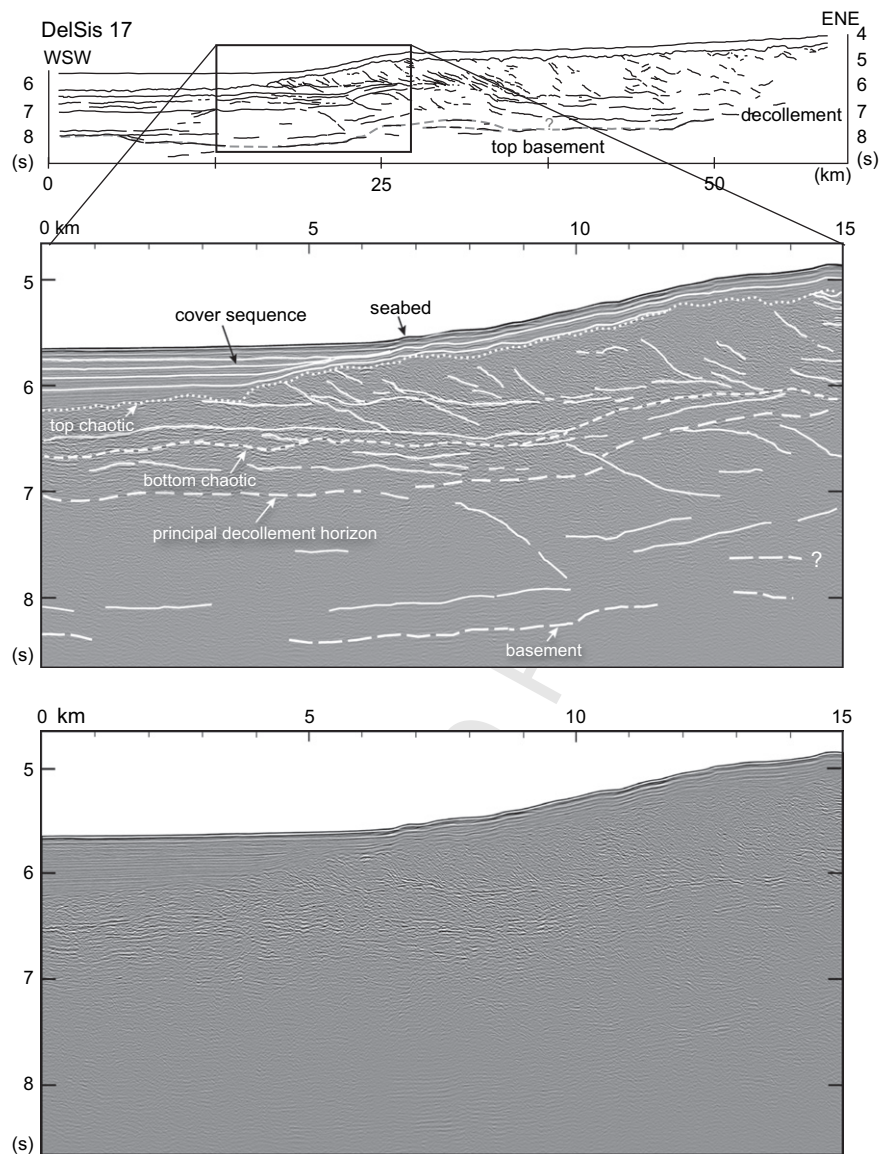


Fig. 7. Seismic section from DelSis Line 17. Top: Line drawing of seismic section, which was migrated with a velocity of 1500 m/s, showing the major reflectors and other reflectors illustrative of the structure. The position of the top of basement (oceanic crust), which is derived from nearby Sismar lines in addition to this section, is shown as a dashed grey line. Middle: The part of the seismic section shown by the box in the line drawing. The interpretation, depicted in the line drawing, is shown in white. Vertical exaggeration at the seafloor is 2.6. Bottom: The part of the seismic section shown by the box in the line drawing, without interpretation.

a handful that exhibit a similar geometry; Makran (Fruehn et al., 1997; Kopp et al., 2000), Hikurangi (Davey et al., 1986), Barbados Ridge (Westbrook et al., 1988), the Calabrian Prism (Cernobori et al., 1996) and the Mediterranean Ridge (Reston et al., 2002; Chamot-Rooke et al., 2005). These wedges are characterized by a very shallow surface slope ($<2^\circ$) and very shallow basal dip ($1\text{--}3^\circ$), resulting in similarly low wedge tapers.

The Mediterranean Ridge accretionary complex displays the most similar geometry (identical 1° surface slope and 1° basal dip), which has been attributed to the mechanical effects of a very weak decollement (Reston et al., 2002). For the Mediterranean Ridge there is a 1–2 km thick layer of Messinian evaporates (primarily gypsum, anhydrite and halite) observed outboard of the deformation front, which is tectonically thickened within the accretionary complex. The decollement layer is interpreted to pass beneath the evaporites, lying within overpressured marls and muds (Reston et al., 2002). These lithologic units can generate very high pore fluid pressures (close to lithostatic) and thus produce an extremely low basal friction (Davis et al., 1983).

3.3. Mud volcanoes

Mud volcanoes can form on passive margins that are affected by halokinesis and in thick rapidly deposited fan systems, such as that of the Niger delta (Kopf, 2002), but are most common in accretionary wedges, e.g. the Barbados Ridge (Westbrook and Smith, 1983; Brown and Westbrook, 1988; Faugeres et al., 1997; Deville et al., 2006) and the Mediterranean Ridge (Huguen et al., 2004; Chamot-Rooke et al., 2005). In accretionary wedges, the compression and tectonic burial of accreted and underthrust sediment and diagenetic processes, such as the smectite-illite transition, leads to the development of excess fluid pressure and subsequent dewaterring to the surface that mobilises mud from argillaceous units on its upward path.

Active mud volcanoes had been previously identified primarily across the upper (eastern) portion of the Cadiz accretionary wedge, with the deepest and westernmost mud volcano, Bonjardim, located at $9^\circ 30'W$, at 3100 m water depth (Pinheiro et al., 2003). From the investigation of features identified in Delila bathymetric

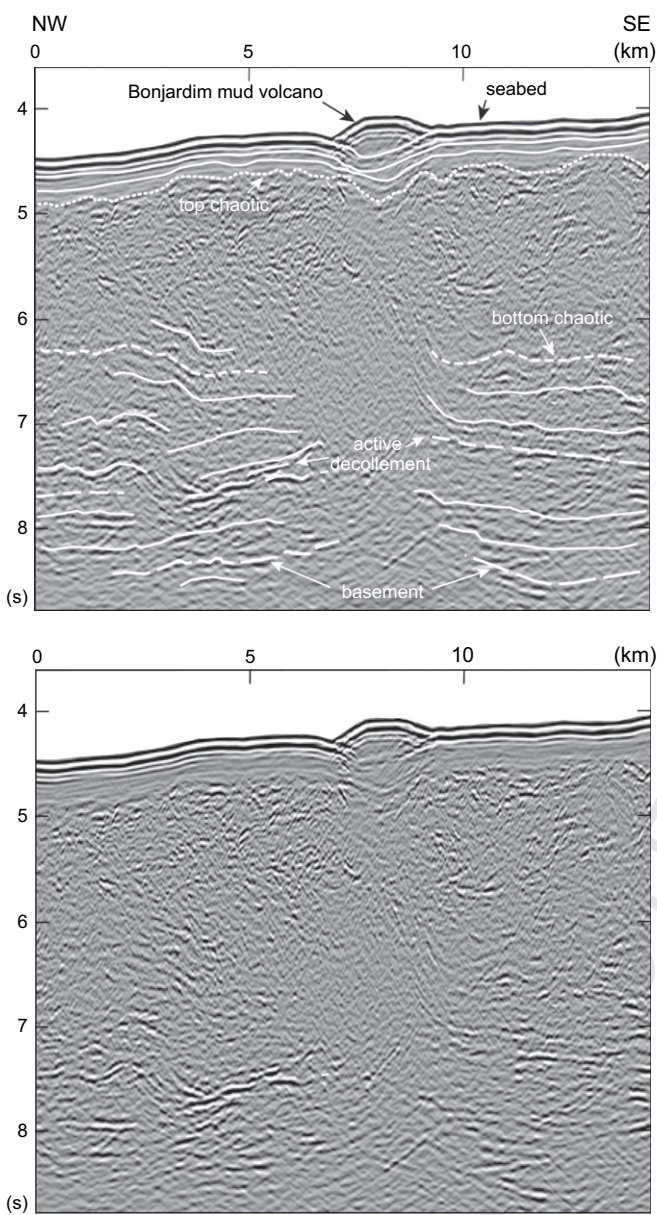


Fig. 8. Part of deeply penetrating seismic section through the Bonjardim mud volcano from SISMAR Line 22. The section is migrated. The section shows a layered sequence beneath structurally disrupted units, which include the chaotic unit. The base of the chaotic unit cannot be distinguished easily. The dashed line marking its base is the deepest estimate of the base of the unit. The strong reflector with reversed polarity is interpreted as the active decollement between the deformed sediments of the wedge above and the sequence of layered sediments beneath, which are under-compacted for their present depth beneath the wedge. The view in the section is predominantly down dip, and there is repetition of the units above the decollement caused by thrusting. The vertical offset of what appears to be the active decollement is likely to be across a lateral ramp. Vertical exaggeration at the seafloor is 3.25.

data and seabed acoustic reflectivity, the existence of four new mud volcanoes was confirmed during the TTR-15 cruise, further south (Semenovich, Soloviev, Carlos Teixeira), and further west, at the deformation front in 4300 m water depth (Porto) (Pinheiro et al., 2006).

The structure of Bonjardim mud volcano is shown by seismic sections SIS-22 (Fig. 8) and DelSis-9 (Fig. 11). Beneath the mud volcano, the structure of the wedge is seismically incoherent, but at its margins deep reflectors bend upward towards the mud volcano (Fig. 8). A reflector with reverse polarity, which is likely to be the

active decollement is located between the deformed sediments of the wedge above and the sequence of layered sediments beneath. At a regional scale, the decollement on profile SIS-22 in the vicinity of Bonjardim mud volcano is located at about 7.5 s TWT, which corresponds to a depth of 8 km, (about 5.5 km beneath the seafloor) (Thiebot and Gutscher, 2006). Locally, this reflector seems perturbed and vertically offset beneath Bonjardim mud volcano. It appears that the volcano is situated above a lateral ramp in the decollement here, which may offer pathways for deep sourced fluids that created the mud volcano. This is in accord with the conclusion of Hensen et al. (2007) that most of the water in mud sampled from the Bonjardim mud volcano was generated by clay dehydration at temperatures in the range 60–150 °C. In addition, enrichment of the minor elements Li and B indicate high-temperature alterations (>150 °C) related to fluid mobilisation along fault systems cutting deeply into the underlying basement (Hensen et al., 2007).

Bonjardim mud volcano is about 450 m thick and has a width of about 2.5 km (Fig. 11). The cover sequence and underlying units in the wedge are depressed beneath the volcano, presumably as a consequence of the removal of material from the wedge to create the mud volcano. The base of the mud volcano lies at least as deep as a horizon in the cover sequence that either side of the mud volcano is 60 m beneath the present seabed. The cover sequence at

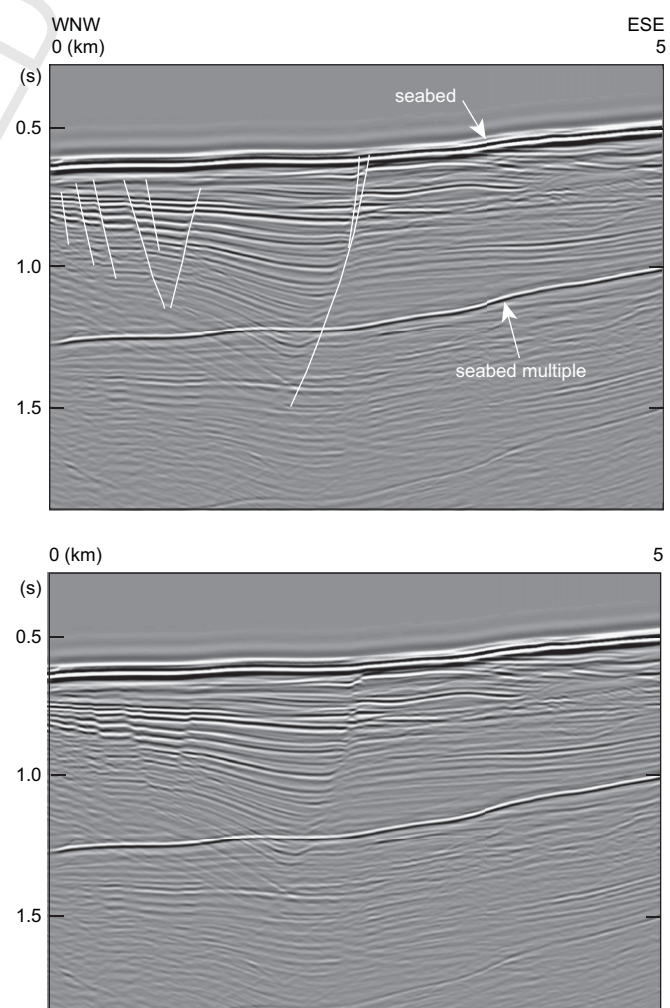
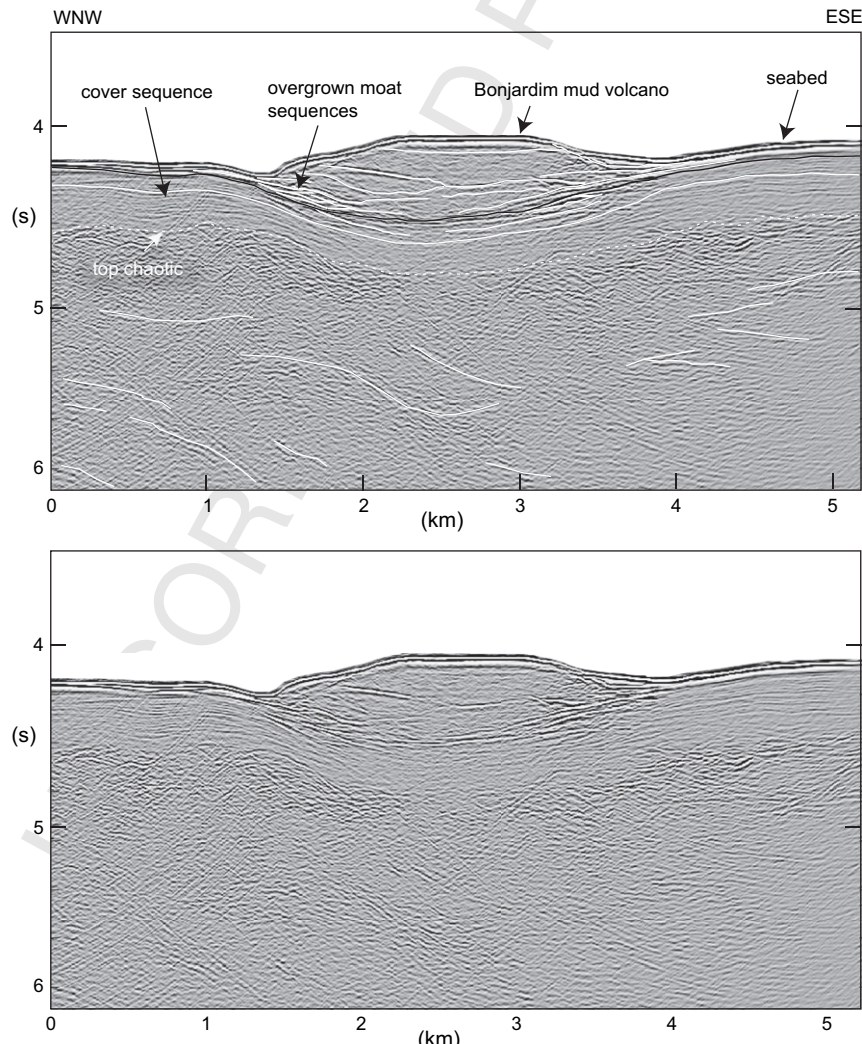
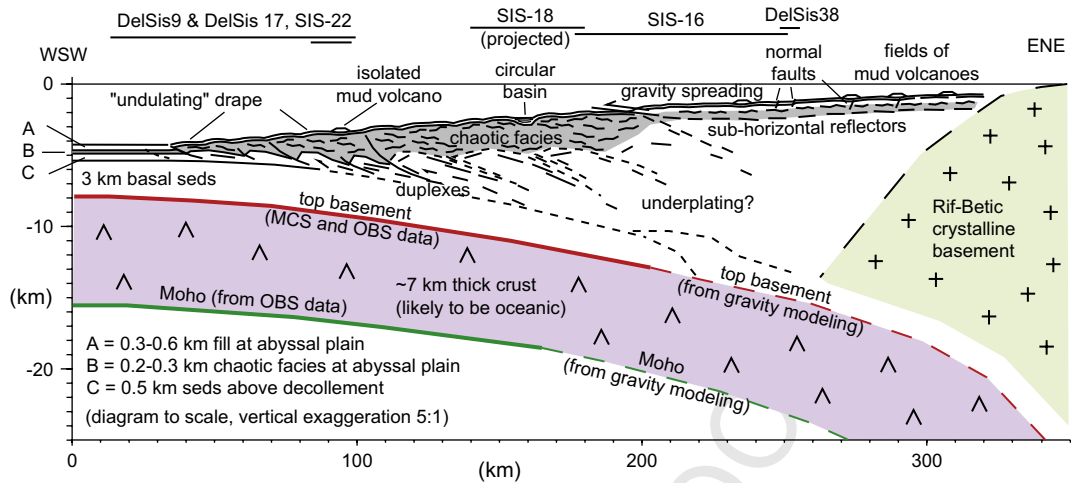


Fig. 9. Top: Part of seismic section from DelSis Line 38, showing major listric normal fault and associated antithetic faults, highlighted in white. Vertical exaggeration at the seafloor is 3.0. Bottom: Seismic section without superimposed interpretation.



Bonjardim is about 300-m thick. So, if the chaotic units beneath are of earliest Pliocene age (5 Ma) and the sedimentation rate has remained constant, the age of the mud volcano is 1.0 Ma. Piston cores taken during the Delsis cruise show that recent sedimentation rates are in the range 40–60 m/my, indicating that the age of the mud volcano lies in the range 1.0–1.5 Ma. Although one must take care in the interpretation of a 2D seismic image of a 3D structure that apparently deeper reflectors are not out-of-plane reflections, there are reflectors, particularly beneath the eastern side of the volcano, which may represent deeper, earlier mud flows. The deepest of these is just above a horizon, marked in white on Fig. 11, that either side of the mud volcano is at a depth of 125 m. If correct, this would double the age of the first extrusions of mud. The presence of seismically visible reflectors within and around the mud volcano indicates that the eruption of flows has been episodic interspersed by periods of hemipelagic sedimentation that provides the contrast in acoustic impedance with the mud flows. Early mud flows filling the moat have been covered by the main edifice of the mud volcano and appear to be locally interbedded with the cover sequence.

Overall, only a few mud volcanoes are scattered on the lower accretionary wedge. Most are situated in the shallowest portion above 1200 m water depth. This is the region that shows some morphological evidence of "raft-tectonics" and where some normal faulting has been observed (Figs. 9 and 10). Perhaps this surface extension associated with the downslope gravitational movement, opens pathways for the escape of overpressured fluids and mud. Such a link has been reported from work on the Moroccan mud volcano field (Van Rensbergen et al., 2005) and is schematically suggested in Fig. 10. Additional work on the geochemistry of fluids in the mud volcanoes should be able to identify the depth of the dewatering processes responsible for their formation (Haese et al., 2006; Hensen et al., 2007).

3.4. Presence of salt

The tops of salt domes are evident in the bathymetry of NW Moroccan margin south of 35°N (Figs. 2–4). Salt diapirs are noted in existing compilations (Somoza et al., 2003) and Triassic salt was drilled during ODP Leg 79 (Hinz et al., 1982). The salt diapirs interact with the SW deformation front of the accretionary wedge and are present within its lower slope (Figs. 2–4). One such bathymetric high (labelled P in Fig. 4B) was sampled by coring during the R/V Sonne GAP cruise. The high salinity of interstitial fluids and high heat-flow anomaly confirmed that it is indeed a salt dome (Kopf et al., 2003). On the SW Spanish margin north of 36.3°N Triassic salt is known from industry drilling data (Maestro et al., 2003) and on the southern Portuguese margin north of 36.1°N salt domes are observed on the basement high (Guadalquivir Ridge/Portimao Bank) (Figs. 3 and 4). It is unknown if salt exists beneath the central portion of the Gulf of Cadiz, presumably underlain by oceanic crust. A gravity core, on the upper accretionary wedge (1740 m water depth) sampled Mediterranean – Messinian faunal associations in the shallow sediments (1 m depth) (Auzende et al., 1981), however, it is unknown if any Messinian evaporites are associated with these strata and it is unclear how one could paleogeographically explain their presence west of Gibraltar.

The morphology observed in the Gulf of Cadiz, with abundant sub-circular depressions, and elongate curvilinear ridges, showing axial troughs is very similar to bathymetric images acquired in the Gulf of Mexico, where a gravitational salt-nappe is advancing to the south, downslope from the southern Louisiana continental margin (Winker and Booth, 2000) (Fig. 8). The Gulf of Mexico also has dome shaped diapirs on the adjacent deep sea-floor. Interestingly, the structures in the Gulf of Mexico appear to be at least twice the size of the structures observed in the Gulf of Cadiz. In the Gulf of Mexico,

the depressions are 20–30 km in size, and the salt domes 5–20 km in size, whereas in the Gulf of Cadiz, the corresponding features are 5–15 and 5–10 km in size, respectively (Fig. 12). Another interesting similarity, is that the steepest portion of the advancing salt nappe, is the deformation front, where slopes of up to 10° are observed, whereas the higher portions toward the continent are almost flat (Fig. 13a). Similarly, in the Gulf of Cadiz, the fronts of the two lobes show steep slopes (on the order of 10°) (Fig. 4b), while the relief is flatter above (Fig. 13b). The overall slope of the lower accretionary wedge is only 1° (below the gravitational lobes) and the steepest slopes on the lower wedge are only about 2–3° (except near the indenter where locally 5° is reached) suggesting that the deformation processes in the lobes and in the lower accretionary wedge are different (Fig. 13b).

Finally, the presence of salt diapirs within the uppermost layers of the accretionary wedge may help explain the abundant sub-circular depressions. Near the SW edge of the accretionary wedge, numerous salt domes are incorporated into the wedge. As these diapirs rise closer to the surface, they may interact with the seawater through fluid circulation, which will eventually lead to their dissolution. Such dissolution would gradually leave a void, similar to karst topography in limestone regions on land. As the hole enlarges, the surface would fill by hemipelagic sedimentation and the overall compressive stress regime near the surface of the wedge, could lead to the side-walls pushing in to try to fill the void. While this is not the only possible explanation for the formation of the circular basins, some type of mass removal process must probably be invoked as there is no obvious link to tectonic structures at depth, nor is a coherent tectonic pattern visible in the morphology. The roughly similar size of the salt domes and the depressions (though the latter are commonly somewhat larger) seems to lend some credence to this hypothesis. Lastly, preliminary work performed on the fluid geochemistry of shallow water mud volcanoes (Ginsburg and Gemini) suggests that "the dissolution of local evaporitic sequences", (anhydrite or gypsum) is required to explain high sulfate concentrations (Hensen et al., 2005; 2007), thus further supporting the salt layer hypothesis.

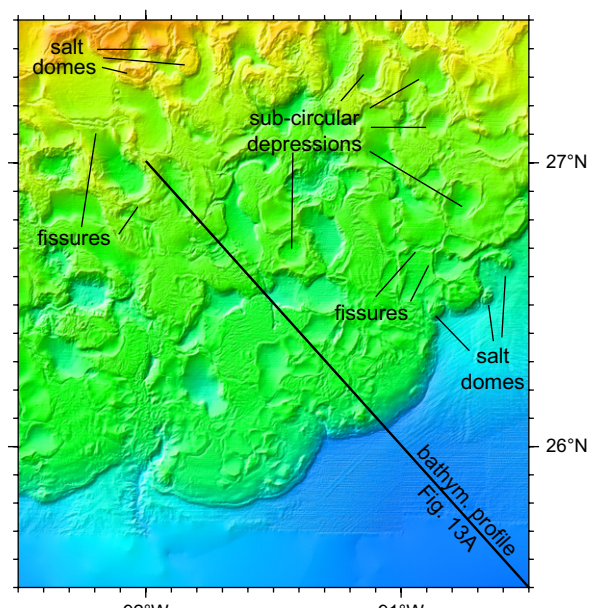


Fig. 12. High-resolution bathymetry (shaded hill relief image) from the Gulf of Mexico off the Southern Louisiana continental slope. Data from the National Geophysical Data Center, Coastal Relief Model (Divins and Metzger, 2006).

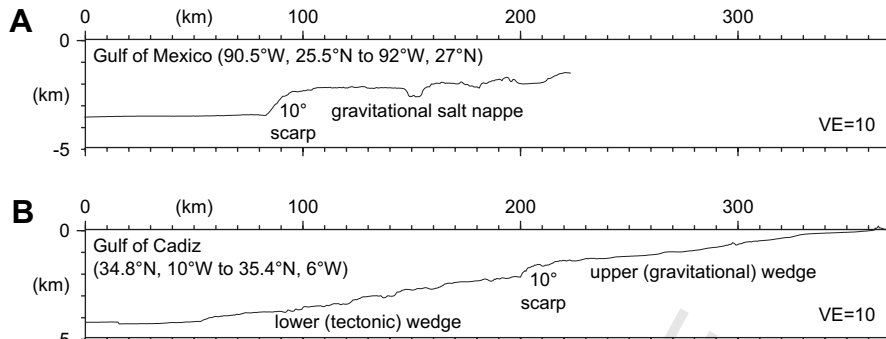


Fig. 13. 2-D bathymetric profiles (vertical exaggeration 10:1). (A) Northern Gulf of Mexico salt nappe and (B) Gulf of Cadiz. Note the similar steep scarps at the leading edge of the gravitationally spreading mass. Note also the difference in the lower wedge slope (constant shallow angle), with respect to the gravitationally controlled upper slope.

4. Conclusions

The morphological and structural data presented here document simultaneous tectonic shortening and gravitational spreading in the Gulf of Cadiz accretionary wedge. A slowing of the E-W convergence in the Gibraltar arc-Gulf of Cadiz region since 5 Ma from 2 to 0.5 cm/yr is suggested by geodynamic modeling (Gutscher et al., 2002) and current GPS data (Fernandes et al., 2007). This may offer an explanation for the diffuse deformation in the transparent layer, characterized by blind-thrusts, and strain distributed over a broad region, rather than discrete thrusts penetrating the entire sedimentary section. The extremely shallow surface angle and taper indicate a very weak basal detachment. The east dipping decollement and top basement interfaces require tectonic thickening, through frontal and/or basal thrusting. However, there is evidence for raft-tectonics, dissolution processes and gravitational instabilities upslope on the shallower portion of the wedge. Two morphological lobes are observed (at roughly the 2000 m depth contour) with a steep local deformation front (up to 10°). These appear to define the boundary of a gravitationally spreading upper wedge overlying a weak sub-horizontal upper detachment. A slowing in the convergence rate could also help accentuate slow deformation processes like the plastic flow of the “gravitationally spreading” upper slope of the accretionary wedge. Mud volcanoes are most abundant here, in the flat basin on the upper slope and may mark the position of the edge of the backstop at depth (Chamot-Rooke et al., 2005) or alternatively, their position may be related to local normal or transtensional faults in the gravitationally spreading lobes. The possible existence of salt or over-pressured mud is suggested by the sub-circular basins observed at the surface, the morphologic similarities to the Gulf of Mexico salt nappe, and by the very low effective friction of the detachment layers.

Acknowledgments

Thanks to the Captain and the crew of the Dom Carlos and to the Instituto Hidrografico for acquisition and processing of the Delila bathymetric data. We thank A. Kopf for use of the GAP bathymetric data (Sonne Cruise SO-175, Nov./Dec. 2003) included in the bathymetric compilation. We gratefully acknowledge financial support through the French GDR Marges project as well as the ESF Euromargins programme contract no. 01-LEC-EMA09F and from EU Specific Programme “Integrating and Strengthening the European Research Area”, Sub-Priority 1.1.6.3, “Global Change and Ecosystems”, contract no. 037110 (NEAREST). We thank the reviewers for constructive comments. Most of the figures were drafted using GMT software (Wessel and Smith, 1991). This paper is IUEM contribution number 1067.

References

- Auzende, J.M., Olivet, J.-L., Pastouret, L., 1981. Structural and paleogeographical implications of the existence of Messinian layers west of Gibraltar. *Marine Geology* 43, 9–18.
- Bonin, J., Olivet, J.L., Auzende, J.M., 1975. Structure en nappe à l'ouest de Gibraltar. *Comptes rendus de l'Academie des Sciences, Paris* 280, 559–562.
- Brown, K.M., Westbrook, G.K., 1988. Mud diapirism and subcretion in the Barbados Ridge accretionary complex. *Tectonics* 7, 613–640.
- Calvert, A., Sandvol, E., Seber, D., Barazangi, M., Roecker, S., Mourabit, T., Vidal, F., Alguacil, G., Jabour, N., 2000. Geodynamic evolution of the lithosphere and upper mantle beneath the Alboran region of the western Mediterranean: constraints from travel time tomography. *Journal of Geophysical Research* 105, 10871–10898.
- Cernobori, L., Hirn, A., McBride, J.H., Nicolich, R., Petronio, L., Romanelli, M., Streamers/Profiles Working Groups, 1996. Crustal image of the Ionian basin and its Calabrian margins. *Tectonophysics* 264, 175–189.
- Chamot-Rooke, N., Rabaut, A., Kreemer, C., 2005. Western Mediterranean Ridge mud belt correlates with active strain at the prism-backstop geological contact. *Geology* 33, 861–864.
- Contriucci, I., Klingelhofer, F., Perrot, J., Bartolome, R., Gutscher, M.-A., Sahabi, M., Malod, J., Rehault, J.-P., 2004. The crustal structure of the NW-Moroccan continental margin from wide-angle and reflection seismic data. *Geophysical Journal International* 159, 117–128.
- Davey, F.J., Hampton, M., Childs, J., Fisher, M.A., Lewis, K., Pettinga, J.R., 1986. Structure of a growing accretionary prism, Hikurangi margin, New Zealand. *Geology* 14, 663–666.
- Davis, D., Suppe, J., Dahlen, F., 1983. Mechanics of fold and thrust belts and accretionary wedges. *Journal of Geophysical Research* 88, 1153–1172.
- Deville, E., Guerlais, S.-H., Callec, Y., Griboulard, R., Huyghe, P., Lallement, S., Mascle, A., Mark, M., Schmitz, J., and the Collaboration of the Caramba Working Group, 2006. Liquefied vs stratified sediment mobilization processes: Insight from the South of the Barbados accretionary prism. *Tectonophysics* 428, 33–47.
- Divins, D.L., Metzger, D., 2006. NGDC coastal relief model. Available from: <http://www.ngdc.noaa.gov/mgg/coastal/coastal.html> [accessed 19.10.06].
- Dominguez, S., Lallemand, S.E., Malavieille, J., von Huene, R., 1998. Upper plate deformation associated with seamount subduction. *Tectonophysics* 293, 207–224.
- Duggen, S., Hoernle, K., van den Bogaard, P., Harris, C., 2004. Magmatic evolution of the Alboran Region: the role of subduction in forming the western Mediterranean and causing the Messinian Salinity Crisis. *Earth Planet. Sci. Lett.* 218, 91–108.
- Duval, B., Cramez, C., Jackson, M.P.A., 1992. Raft tectonics in the Kwanza Basin, Angola. *Marine and Petroleum Geology* 9, 389–404.
- Fadil, A., VERNANT, P., McClusky, S., Reilingher, R., Gomez, F., Ben Sari, D., Mourabit, T., Feigl, K., Barazangi, M., 2006. Active tectonics of the western Mediterranean: evidence for roll-back of a delaminated subcontinental lithospheric slab beneath the Rif Mountains Morocco. *Geology* 34, 529–532.
- Faugeres, J.C., Gonther, E., Bobier, C., Griboulard, R., 1997. Tectonic control on sedimentary processes in the southern termination of the Barbados Prism. *Marine Geology* 140, 117–140.
- Fernandes, R.M.S., Miranda, J.M., Meijninger, R.M.L., Bos, M.S., Noomen, R., Bastos, L., Ambrosius, B.A.C., Riva, R.E.M., 2007. Surface velocity field of the Ibero-Maghrebian segment of the Eurasia-Nubia plate boundary. *Geophysical Journal International* 169, 315–324.
- Fruehn, J., White, R.S., Minshull, T.A., 1997. Internal deformation and compaction of the Makran accretionary wedge. *Terra Nova* 9, 101–104.
- Fukao, Y., 1973. Thrust faulting at a lithospheric plate boundary: the Portugal earthquake of 1969. *Earth and Planetary Science Letters* 18, 205–216.
- Gaulier, V., Mart, Y., Bellalche, G., Vendeville, B., Mascle, J., Zitter, T., The Second Leg PRISMED II Scientific Party, 2000. Salt tectonics in and around the Nile deep-sea fan: insights from the PRISMED II cruise. In: Vendeville, B.C., Mart, Y., Vigneresse, J.L. (Eds.), *Salt, Shale, and Igneous Diapsirs in and Around Europe*. Geological Society of London Special Publication, vol. 174, pp. 111–129.
- Gracia, E., Danobeitia, J.J., Verges, J., Parsifal Team, 2003a. Mapping active faults offshore Portugal (36°N–38°N): implications for seismic hazard assessment along the southwest Iberian margin. *Geology* 31, 83–86.

- 1562 Gracia, E., Danobeitia, J.J., Verges, J., Bartolome, R., 2003b. Crustal architecture and
1563 tectonic evolution of the Gulf of Cadiz (SW Iberian margin) at the convergence
1564 of the Eurasian and African plates. *Tectonics* 22 (4), 1033, doi:10.1029/
1565 2001TC901045.
- 1566 Gutscher, M.-A., Malod, J., Rehault, J.-P., Contrucci, I., Klingelhoefer, F., Mendes-
1567 Victor, L., Spakman, W., 2002. Evidence for active subduction beneath Gibraltar.
1568 *Geology* 30, 1071–1074.
- 1569 Gutscher, M.-A., 2004. What caused the Great Lisbon earthquake? *Science* 305,
1570 1247–1248.
- 1571 Gutscher, M.-A., Baptista, M.A., Miranda, J.M., 2006. The Gibraltar Arc seismogenic
1572 zone (part 2): constraints on a shallow east dipping fault plane source for the
1573 1755 Lisbon earthquake provided by tsunami modeling and seismic intensity.
1574 *Tectonophysics* SP Vol. "Natural Laboratories on Seismogenic Faults" 427, 153–
1575 166, doi:10.1016/j.tecto.2006.02.025.
- 1576 Haese, R.R., Hensen, C., de Lange, G.J., 2006. Pore water geochemistry of eastern
1577 Mediterranean mud volcanoes: Implications for fluid transport and fluid origin.
1578 *Marine Geology* 225, 191–208.
- 1579 Hensen, C., Nuzzo, M., Hornbrook, E.R.C., Brueckmann, W., Magalhaes, V.H., Parkes,
1580 R.J., Pinheiro, L., March 2005. The origin of mud volcano fluids in the Gulf of
1581 Cadiz. (Abstract). In: Proc. IMPACTS Workshop, Brest.
- 1582 Hensen, C., Nuzzo, M., Hornbrook, E.R.C., Pinheiro, L., Bock, B., Magalhaes, V.H.,
1583 Brückmann, W., 2007. Sources of mud volcano fluids in the Gulf of Cadiz –
1584 indications for hydrothermal input. *Geochimica et Cosmochimica Acta*,
doi:10.1016/j.gca.2006.11.022.
- 1585 Hinz, K., Winterer, E.L., Baumgartner, P.O., Bradshaw, M.J., Channel, J.E.T.,
1586 Jaffrezo, M., Jansa, L.F., Leckie, R.M., Moore, J.N., Rullkötter, J., Schaftehaar, C.,
1587 Steiger, T.H., Vuchev, V., Wiegand, G.E., 1982. Preliminary results from DSDP Leg
1588 79 seaward of the Mazagan Plateau of Morocco. In: von Rad, U., Hinz, K.,
1589 Sarnthein, M., Seibold, E. (Eds.), *Geology of the Northwest African Continental
1590 Margin*. Springer-Verlag, Berlin-Heidelberg, pp. 23–33.
- 1591 Hudec, M.R., Jackson, M.P.A., 2002. Structural segmentation, inversion, and salt
1592 tectonics on a passive margin: evolution of the Inner Kwanza Basin, Angola.
1593 Geological Society of America Bulletin 114, 1222–1244.
- 1594 Huguen, C., Mascle, J., Chaumillon, E., Kopf, A., Woodside, J., Zitter, T., 2004. Struc-
1595 tural setting and tectonic control of mud volcanoes from the central Medi-
1596 terranean Ridge (Eastern Mediterranean). *Marine Geology* 209, 245–263.
- 1597 IOC, IHO, BODC, 2003. Centenary Edition of the GEBCO Digital Atlas. Published on
1598 CD-ROM on behalf of the Intergovernmental Oceanographic Commission and the
1599 International Hydrographic Organization as part of the General Bathymetric
1600 Chart of the Oceans. British Oceanographic Data Centre, Liverpool.
- 1601 Jimenez-Munt, I., Fernandez, M., Torne, M., Bird, P., 2001. The transition from linear
1602 to diffuse plate boundary in the Azores–Gibraltar region. *Earth and Planetary
1603 Science Letters* 192, 175–189.
- 1604 Johnston, A., 1996. Seismic moment assessment of earthquakes in stable continental
1605 regions – III. New Madrid, 1811–1812, Charleston 1886 and Lisbon 1755.
1606 *Geophysical Journal International* 126, 314–344.
- 1607 Kopf, A., 2002. Significance of mud volcanism. *Reviews of Geophysics* 40, 1005,
doi:10.1029/2000RG000093.
- 1608 Kopf, The SO175 Scientific Party, 2003. Report and Preliminary Results of Sonne
1609 Cruise SO175. Miami to Bremerhaven 12 Nov. 2003–30 Dec. 2002. Berichte
Fachbereich Geowissenschaften, Univ. Bremen, 218 pp.
- 1610 Kopp, C., Fruehn, J., Flueh, E.R., Reichert, C., Kukowski, N., Bialas, J., Klaeschen, D.,
1611 2000. Structure of the Makran subduction zone from wide-angle and reflection
1612 seismic data. *Tectonophysics* 329, 171–191.
- 1613 Lallemand, S., Schnürle, P., Malavieille, J., 1994. Coulomb theory applied to accre-
1614 tionary and nonaccretionary wedges: possible causes for tectonic erosion and/
1615 or frontal accretion. *Journal of Geophysical Research* 99, 12033–12055.
- 1616 Lonergan, L., White, N., 1997. Origin of the Betic-Rif mountain belt. *Tectonics* 16,
504–522.
- 1617 Maestro, A., Somoza, L., Medialdea, T., Talbot, C.J., Lowrie, A., Vazquez, J.T., Diaz-del-
1618 Rio, V., 2003. Large-scale slope failure involving Triassic and Middle Miocene
1619 salt and shale in the Gulf of Cadiz. *Terra Nova* 15, 380–391.
- Martinez-Solares, J.M., Lopez, A., Mezcua, J., 1979. Isoseismal map of the 1755 Lisbon
earthquake obtained from Spanish data. *Tectonophysics* 53, 301–313.
- Medialdea, T., Vegas, R., Somoza, L., Vazquez, J.T., Maldonado, A., Diaz-del-Rio, V.,
Maestro, A., Cordoba, D., Fernandez-Puga, M.C., 2004. Structure and evolution of
the "olistostrome" complex of the Gibraltar Arc in the Gulf of Cadiz (eastern
Central Atlantic): evidence from two long seismic cross-sections. *Marine
Geology* 209, 173–198.
- Mulder, T., Voisset, M., Lecroart, P., Le Drezen, E., Gonthier, E., The Cadisar Shipboard
Party, 2003. The Gulf of Cadiz: an unstable giant contouritic levee. *Geo-Marine
Letters* 23, 7–18.
- Mulder, T., Lecroart, P., Hanquiez, V., Marches, E., Gonthier, E., Guedes, J.C.,
Thiebot, E., Jaaidi, B., Kenyon, N., Voisset, M., Perez, C., Sayago, M., Fuchey, Y.,
Bujan, S., 2006. The western part of the Gulf of Cadiz: contour currents and
turbidity currents interactions. *Geo-Marine Letters* 26, 31–41.
- Pinheiro, L.M., Ivanov, M.K., Sautkin, A., Akhmanov, G., Magalhaes, V.H.,
Volkonskaya, A., Monteiro, J.H., Somoza, L., Gardner, J., Hamouni, N.,
Cunha, M.R., 2003. Mud volcanism in the Gulf of Cadiz: results from the TTR-10
cruise. *Marine Geology* 195, 131–151.
- Pinheiro, L.M., et al., 2006. MV Seis: tectonic control, deep crustal structure and
fluid escape pathways in the Gulf of Cadiz Mud Volcano Field. EuroMargins
Interim Report, ESF Project 01-LEC-EMA24F.
- Platt, J.P., Vissers, R.L.M., 1989. Extensional collapse of thickened continental lith-
osphere: a working hypothesis for the Alboran Sea and Gibraltar arc. *Geology* 17, 540–543.
- Reston, T.J., von Huene, R., Dickmann, T., Klaeschen, D., Kopp, H., 2002. Frontal
accretion along the western Mediterranean Ridge: the effect of Messinian
evaporites on wedge mechanics and structural style. *Marine Geology* 186, 59–
82, doi:10.1016/S0025-3227(02)00173-1.
- Sartori, R., Torelli, L., Zitellini, N., Peis, D., Lodolo, E., 1994. Eastern segment of the
Azores–Gibraltar line (central-eastern Atlantic): an oceanic plate boundary
with diffuse compressional deformation. *Geology* 22, 555–558.
- Somoza, L., Diaz-del-Rio, V., Leon, R., Ivanov, M., Fernandez-Puga, M.C.,
Gardner, J.M., Hernandez-Molina, F.J., Pinheiro, L.M., Rodero, J., Lobato, A.,
Maestro, A., Vazquez, J.T., Medialdea, T., Fernandez-Salas, L.M., 2003. Seabed
morphology and hydrocarbon seepage in the Gulf of Cadiz mud volcano area:
acoustic imagery, multibeam and ultra-high resolution seismic data. *Marine
Geology* 195, 153–176.
- Terrinha, P., Pinheiro, L.M., Henriet, J.-P., Matias, L., Ivanov, A.K., Monteiro, J.H.,
Akhmetzhanov, A., VolkonskayaCunha, M.R., Shaskin, P., Rovere, M., 2003.
Tsunamigenic–seismogenic structures, neotectonics, sedimentary processes
and slope instability on the Southwest Portuguese margin. *Marine Geology* 195,
1–19.
- Terrinha, P., Matias, L., Vicente, J., Duarte, J., Luís, J., Pinheiro, L., Lourenço, N., Diez, S.,
Rosas, F., Magalhães, V., Valadares, V., Zitellini, N., Roque, C., Mendes Victor, L.,
and Matespro Team. Strain partitioning and morpho-tectonics at the Iberia-
Africa plate boundary from multibeam and seismic reflection data. *Marine
Geology*, in press.
- Thiebot, E., Gutscher, M.-A., 2006. The Gibraltar Arc seismogenic zone (part 1):
constraints on a shallow east dipping fault plane source for the 1755 Lisbon
earthquake provided by seismic data, gravity and thermal modeling. *Tectono-
physics* SP Vol. "Natural Laboratories on Seismogenic Faults" 427, 135–152,,
doi:10.1016/j.tecto.2006.02.024.
- Torelli, L., Sartori, R., Zitellini, N., 1997. The giant chaotic body in the Atlantic off
Gibraltar: new results from a deep seismic reflection survey. *Marine and
Petroleum Geology* 14, 125–138.
- Tortella, D., Torne, M., Perez-Estaun, A., 1997. Geodynamic evolution of the eastern
segment of the Azores–Gibraltar Zone: the Gorringe Bank and Gulf of Cadiz
region. *Marine Geophysical Research* 19, 211–230.
- Van Rensbergen, P., Depreiter, D., Pannemans, B., Henriet, J.-P., 2005. Seafloor
expression of sediment extrusion and intrusion at the El Arraiche mud volcano
field, Gulf of Cadiz. *Journal of Geophysical Research* 110, F02010, doi:10.1029/
2004JF000165.
- Wessel, P., Smith, W.H.F., 1991. Free software helps map and display data. *EOS* 72, 441.
- Westbrook, G.K., 1982. The Barbados ridge complex: tectonics of a mature forearc
system. In: Leggett, J.K. (Ed.), *Tectonics and Sedimentation in Modern and
Ancient Trenches and Forearcs*. Spec. Publ. Geological Society of London, Special
Publication, vol. 10, pp. 275–290.
- Westbrook, G.K., Smith, M.J., Peacock, J.H., Poultre, M.J., 1982. Extensive under-
thrusting of undeformed sediment beneath the accretionary complex of the
Lesser Antilles subduction zone. *Nature* 300, 625–628.
- Westbrook, G.K., Smith, M.J., 1983. Long decollements and mud volcanoes: evidence
from the Barbados Ridge complex for the role of high pore-fluid pressure in the
development of an accretionary complex. *Geology* 11, 279–283.
- Westbrook, G.K., Ladd, J.W., Buhl, P., Bangs, N., Tiley, G.J., 1988. Cross section of an
accretionary wedge: Barbados Ridge complex. *Geology* 16, 631–635.
- Winkler, C.D., Booth, J., 2000. Sedimentary dynamics of the salt-dominated conti-
nental slope, Gulf of Mexico: integration of observations from the seafloor,
near-surface, and deep subsurface. In: CCSEPM Foundation 20th Annual
Research Conference, Deep-water Reservoirs of the World, pp. 1059–1086
(CD-ROM publication).
- Zitellini, N., et al., 2001. Source of 1755 Lisbon earthquake and tsunami investigated.
Eos Transactions, American Geophysical Union 82, 285–291.

Internet newsletters



16/08/2008 - 12h11

Estação da UE para alerta de tsunami é retirada de mar luso

Por Cecília Malheiro, da Agência Lusa

Faro, 16 ago (Lusa) - Uma equipe de cientistas a bordo do navio italiano "Urania" retirou esta semana do fundo do mar do Algarve, sul de Portugal, a primeira estação europeia de alerta precoce de tsunamis, operação considerada bem sucedida.

"Retiramos todos os equipamentos com uma taxa de sucesso de 100%, mas, agora, vamos levar entre um e dois anos analisando-os com uma equipe de cerca de 10 pessoas", declarou à Agência Lusa o cientista Nevio Zitellini, coordenador da instalação do Geostar a 150 quilômetros da ponta do Cabo de Sagres, em Portugal.

O Geostar havia sido instalado há um ano, no Banco de Goringe, perto do Golfo de Cádiz, local do epicentro de um terremoto em 1755. Por causa da forte atividade tectônica, a área é exposta ao risco de tremores e tsunamis.

Financiado pela União Europeia, projeto conta com a participação de cientistas de Espanha, Itália, Marrocos, França e Alemanha.

O observatório é equipado com sismógrafos e sensores capazes de efetuar levantamentos geológicos e geofísicos no fundo do mar. Durante o ano em que ficou submerso, foram recolhidos 500 gigabytes de informação pelo Geostar e por 24 "buoy" - máquinas que servem para registrar pequenos tremores de terra.

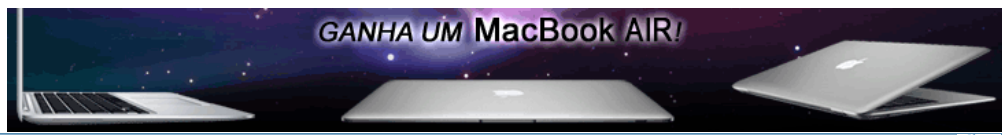
A informação será analisada e conclusões preliminares serão divulgadas em outubro, em Berlim, cidade em que vão se reunir os cientistas ligados ao projeto, indicou Nevio Zitellini, que pertence ao Instituto de Ciências Marítimas de Bolonha.

"Saber quando vai aparecer uma onda gigante e poder alertar em tempo hábil as pessoas de todo o mundo, principalmente as que estão junto à costa marítima, é um dos grandes objetivos do projeto europeu Nearest", explicou.

Antes do Mediterrâneo, já existia © 1996-2008 UOL - O melhor conteúdo. Todos os direitos reservados.
Hospedagem: UOL Host um equipamento capaz de alertar a população europeia de uma onda gigante na Ásia.

Após o fim do projeto "Nearest", o cientista Nevio Zitellini pretende estudar quais regiões seriam mais afetadas no sul da Península Ibérica no caso de ocorrer um tsunami.

Faça do IOLDiário a sua homepage
Adicione o IOLDiário aos seus favoritos



Informação Desporto Horas Vagas Pesquisas Classificados Compras Serviços Correio



31 Outubro 2008

ÚLTIMA HORA SOCIEDADE DESPORTO FOTOS VÍDEOS BLOGUES

POLÍTICA ECONOMIA INTERNACIONAL AMBIENTE MODA&SOCIAL ESTA É BOCA ACREDITE SE QUISER

TECNOLOGIA MÚSICA CINEMA

PESQUISAR

■ TECNOLOGIA

[brasil](#) [eua](#) [governo](#) [inglaterra](#) [lisboa](#) [pj](#) [portugal](#)

[portugaldiário](#)

O que são tags?

16-08-2008 - 18:58h

5 artigos de **Tecnologia** [seguinte](#)

Estação para alerta de tsunamis retirada das águas algarvias

Primeiro equipamento europeu do género foi recolhido com sucesso para que os dados possam ser analisados

Por: Redacção / Cecília Malheiros/Lusa

Vota
votos

Resultado

print comentar

PUB COFIDIS. Até 4.000€. O poder de escolher é seu!



Uma equipa de cientistas a bordo do navio italiano «Urânia» retirou esta semana do fundo marítimo do Algarve a primeira estação europeia de alertas precoce de tsunami, onda gigante, uma operação que decorreu total sucesso, afirmam.

«Retirámos todos os equipamentos com uma taxa de sucesso de 100 por cento, mas agora vamos levar entre um a dois anos a analisá-los com uma equipa de cerca de 10 pessoas», declarou à Agência Lusa o cientista Nevio Zitellini, coordenador pela colocação do Geostar ao largo do Cabo de Sagres.

«Saber quando é que vai aparecer uma onda gigante e poder alertar em tempo útil as pessoas de todo o mundo, mas também e principalmente as que estão junto à costa marítima é um dos grandes objectivos do projecto europeu Nearest», explicou Nevio Zitellini.

O observatório colocado no fundo do mar foi baptizado de Geostar e serve para medir os níveis sísmicos da área e estudar um eventual tsunami.

Colocada há um ano a 80 milhas, cerca de 150 quilómetros, da ponta do Cabo de Sagres, o observatório Geostar está equipado com sismógrafos e sensores capazes de efectuar levantamentos geológicos e geofísicos e prevenir eventuais tsunamis a partir do fundo do mar.

O Geostar foi colocado no Banco de Goringe, a cerca de 80 milhas a sudoeste de Sagres, e perto do Golfo de Cadiz, local do epicentro do sismo de 1755.

Durante um ano, foram recolhidos «500 gigabytes» de informação pelo Geostar e por 24 «buoy» - máquinas que serviram para registar os

OFERTA LIMITADA

GRÁTIS: um disco rígido de 160 GB

ao comprar o **CorelDRAW GRAPHICS SUITE X4**

COMPRE JA >>

Última hora

Filtrar

[última hora](#) | [+ lidos](#) | [+ votados](#) | [+](#) [comentados](#)

15:53 | Política

Autarquias: ministra da Educação «sem pressa»

15:52 | Desporto

Sidnei: «Sabemos das dificuldades que vamos encontrar em Guimarães»

15:25 | Música

Michael Jackson nega regresso dos «Jackson 5»

15:06 | Sociedade

Presidente da EMEL pede demissão

15:02 | Internacional

Tabaco mata 2600 fumadores passivos por ano

Primeira Página



PS a subir, perto da maioria absoluta

Fim-de-semana com chuva e vento

Polícia apanha ladrão pela... 15ª vez

pequenos tremores de terra e que foram colocadas no fundo do mar ao largo de Sagres na mesma altura do Geostar.

Toda a informação vai ser posteriormente analisada, mas as conclusões preliminares vão ser divulgadas em Outubro em Berlim, local onde os cientistas relacionados com o projecto da estação europeia para alerta de tsunamis vão reunir-se, indicou o coordenador Nevio Zitellini, do Instituto de ciências Marítimas em Bolonha (Itália).

«É uma das maiores experiências deste género feitas em todo o mundo»

A primeira estação europeia para alerta de tsunamis colocada no Algarve conta com a participação de cientistas de Espanha, Itália, Marrocos, França e Alemanha, mas este mês a expedição do Urania termina.

O observatório Geostar ficou submerso numa área de risco de sismos e tsunamis - devido ao facto de ter forte actividade tectónica - e, durante cerca de um ano, estudou a área junto ao Algarve.

Na Ásia já existe equipamento capaz de alertar as populações da existência de tsunamis, mas no Mediterrâneo a estratégia tem de ser diferente e o desafio é realizar a vigilância dos tsunamis na falha tectónica.

«É uma das maiores experiências deste género feitas em todo o mundo», adiantou Paolo Favali, cientista do Instituto Nacional de Geofísica e Vulcanologia de Roma, Itália, que integra o projecto financiado pela União Europeia.

Após o fim do projecto europeu «Nearest», o cientista Nevio Zitellini tem intenções de desenvolver um outro estudo relacionado com o estudo das zonas mais afectadas no Algarve e sul de Espanha caso haja um tsunami.

O objectivo é trabalhar com as autoridades locais para desenvolver um método de alertar a população sobre a chegada de uma onda gigante.

[Esta notícia no seu telemóvel](#)

Vota Resultado votos |  | A | A | A |  print |  enviar |  comentar

MAIS NOTÍCIAS:

- » PortugalDiário em 140 caracteres, no **Twitter**
- » «Beatles» chegam ao mundo dos jogos
- » Google e Yahoo ameaçam quebrar parceria comercial
- » Telescópio Espacial Hubble já está em funcionamento
- » PoDTec: a Internet «sem velocidade» em Portugal e a Táxi TV
- » Diga ao seu chefe que pode ir ao Hi5 no trabalho
- » MTV concorre com Youtube

5 artigos de: **Tecnologia** [seguinte](#)

[Ficha Técnica](#)

[Estatuto Editorial](#)

[Publicidade](#)



Copyright © 2008 www.iol.pt

Meios Media Capital: Agência Financeira | Maisfutebol | Rádio Clube Português | TVI

Meios Associados: Imprensa: AS | Cinco Dias | EL País | Rádio: Cadena SER | Los 40 | TV: Cuatro | Plus

[Crise: Espanha à beira da recessão](#)

[Para que serve o «dia das bruxas»?](#)

[Apanhado médico falso que tratava crianças](#)

[Mais de 80 escolas pedem suspensão da avaliação](#)

DOS LEITORES

FÓRUM: Acha que tem havido caça à multa em Portugal?

BLOG: Angariação de fundos online

O MELHOR: Fraude CGD



DESPORTO

E-golo: mercado fecha às 18 horas



CELEBRIDADES

Hello Kitty Hello Music



CINEMA

Família de Jennifer Hudson cria fundação



MÚSICA

Róisin Murphy torna-se «mulher furacão» no Coliseu

[Teckpoint, Ida - Algarve Nº 1 em Vídeo Vigilância Digital Tecnologia Ip Megapixel, Ptz, Nvr](#)
[www.teckpoint.pt Aminhafesta® Soluções para animação de eventos! Animação Dj, Karaoke e muito mais..](#) [www.aminhafesta.pt Lista de Baptizado Dezenas de Lojas para a Lista de Baptizado do seu Bébé com Descontos](#)
[www.presentes.pt/baptizado/ Hotéis no Algarve Reserve já o seu Hotel](#)



Click here to download plugin.

Ciência e Tecnologia

Mar algarvio monitorizado

31-10-2007 16:19:00

No mês em que se assinalam 252 anos sobre o terramoto que devastou Lisboa e o Algarve fica completa a primeira rede de sismómetros colocada no fundo do mar algarvio para estudar a actividade sísmica da região.

Durante um ano, 24 sismómetros colocados entre o Golfo de Cadiz e o Banco de Gorrige vão medir a actividade sísmica da área onde se pensa que tiveram origem os terramotos de 1755 e 1969, este menos devastador, mas que também gerou um tsunami.

Segundo disse à Lusa Maria Ana Baptista, responsável pelo projecto e especialista em tsunamis, o objectivo não é detectar a ocorrência de sismos, mas medir fenómenos de pequena intensidade para obter dados referentes àquela área.

Esta é a primeira experiência do género a acontecer no Algarve, mas já aconteceu noutras zonas do país, nomeadamente em Peniche, nos Açores e na costa alentejana.

A rede de sismómetros, que fica completa em Novembro, começou a ser instalada em Setembro na zona compreendida entre o local onde está a estação "Geostar" e o Banco de Gorrige (complexo de montes submarinos).

Aquela estação piloto - localizada a cerca de 150 quilómetros da ponta de Sagres, perto do Golfo de Cadiz - é a primeira vocacionada para o alerta precoce de tsunamis e permite detectar a ocorrência de grandes sismos.

O terramoto de 01 de Novembro de 1755, sobre o qual passam quinta-feira 252 anos, arrasou dois terços da cidade de Lisboa, mas teve também efeitos muito devastadores na região algarvia, tendo deixado submersas povoações inteiras.

Por ser menos habitada que Lisboa, a região acabou por não registar tantas vítimas, mas o terramoto abalou severamente o Barlavento (parte ocidental do Algarve), sobretudo a cidade de Lagos, embora tenha também causado fortes estragos em Faro.

Segundo a investigadora do Instituto Superior de Engenharia de Lisboa (ISEL), a onda gigante que sucedeu ao terramoto destruiu todas as construções que se erguiam nas ilhas barreira da Ria Formosa, entre Loulé e Tavira.

"Se a onda gigante galgou a Ilha de Faro, cuja altura actual é de dez metros, o seu tamanho teria de ter sido superior", observa a especialista, que explica que a massa de água que a formava deveria ter cerca de 100 quilómetros de dimensão.

"Normalmente a massa de água forma-se ao longo do comprimento da falha que origina o tsunami",

explica Maria Ana Baptista, que sublinha que estas ondas "são muito diferentes" das causadas pelo vento.

O tsunami que se seguiu ao terramoto de 1755 deixou muitas vilas algarvias submersas, algumas delas acabaram por ser reconstruídas por detrás da linha de costa, mais longe do mar do que na sua localização original.

"A vila de Armação de Pêra e Quarteira ficaram totalmente devastadas e tiveram de ser reconstruídas", exemplifica, explicando tratar-se de zonas extremamente vulneráveis, por estarem muito expostas.

No caso da capital algarvia, a vulnerabilidade a um possível tsunami é menor, por estar protegida pela Ilha de Faro, o mesmo acontecendo com as povoações que têm ilhas à sua frente, como Olhão ou Tavira.

A instalação da rede de sismómetros é financiada pela União Europeia e está integrada num projecto mais abrangente, o NEAREST, que se dedica à investigação sobre potenciais fontes de tsunamis localizadas perto da costa.





Procurar

denota conteúdo de acesso restrito

Favorito

Segunda-feira, 6 de Outubro de 2008

REGISTOE-mail
Senha
Recuperar senha
Ainda não se registou?**PUBLICIDADE**

170^x₂₁₀
Pixel
é a medida para
SEU anúncio
PUBLICITÁRIO

- › Home
- › Política
- › Economia
- › Regional
- › Desporto
- › Cultura
- › Educação
- › Gramofone

[Todas as secções »](#)**CLASSIFICADOS**

Imobiliário
[Vende-se T3 - LAGOA](#)

Imobiliário
[Procura-se PRETENDO ARRENDAR CASA R/C SEM MOBÍLIA](#)

Veículos
[Vende-se DUMPER BEDFORD](#)
[Mais classificados »](#)
[Como fazer um anúncio classificado »](#)

BLOCO NOTAS

Lagos
[José Fortunato expõe «J'aime les arbres»](#)

Algarve
[Agenda Cultural](#)

Algarve
[Cinemas](#)

[Próximos eventos »](#)

Farmácias
[Tabela de marés](#)

Restaurante «Pizza Pasta Fantasia», na Quinta do Lago

[Mais restaurantes »](#)**DOSSIERS**

- › Tecnologias
- › Portimão, Cidade do Mundo
- › Mundo
- › Media & Comunicação
- › PROTAG

[Todos os temas »](#)**PUBLICIDADE**

Regional

1º estação europeia para alerta de tsunamis retirada com sucesso das águas algarvias

elisabete rodrigues

[Ver Fotos »](#)

Bóia gigante do sistema de alerta de tsunamis

grandes objectivos do projecto europeu Nearest", explicou Nevio Zitellini.

Uma equipa de cientistas a bordo do navio italiano "Urania" retirou esta semana do fundo marítimo do Algarve a primeira estação europeia de alertas precoce de tsunamis (onda gigante), uma operação que decorreu total sucesso, afirmam.

"Retirámos todos os equipamentos com uma taxa de sucesso de 100 por cento, mas agora vamos levar entre um a dois anos a analisá-los com uma equipa de cerca de 10 pessoas", declarou à Agência Lusa o cientista Nevio Zitellini, coordenador pela colocação do Geostar ao largo do Cabo de Sagres.

"Saber quando é que vai aparecer uma onda gigante e poder alertar em tempo útil as pessoas de todo o mundo, mas também e principalmente as que estão junto à costa marítima é um dos

O observatório colocado no fundo do mar foi baptizado de Geostar e serve para medir os níveis sísmicos da área e estudar um eventual tsunami.

Colocada há um ano a 80 milhas (150 quilómetros) da ponta do Cabo de Sagres, o observatório Geostar está equipado com sismógrafos e sensores capazes de efectuar levantamentos geológicos e geofísicos e prevenir eventuais tsunamis a partir do fundo do mar.

O Geostar foi colocado no Banco de Goringe, a cerca de 80 milhas a sudoeste de Sagres, e perto do Golfo de Cadiz, local do epicentro do sismo de 1755.

Durante um ano, foram recolhidos "500 gigabytes" de informação pelo Geostar e por 24 "buoy" - máquinas que serviram para registrar os pequenos tremores de terra e que foram colocadas no fundo do mar ao largo de Sagres na mesma altura do Geostar.

Toda a informação vai ser posteriormente analisada, mas conclusões preliminares vão ser divulgadas em Outubro em Berlim, local onde os cientistas relacionados com o projecto da estação europeia para alerta de tsunamis vão reunir-se, indicou o coordenador Nevio Zitellini, do Instituto de ciências Marítimas em Bolonha (Itália).

A primeira estação europeia para alerta de tsunamis colocada no Algarve conta com a participação de cientistas de Espanha, Itália, Marrocos, França e Alemanha, mas este mês a expedição do Urania termina.

O observatório Geostar ficou submerso numa área de risco de sismos e tsunamis - devido ao facto de ter forte actividade tectónica - e, durante cerca de um ano, estudou a área junto ao Algarve.

Na Ásia já existe equipamento capaz de alertar as populações da existência de tsunamis, mas no Mediterrâneo a estratégia tem de ser diferente e o desafio é realizar a vigilância dos tsunamis na falha tectónica.

"É uma das maiores experiências deste género feitas em todo o mundo", adiantou Paolo Favali, cientista do Instituto Nacional de Geofísica e Vulcanologia de Roma, Itália, que integra o projecto financiado pela União

NEWSLETTER

Subscreva a nossa newsletter e receba as notícias na sua caixa de correio.

[Ainda não subscreveu?](#)**EDIÇÃO IMPRESSA**

Edição nº 1625

[Todas as edições »](#)**MULTIMÉDIA**

- › Desfile dos caloiros levou boa disposição às ruas de Faro
- › Espectáculo da velocidade voltou com o Pax Rally
- › Lágrimas e festa receberam Ana Cabecinha no Pechão



Europeia.

[Todas as galerias »](#)

O Geostar foi retirado do fundo do mar pelo navio italiano de investigação científica baptizado de "Urania - nave oceanográfica", que pesa 1200 toneladas e tem 87 metros de comprimento, 11 de largura e 18 metros de mastro.

INQUÉRITO
Não se encontra inquérito activo.

Após o fim do projecto europeu "Nearest", o cientista Nevio Zitellini tem intenções de desenvolver um outro estudo relacionado com o estudo das zonas mais afectadas no Algarve e sul de Espanha caso haja um tsunami.

[Ver resultados »](#)

O objectivo é trabalhar com as autoridades locais para desenvolver um método de alertar a população sobre a chegada de uma onda gigante.

17 de Agosto de 2008 | 09:53
cecilia malheiro, Agência Lusa

Notícias Relacionadas

Progressos do estudo sobre risco sísmico e tsunamis são apresentados hoje em Faro pelo MAI

20 de Fevereiro de 2008 | 00:10

Ministro Rui Pereira preside à apresentação do Plano de Risco Sísmico e de Tsunamis do Algarve

19 de Fevereiro de 2008 | 10:30

Bóia gigante de sistema de alerta de tsunamis recuperada

22 de Outubro de 2007 | 11:29

1ª Estação europeia de alerta de tsunamis no fundo do mar a 150 km do Algarve

18 de Agosto de 2007 | 17:28

Portugal não tem sistema de alerta precoce para tsunamis para proteger a 100 % a população

16 de Julho de 2007 | 15:29

Algarve vai ter estudo sísmico e de previsão de tsunamis

22 de Fevereiro de 2006 | 00:34

Cientistas procuram origem do tsunami de 1755

31 de Outubro de 2005 | 09:54

Investigador fala sobre o risco de Tsunamis no Algarve

16 de Outubro de 2005 | 15:17

assine o barlavento

Para quem gosta de saber tudo.

Com 30 anos de vida, o barlavento é hoje uma referência no Algarve. Sempre no caminho da verdade. Sempre directo ao que interessa. Conta tim-tim por tim-tim o que precisa de saber sobre política, desporto, economia, cultura, ambiente, educação e muito mais. Agora, com uma edição online, inteiramente grátis para os assinantes da edição impressa. 30 anos de Algarve num só jornal.

Assine o barlavento

por apenas 30 € anuais



CORRA PELA VIDA
mama maratona 2008 12 Out 10h00 Parque de Feiras e Exposições PORTIMÃO

Organização:


Parceria Institucional:


[Contacte o barlavento](#) | [Publicidade](#) | [Nós](#) | [Ficha Técnica](#) | [Assine o barlavento](#) | [Newsletter](#) | [Política de Privacidade](#)

© Mediregião - Edição e Distribuição de Publicações, Lda
website [e-solutions](#)

Diário de Notícias

http://dn.sapo.pt/2007/11/20/sociedade/sistema_alerta_tsunamis_atlantico_te.html

Sistema de alerta de tsunamis no Atlântico em testes já em Janeiro

FILOMENA NAVES



Sistema de alerta de tsunamis no Atlântico em testes já em Janeiro

Reunião de Lisboa decisiva para arranque do sistema inicial de alerta

O primeiro sistema de alerta de tsunamis para o Atlântico e Mediterrâneo pode entrar já em fase de testes a partir de Janeiro de 2008, mas esse arranque está dependente do resultado da reunião internacional, promovida pela Unesco, que amanhã começa em Lisboa. Tudo vai depender de uma instituição científica europeia - parece haver uma candidatura viável - poder assumir já a coordenação dessa rede. Mas isso só se saberá na sexta-feira.

Para Portugal poderá estar também em cima da mesa, nesta 4.ª reunião de grupo intergovernamental para o futuro sistema de alerta, a hipótese da futura coordenação regional para a bacia atlântica. Uma questão que "depende da vontade política e de uma verba anual de 200 mil euros para recursos humanos, já que a capacidade técnico-científica existe", adiantou ao DN Luís Matias, investigador do Centro de Geofísica da Universidade de Lisboa-Instituto D. Luís e um dos delegados portugueses ao projecto.

Promovido pela Comissão Oceanográfica Internacional (COI), da Unesco, o futuro sistema de alerta de tsunamis para o Atlântico, Mediterrâneo e Mares Adjacentes, deverá estar em funcionar em pleno em 2011. Mas, para isso, a primeira fase terá que estar concluída em Janeiro, para que um sistema inicial automático possa iniciar já um período de testes.

Sem verbas próprias, este sistema de alerta assentará nas infra-estruturas de cada país, com as respectivas estações sísmicas e de medição de marés, transmissão de dados em tempo real para um ponto focal nacional e, daí, para os centros de coordenadores. Nesta fase haverá apenas uma instituição coordenadora. No futuro, estão previstos centros de coordenação regional.

Fazer o balanço dos progressos realizados até agora e aprovar a instituição coordenadora para a primeira fase, se

se concretizar a candidatura necessária, estão na agenda da reunião de Lisboa.

Para Portugal, estará também em cima da mesa a possibilidade de assumir futuramente a coordenação regional para a bacia Atlântica.

Para Maria Ana Baptista, especialista em tsunamis, investigadora do Centro de Geofísica da Universidade de Lisboa e coordenadora do grupo de trabalho português para os tsunamis no âmbito da COI, "seria uma importante oportunidade para o País, dada a nossa localização geográfica". Mas, sublinha, "cabe ao Governo dar esse passo". Na competição por esse papel está, de resto, o Reino Unido, que na última reunião dos delegados internacionais, realizada em Bona, em Fevereiro, já manifestou a intenção de o assumir.

"Pela nossa localização geográfica, dado que estamos na primeira linha de impacto de um tsunami nesta região atlântica, e pelo investimento científico que estamos a fazer nesta área, temos todo o interesse em ficar com essa coordenação em Portugal, no Instituto de Meteorologia", explicam Luís Matias e Maria Ana Baptista. "Neste momento", garante Luís Matias, "temos todos os requisitos, excepto uma verba anual de cerca de 200 mil euros para recursos humanos, que garantam o trabalho 24 horas por dia, necessário num sistema de alerta. E isso depende da vontade política".

NEWS N. 16933

Progetto UE potenzierà il sistema di allarme tsunami

Fonte: CORDIS - NEWS n.28909 del 02-01-2008

Tipo di informazione: RISULTATO

In conseguenza alla calamità dello tsunami avvenuta nel 2004 un progetto finanziato dall'UE ha avviato i lavori per mettere a disposizione dell'intera regione dell'Oceano indiano un sistema di allarme precoce.

Sulla base del lavoro condotto nel quadro del progetto German Indonesian Tsunami Early Warning System (GITEWS), il Distant Early Warning System (DEWS) sta sviluppando una piattaforma tecnologica per evitare che la tragedia del 2004 si ripeta.

«In seguito ai progressi compiuti nell'ambito del progetto GITEWS, è arrivato il momento di fornire a più paesi della regione dell'Oceano indiano, come la Thailandia o lo Sri Lanka, un accesso tempestivo alle informazioni di allerta, nonché dati in tempo reale sull'oceano e i terremoti», ha dichiarato uno degli undici partner del progetto, il dott. Joachim Wächter del Centro di ricerca geofisica (GFZ) di Potsdam (Germania).

Finanziato nell'ambito del Sesto programma quadro dell'UE (6°PQ), il progetto DEWS mira a rafforzare le capacità di allerta della regione, creando un sistema di allarme precoce tsunami aperto e interoperabile per l'Oceano indiano.

Il sistema di rilevamento degli tsunami si baserà su una piattaforma di sensori aperta e su sistemi di sensori integrati per il monitoraggio dei terremoti (sismico), del livello del mare (misuratore delle maree, boe) e degli spostamenti del terreno (stazioni GPS terrestri).

Questi sistemi di sensori costituiranno una delle più importanti innovazioni del progetto, poiché saranno responsabili dell'invio di dati affidabili dal fondale marino alla stazione di allarme.

Sulla base di questi progressi il progetto intende migliorare la qualità e il flusso dei suoi messaggi di allerta al pubblico, alle autorità pertinenti e alle forze responsabili della gestione delle emergenze, sia a livello nazionale sia internazionale.

Infine, un ulteriore obiettivo del progetto sarà quello di trasferire il suo sistema DEWS ad altre zone del mondo a rischio tsunami. Questo compito verrà svolto attraverso un'azione supplementare nel bacino del Mediterraneo.

Il progetto ha una durata di quattro anni ed è finanziato dall'UE con uno stanziamento di fondi dell'ordine di 6,5 Mio EUR.

Fonte: Progetto DEWS (Distant Early Warning System)

Quadro di finanziamento

6FP-IST - Tecnologie della società dell'informazione: priorità tematica 2 nell'ambito del gruppo di attività 'Integrare e rafforzare lo Spazio europeo della ricerca' del VI Programma Quadro di RST



© Comunità europee, 1990-2008

Tali informazioni sono tratte da **CORDIS**, il servizio d'informazione comunitario in materia di R&S, messo a disposizione dell'Unione europea per favorire lo scambio di informazioni fra i vari operatori attivi nel settore della R&S e dell'innovazione tecnologica

I testi presenti nel sito non rivestono carattere di ufficialità e non sono in alcun modo sostitutivi della documentazione cartacea ufficiale

FIRST Finanziamenti per l'Innovazione, la Ricerca e lo Sviluppo Tecnologico

© Copyright

Jornal de Notícias

Alerta de tsunamis terá dados daqui a um ano

Uma equipa de cientistas a bordo do navio italiano "Urania" retirou esta semana do fundo marítimo do Algarve a primeira estação europeia de alerta precoce de tsunamis, uma operação que decorreu total sucesso.

"Retirámos todos os equipamentos com uma taxa de sucesso de 100 por cento, mas agora vamos levar entre um a dois anos a analisá-los com uma equipa de cerca de 10 pessoas", declarou o cientista Nevio Zitellini, coordenador pela colocação do Geostar ao largo do cabo de Sagres.

O objectivo maior do projecto europeu Nearest é "saber quando é que vai aparecer uma onda gigante e poder alertar em tempo útil as pessoas de todo o mundo, mas também e principalmente as que estão junto à costa marítima", explicou Nevio Zitellini.

O observatório colocado no fundo do mar foi baptizado de Geostar e serve para medir os níveis sísmicos da área e estudar um eventual tsunami. Colocada há um ano a 80 milhas (150 quilómetros) da ponta do Cabo de Sagres, o observatório Geostar está equipado com sismógrafos e sensores capazes de efectuar levantamentos geológicos e geofísicos e prevenir eventuais tsunamis a partir do fundo do mar.

O Geostar foi colocado no Banco de Goringe, a cerca de 80 milhas a sudoeste de Sagres, e perto do Golfo de Cadiz, local do epicentro do sismo de 1755.

Durante um ano, foram recolhidos "500 gigabytes" de informação pelo Geostar e por 24 "buoy" - máquinas que serviram para registar os pequenos tremores de terra e que foram colocadas no fundo do mar ao largo de Sagres na mesma altura do Geostar.

Toda a informação vai ser posteriormente analisada, mas conclusões preliminares vão ser divulgadas em Outubro em Berlim, local onde os cientistas relacionados com o projecto da estação europeia para alerta de tsunamis vão reunir-se, indicou o coordenador Nevio Zitellini, do Instituto de ciências Marítimas em Bolonha.

O observatório Geostar ficou submerso numa área de risco de sismos e tsunamis - devido ao facto de ter forte actividade tectónica - e, durante cerca de um ano, estudou a área junto ao Algarve.

Na Ásia já existe equipamento capaz de alertar as populações da existência de tsunamis, mas no Mediterrâneo a estratégia tem de ser diferente e o desafio é realizar a vigilância dos tsunamis na falha tectónica. "É uma das maiores experiências deste género feitas em todo o mundo", adiantou Paolo Favali, cientista do Instituto Nacional de Geofísica e Vulcanologia de Roma, que integra o projecto financiado pela UE.

O Geostar foi retirado do fundo do mar pelo navio italiano de investigação científica baptizado de "Urania - nave oceanográfica", que pesa 1200 toneladas e tem 87 metros de comprimento e 11 de largura.

CECÍLIA MALHEIRO*

publicado a 2008-08-17 às 00:30



Patrocínio

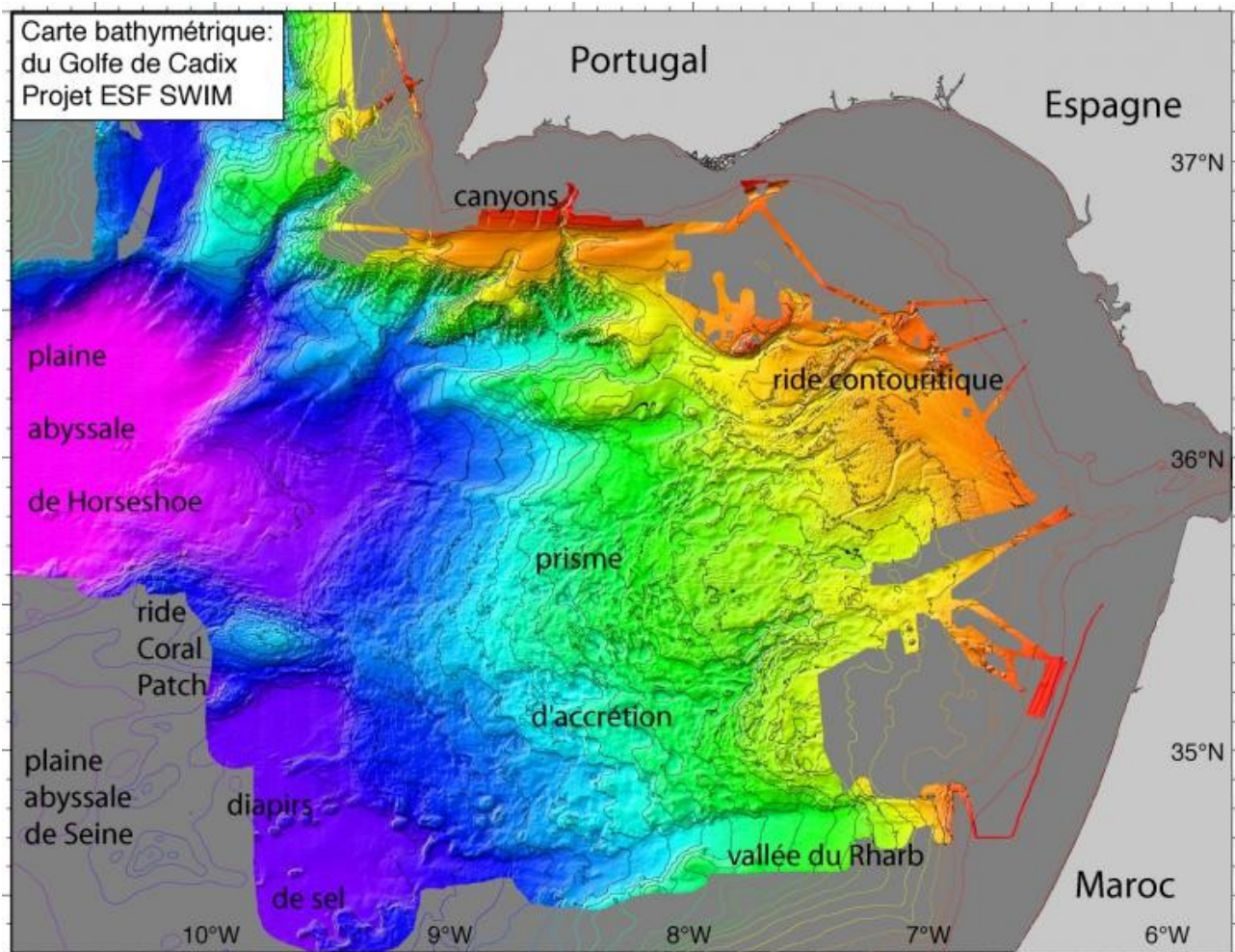
Para mais detalhes consulte:

http://www.jn.pt/PaginaInicial/Nacional/Interior.aspx?content_id=980502

GRUPO CONTROLINVESTE

Copyright © - Todos os direitos reservados

Semaine du 24 mars 2008



Cette image montre le relief sous-marin de la baie de Cadix, à l'Ouest de Gibraltar. Elle a été obtenue dans le cadre d'un projet européen par des chercheurs Italiens, Espagnols, Français, Portugais, Britanniques, Belges à la suite de plusieurs campagnes océanographiques. Dans cette région, un pan de la plaque africaine plonge en subduction dans le manteau. Les chercheurs pensent que cette situation a engendré le tragique séisme de Lisbonne survenu le 1er novembre 1755. D'une magnitude estimée entre 8,5 et 9 sur l'échelle de Richter, il a été suivi d'un tsunami qui a détruit les ports du Golfe de Cadix.

Sur cette carte le continent est en gris clair, le plateau continental et les grandes plaines abyssales dont la bathymétrie n'a pas été mesurée sont en gris foncé. On observe de beaux canyons profond près du Portugal, la zone rugueuse en orangé, vert, bleu (prisme d'accrétion) est une accumulation de sédiments lié à la probable subduction. Le rose correspond à une profondeur supérieure à 5000 mètres.

Contact(s)

[Marc-André Gutscher](#)

Participation to Congresses

AGU FALL MEETING; 10-14 December 2007; San Francisco, CA, USA

An innovative tsunami detector operating in tsunami generation environment

- Chierici, F (chierici@ira.inaf.it), ira-inaf, via gobetti 101, bologna, 40129, Italy
- beranzoli, l (beranzoli@ingv.it), ingv, via vigna murata, roma, 00100, Italy
- embriaco, d (embriaco@ingv.it), ingv, via vigna murata, roma, 00100, Italy
- favali, p (paolofa@ingv.it), ingv, via vigna murata, roma, 00100, Italy
- marinaro, g (marinaro@ingv.it), ingv, via vigna murata, roma, 00100, Italy
- monna, s (monna@ingv.it), ingv, via vigna murata, roma, 00100, Italy
- pignagnoli, l (luca.pignagnoli@bo.ismar.cnr.it), ismar-cnr, via gobetti 101, bologna, 40129, Italy
- zitellini, n (nevio.zitellini@bo.ismar.cnr.it), ismar-cnr, via gobetti 101, bologna, 40129, Italy
- bruni, f (bruni@tecnomare.it), tecnomare-eni s.p.a., campo s. angelo, venezia, 30100, Italy
- furlan, f (furlan@tecnomare.it), tecnomare-eni s.p.a., campo s. angelo, venezia, 30100, Italy
- gasparoni, f (gasparoni@tecnomare.it), tecnomare-eni s.p.a., campo s. angelo, venezia, 30100, Italy

On August 25th 2007 a tsunami detector installed onboard the multi-parameter observatory GEOSTAR was successfully deployed at 3200 b. s. l. in the Gulf of Cadiz, Portugal. This activity is within the NEAREST EC Project (<http://nearest.bo.ismar.cnr.it/>). Among other deliverables, the NEAREST project will produce and test the basic parts of an operational prototype of a near field tsunami warning system. This system includes an onshore warning centre, based on the geophysical monitoring networks which are already operating, and a tsunami detector deployed on board GEOSTAR at the sea bottom. On land the warning centre is in charge of collecting, integrating, and evaluating data recorded at sea. At the sea bottom data is recorded and processed by an advanced type of tsunami detector which includes: a pressure sensor, a seismometer and two accelerometers. The detector communicates acoustically with a surface buoy in two-way mode. The buoy is equipped with meteo station, GPS and tiltmeter and is connected to a shore station via satellite link. The prototype is designed to operate in tsunami generation areas for detection-warning purpose as well as for scientific measurements. The tsunami detector sends a near real time automatic alert message when a seismic or pressure threshold are exceeded. Pressure signals are processed by the tsunami detection algorithm and the water pressure perturbation caused by the seafloor motion is taken into account. The algorithm is designed to detect small tsunami waves, less than one centimetre, in a very noisy environment. Our objective is to combine a novel approach to the tsunami warning problem, with a study of the coupling between the water column perturbations and sea floor motion, together with the long term monitoring of geophysical, geochemical and oceanographic parameters. <http://nearest.bo.ismar.cnr.it/>



An innovative tsunami detector operating on a multiparameter seafloor observatory

F.Chierici (1), D. Embriaco (2), L. Pignagnoli (3), L. Beranzoli (2), P. Favali (2), G. Marinaro (2), S. Monna (2), F. Bruni (4), F. Furlan (4), F. Gasparoni (4)
(1) IRA-INAF, sez. Bologna, Italy, (2) INGV, sez. Roma 2, Italy, (3) ISMAR-CNR, sez. Bologna, Italy, (4) Tecnomare-ENI SpA

During the cruise of the Italian research vessel URANIA on August 2007, a new tsunami detector was successfully deployed at 3200 b. s. l. in the Gulf of Cadiz, Portugal. The new detector is installed on board the multi-parameter abyssal observatory GEOSTAR.

This activity is a task of NEAREST EC Project (<http://nearest.bo.ismar.cnr.it/>).

Among other tasks, the NEAREST project will produce and test the basic parts of an operational prototype of a near field tsunami warning system. The warning system includes an onshore warning centre based on the seismic and tide gauges monitoring networks which are already operating in the area of Gulf of Cadiz and connected in real time with many warning receiving shore stations, a buoy equipped with meteo-station and two way acoustic and satellite links, and the tsunami detector installed on board GEOSTAR. The warning centre is in charge of collecting, integrating, and evaluating data recorded at sea.

In the observatory at the sea bottom, data are recorded and processed by the tsunami detector which includes a pressure sensor, a seismometer and two accelerometers. The observatory communicates acoustically with a surface buoy in two-way mode. The buoy is equipped with meteo station and GPS and it is connected to the shore station via satellite dual-link.

The prototype is designed to operate in tsunami generation areas for detection-warning

purpose as well as for scientific measurements during long term monitoring. The pressure data are processed in real time on the sea floor observatory by a tsunami detection algorithm able to detect small tsunami waves, less than one centimetre, in a very noisy environment. At the same time the seismic data are analysed using a STA/LTA algorithm.

The tsunami detector sends a near real time automatic alert message when a seismic or a pressure signal exceeds a selectable threshold indicating a strong local earthquake or a tsunami wave event. After the detection of an event, the seafloor observatory will start sending updated pressure data to the shore station. Our objective is to combine a novel approach to the tsunami warning problem, with a study of the coupling between the water column perturbations and sea floor motion, together with the long term monitoring of geophysical, geochemical and oceanographic parameters.

Geomorphologic domains of the Gulf of Cadiz from swath multibeam bathymetry

V. Valadares (1,2), P. Terrinha (2), J. C. Duarte(1,2), E. Grácia (3), N. Zitellini (4),
M. A. Gutscher (5), F. Rosas (1), L. M. Matias (6)

- (1) LATTEX – IDL, Lisbon, Portugal, (2) DGM-INETI, Alfragide, Portugal, (3)
UTM-CMIMA-CSIC, Barcelona, Spain, (4) ISMAR-CNR, Bologna, Italy, (5)
IUEM-UGBO-CNRS, Plouzané, France

The SWIM bathymetric dataset covers an area of approximately 180.000km², was obtained after compilation of 19 multibeam bathymetry surveys. Terrain analysis and detailed morphological interpretation of this dataset on a 100m cell-size map allowed the identification of a diversity of morphological domains that result from the combined or individual action of oceanographic, sedimentological and tectonic processes. The available multi-channel seismic reflection profiles, high resolution profiles and the multibeam probe backscatter images were also used to establish the different domains and their borders as well as the structural and tectonic control of the buried structures on the present day morphology.

After thorough seafloor mapping the following domains were characterized: submarine mountains, abyssal plains, abyssal hills, axial areas of submarine canyons and gullies associated with steep walls, plateaus, contourites and other sedimentary and erosional structures associated with the Mediterranean Outflow Water (MOW) , the Gulf of Cadiz accretionary wedge with its mud volcanoes, salt domes and sub-circular basins, continental shelf, diapiric ridges, basement outcrops, submarine deep scours and volcanic edifices.

The Central longitudinal part of the Gulf of Cadiz shows three different morphologies, the Horseshoe Abyssal Plain, the mouth of the South Portugal canyons and the accretionary wedge. In the East the interaction of the MOW with the seafloor creates erosional and depositional features that extend as contourites bodies along the South and Southwestern Portuguese slope. The Northern part exhibits the Portuguese shelf, the deeply incised continental slope and the MOW contourites depositional system, . Scattered structures of mass wasting deposits exist the Gulf of Cadiz, generally associated with active fault scarps.

Tsunami Warning prototype in the frame of the EC NEAREST project.

FRANCESCO CHIERICI (*), NEVIO ZITELLINI (**), PAOLO FAVALI (***)^{*}, LAURA BERANZOLI (***)^{*}, LUCA PIGNAGNOLI (**), DAVIDE EMBRIACO (***)^{*}, GABRIELA CARRARA (**), GIUDITTA MARINARO (***)^{*}, NADIA LO BUE (***)^{*}, STEPHEN MONNA (***)^{*}, FRANCESCO GASPARONI (°), FLAVIO FURLAN (°), FEDERICO BRUNI (°)

ABSTRACT

Prototipo di Tsunami Warning nel quadro del progetto EC NEAREST

Nell' ambito del progetto NEAREST finanziato dalla EC sono stati sviluppati alcuni elementi di un sistema di allerta per tsunami, fra i quali un prototipo di detector di onde anomale installato a bordo dell' osservatorio abissale GEOSTAR: l' osservatorio con il detector di onde anomale ha operato per un anno nel Golfo di Cadice, a 3200m di profondità

Key words: *seafloor observatories, tsunami detection, 1775 earthquake, Cadiz Gulf*

INTRODUCTION

On August 25th 2007 a tsunami detector installed onboard the multiparametric observatory GEOSTAR (FAVALI *et alii*, 2006) was successfully deployed at 3200 b.s.l. in the Gulf of Cadiz, Portugal (Fig. 1). This activity is within the NEAREST EC Project (<http://nearest.bo.ismar.cnr.it/>). Among other deliverables, the NEAREST project will produce and test the basic parts of an operational prototype of a near field tsunami warning system. This system includes an onshore warning centre, based on the geophysical monitoring networks which are already operating, and a tsunami detector installed on board GEOSTAR. On land the warning centre is in charge of collecting, integrating, and evaluating data recorded at sea. At the sea bottom, data are recorded and processed by an advanced type of tsunami detector which includes a pressure sensor, a seismometer and two accelerometers. The detector communicates acoustically with a surface buoy in two-way mode. The buoy is equipped with meteo station, GPS and tiltmeter and is connected to a shore station via satellite dual-link. The prototype is designed to operate in tsunami generation areas for detection-warning purpose as well as for scientific measurements. The tsunami detector sends a near-real-time automatic alert message (Fig. 2) when a seismic or pressure threshold are exceeded. Pressure signals are processed by the tsunami detection algorithm and the water pressure perturbation caused by the seafloor motion is taken

into account. The algorithm is designed to detect small tsunami waves, less than one centimetre, in a very noisy environment. Our objective is to combine a novel approach to the tsunami warning problem (DART website), with a study of the coupling between the water column perturbations and seafloor motion, together with the long term monitoring of geophysical, geochemical and oceanographic parameters.

NEAREST PILOT EXPERIMENT IN CADIZ GULF

The Gulf of Cadiz is a highly populated area, prone to devastating earthquakes and tsunamis (e.g., 1755 Lisbon earthquake, BAPTISTA *et alii*, 2003). More than ten years of geological and geophysical investigations offshore SW Iberia have been collected (multibeam bathymetry, side-scan sonar, high-resolution and multichannel seismics, and sampling which probed the first kilometres of the upper crust at various resolution) (see Fig. 1).

Recognition and mapping of active tectonic structures likely to

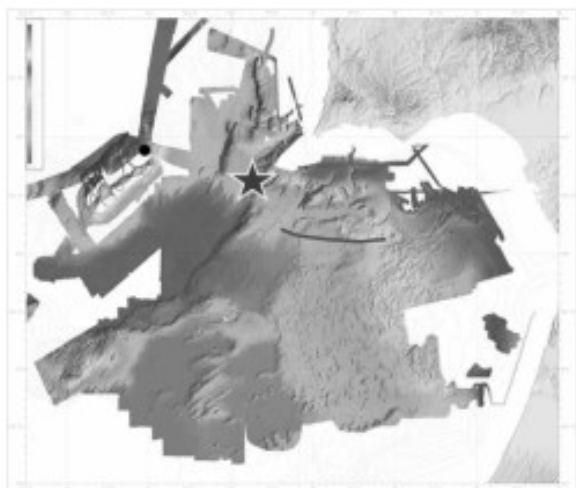


Fig. 1: Deployment site in the Gulf of Cadiz

(**) Istituto di Radio Astronomia-INAF

(**) Istituto di Scienze Marine-CNR

(***) Istituto Nazionale di Geofisica e Vulcanologia (INGV)

(°) Tecnomare S.p.A.

generate large earthquakes and tsunamis have been performed.

THE TSUNAMI DETECTOR

The tsunami detector is capable of real-time recognition and transmission of sea water anomalies and seismic signals to

shore stations. The new Tsunami detector (grey labels in the sensors in the table below), is installed onboard the pre-existent GEOSTAR multiparameter abyssal observatory, that can collect a wide variety of different geophysical and oceanographic data (Fig. 3).

Sensor	rate	Acquisition
Triaxial broad band seismometer	100Hz - comp. (0.016-100 Hz f.r)	3Continuous + triggered events
Triaxial accelerometer	100Hz - comp.	3Continuous + triggered events
Hydrophone	100Hz	Continuous
Pressure sensor	15sec or sec	1-5Continuous
Accelerometer	100Hz - Gsensor	6Only on triggered events

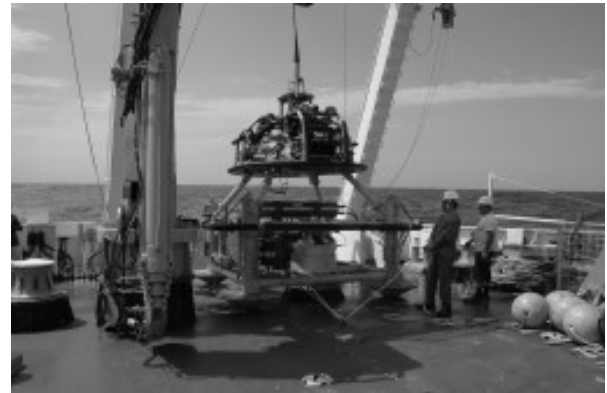
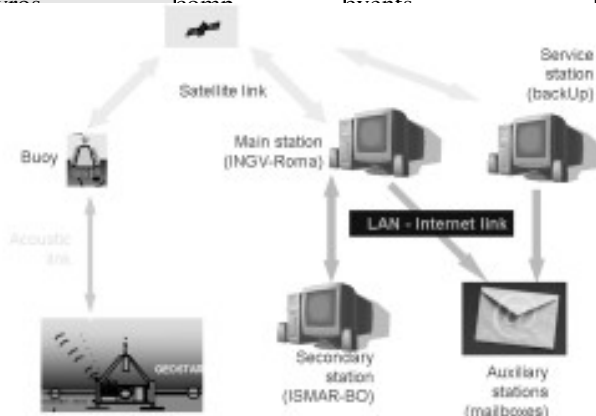


Fig. 3: GEOSTAR observatory

to the assigned threshold (MOFJELD, 2000). Fig.2

REFERENCES

BAPTISTA M. A., MIRANDA J.M., CHIERICI F. & ZITELLINI N. (2003). - *New study of the 1755 earthquake source based on multi-channel seismic survey data and tsunami modelling*, Natural Hazards and Earth System Sciences, **3(5)**, 333-340.

DART DATA WEB SITE:
<http://www.ngdc.noaa.gov/seg/hazard/DARTData.shtml>.

MOFJELD H.O. (2000) - *Tsunami Detection Algorithm* Available at:
http://nctr.pmel.noaa.gov/tda_documentation.html

FAVALI P., BERANZOLI L., D'ANNA G., GASPARONI F., MARVALDI J., CLAUSS G., GERBER H.W., NICOT M., MARANI M.P., GAMBERI F., MILLOT C. & FLUEH E.R. (2006) – *A fleet of multiparameter observatories for geophysical and environmental monitoring at seafloor*, Ann. Geophys., **49**, 2/3, 659-680.

The tsunami detection procedure is based on trigger on pressure and seismic events:

- Seismometer: trigger on local strong earthquakes (STA/LTA);
- Pressure: detection of sea level anomalies (Tsunamis wave): trigger on processed sea level data compared

P. Costa*, C. Andrade*, M. C. Freitas*, M. A. Oliveira*, R. Taborda** and C. M. da Silva*

High energy boulder deposition in Barranco and Furnas lowlands, western Algarve (south Portugal)

*Centro de Geologia; **LATTEX-IDL. Universidade de Lisboa, Faculdade de Ciências, Departamento de Geologia. Campo Grande, Edifício C6-3 piso, 1749-016 Lisboa, Portugal, fax: +351 21 750 00 64. e-mail: ppcosta@fc.ul.pt; candrade@fc.ul.pt; cfreitas@fc.ul.pt; maoliveira@fc.ul.pt; rtaborda@fc.ul.pt; paleocarlos@fc.ul.pt

Keywords: Tsunami, storms, boulders, sediment transport, bioerosion, southern Portugal

Abstract

Peculiar accumulations of perforated marine boulders resting above spring tide level, extending several hundreds of meters inland and exceeding the width of present day washovers were detected in two lowlands of the Algarve coast. Their marine source is evidenced by well developed macrobioerosion sculpturing and *in situ* skeletal remains of endolithic shallow marine bivalves. The proportion of bored clasts decreases with distance from the shore but no trend in size variation with distance was found. The study of the fossils within the boulders indicates that downwearing during transport and redeposition was not significant and suggests a recent age for the deposit. Data presented here suggests simultaneous entrainment of coarse particles from the shallow sea floor followed by rapid shoreward suspended-dominated transport and inland non-graded redeposition excluding significant sorting by weight or dimension. The application of two distinct threshold criteria for the initiation of submerged particle movement under waves leads to contradictory inferences regarding the minimum wave height required for particle entrainment and nature of the driving mechanism: storm *versus* tsunami. Consideration of the low-energy wave regime of this coast and contrasts existing between the boulder accumulations and present-day storm-deposits suggests that they were most probably emplaced by a tsunami inundation.

Introduction

The south Algarve coast of Portugal is an area rarely subjected to extreme storms or tsunamis, though both types of events have been recurrent. The most devastating tsunami that affected the Portuguese coast in historical times took place in AD 1755 and several studies discussed sandy sedimentation associated to that event in Portugal and elsewhere, in contrast with few reports on deposition of larger particles. Here, we present first results obtained in the scope of Project NEAREST (*integrated observations from nearshore sources of tsunamis: towards an early warning system*), on the characterization of boulder-sized clasts from two coastal lowlands (Barranco and Furnas) of the western section of the south Algarve coast and discuss entrainment and depositional mechanisms and the location of their source area.

The westernmost section of the southern Algarve coast is high (*circa* 40m above mean sea level) and rocky, sea cliffs cutting resistant Jurassic limestones and dolomites (Fig. 1). The drainage system consists of few ephemeral rivulets running in deeply incised canyon-shaped valleys. In their downstream sections the valleys are flat-floored and choked with alluvial mud, the valley bottom resting some 2-3m above mean sea level. The narrow alluvial floodplains are limited seawards by beaches, usually made of a thin veneer of sand covering shingle, in agreement with the sand-starved character of this coast, and backed by overwash fans, essentially made of sand and eventually including scattered boulders, reaching up to 100m in width.

Barranco and Furnas are narrow flat-floored canyons, the stream flowing across small floodplains, which consist of sandy mud and abundant heterometric angular pebbles, cobbles and occasional boulders, mixed with lithic and quartz gritt. Towards the beach the

stream deposits spread into a thin discontinuous gravelly fan, resting upon the alluvial mud and merging with backbeach sand. Here, the gravel is a mixture of fluvial and marine-sourced pebbles to boulders bearing macrobioerosion features.

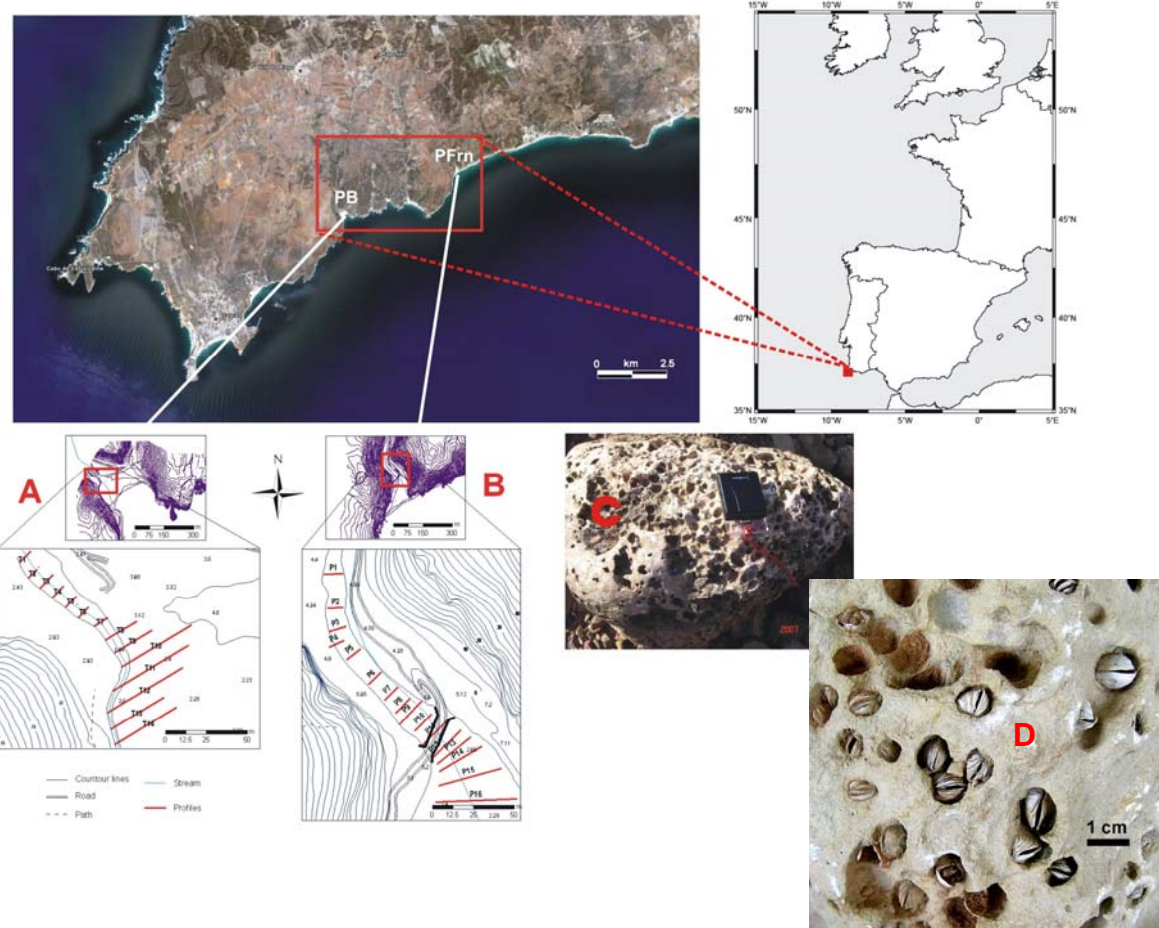


Fig. 1- General overview of the study areas. PB- Praia do Barranco. PFrn- Praia das Furnas. Red lines in [A] and [B] indicate profiles where boulders have been measured; [C] and [D] – perforated boulders; note endolithic shells (photos: Google Earth, P.J.M. Costa, C. M. Silva).

Marine boulder deposits

Marine-borne pebbles, cobbles and boulders found in Barranco and Furnas extend up to 250-300m inland from the berm crest (Table 1) above the spring high-tide line; they were not found at higher elevations, namely in the confining valley slopes. Their marine source is evidenced by well developed macrobioerosion sculpturing that includes ichnofossils produced by marine organisms such as clionid sponges (*Entobia* isp. bioerosion structures) and boring bivalves (*Gastrochaenolites* isp. bioerosion structures) as well as numerous *in situ* and extremely well preserved skeletal remains of the endolithic shallow marine *Petricola lithophaga* bivalve inside their original borings (Fig. 1D). These features indicate that each of these clasts has been originally sculptured and bored in a very shallow, infra- to low mesolittoral, non depositional and rocky marine environment, preceding its entrainment and redeposition inland and also suggest a recent date for its emplacement. Today, environments with these characteristics can be found along the western Algarve littoral. Most of the endolithic bivalve shells preserved *in situ* within the boulders showed both valves still articulated and clearly protruding outside their borings, sticking out above the host-rock surface. Given their fragile nature, this implies the absence of prolonged activity of downwearing of the boulders during transport and redeposition. This suggests simultaneous entrainment of coarse lithic particles from the shallow sea floor, rapid shoreward transport as

suspended load (with minimum particle-particle and particle-bottom interaction, therefore excluding sliding, rolling and frequent saltation) followed by deposition inland.

In order to search for a pattern of spatial distribution in size, a number of regularly spaced cross valley profiles were surveyed upstream of the beach at each site; the number of clasts bearing macrobioerosion features in each profile was noted and the largest boulders measured (Fig. 1A, B, Table 1). The results showed that there is no clear trend in size variation with distance, whereas the number of bored clasts is higher in the vicinity of the beach and rapidly drops further inland. These results are consistent with their lifting from the shallow marine zone and inland transportation excluding size selection and suggest that deposition was essentially a non-gradational process.

Table 1- Characteristics of boulders of Furnas and minimum height of tsunami (Ht) and wind (Hw) waves required to exceed the threshold of movement (see text for explanation).

Profile	A-axis (m)	B-Axis (m)	C-axis (m)	Distance to coast (m)	Volume (m ³)	Weight (kg)	Ht (m)	Hw (m)
P1	0.44	0.30	0.23	253	0.030	78.94	0.19	0.77
P2	0.40	0.33	0.16	234	0.021	54.91	0.29	1.16
	0.27	0.26	0.23	234	0.016	41.98	0.16	0.64
	0.56	0.30	0.18	234	0.030	78.62	0.23	0.92
P3	0.75	0.55	0.30	221	0.124	321.75	0.40	1.61
	0.44	0.33	0.28	221	0.041	105.71	0.19	0.77
P4	0.48	0.25	0.24	212	0.029	74.88	0.15	0.59
P5	0.60	0.30	0.17	203	0.031	79.56	0.24	0.96
	0.60	0.40	0.30	203	0.072	187.20	0.24	0.96
P6	0.60	0.50	0.30	183	0.090	234.00	0.34	1.37
	0.35	0.25	0.20	183	0.018	45.50	0.17	0.66
P7	0.40	0.18	0.15	171	0.011	28.08	0.13	0.53
P8	0.29	0.22	0.22	162	0.014	36.49	0.13	0.54
P9	1.60	1.00	0.50	156	0.800	2080.00	0.74	2.95
P11	0.48	0.36	0.15	140	0.026	67.39	0.35	1.41
P12	0.45	0.40	0.25	132	0.045	117.00	0.28	1.11
P13	0.76	0.40	0.40	127	0.122	316.16	0.19	0.78
P14	0.90	0.46	0.40	121	0.166	430.56	0.24	0.96
P15	0.80	0.54	0.25	109	0.108	280.80	0.45	1.82
P16	1.15	0.60	0.55	95	0.379	986.70	0.28	1.13

Entrainment and transport of boulders

Noormets et al. (2004) indicated that tsunamis as well as large swell waves are capable of quarrying large boulders from the rocky shore, provided that sufficient initial fracturing is present. However, wind waves are seldom capable of emplacing large blocks onto the emerged platform (due to the rapid disintegration of the waves after breaking) in contrast with tsunamis, which have longer duration and attain higher velocities (Goto et al., 2007 indicate 8 -15ms⁻¹ for the 2004 tsunami in Thailand).

Nott (1997, 2003) presented a set of equations relating the forces involved in the transport of submerged boulders in coastal areas. Application of these equations to the boulders of Barranco and Furnas indicate that low energy storms have the capacity to move them. The heaviest particle detected at Furnas could be moved by a storm with Hw of only 2.94m (Table 1). Moreover, all boulders could have been moved by wind waves smaller than 3m.

Komar and Miller (1974) and Soulsby (1997) addressed the issue of threshold wave height required to induce motion of particles resting in the sea floor and compared computed results with experimental data. Application of Airy wave theory in combination with the latter solutions to the most frequent boulder size (B-axis~0.3m) in both Algarve field sites indicates a threshold wave height of about 5m at depths of 3m (the same depth implied in Nott's

approach) and the height should increase to at least 8m in the case of the largest boulder (B-axis~1m). This set of results practically rules out a wind-generated wave origin for the boulder deposits, in clear contrast with the former conclusion. The large discrepancies found between results yielded by the two approaches may reside in different assumptions on the mode of particle threshold (sliding or rolling) and on the length scales of particles and of sea bottom roughness, issues that are not clearly discussed in those papers, but that Wiberg and Smith (1987) indicate as governing significant changes in near-bottom critical shear stress. Regardless the physical aspects, it is worth to note that the wave climate in the Algarve is one of low-energy. On average, once every winter a SW storm raises waves with significant height of about 3m and mean period of 7-8s (Capitão, 1992). Taking exceedance of threshold of movement according to Nott's solutions as implying the entrainment and landward transport of gravel particles from the nearshore during storms, formation of boulder storm-ridges and washovers with abundant perforated clasts containing *in situ* shells of endolithic marine bivalves and other bioerosion structures should be quite common during winter along the rocky coast of Algarve, and this is clearly not the case. In addition, there is a substantial difference between attaining the threshold of particle movement under waves and sustaining its continuous transportation upslope in the direction of wave travel for a distance exceeding several wavelengths. Based on the results and discussion stated above, we hypothesize a tsunami origin for the Barranco and Furnas boulders.

Conclusions

Boulders accumulated at Barranco and Furnas lowlands were entrained from the sea floor and rapidly transported without significant wearing out before redeposition up to 300m inland by an exceptionally high energy inundation episode. The deposit includes numerous bored particles with *in situ* shells of endolithic marine bivalves and other bioerosion structures, that show no trend in size variation with distance to the shore, though the number of bored clasts is higher in the vicinity of the beach and rapidly drops inland. These results are consistent with their lifting from the shallow marine zone and inland transportation excluding size selection and suggest that deposition was essentially a non-gradational process.

Application of two distinct threshold criteria resulted in contrasting values of minimum wave height required for particle entrainment and in different driving mechanisms (storm versus tsunami). The low-energy wave regime and nature of storm washovers in the Algarve coast suggest a tsunami as the most probable cause for the emplacement of these boulders.

References

- Capitão R. (1992). Wave climatology of the Portuguese coast. Clima de agitação marítima na costa portuguesa. Unp. Tech. Rep. NATO PO-Waves TFOM 10/92, Instituto Hidrográfico, Lisboa, 14 pp.
- Goto K., Chavanich S., Imamura F., Kunthasap P., Matsui K., Minoura K., Sugawara D. and Hideaki Y. (2007). Distribution, origin and transport process of boulders deposited by the 2004 Indian Ocean tsunami at Pakarang Cape, Thailand. Sed. Geol. 202, 821-837.
- Komar P. and Miller M. C. (1975). On the comparison of the threshold of sediment motion under waves and unidirectional currents with a discussion of the practical evaluation of the threshold. Jour. Sed. Petrology 45, 362-367.
- Noormets R., Crook K.A.W. and Felton E.A. (2004). Sedimentology of rocky shorelines: 3. Hydrodynamics of megaclasts emplacement and transport on a shore platform, Oahu, Hawaii. Sediment. Geol. 172, 41-65.
- Nott J.F. (1997). Extremely high-energy wave deposits inside the Great Barrier Reef, Australia: determining the cause — tsunami or tropical cyclone. Mar. Geol. 141, 193–207.
- Nott J.F. (2003). Waves, coastal boulders and the importance of the pre-transport setting. Earth Planet. Sci. Lett. 210, 269–276.
- Soulsby, R. (1997) – Dynamics of marine sand. A manual for practical applications. Thomas Telford, London, 249 pp.
- Wiberg P. and Smith J. D. (1987). Calculations of the critical shear stress for motion of uniform and heterogeneous sediments. Water Res. Research 23, 8, 1471-1480.

OSL dating of clastic deposits generated by extreme marine coastal floods (Algarve, Portugal)

P.P. Cunha^a, J.P. Buylaert^b, A.S. Murray^b, C. Andrade^c, M.C. Freitas^c, F. Fatela^c, J.M. Munhá^c & A.A. Martins^d

^a Dep. of Earth Sciences, Instituto do Mar, Univ. Coimbra, Portugal, pcunha@dct.uc.pt

^b Nordic Lab. for Luminescence Dating, Dep. of Earth Sciences, Aarhus Univ., Denmark

^c Univ. Lisboa, Faculdade de Ciências, Centro de Geologia, Portugal

^d Centro de Geofísica, Dep. Geociências Univ. Évora, Portugal

Project funding: NEAREST - EU-037110-GOCE-2006 and GETS FCT-PDTC/CTE-GEX/65948/2006

In order to investigate signatures of coastal high-energy single event deposition, capable of distinguishing between storm-and tsunami-induced flooding, and also to improve the database on the geological record of tsunami flooding of the Portuguese coast in the Late Holocene, two sites in the Algarve (South Portuguese coast) were investigated by the excavation of trenches, stratigraphic description and sampling for sedimentological, geochemical and biostratigraphical analysis, and for OSL dating. At both sites sand layers were identified, intercalated in estuarine muds. At the Boca do Rio site a ~10 cm-thick sand layer 80-115 cm below the modern surface has been previously identified as being deposited by the 1755 tsunami and dated by thermoluminescence (Dawson et al., 1995). The historical data indicates that this event occurred in full sunlight. More to the west, in a 1m deep trench excavated at Martinhal lowland, two sandy layers overlain by muds were also identified and sampled. The sedimentological characteristics of these sandy beds indicate a marine source (good sorting and richness in marine quartz and bioclasts); they are also presumed to have originated with extreme marine coastal floods.

Luminescence ages from the sandy layers were derived using a standard quartz SAR OSL protocol suitable for young samples. Coarse grained (180-250µm) quartz extracts were prepared using conventional sample preparation techniques. Measurements were made on large aliquots; the quartz OSL signal from this material is clearly dominated by the fast component. Preheat plateau and thermal transfer tests suggested preheat temperatures should be $\leq 220^{\circ}\text{C}$; a preheat of 200°C for 10s and a cut heat of 180°C was selected for all D_e measurements. The overall applicability of our measurement protocol was confirmed by dose recovery tests (measured to given dose ratios: 1.04 ± 0.02 , n=24). High resolution laboratory gamma-spectrometry was used to determine dose rates, which lie in the range 0.80 to 2.50 Gy·ka⁻¹. The preliminary ages are: Boca do Rio - 340 ± 20 y; Martinhal - 390 ± 30 y (upper level) and $1,560 \pm 80$ y (lower level); the younger two of these are taken to record the AD 1755 tsunami. Although the age of this event may be slightly overestimated, the offset is small, and gives us confidence that the earlier age obtained for a previous extreme coastal flood is accurate.

Dawson, A.G., Hindson, R., Andrade, C., Freitas, C., Parish, R. & Bateman, M. (1995) Tsunami sedimentation associated with the Lisbon Earthquake of November 1st 1755 AD: Boca do Rio, Algarve-Portugal. *The Holocene*, 5 (2), 209-215.

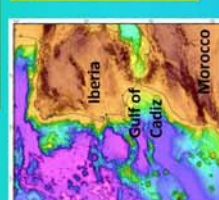
Scientific Poster

Geomorphologic domains of the Gulf of Cadiz from swath multibeam bathymetry

Valadares^{1,2}, P. Terrinha², J. C. Duarte^{1,2}, E. Grácia³, N. Zitellini⁴, M. A. Gutscher⁵, F. Rosas¹, L. M. Matias⁶

(1) ATTEST - ID - Lisbon, Portugal (2) DGM-METI - Lisbon, Portugal (3) UTM-CMIMA-CSIC, Barcelona, Spain, (4) SMAR-CNR, Bologna, Italy (5) IEM-UGBO-CNRS, Plouzané, France, (6) CGU - ID - Lisbon, Portugal

valadares@ineti.pt



卷之三

The SWIM bathymetric dataset covers an area of approximately 180,000km², was obtained after compilation of 19 multibeam bathymetry surveys. Terrain analysis and detailed morphological interpretation of this dataset, on a 100m cell-size map allowed the identification of a diversity of morphological domains that result from the combined or individual action of oceanographic, sedimentological and tectonic processes. The available multi-channel seismic reflection profiles, high resolution profiles and the multibeam probe backscatter images were also used to establish the different

Morphotectonic Domains

卷之三

The Gulf of Cadiz shows three different morphologies: the Central longitudinal part of the Gulf of Cadiz shows three different morphologies: the Sesmeiro Abyssal Plain, the mouth of the South Portugal canyons and the accretionary wedge. In the East, the interaction of the Mediterranean Outflow Water (MOW) with the continental shelf creates erosional and depositional features that extend as continental bodies along the South and Southwestern Portuguese slope, as well as sedimentary features that mask undulate surface of the accretionary wedge. The Northern part of the Gulf of Cadiz exhibits the Portuguese shelf, the deeply incised continental slope and the MOW contours of a positionnal system. Scattered structures of mass transport deposits exist throughout the Gulf of Cadiz and its southwest Portuguese Margin, generally associated with active fault

18

Upper slope The upper slope corresponds to the continental shelf borders the northern and southern margins of the Gulf of Cadiz as a relatively smooth, shallow, gently dipping part of the sea.

Tallers The Cadiz Valley is a flat, relatively smooth and wide valley that displays minor structures and is inferior formed by bottom currents and sediment instabilities.

The Horseshoe Valley is very gently dipping (below 0.3°) and its bottom is very wide.

between 20 and

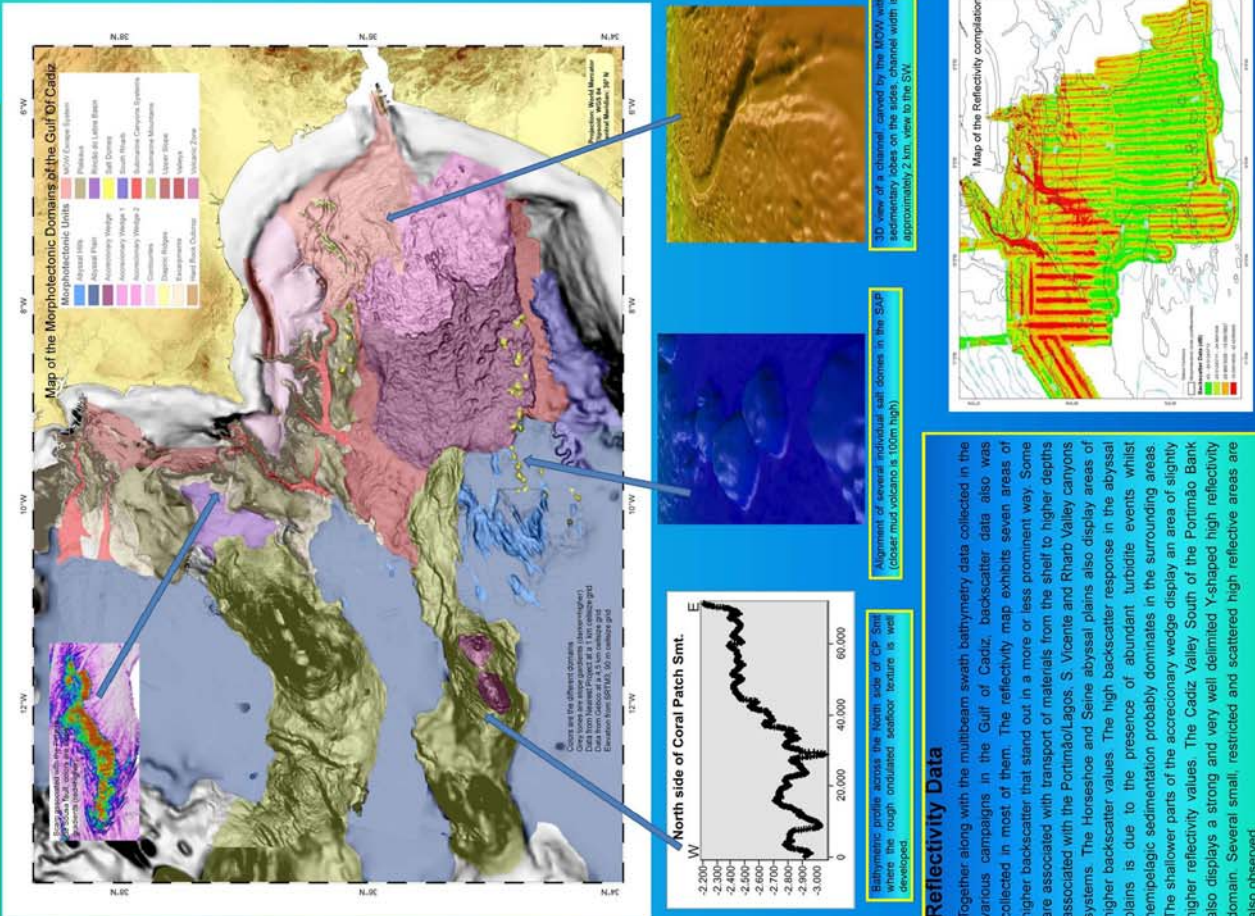
This domain is characterized by the outcrop of basement rock in two areas one near the Marqués de Pontevedra and the Pereira de Sousa fault scarps. It is relatively flat, dips gently to the West and has a N-S orientation. The basement consists of the Gorringe Submarine Mountain, the Marques de Pontevedra plateau and the Pereira de Sousa fault scarps. It is relatively flat, dips gently to the West and has a N-S orientation.

contourites

contourlines present a very smooth and flat surface (less than 1°) with a well defined steep front that can reach up to 7°. They occur in the shallow parts of the area South of Agarveiro, east of 7° 30' W, extending in length more than 150 km. There are 3 bodies: Faro, Abuleira and Pombaline drifts. They are related to the MOW currents and their interaction with continental slope.

This is a comic

This domain is made up of two volcanic edifices of basaltic nature that seat on top of the Corral Patch Seamount. They display a distinct seabed texture probably related to the presence of lava flows or other volcanic related formations.



Reflectivity Data

Together along with the multibeam swath bathymetry data collected in the various campaigns in the Gulf of Cadiz, backscatter data also was collected in most of them. The reflectivity map exhibits seven areas of higher backscatter that stand out in a more or less prominent way. Some are associated with transport of materials from the shelf to higher depths associated with the Portimão/Lagos, S. Vicente and Riaibr Valley canyons systems. The Honeymoon and Saine abyssal plains also display areas of higher backscatter values. The high backscatter response in the abyssal plains is due to the presence of abundant turbidite events whilst hemipelagic sedimentation probably dominates in the surrounding areas. The shallower parts of the accretionary wedge display an area of slightly higher reflectivity values. The Cadiz Valley South of the Pontimão Bank also displays a strong and very well delimited Y-shaped high reflectivity domain. Several small, restricted and scattered high reflective areas are also observed.

Material to distribute



NEAREST (2006-2009) – EC project of the 6° FP

Coordinator: Consiglio Nazionale delle Ricerche – ISMAR
Nevio Zitellini

Partners:



Alfred Wegener Inst. für Polar und Meeresforschung
(Germany)



Consejo Superior de Investigaciones Científicas
(Spain)



Technische Fachhochschule Berlin
(Germany)

Université de Bretagne Occidentale
(France)



Istituto Nazionale di geofisica e Vulcanologia
(Italy)

Universidad de Granada – Instituto Andaluz de Geofísica
(Spain)



Centre National pour la Recherche Scientifique et Technologique
(Morocco)

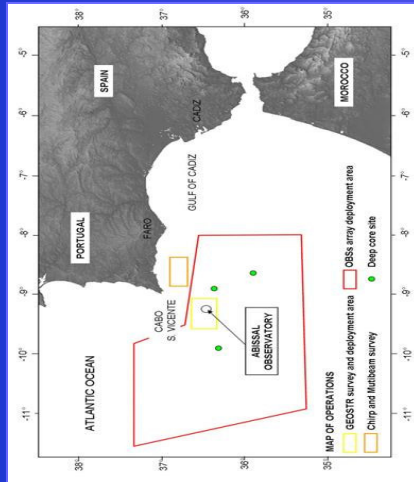


Istituto de Meteorologia
(Portugal)

XISTO Développement S.A.
(Portugal)



Integrated Observations from NEAR shore sources of Tsunamis: towards an early warning system



NEAREST project is addressed to the identification and characterization of potential tsunami sources located near shore in the Gulf of Cadiz; the improvement of near-real time detection of signals by a multiparameter observatory for the characterisation of potential tsunamigenic sources to be used in the development of an Early Warning System (EWS) Prototype;

the improvement of integrated numerical models enabling more accurate scenarios of tsunami impact and the production of accurate maps in selected areas of the Algarve (SW Portugal), highly hit by the 1755 tsunamis. In this area, highly populated and prone to devastating earthquakes and tsunamis, excellent geological/geophysical knowledge has already been acquired in the last decade. The methodological approach will be based on the cross-checking of multiparameter time series acquired on land by seismic and tide gauge stations on the seafloor and in the water column by broad band Ocean Bottom Seismometers and a multiparameter deep-sea platform, this latter equipped with real-time communication to an onshore warning centre. Land and sea data will be integrated to be used in a prototype of EWS. NEAREST will search for sedimentological evidence of tsunamis events and will try to measure the key parameters for the comprehension of the tsunami generation mechanisms. The proposed method can be extended to other near-shore potential tsunamigenic sources, as for instance the Central Mediterranean (Western Ionian Sea), Aegean Arc and Marmara Sea.

<http://www.nerest.bo.ismar.it>

The 1755 Lisbon earthquake



The 1755 Lisbon earthquake, known as the Great Lisbon Earthquake, took place on November 1, 1755 at around 9:40 AM. The earthquake was followed by a tsunami and fire, which caused near-total destruction of Lisbon, Portugal and adjoining areas.

A devastating fire following the earthquake destroyed a large part of Lisbon, and a very strong tsunami caused heavy destruction along the coasts of Portugal, southwest Spain, and western Morocco. Moderate damage was done in Algiers and in southwest Spain. Shaking was also felt in France, Switzerland, and Northern Italy.

The geologists estimate for the Lisbon earthquake a Richter Magnitude of 9, with epicenter in the Atlantic Ocean about 200 km west-southwest of Cape St. Vincent. Death toll is estimated between 60,000 to 100,000 people. The Lisbon earthquake is still at present the most destructive in history.

What is a tsunami ?

A tsunami is a series of waves created when a water mass in an ocean basin, is rapidly displaced. Submarine earthquakes, eruptions and landslides have the potential to generate a tsunami.

A tsunami has a much smaller amplitude (wave height) offshore, and a very long wavelength (often hundreds of kilometers long). So they generally pass unnoticed at sea, forming only a slight swell usually about 300 mm above the normal sea surface. A tsunami can occur at any state of the tide and even at low tide state can inundate coastal areas as well.

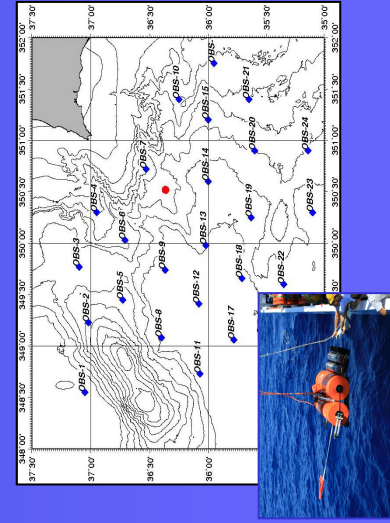
The effects of a tsunami can be devastating due to the immense volumes of water and energy involved.

The NEAREST pilot experiment

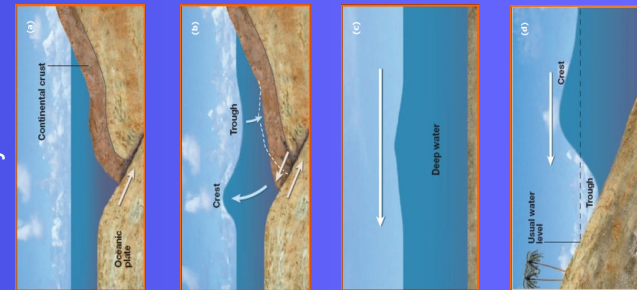
In the framework of the NEAREST project, a long-term Pilot Experiment of integrated land-marine monitoring was planned. The experiment is dedicated both to long-term acquisition of seismological data in the area of the tsunamigenic sources of the Lisbon 1755 earthquake and to validate a prototype of *tsunameter*. Started in August '07, the experiment is still on-going and will last till August '08.

The GEOSTAR observatory, manoeuvred from ship-board through the special vehicle MODUS, was deployed south-west of Cape St. Vincent for a multidisciplinary monitoring (geophysical and oceanographic). GEOSTAR relies on a surface buoy for the communication to land and transmits short messages on the status of the observatory and parameters of significant events.

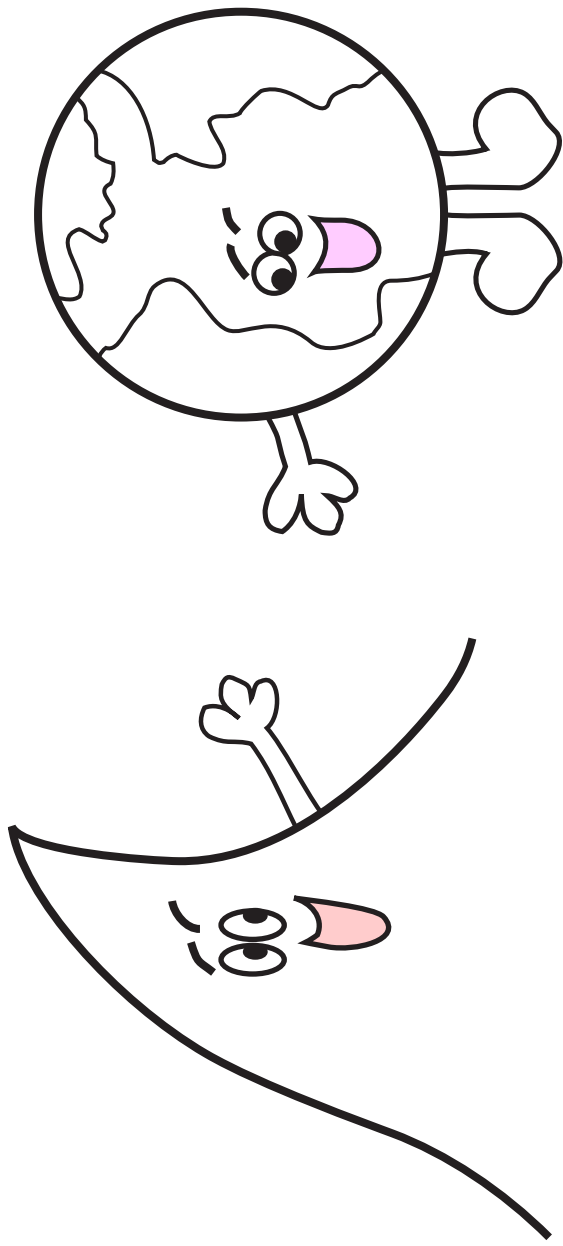
In the NEAREST Pilot Experiment, GEOSTAR was equipped for the first time with an innovative *tsunameter* able to detect pressure variations in deep water related to earthquake kick-off by automatically cross-checking the seismological signals and the water pressure variations.



Around GEOSTAR, over a large area (about 240 x 200 km) off Portugal and Morocco including the seismogenic source of the Lisbon earthquake, 25 Ocean Bottom broad-band Seismometer and Hydrophones (OBS-H) were distributed in order to carry out a long-term seismological monitoring.



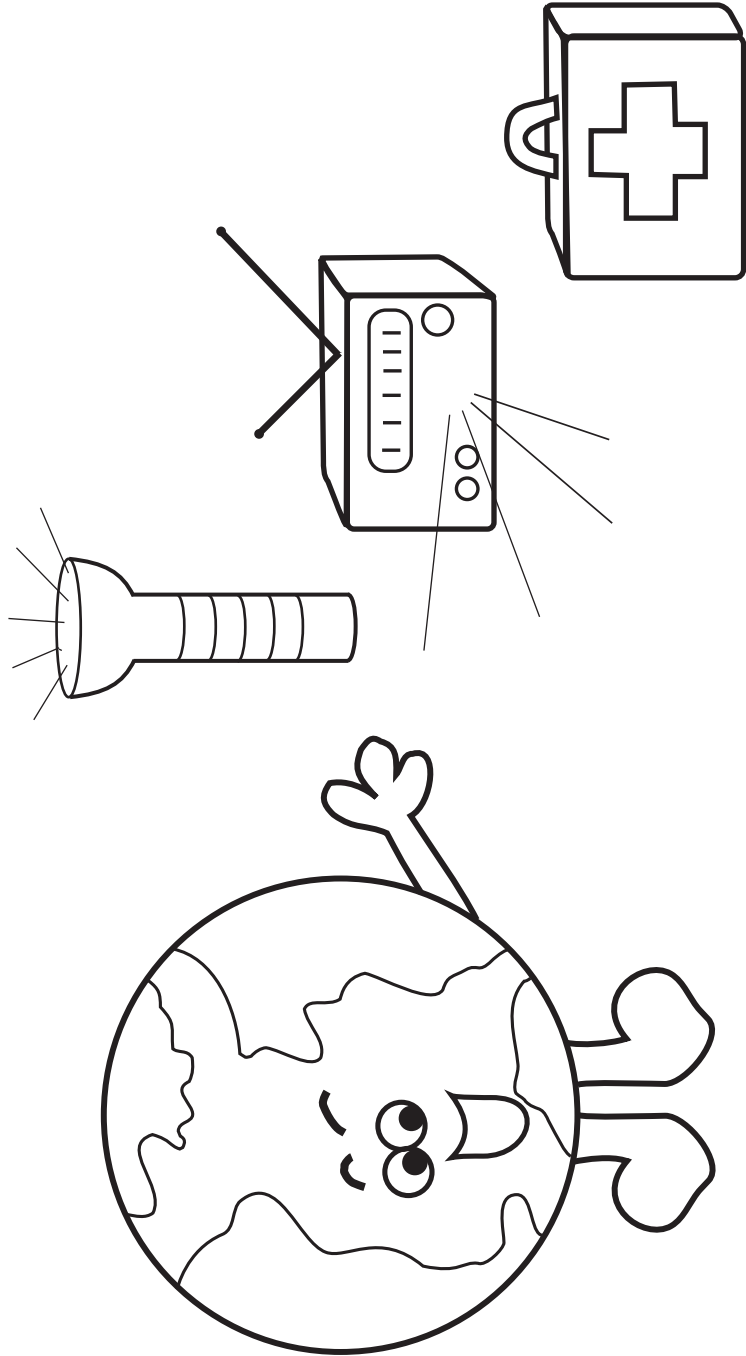
PRESENTING.....



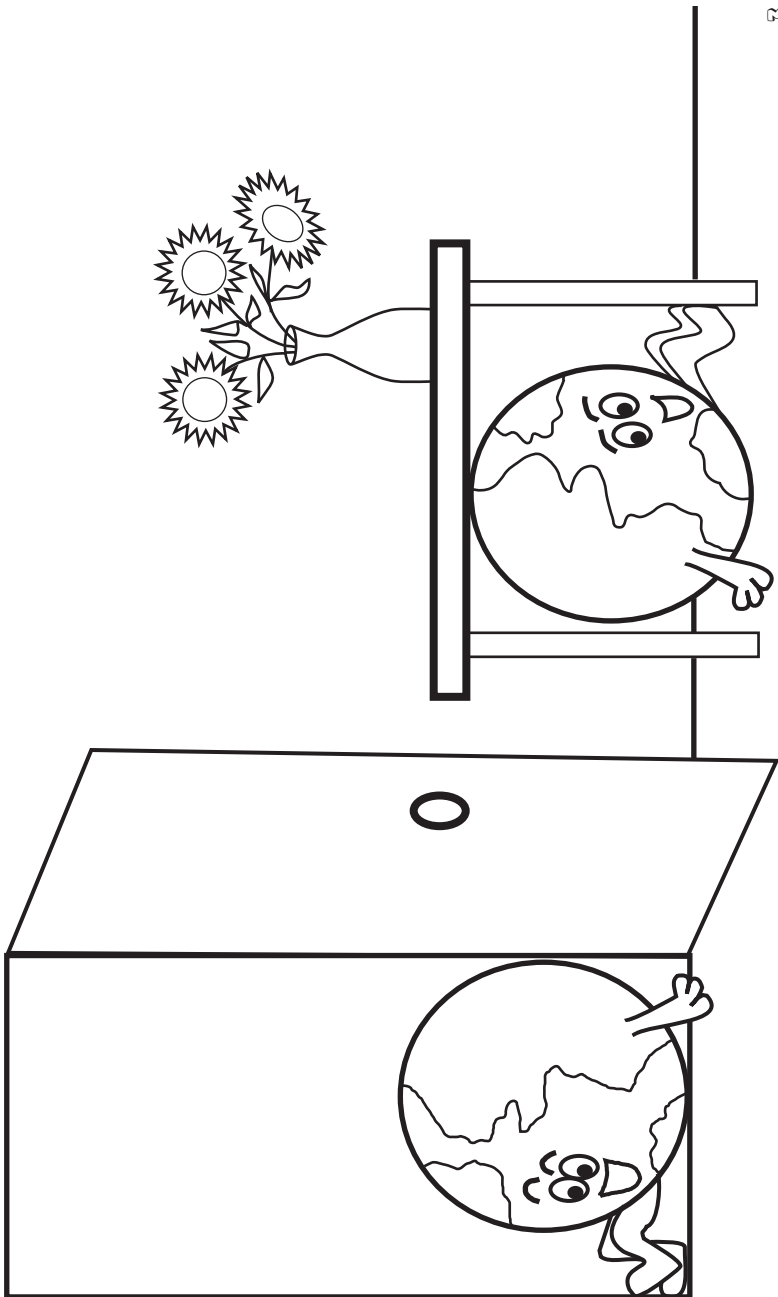
ERNIE
AND
EARTHQUAKE

TOMMY
AND
TSUNAMI

ERNIE EARTHQUAKE SAYS BE PREPARED!
HAVE A FLASHLIGHT, RADIO AND
FIRST AID KIT HANDY!

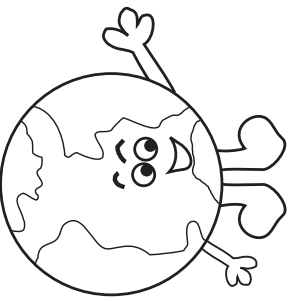


SAFEST PLACE DURING AN EARTHQUAKE
IS IN A DOORWAY OR UNDER A
DESK OR TABLE



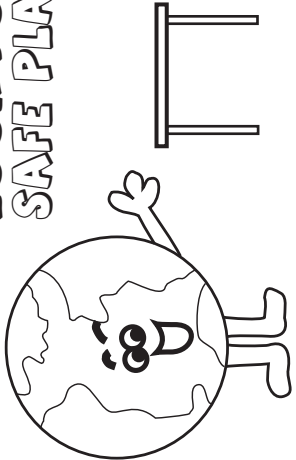
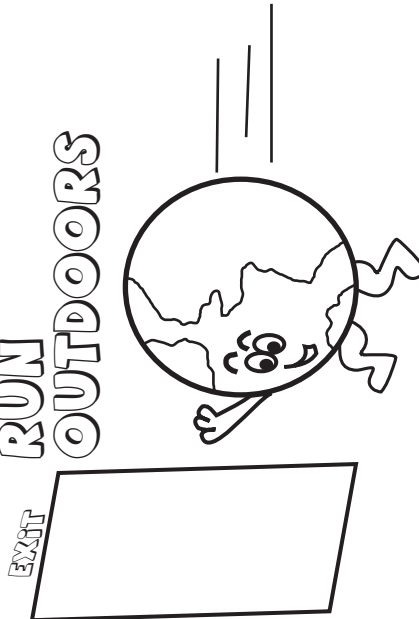
DURING EARTHQUAKES

DON'T 

DO 

STAY COOL
AND CALM
LISTEN TO
INSTRUCTIONS

IF INDOORS -
STAY THERE...
LOOK FOR A
SAFE PLACE



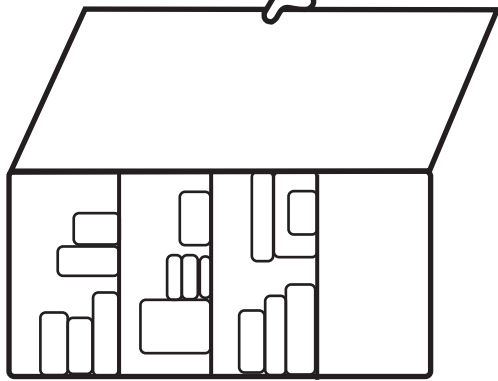
AFTER AN EARTHQUAKE HITS...

- 1) CHECK FOR FIRE AND FIRE HAZARDS
- 2) DO NOT TOUCH DOWNED POWER LINES
- 3) CLEAN UP SPILLED MEDICINES AND OTHER COULD-BE HARMFUL MATERIALS

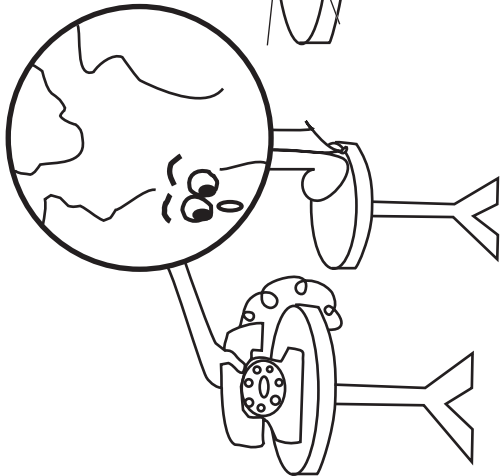


AFTER AN EARTHQUAKE

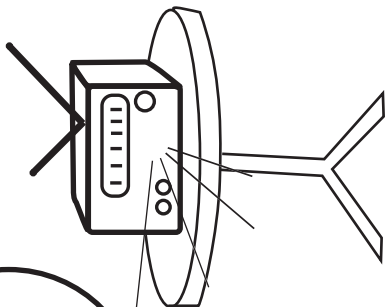
CAREFULLY CHECK
CLOSET AREAS FOR
FALLEN OBJECTS

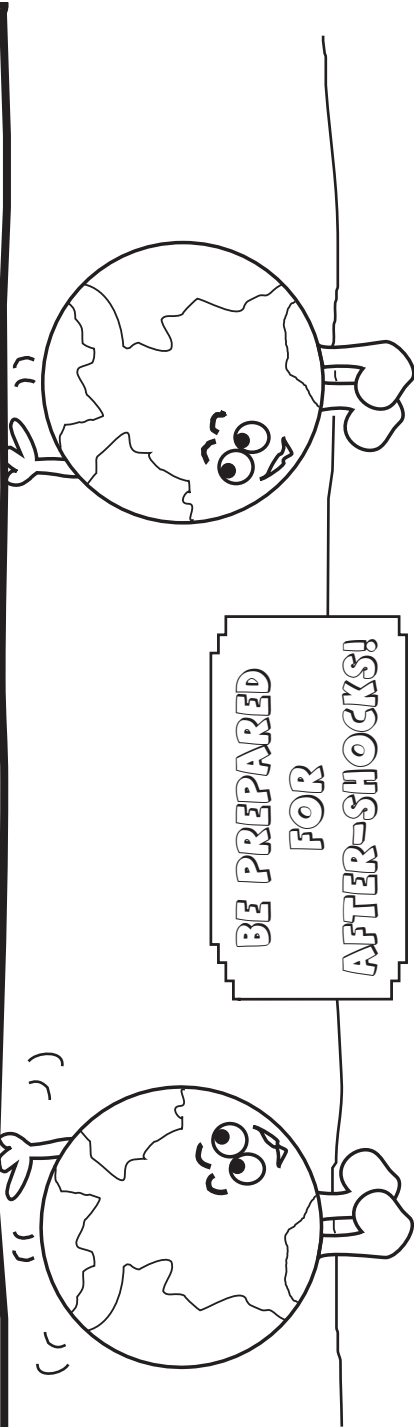
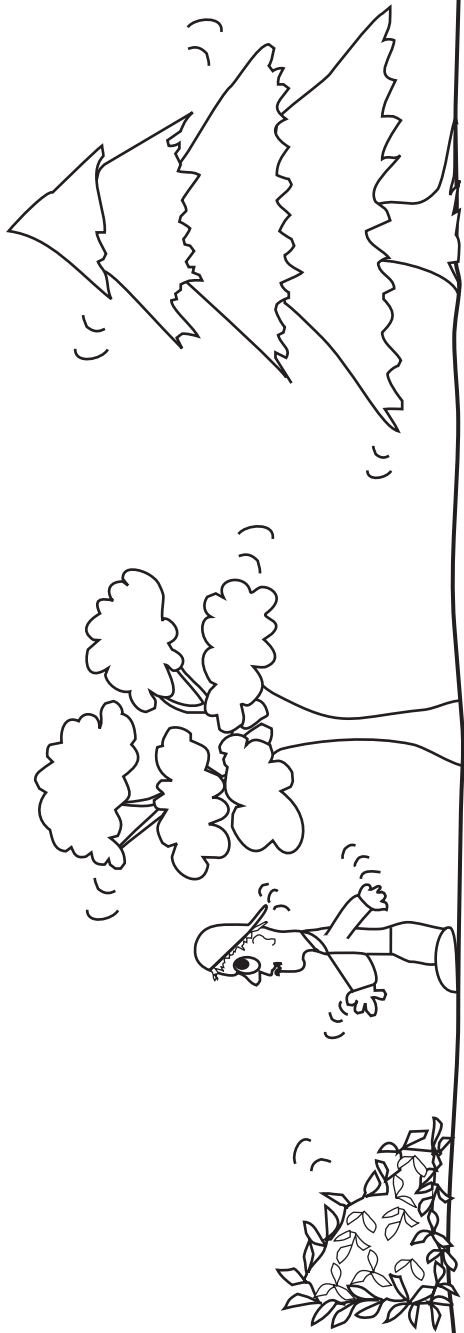


DON'T USE THE
PHONE, EXCEPT IN
EMERGENCIES



STAY TUNED TO
THE RADIO
FOR NEWS





BE ON THE LOOK-OUT!
ONCE AN EARTHQUAKE ARRIVES,
LARGE WAVES, KNOWN AS TSUNAMIS
COULD BE ON THE WAY.



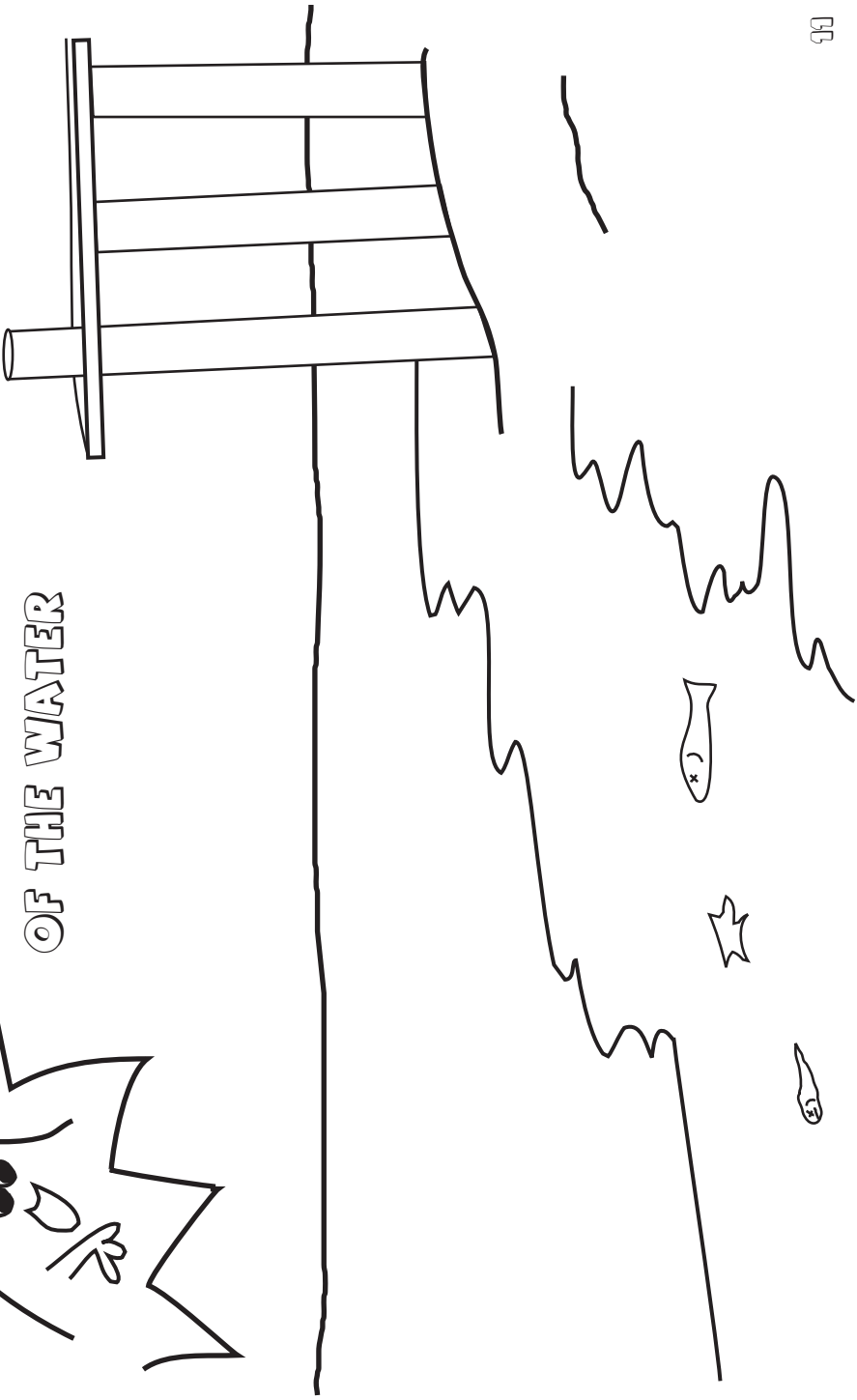
TOMMY TSUNAMI SAY'S:
ALL TSUNAMIS CAN BE
HARMFUL



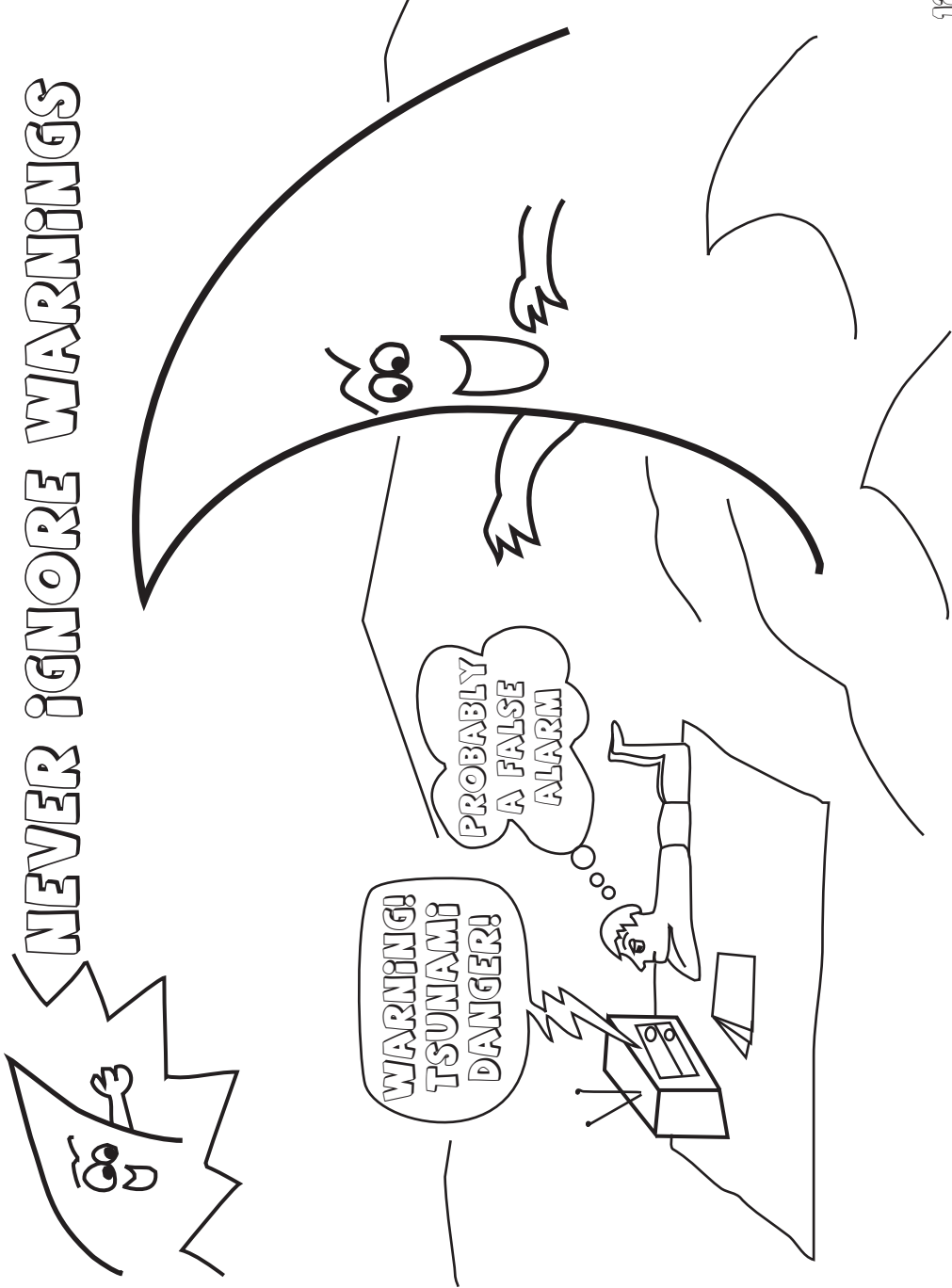
TOMMY TSUNAMI SAYS:
A TSUNAMI ISN'T JUST ONE WAVE
BUT MANY—STAY CLEAR OF
DANGER AREAS!



A SIGN OF UPCOMING TSUNAMIS
IS A SUDDEN RISE OR FALL
OF THE WATER



NEVER IGNORE WARNINGS

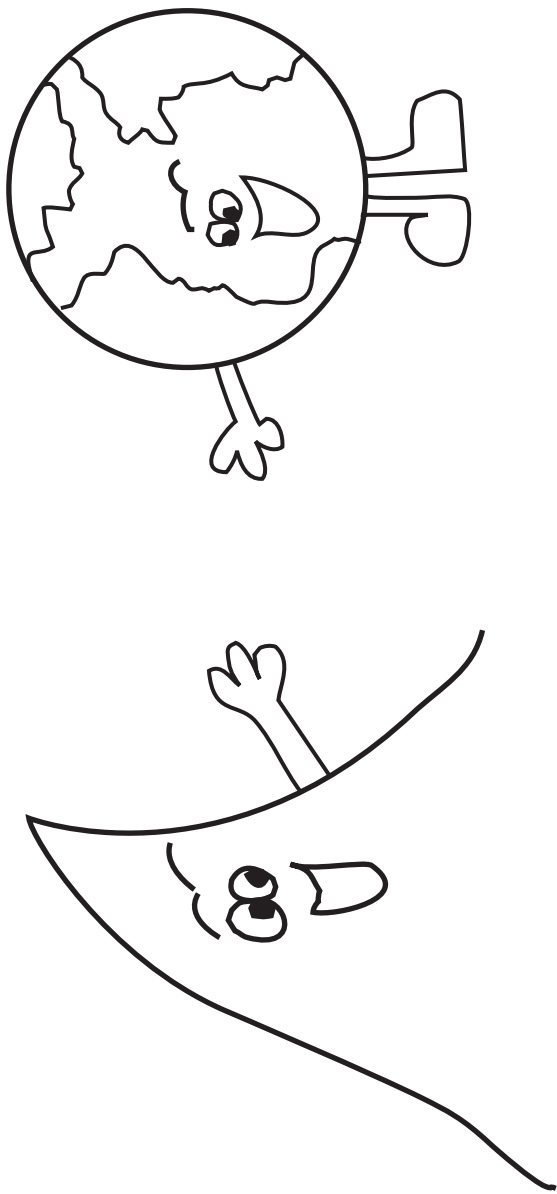




SOONER OR LATER

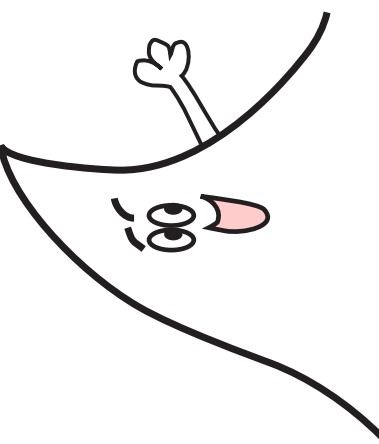
TSUNAMIS VISIT EVERY COASTLINE

**TOMMY TSUNAMI AND ERNIE EARTHQUAKE
WANT YOU TO BE PREPARED AND NOT
AFRAID OF THEIR UNEXPECTED VISITS**



ORIGINAL CONCEPT AND DRAWINGS

BY

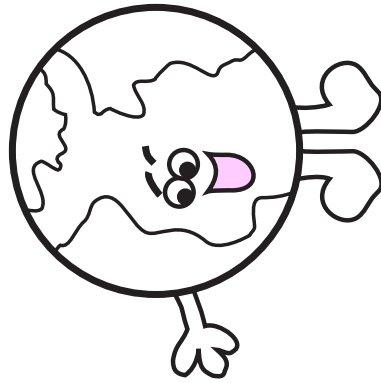


JEWELL HERMON

PDF VERSION

BY

KAREN BIRCHFIELD

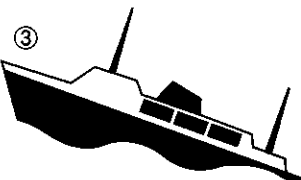


TSUNAMI TRIVIA

(soo-nam-ee)

Circle the correct answer(s):

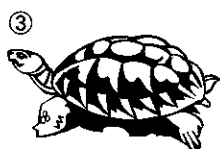
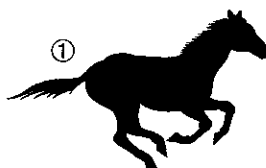
A Tsunami is caused by:



Circle the official tsunami warning sign.



Circle the picture which travels about the same speed as a tsunami.



Circle the states that can experience a tsunami.



Test your detective skills.

Circle the words listed below in the word search puzzle.

Beach	Run uphill
Earthquake	Safe area
Fast	Sand
Geology	Tsunami
Giant wave	Warning
Ocean	Water

H	A	V	E	F	G	R
T	S	U	N	M	I	U
W	A	T	E	U	A	N
A	G	N	A	T	N	U
R	E	T	S	H	W	P
N	O	E	A	S	A	H
I	L	B	F	Q	V	I
N	O	N	E	U	W	L
G	O	E	A	A	A	O
A	Y	C	R	K	D	E
D	A	B	E	C	H	T
B	Y	F	A	S	T	O

List the 25 unused letters to decode the message



 United Nations Educational, Scientific and Cultural Organization



International
Tsunami
Information Centre

Intergovernmental
Oceanographic
Commission (IOC)
United Nations Educational, Scientific and Cultural
Organization (UNESCO)

1, rue Miollis
75 735 Paris Cedex 15
France
Tel: +33 1 45 68 39 83
Fax: +33 1 45 68 58 12
<http://ioc.unesco.org>



United Nations
Educational, Scientific and
Cultural Organization



2005

1945

ACKNOWLEDGMENTS

The International Coordination Group for the Tsunami Warning System in the Pacific of the Intergovernmental Oceanographic Commission of UNESCO, at its Thirteenth Session in Ensenada, Mexico (September 1991), encouraged the preparation of a book designed to inform young persons about tsunamis, the dangers which they present, and what should be done to save lives and property.

The authors of this book are Dr. George Pararas-Carayannis, Ms. Patricia Wilson, and Mr. Richard Sillcox, and the illustrations were created by Mr. Joe Hunt.

To learn more about tsunamis and what you should do when a tsunami is coming, we encourage you to read *The Great Waves*.

This book was revised by the International Tsunami Information Centre in June 2005, and reprinted with the support of the Hawaii State Civil Defense and the U. S. National Tsunami Hazard Mitigation Program.

Bibliographic reference:

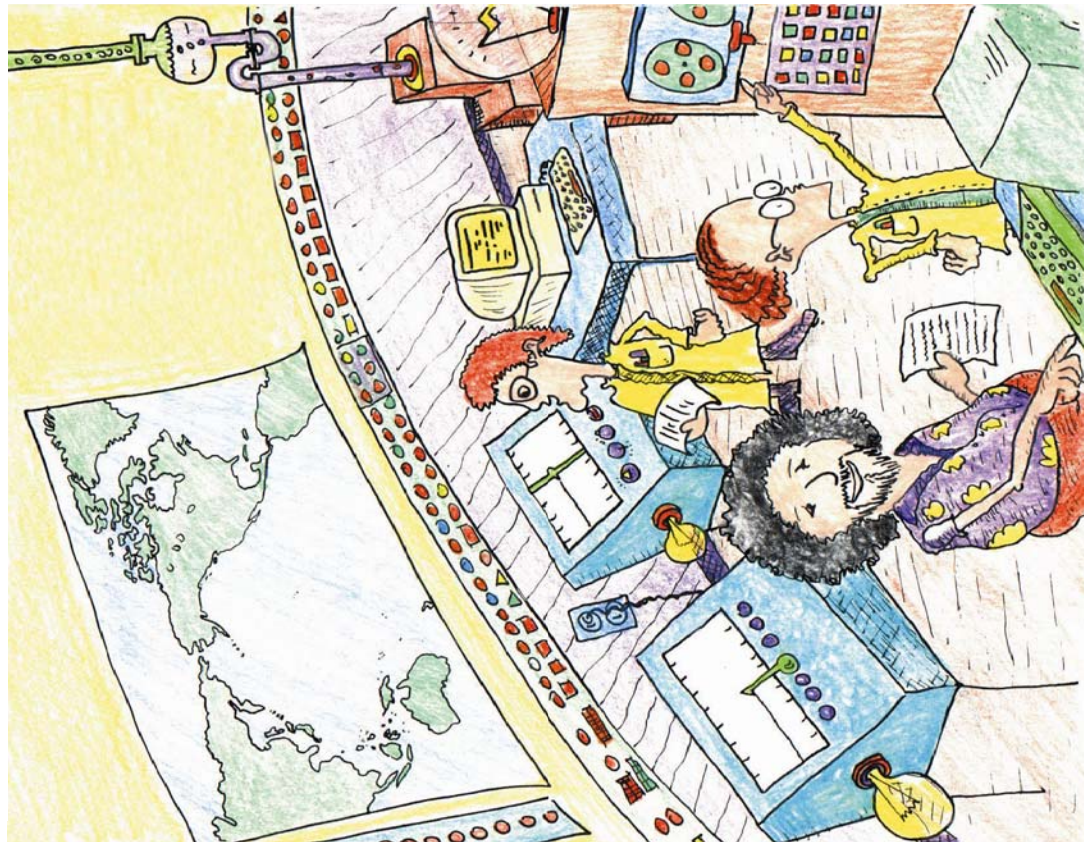
UNESCO-IOC. Tsunami Warning! IOC Information Document No. 1223 (IOC/INF-1/223)
Printed by: Hawaii State Civil Defense
© 2005



United Nations
Educational, Scientific and
Cultural Organization

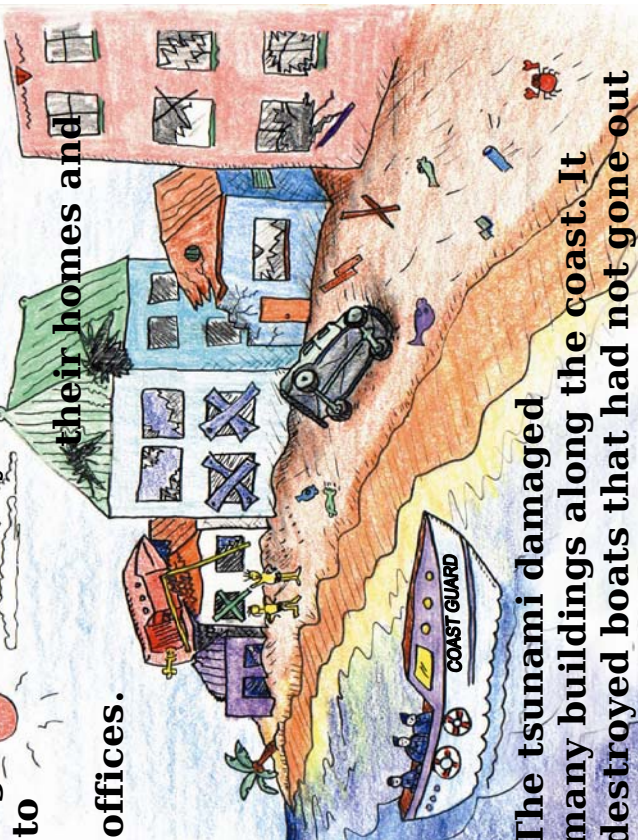


International Tsunami
Information Centre
737 Bishop St., Suite #2200
Honolulu, Hawaii 96813,
U.S.A.
Tel: <1> 808-532-6422
Fax: <1> 808-532-5576
E-mail:
itic.tsunami@noaa.gov



It is nice to know that the scientists at tsunami warning centers are always on watch for the next sign of a tsunami to protect lives today and in the future.

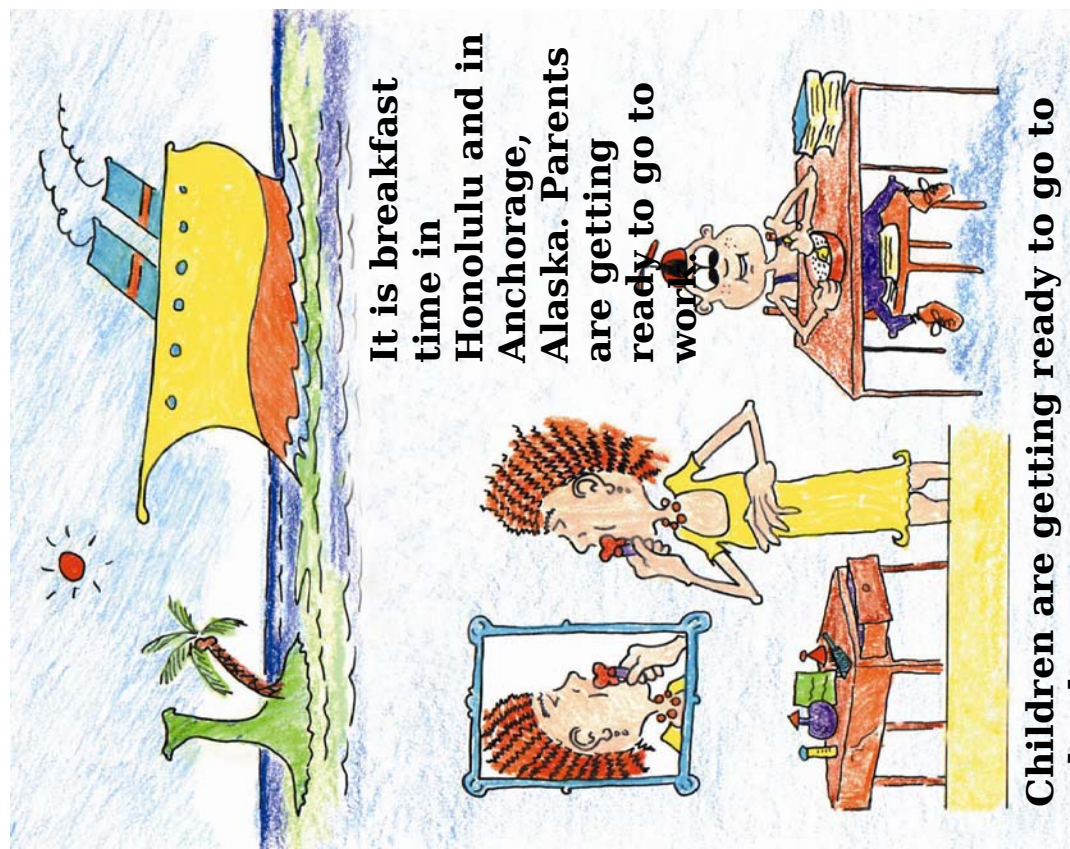
When the tsunami waves become small and do not cause any damage, the Pacific Tsunami Warning Center cancels the TSUNAMI WARNING. Everyone must still wait for the Civil Defense to sound the "ALL-CLEAR" signal to tell everyone it is safe to return to their homes and offices.



The tsunami damaged many buildings along the coast. It destroyed boats that had not gone out to sea. It tossed cars around like they were toys. It tore open walls and roofs of buildings and flooded all the inundation zones.

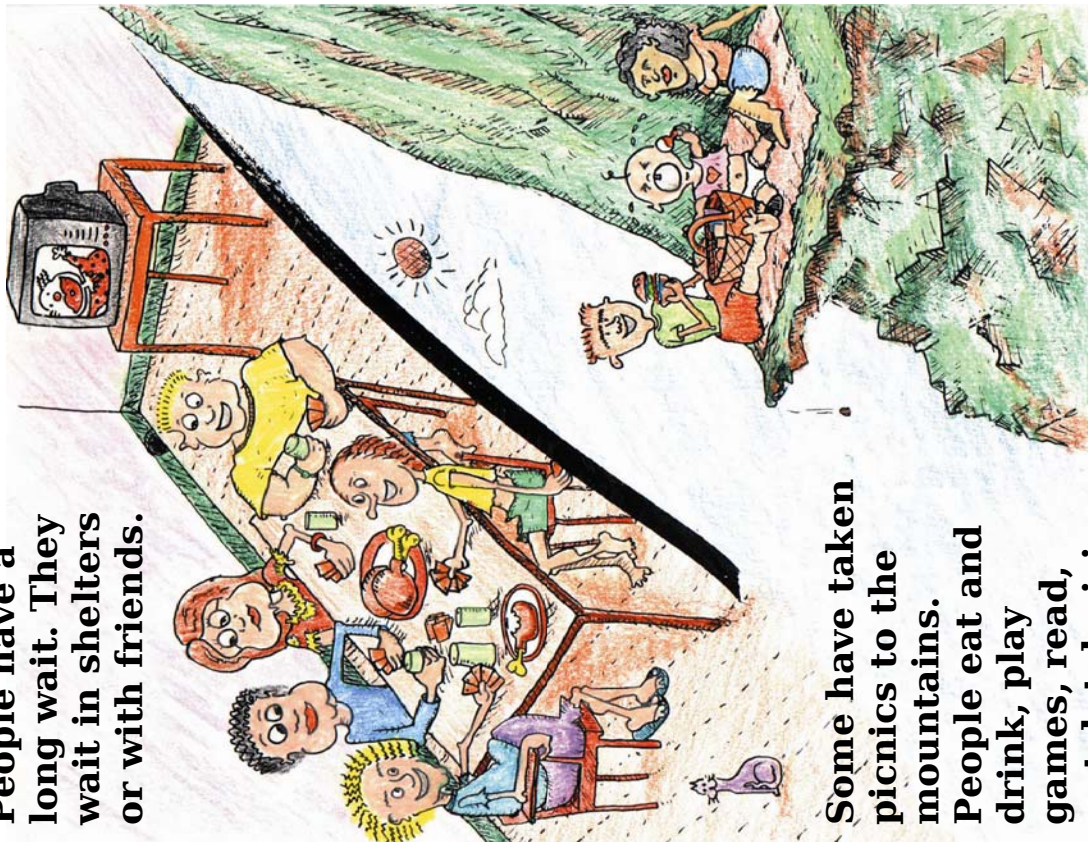
Everyone was glad that no one was hurt. They were prepared and knew what to do.

Over the blue, calm water of the Pacific Ocean, a cruise ship is sailing towards Hawaii. It is warm and sunny in Honolulu. A



Children are getting ready to go to

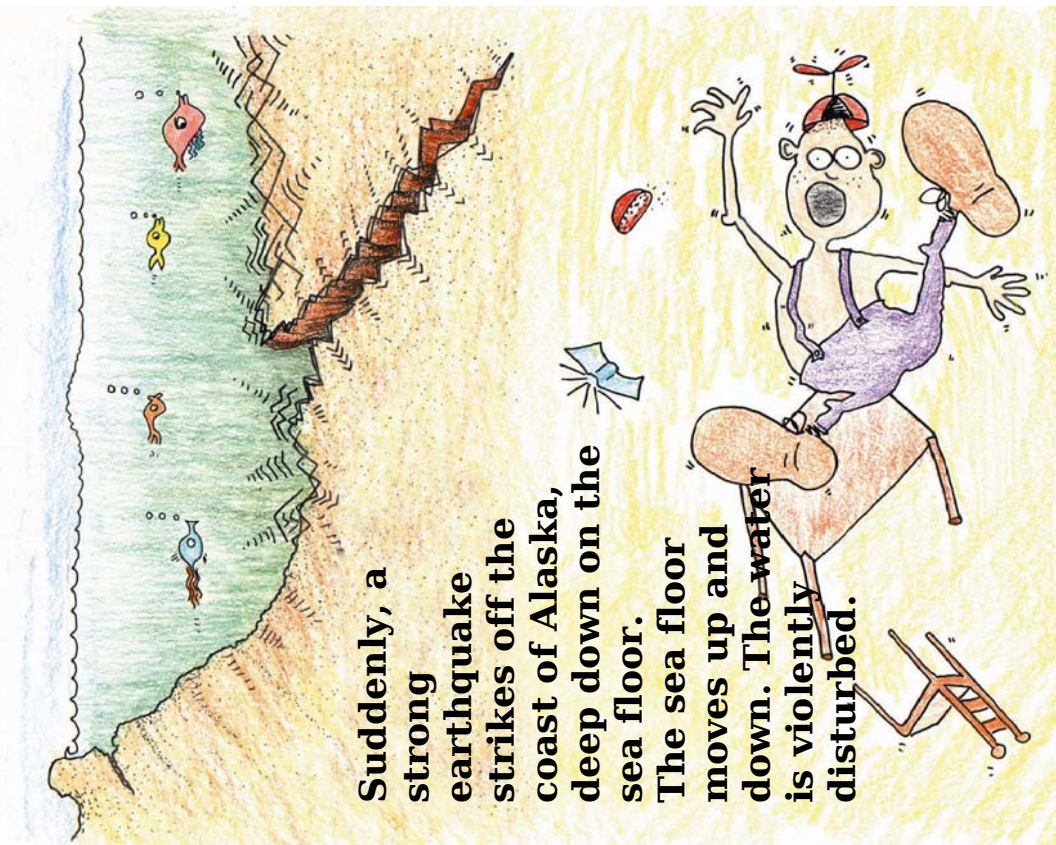
People have a long wait. They wait in shelters or with friends.



Some have taken picnics to the mountains. People eat and drink, play games, read, watch television or listen to the radio. They wait anxiously for the Civil Defense to sound the "ALL-CLEAR" signal.

Suddenly, a strong earthquake strikes off the coast of Alaska, deep down on the sea floor.

The sea floor moves up and down. The water is violently disturbed.



In Alaska, the walls and floors of the houses suddenly start to shake. Chairs topple over. Things rattle and break. Dishes crash to the floor.

At 12 noon, the first tsunami wave arrives. Around some parts of Hawaii, coral reefs help to break the

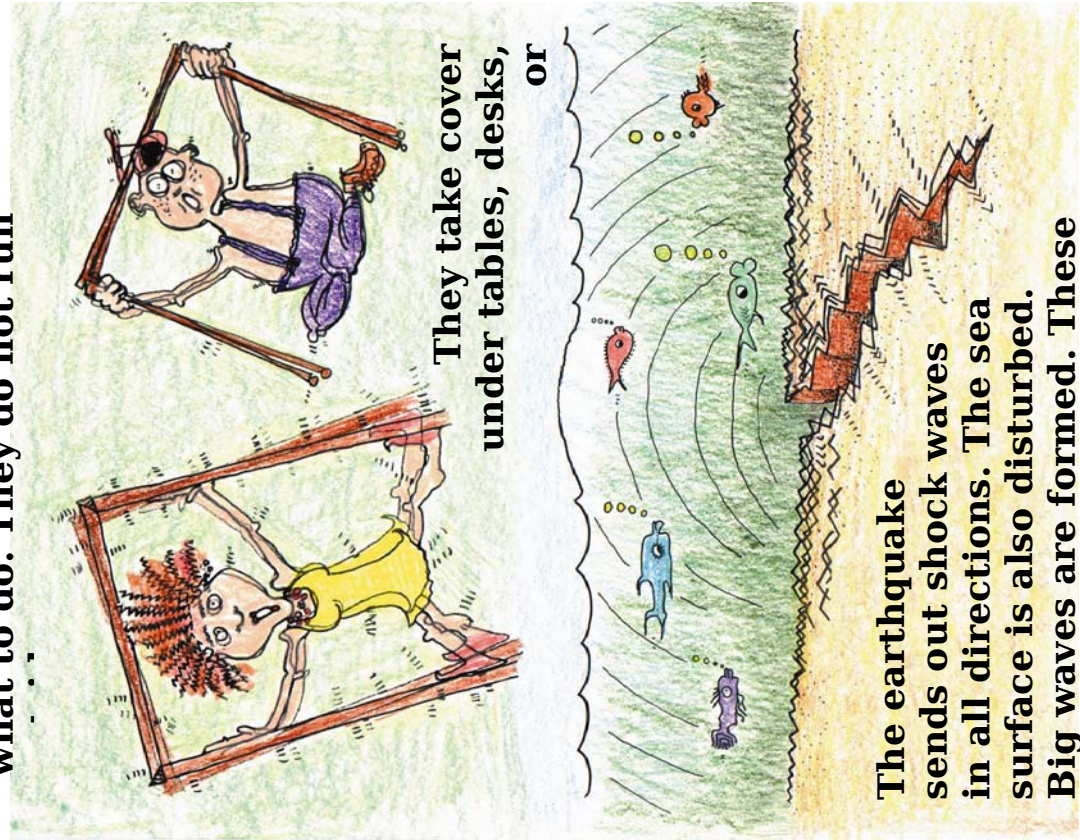


.. Some shores are protected by trees and mangrove forests which lessens the wave force even more. But the waves in these areas can still be large and



But at bays, the waves can be very big because the sides of the bay shorten the length of the wave and push it upwards. There are six waves in this tsunami

It is an earthquake! People know what to do. They do not run

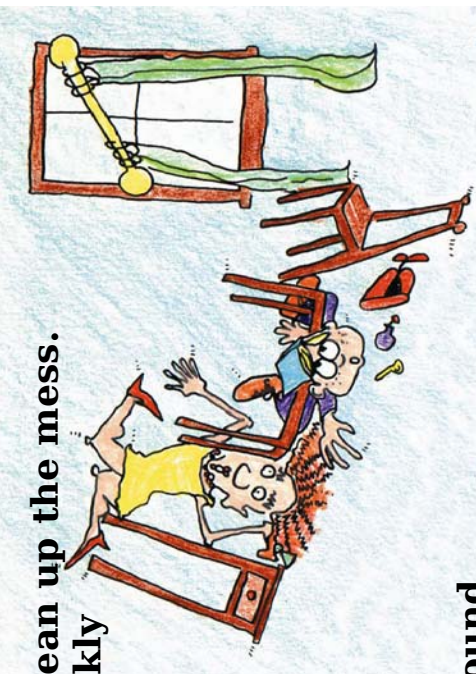


They take cover under tables, desks, or

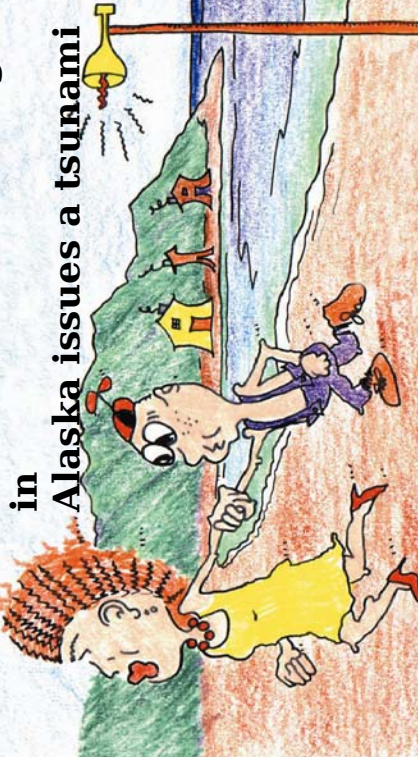
The earthquake sends out shock waves in all directions. The sea surface is also disturbed. Big waves are formed. These powerful waves are called tsunami. These waves travel fast across the sea.

When the shaking stops, people living by sea know what to do. They do not start to clean up the mess.

They quickly leave their homes and move inland away from water to higher ground.

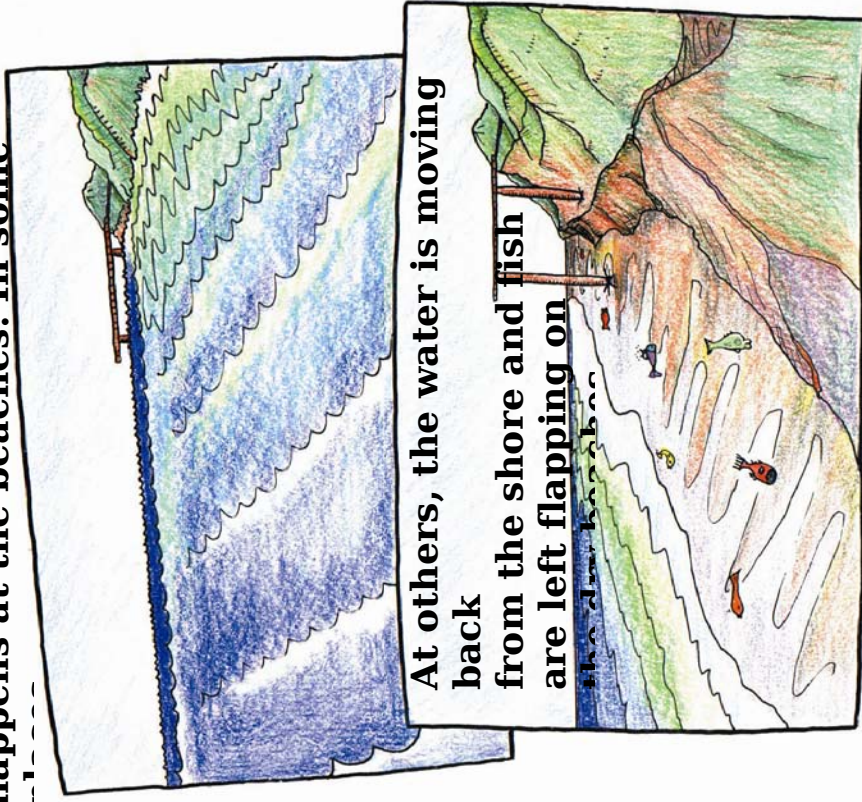


The Tsunami Warning Center in



Then the Alaska Emergency Operations Center sounds sirens to warn people a tsunami is expected. There is not much time. People hurry to safety, away from the

A few minutes later something strange happens at the beaches. In some



At others, the water is moving back from the shore and fish are left flapping on the sand.

Both rising water and receding water are sure signs that a tsunami is arriving soon.

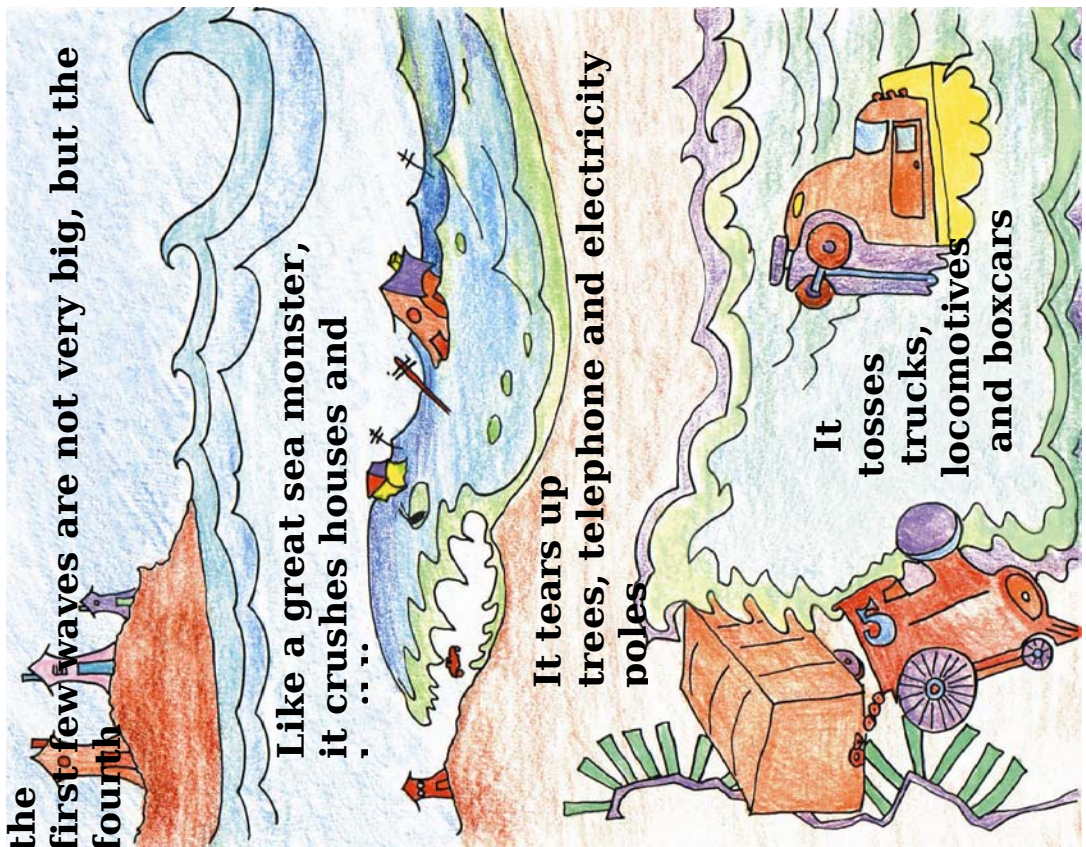
At 11 o'clock, the sirens wail again. The first tsunami wave is expected in less than one hour. Police are busy checking that everyone has evacuated.

They make sure no one has been left behind in the inundation zones. Then they block off the roads so no



At 11:30 a.m., the sirens sound for the last time. There is nothing left to do but wait. Everyone expects the first wave to come

The waves of the tsunami start to roll in 10 minutes after the earthquake. This time the first few waves are not very big, but the fourth

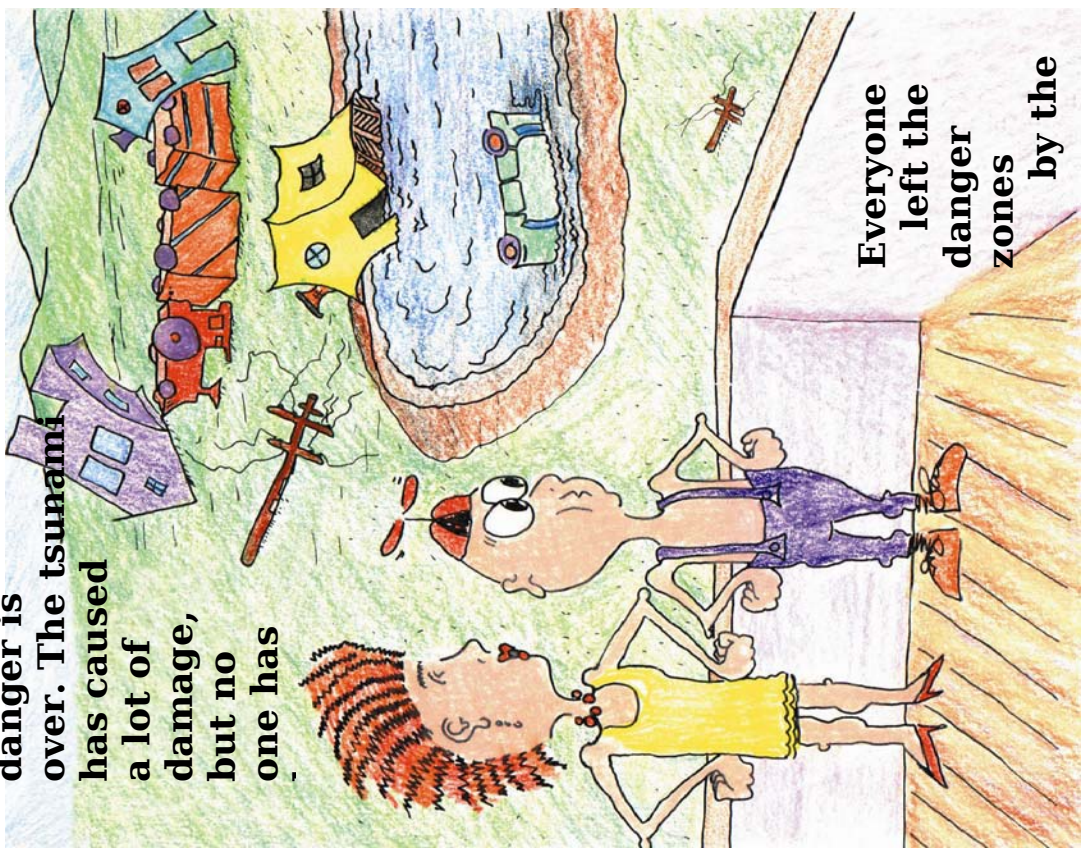


as it sweeps over the land for about a kilometer (km). It pushes and floods everything over a kilometer

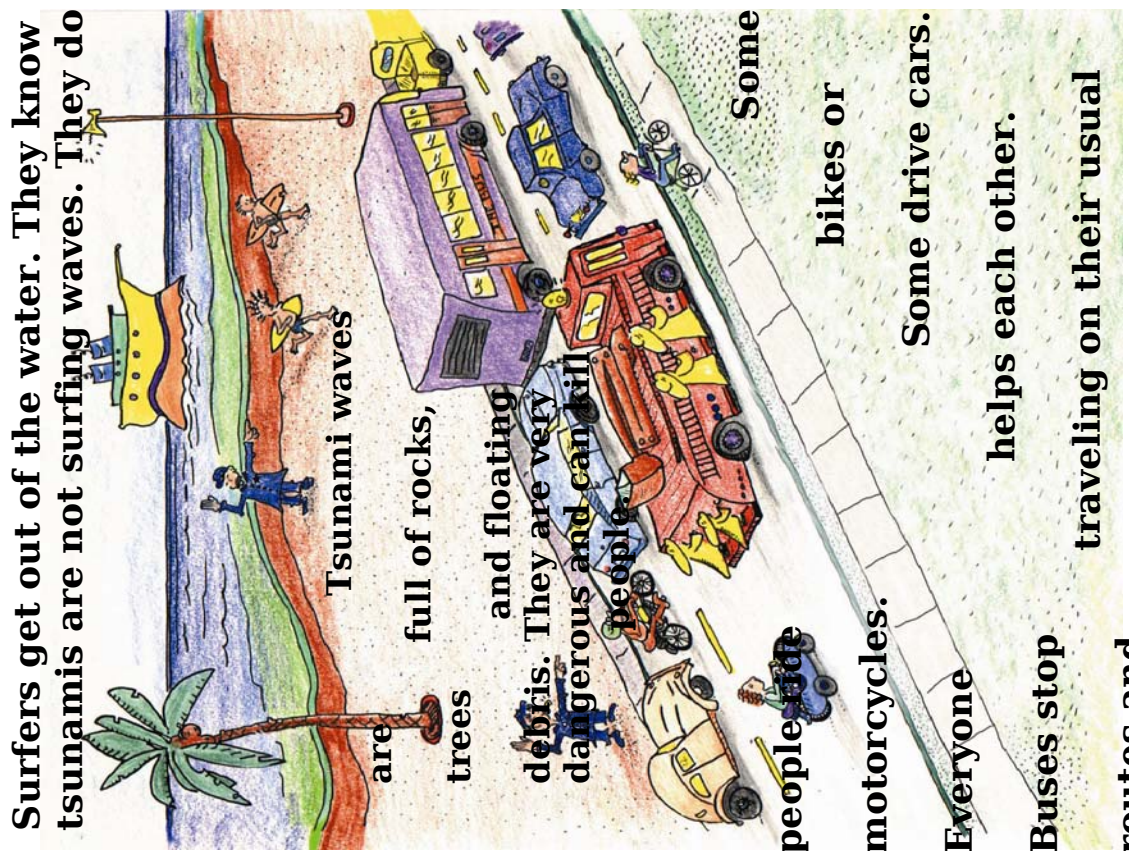
The tsunami waves keep coming but they grow smaller until the danger is over. The tsunami has caused a lot of damage, but no one has

It is 10 o'clock. The tsunami will arrive in two hours. The sirens wail again as a warning. People are leaving the inundation zones.

Surfers get out of the water. They know tsunamis are not surfing waves. They do

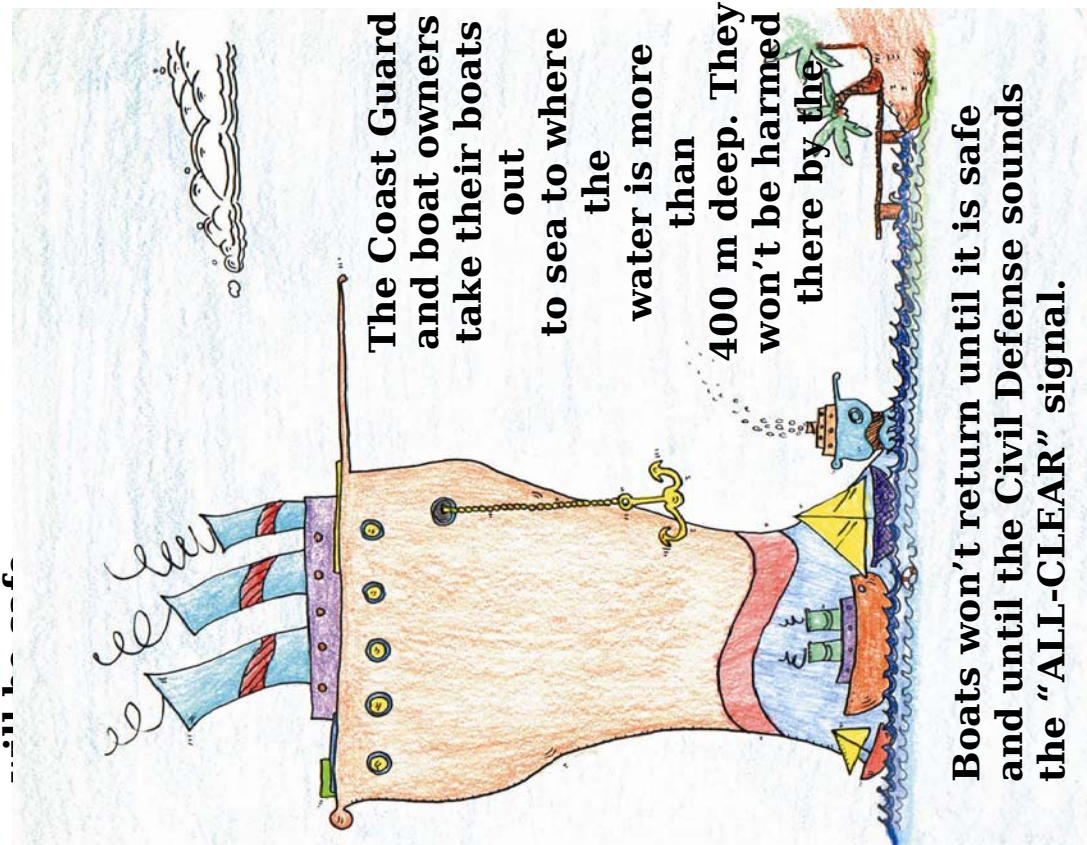


Everyone rushed to safety and higher ground. They evacuated the area and were saved.

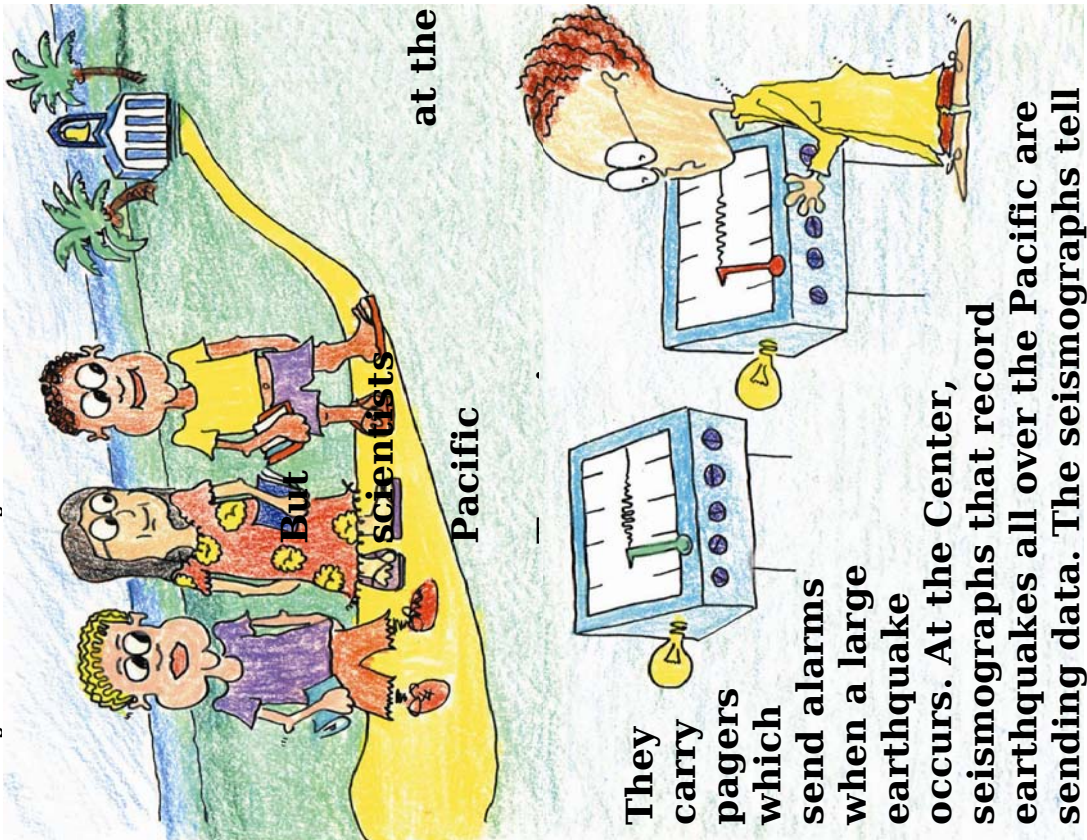


Buses stop traveling on their usual routes and act as shuttle buses between the

In Honolulu, Hawaii breakfast is finished and parents and children leave home. They have not yet heard about the



The cruise ship does not pull into the harbor at Honolulu. It will remain out on the ocean where it

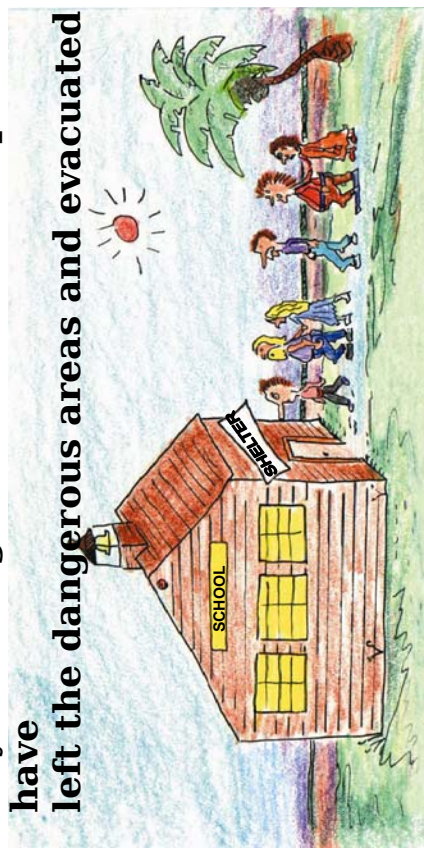


In Honolulu, Hawaii breakfast is

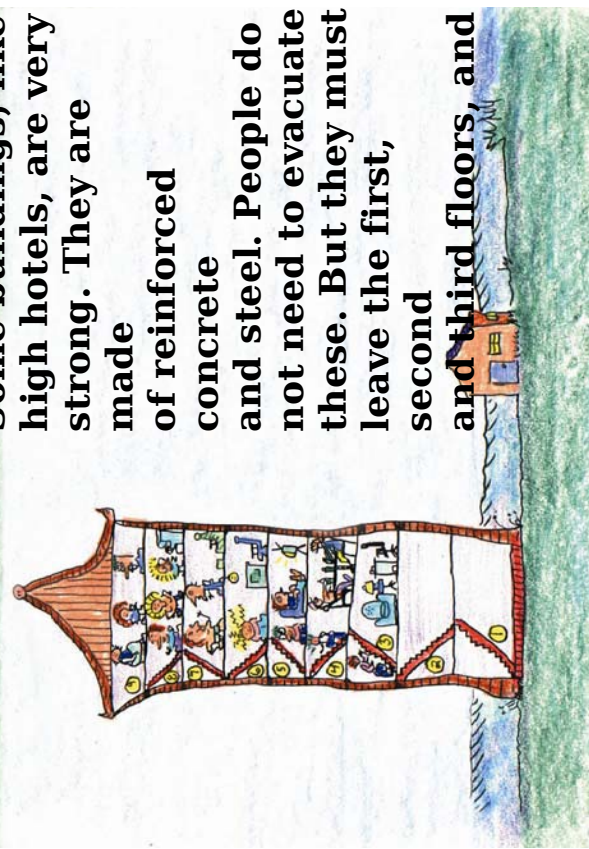
finished

and parents and children leave home. They have not yet heard about the

People move from the inundation zones to safe areas or shelters. Schools outside the danger areas are used as shelters. Anyone can go there to wait. People have left the dangerous areas and evacuated



Some buildings, like high hotels, are very strong. They are made of reinforced concrete and steel. People do not need to evacuate these. But they must leave the first, second and third floors, and



The scientists at the Center work all day and all night in shifts. There is always someone on duty for

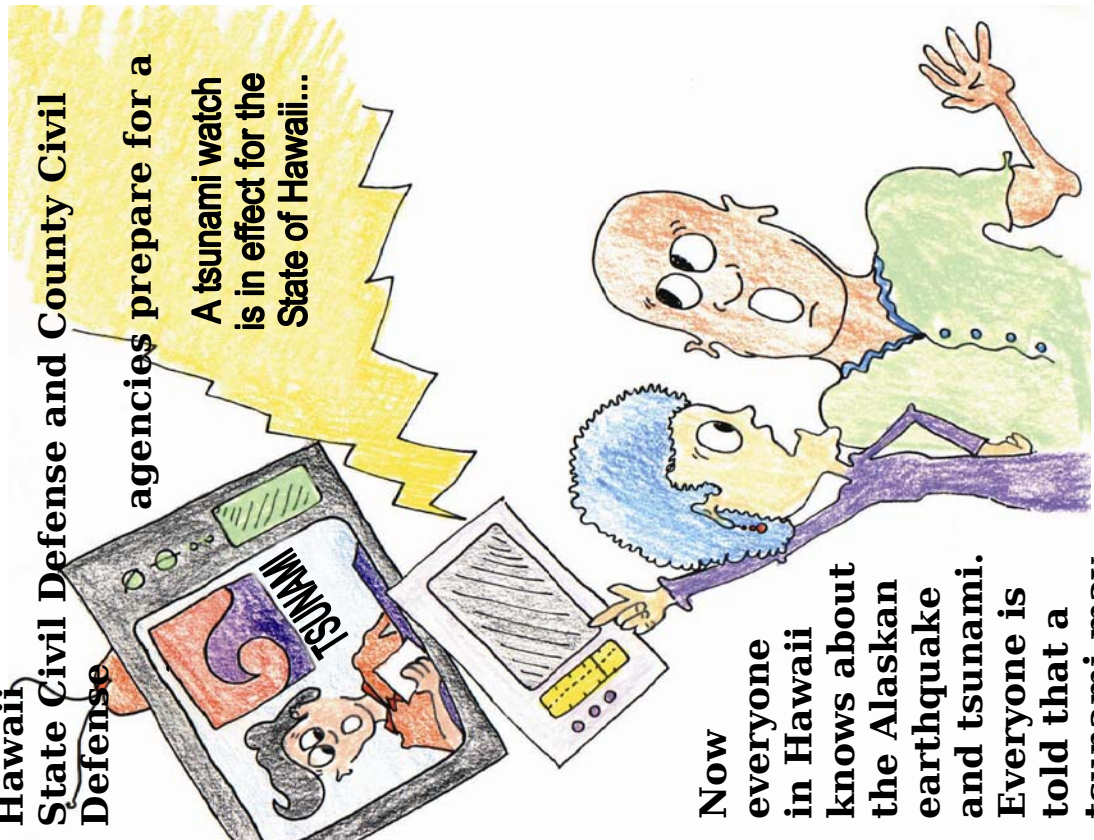


Quickly the scientists send messages to other tsunami warning centers in many countries all around the Pacific Ocean.

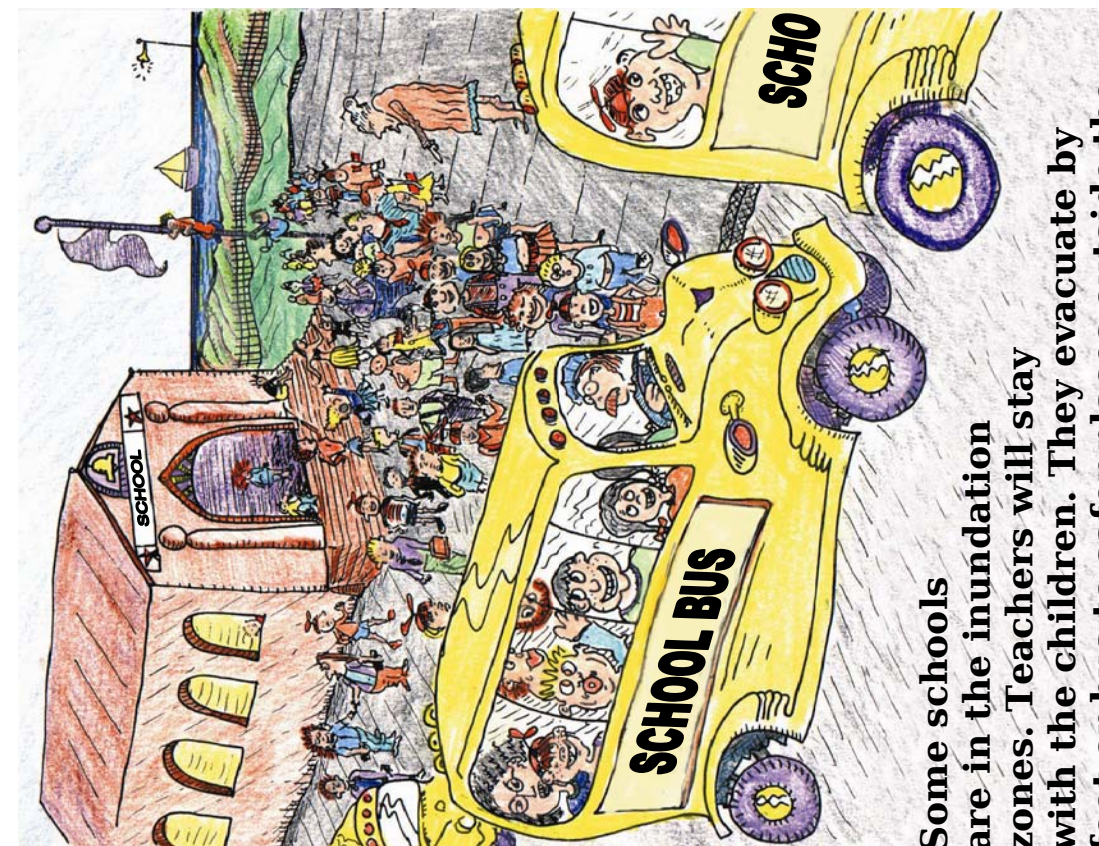
They tell them that the Alaskan earthquake was big and a tsunami is now crossing the Pacific Ocean in all

The scientists at the Pacific Tsunami Warning Center issue a Tsunami Watch. The Hawaii State Civil Defense and County Civil Defense agencies prepare for a

A tsunami watch is in effect for the State of Hawaii...

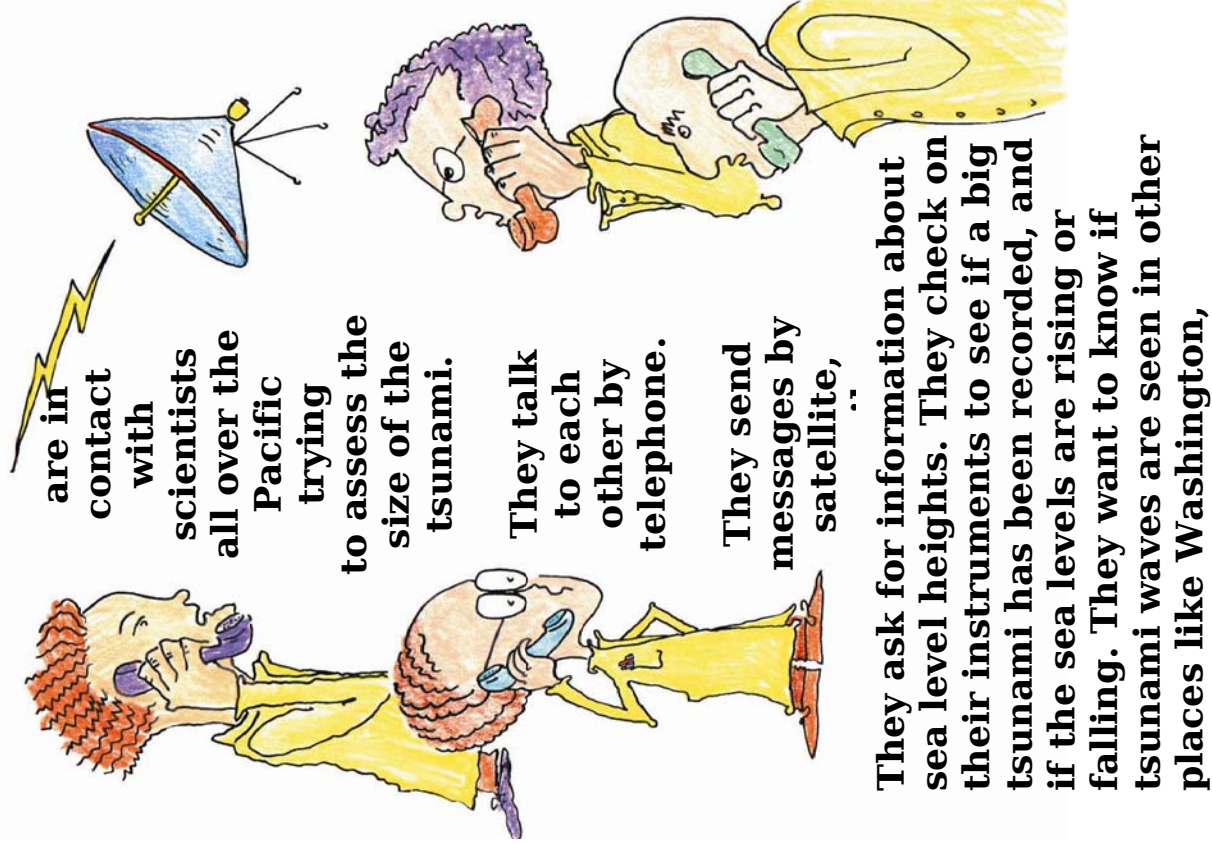


Now everyone in Hawaii knows about the Alaskan earthquake and tsunami. Everyone is told that a tsunami may be on its way across the Pacific Ocean.



Some schools are in the inundation zones. Teachers will stay with the children. They evacuate by foot or bus to safer places outside the inundation zones. They will look after the children until the tsunami danger has passed. Then the parents will come to get

During the Tsunami Watch, the scientists at



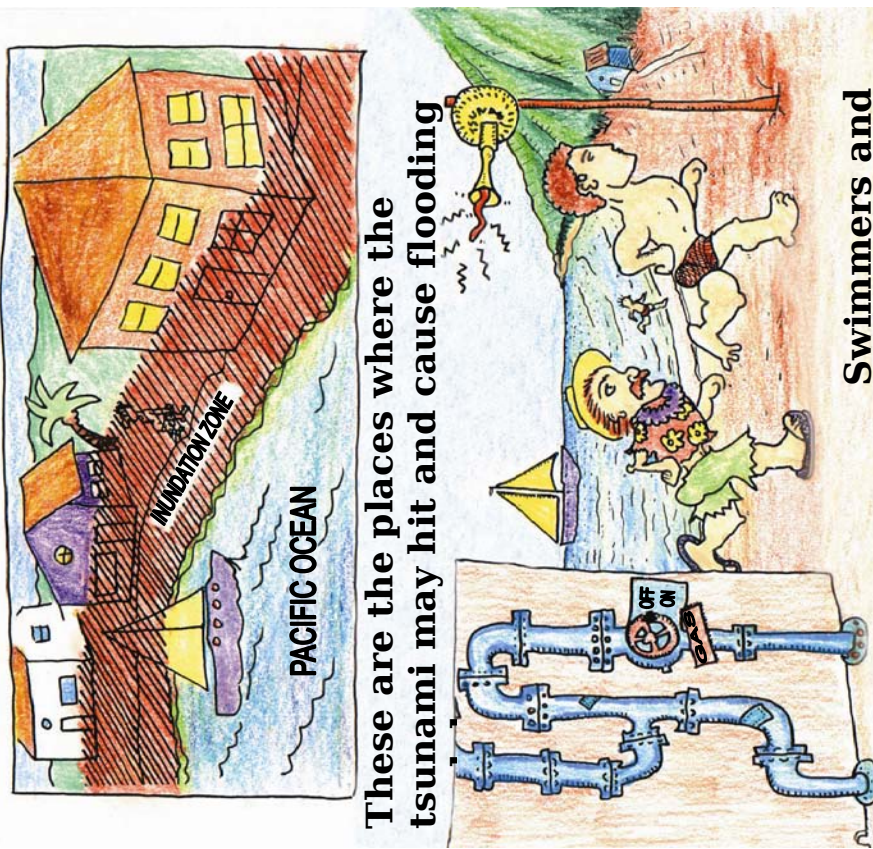
are in contact with scientists all over the Pacific trying to assess the size of the tsunami.

They talk to each other by telephone.

They send messages by satellite,

They ask for information about sea level heights. They check on their instruments to see if a big tsunami has been recorded, and if the sea levels are rising or falling. They want to know if tsunami waves are seen in other places like Washington,

Beaches and low-lying areas along the coast that get flooded are in the tsunami

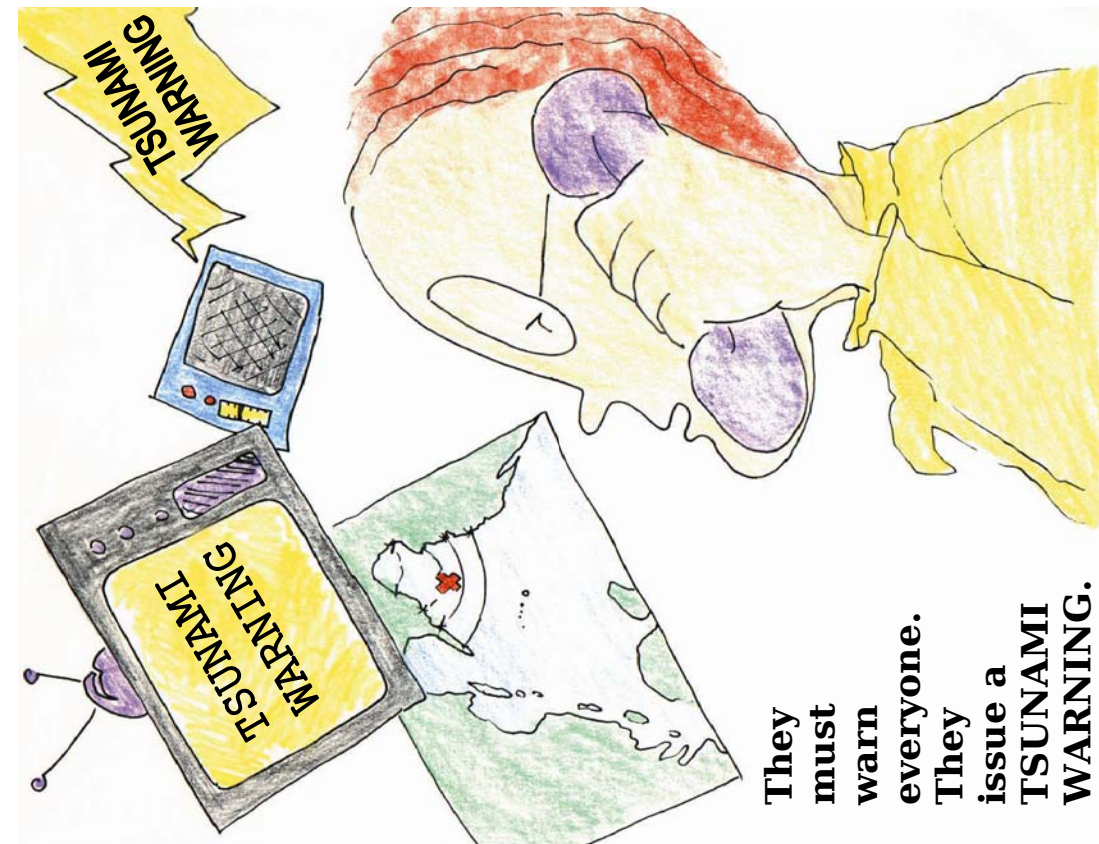
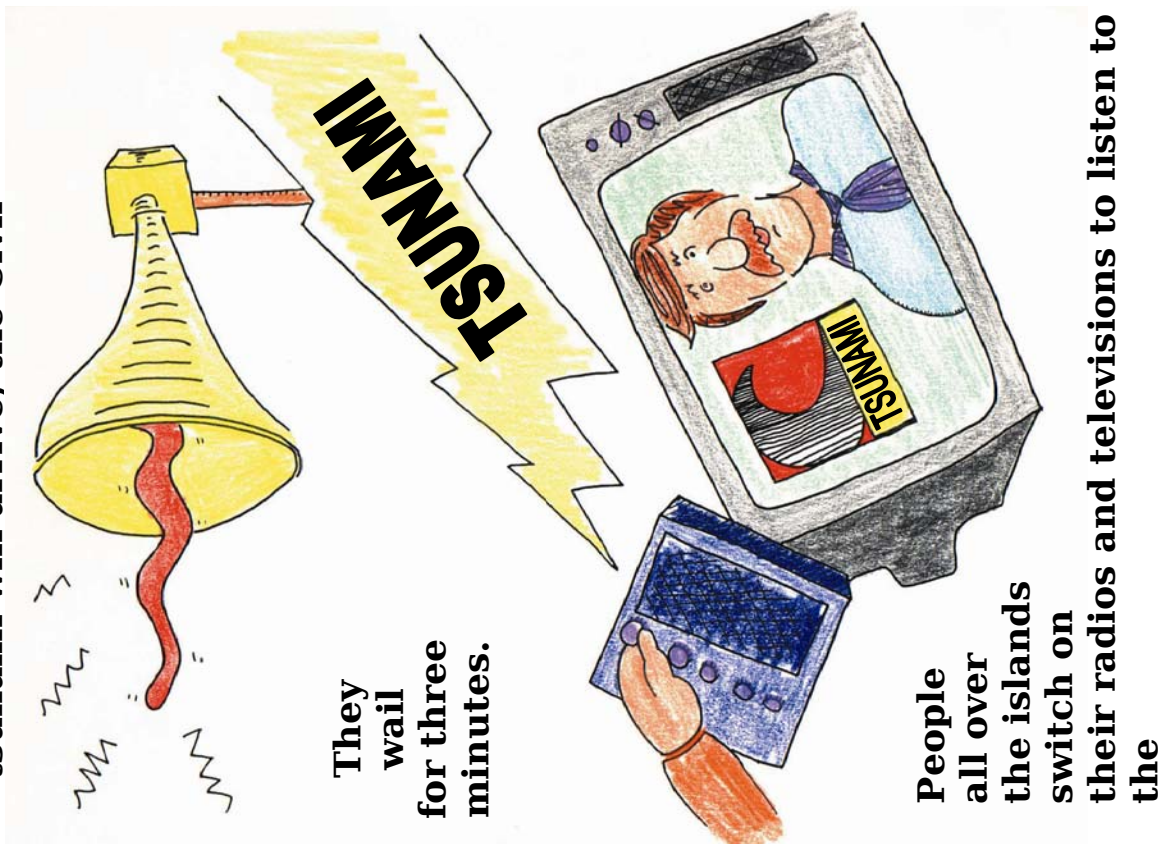


These are the places where the tsunami may hit and cause flooding

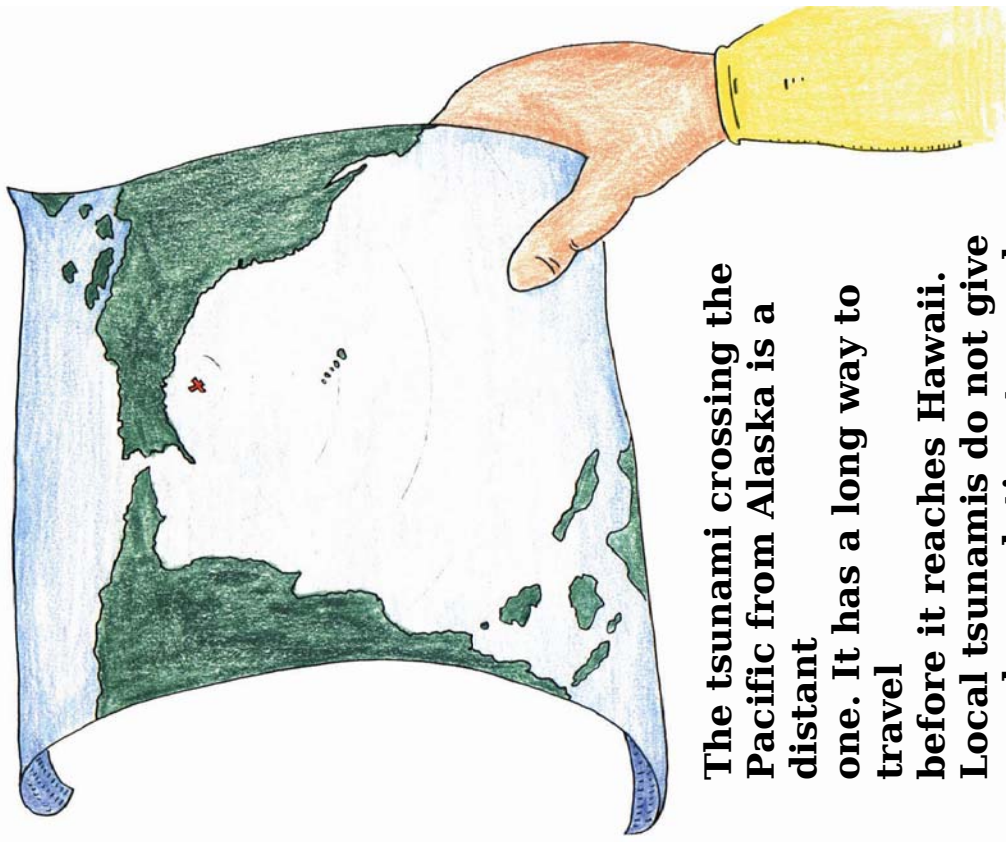
Swimmers and vacation start to leave the beaches. People who live in the inundation zones must evacuate their homes. They switch off water, electricity and gas at the main valves. Hotel staff help their

At 9 o'clock, three hours before
the tsunami will arrive, the Civil

By now the scientists have a lot of
information. They know that a
tsunami



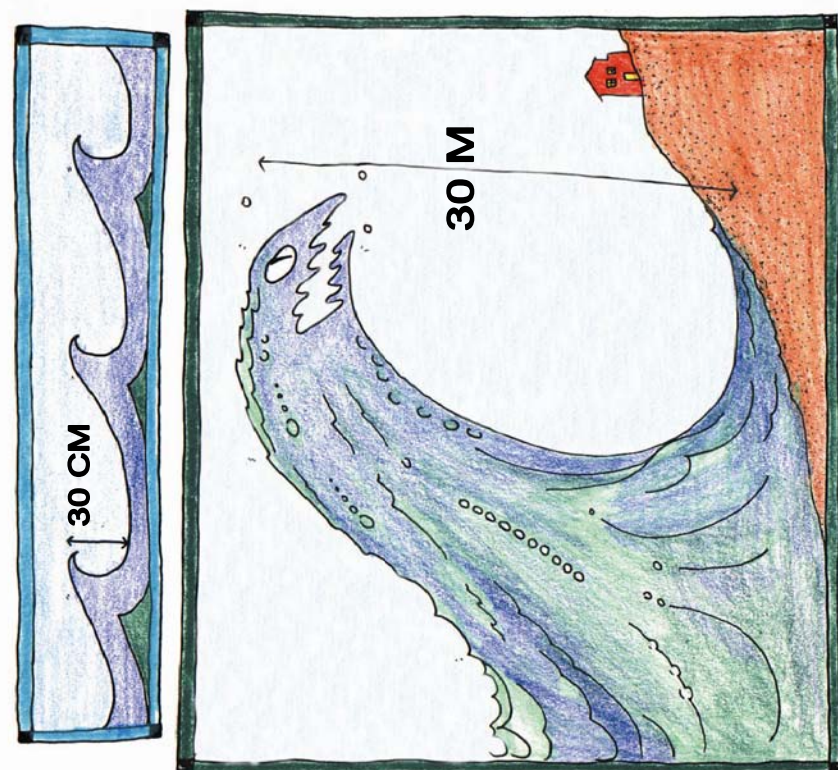
The tsunami that damaged Alaska was a local one because it happened in the same



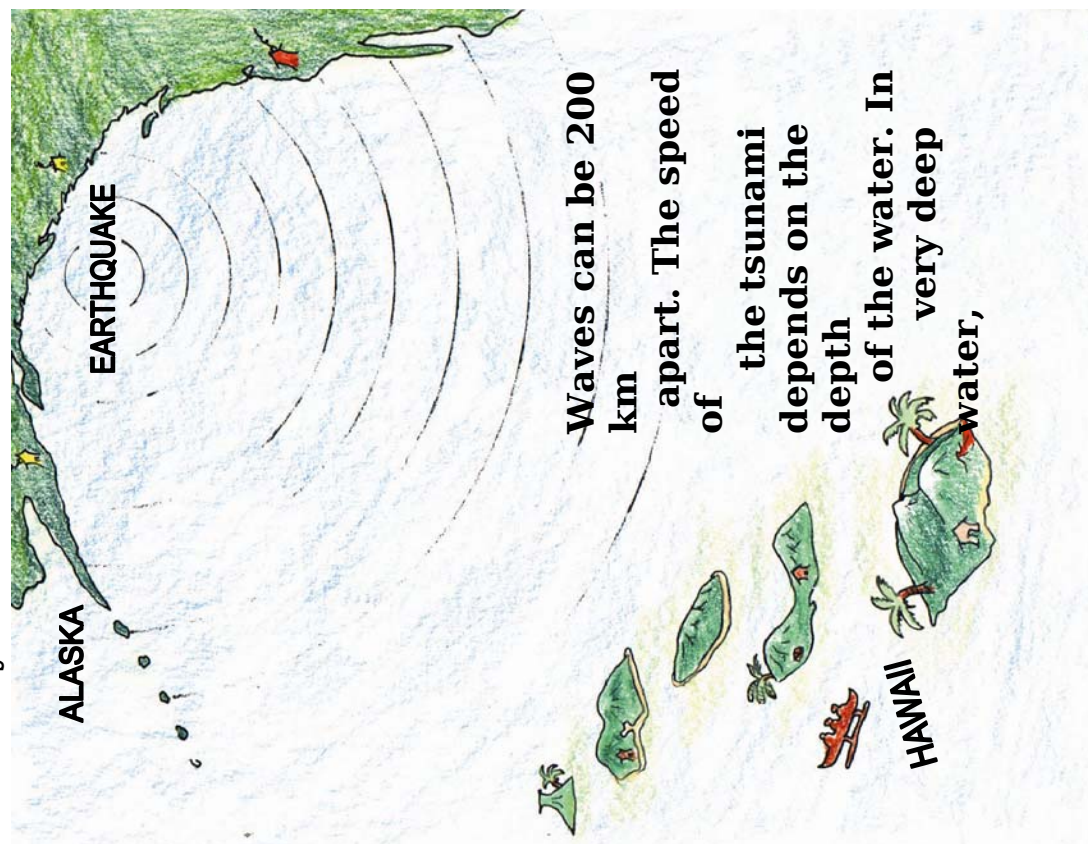
The scientists at the Pacific Tsunami Warning Center can calculate when the first wave of the tsunami will reach Hawaii. It will reach



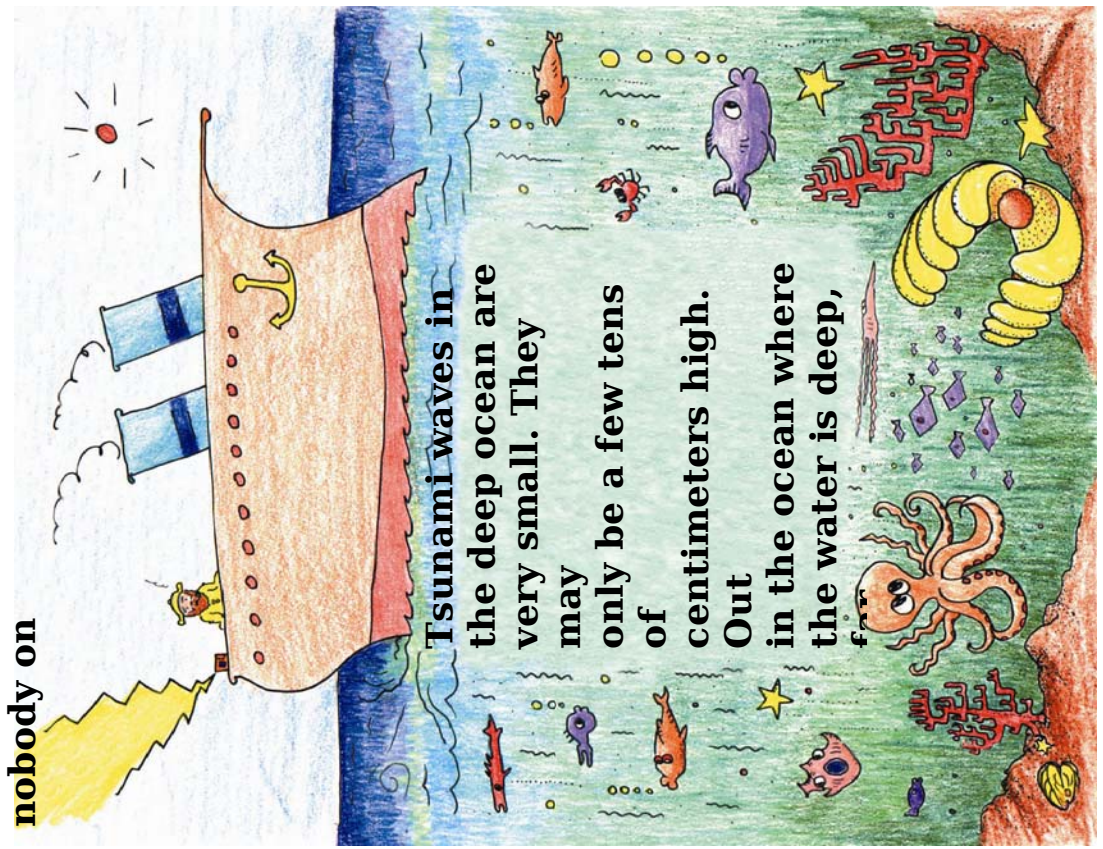
This is when the tsunami waves can become very dangerous. A small wave only 30 centimeters (cm) high in the deep



The tsunami that is on its way to Hawaii is made up of a series of very long waves. A tsunami is made up of many



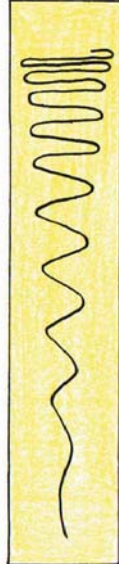
Tsunami waves cannot be felt or seen by ships at sea. The captain of the cruise ship has heard about the tsunami on his radio, but nobody on



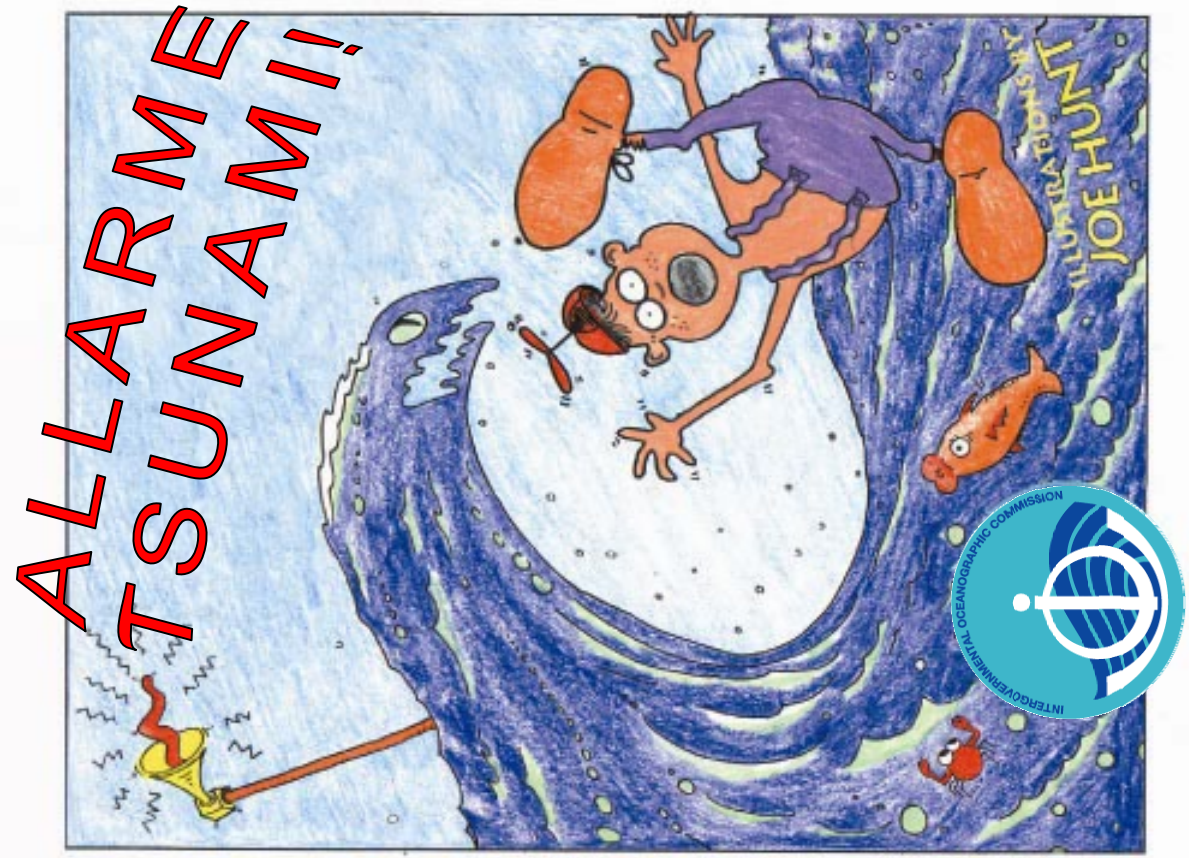
But as the tsunami approaches land, it becomes dangerous. The waves slow down when they hit shallow



In 10 meters of water, a tsunami travels at 40 km/h. That is the speed of a slow car



Although the first wave slows down when it enters shallow water, the second wave is 200 km away, and still traveling faster. It catches up to the first wave. The result is that the distance between the waves does not



 United Nations Educational, Scientific and Cultural Organization



Intergovernmental
Oceanographic
Commission

Intergovernmental Oceanographic Commission (IOC)
United Nations Educational, Scientific and Cultural
Organization (UNESCO)
1, rue Miollis
75 735 Paris Cedex 15
France
Tel: +33 1 45 68 39 83
Fax: +33 1 45 68 58 12
<http://ioc.unesco.org>



United Nations
Educational, Scientific and
Cultural Organization
2005
1945

ACKNOWLEDGMENTS

The International Coordination Group for the Tsunami Warning System in the Pacific of the Intergovernmental Oceanographic Commission of UNESCO, at its Thirteenth Session in Ensenada, Mexico (September 1991), encouraged the preparation of a book designed to inform young persons about tsunamis, the dangers which they present, and what should be done to save lives and property.

The authors of this book are Dr. George Pararas-Carayannis, Ms. Patricia Wilson, and Mr. Richard Sillcox, and the illustrations were created by Mr. Joe Hunt.

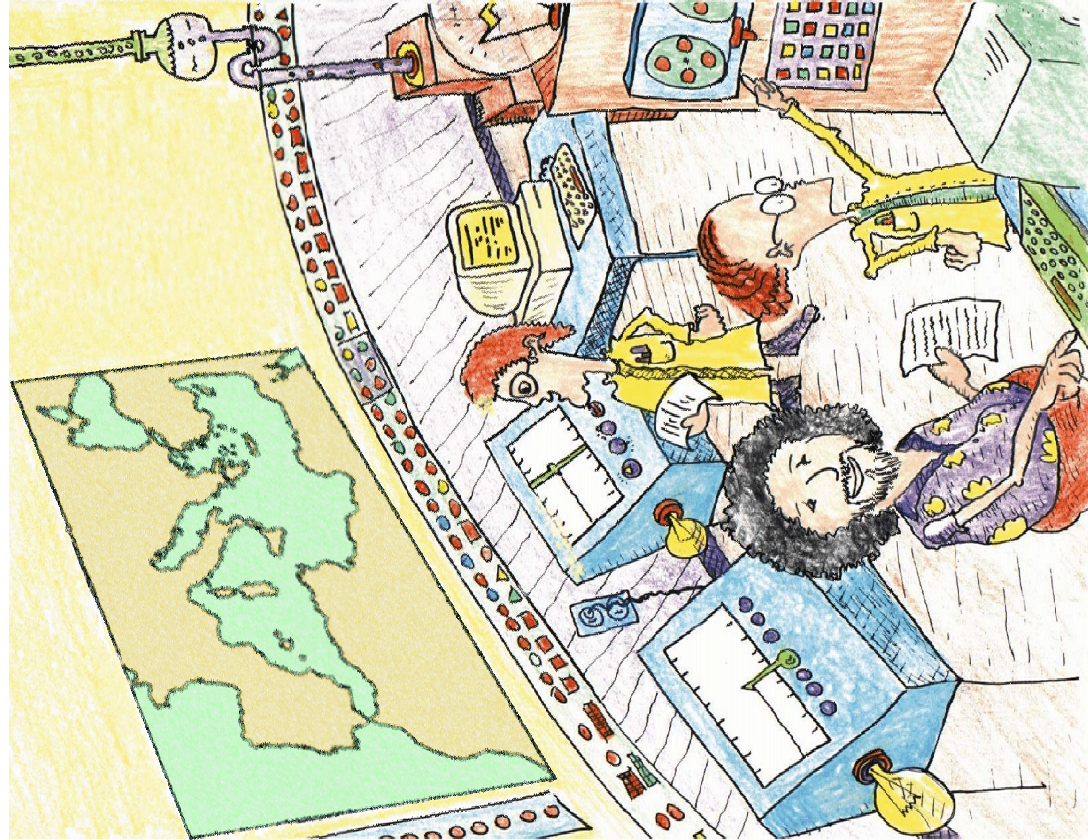
To learn more about tsunamis and what you should do when a tsunami is coming, we encourage you to read *The Great Waves*.

This book was revised by the International Tsunami Information Centre in June 2005, and reprinted with the support of the Hawaii State Civil Defense and the U. S. National Tsunami Hazard Mitigation Program.

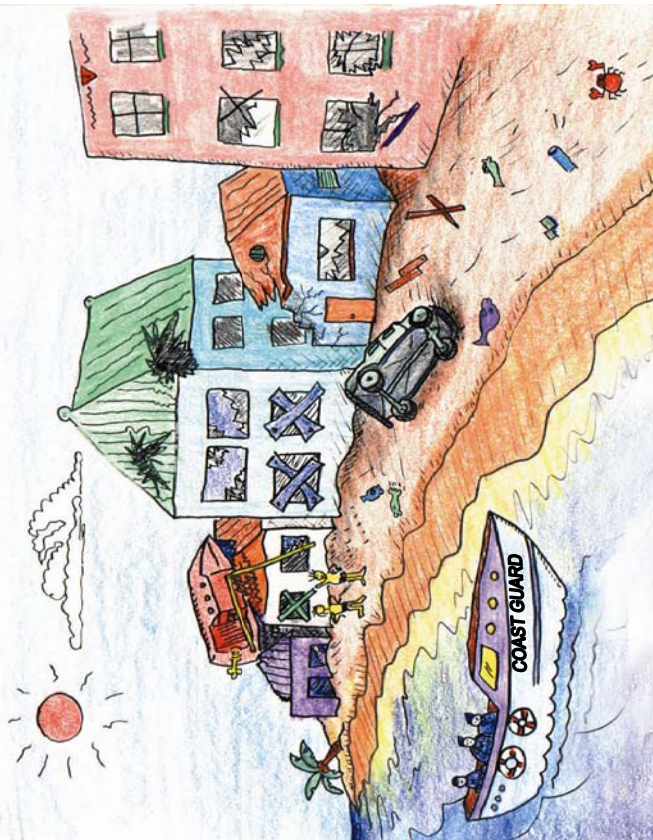
Bibliographic reference:

UNESCO-IOC. Tsunami Warning! IOC Information Document No. 1223 (IOC/INF-1223)
Printed by: Hawaii State Civil Defense
© 2005

E' bello sapere che ci sono scienziati che lavorano nei centri di allarme terremoti e tsunami e che sono sempre all'erta per riconoscere il primo segno di tsunami per proteggere vite umane adesso e nel futuro.



Quando le onde di tsunami sono piccole e non causano alcun danno, i **centri di allarme** annullano l'allerta Tsunami. Ognuno deve aspettare che la protezione civile annunci il cessato allarme in modo che tutti possano rientrare in modo sicuro alle proprie case ed ai posti di lavoro.



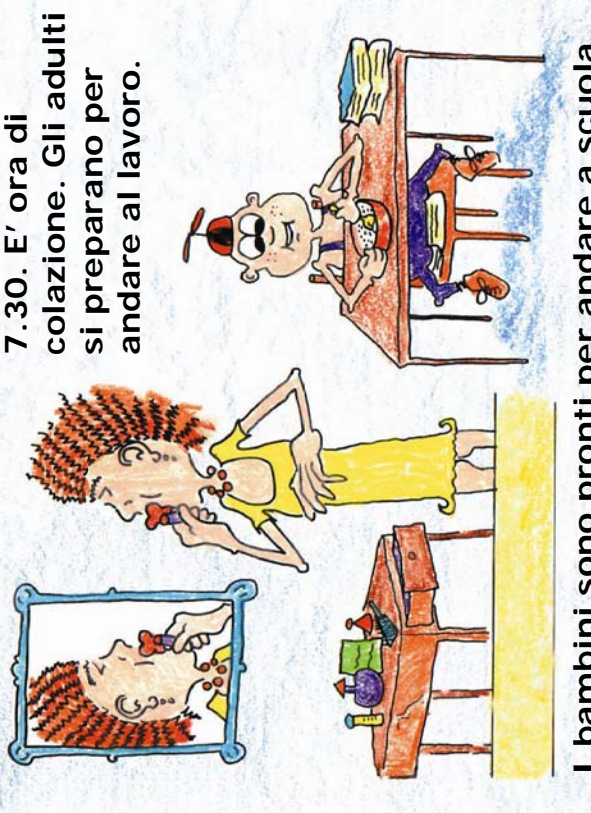
Lo tsunami ha danneggiato molte costruzioni lungo la costa. Ha distrutto quelle barche che non si sono allontanate in mare aperto. Ha lanciato a terra le macchine come se fossero giocattoli. Ha distrutto pareti e tetti ed ha allagato tutte le zone basse. Tutti sono felici che nessuno si sia fatto male. Erano preparati e sapevano cosa fare. Tutti hanno lasciato le aree inondabili quando hanno udito l'allarme tsunami. Le persone adesso lavorano per riparare le loro case in modo da ritornare ad una vita normale.

28

Nelle acque calme e azzurre del Tirreno, una nave da crociera sta navigando verso l'Isola d'Elba.



In Sicilia sono le 7.30. E' ora di colazione. Gli adulti si preparano per andare al lavoro.



I bambini sono pronti per andare a scuola.

1

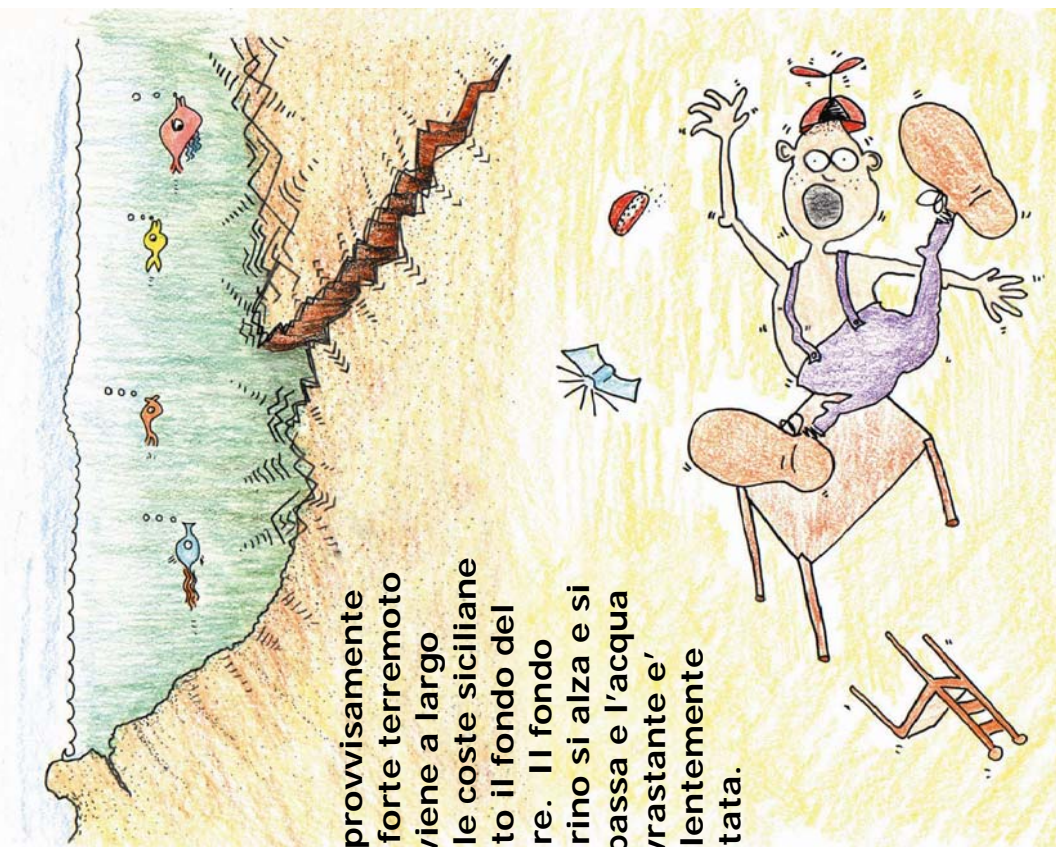
**Le persone
attendono nei rifugi.**



Alcuni hanno colto l'occasione per fare un picnic sulle montagne. Le persone mangiano, devono, giocano, leggono guardano la televisione o ascoltano la radio to the radio. Stanno aspettando il "CESSATO ALLARME" della protezione civile.

27

Improvvisamente un forte terremoto avviene a largo delle coste siciliane sotto il fondo del mare. Il fondo marino si alza e si abbassa e l'acqua sovrastante è violentemente agitata.

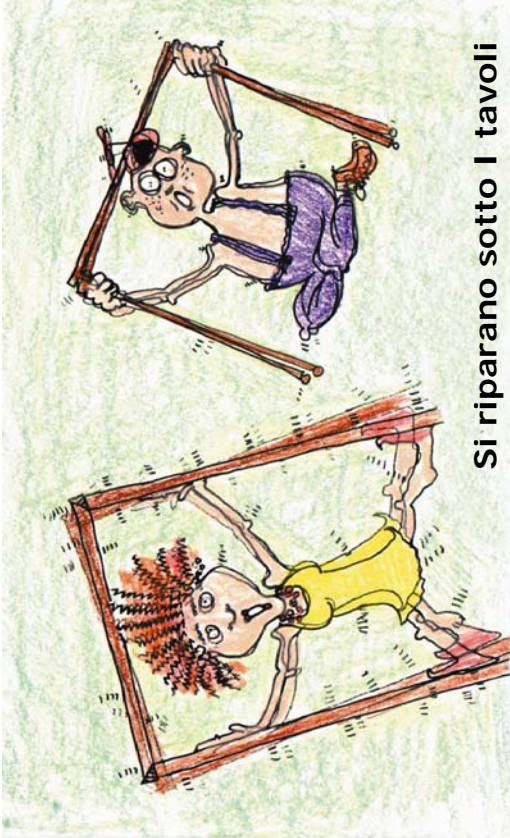


In Sicilia, i muri e i pavimenti delle case improvvisamente iniziano a scutersi. Le sedie si rovesciano. Le stoviglie e i sopramobili sbattono e tintinnano. I piatti si rompono sul pavimento.

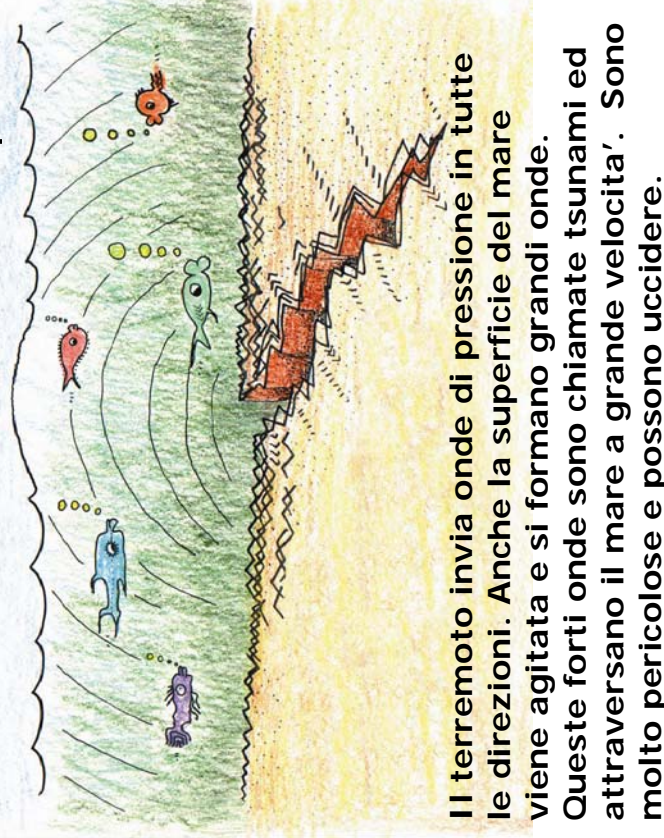
2

Alle 8.40, arriva la prima onda di tsunami.

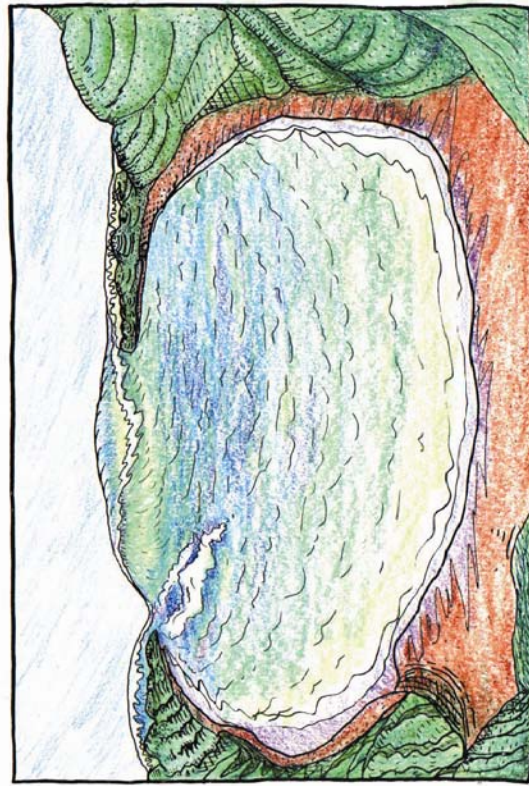
E' un terremoto! Le persone sanno cosa devono fare. Non corrono fuori.



Si riparano sotto i tavoli o nei vani delle porte.



Il terremoto invia onde di pressione in tutte le direzioni. Anche la superficie del mare viene agitata e si formano grandi onde. Queste forti onde sono chiamate tsunami ed attraversano il mare a grande velocita'. Sono molto pericolose e possono uccidere.

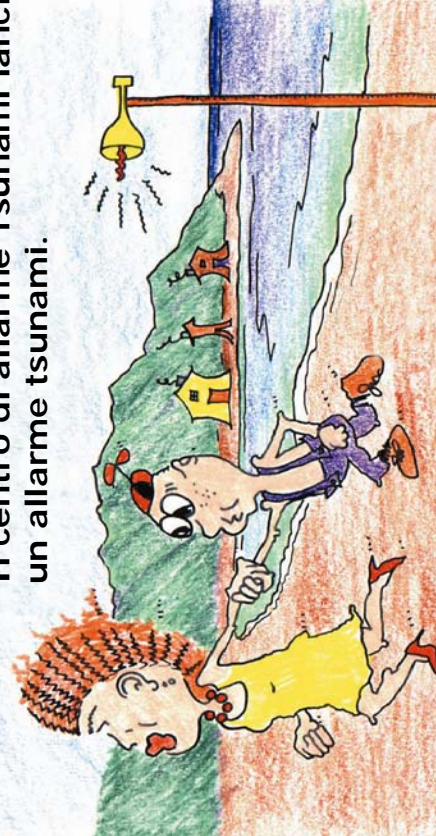


Nelle baie le onde possono diventare molto grandi perche' i lati della baia diminuiscono la lunghezza delle onde e le spingono verso l'alto.

Quando finisce il tremore, le persone che vivono lungo la costa sanno cosa devono fare. Non iniziano a mettere a posto la confusione che si e' creata, ma velocemente lasciano le loro case e si allontanano dalla costa verso zone piu' alte. Loro sanno che i terremoti possono provocare onde di maremoto (tsunami).

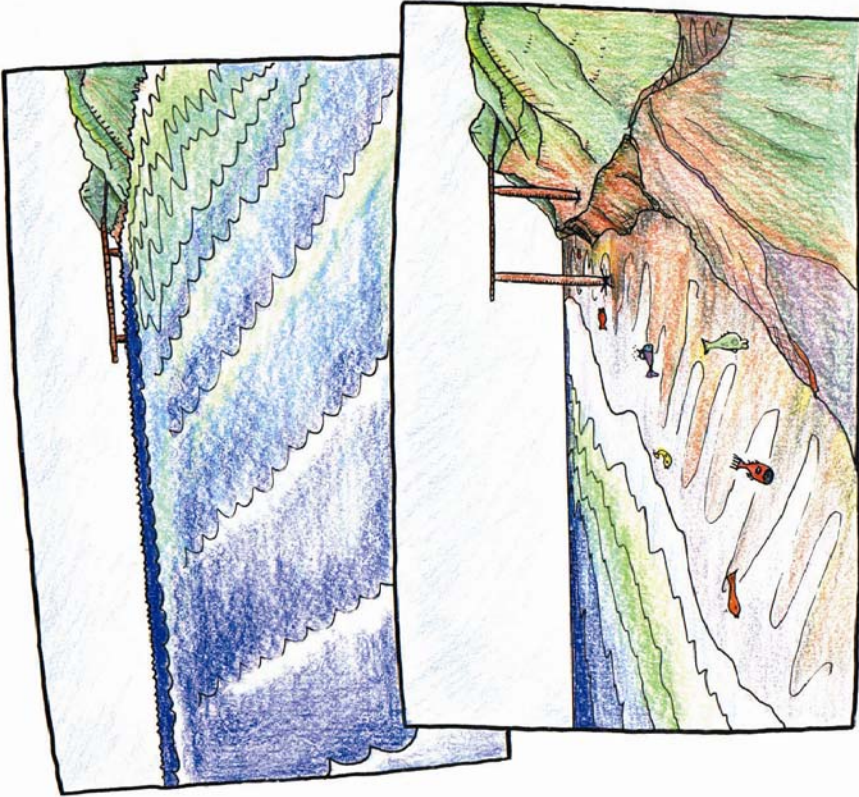


Il centro di allarme Tsunami lancia un allarme tsunami.



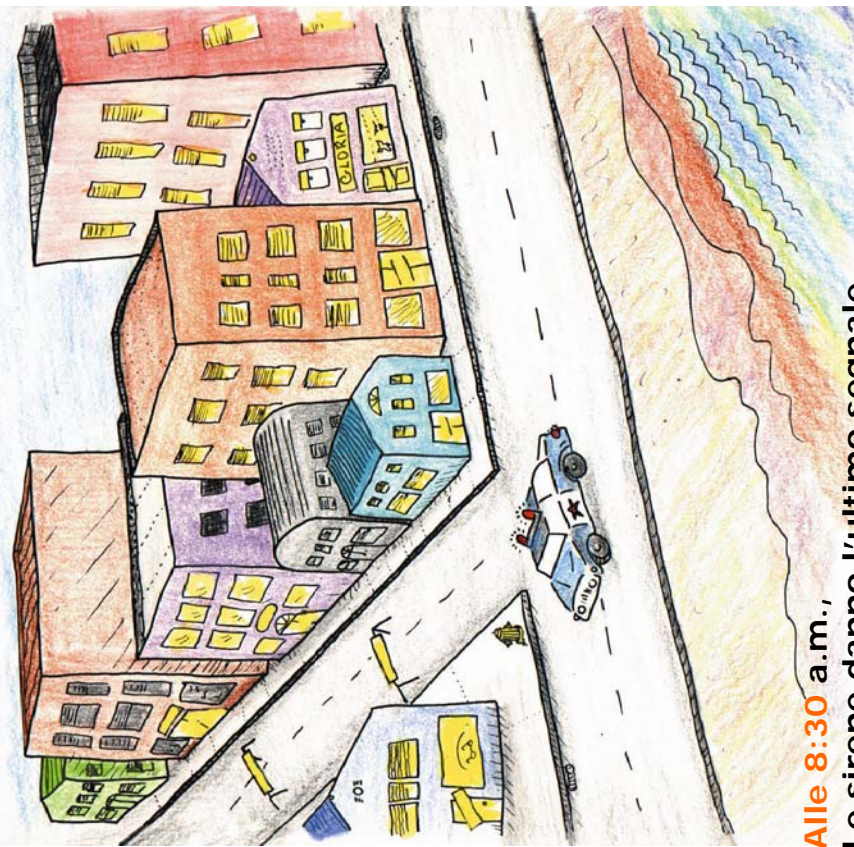
Poi il centro operativo della protezione civile fa suonare le sirene per avvertire la popolazione che sta arrivando uno tsunami. Non c'e' tempo da perdere! Le persone corrono verso la salvezza lontano dalla costa ed aspettano l'arrivo dello tsunami.

Pochi minuti dopo qualcosa di strano inizia ad accadere lungo le spiagge. In alcuni posti il mare risale dolcemente. In altri l'acqua si ritira dalla costa lasciando i pesci a dimenarsi senz'acqua sulla battigia.



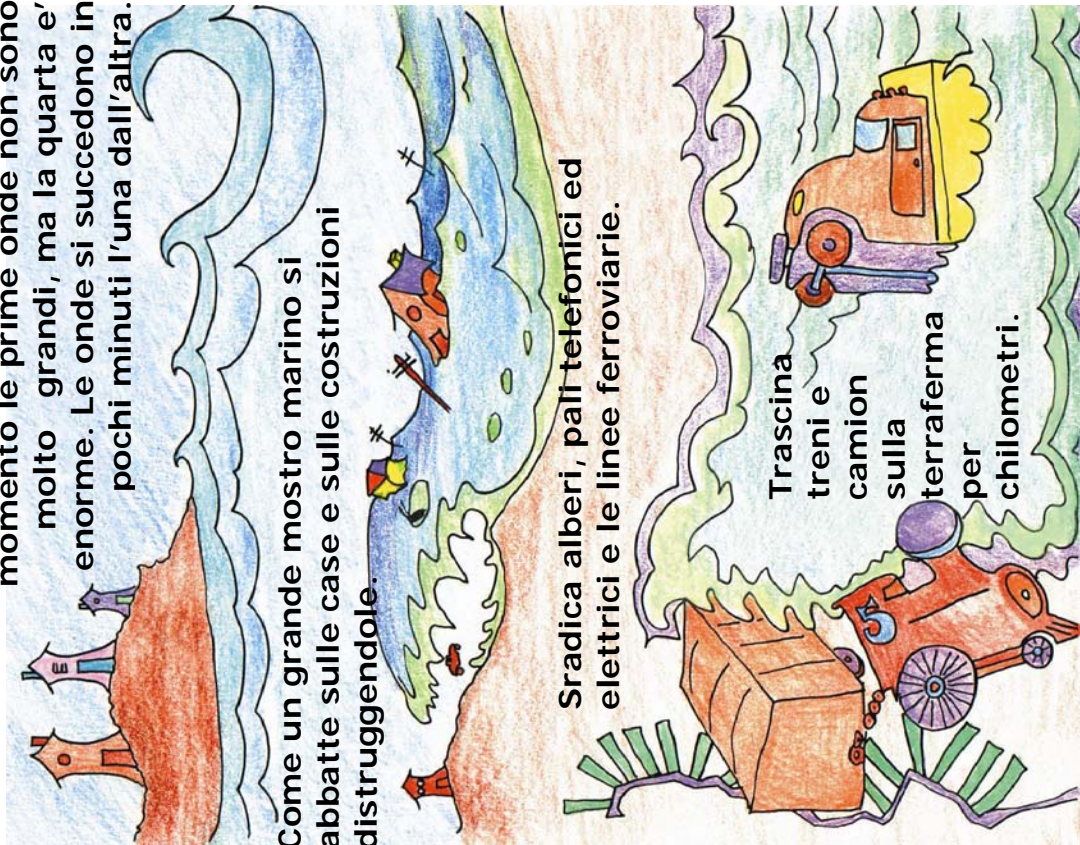
Entrambi I fenomeni sono segni sicuri dell'arrivo imminente di uno tsunami.

Alle 8.20, le sirene suonano ancora. La prima onda di tsunami e' prevista tra meno di venti minuti.
La polizia e' impegnata nel controllare che tutti siano evacuati. Vogliono essere sicuri che nessuno sia rimasto nelle zone di inondazione. Poi bloccano le strade cosi' nessuno puo' tornare nelle zone pericolose.



Alle 8:30 a.m.,
Le sirene danno l'ultimo segnale.
Non c'e' nient'altro da fare che aspettare.
Ognuno aspetta che arrivi l'onda.

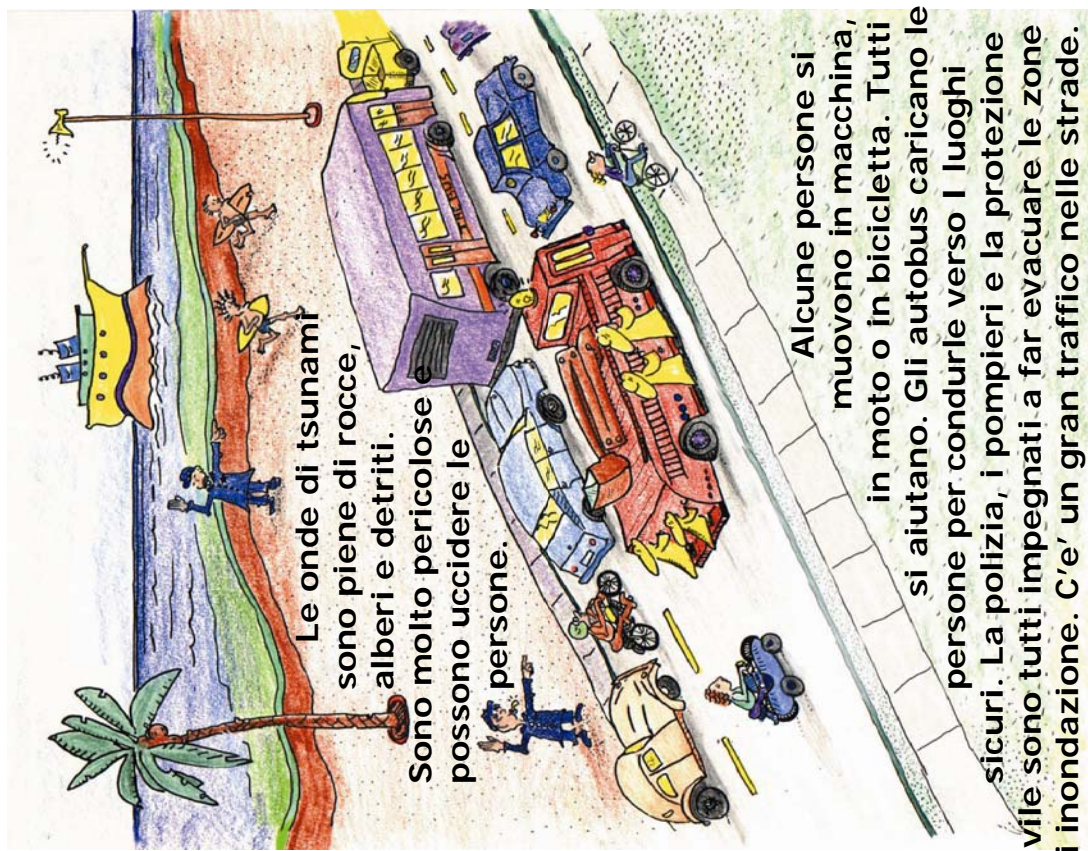
Le onde di tsunami iniziano a muoversi dopo pochi minuti che e' avvenuto il terremoto. In questo momento le prime onde non sono molto grandi, ma la quarta e' enorme. Le onde si succedono in pochi minuti l'una dall'altra.



Sommerge ogni cosa sulla terraferma per piu' di un chilometro dalla linea di costa.

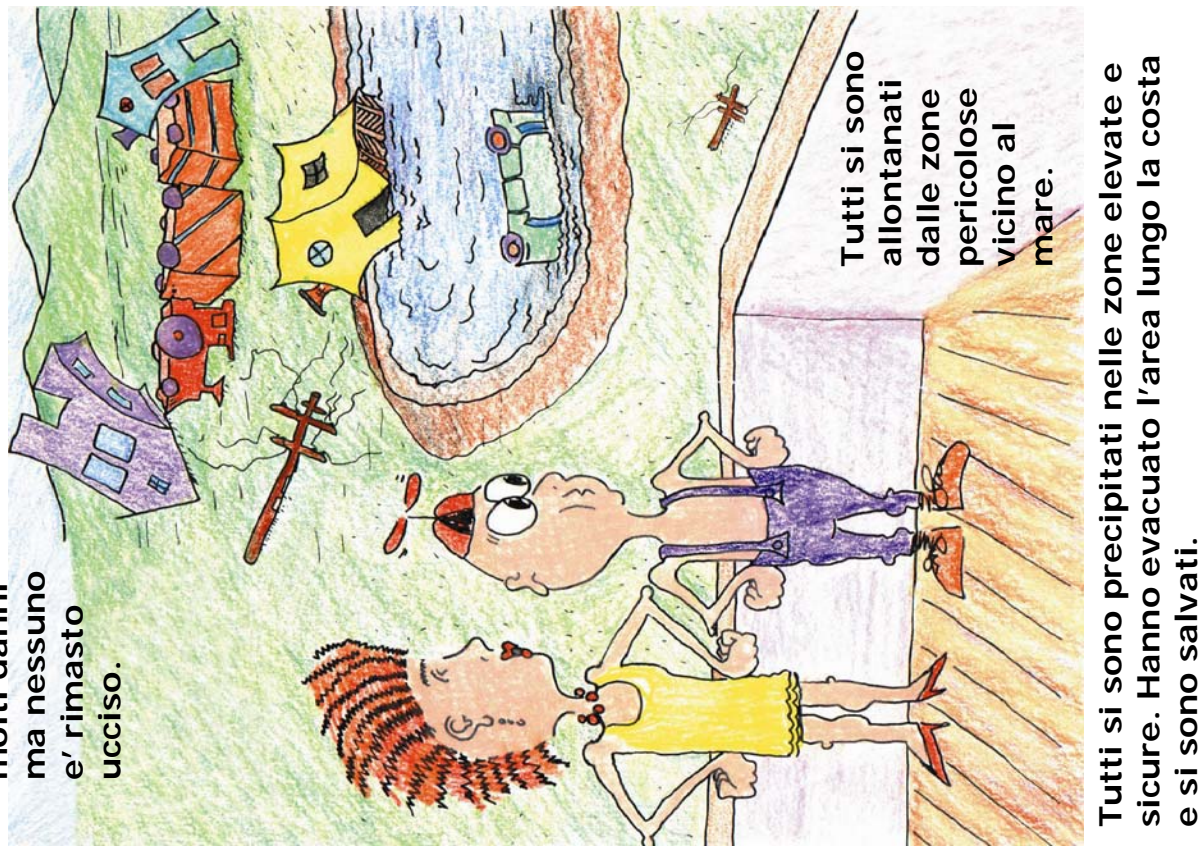
Le onde di tsunami continuano ad arrivare ma crescono sempre meno fino a che il pericolo termina. Lo tsunami ha causato molti danni ma nessuno e' rimasto ucciso.

Sono le 8.10! Lo tsunami arrivera' tra meno di mezz'ora. Le sirene suonano ancora l'allarme. La popolazione sta abbandonando le zone di inondazione.
I surfisti escono dall'acqua perche' sanno che le



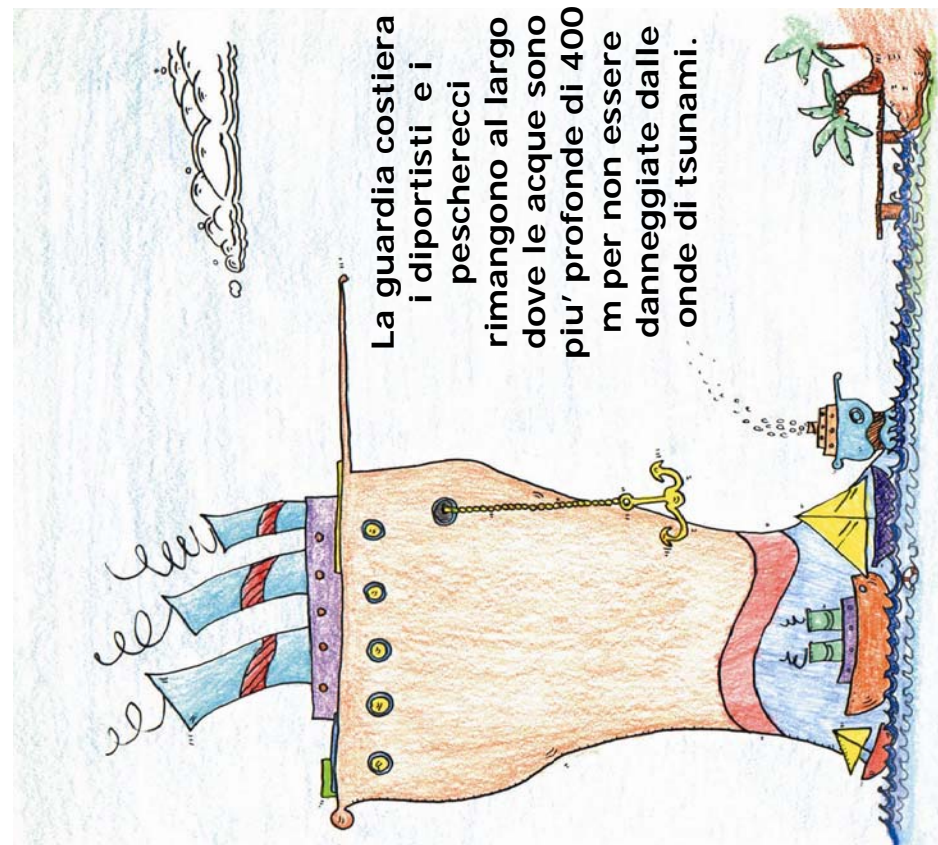
6

23



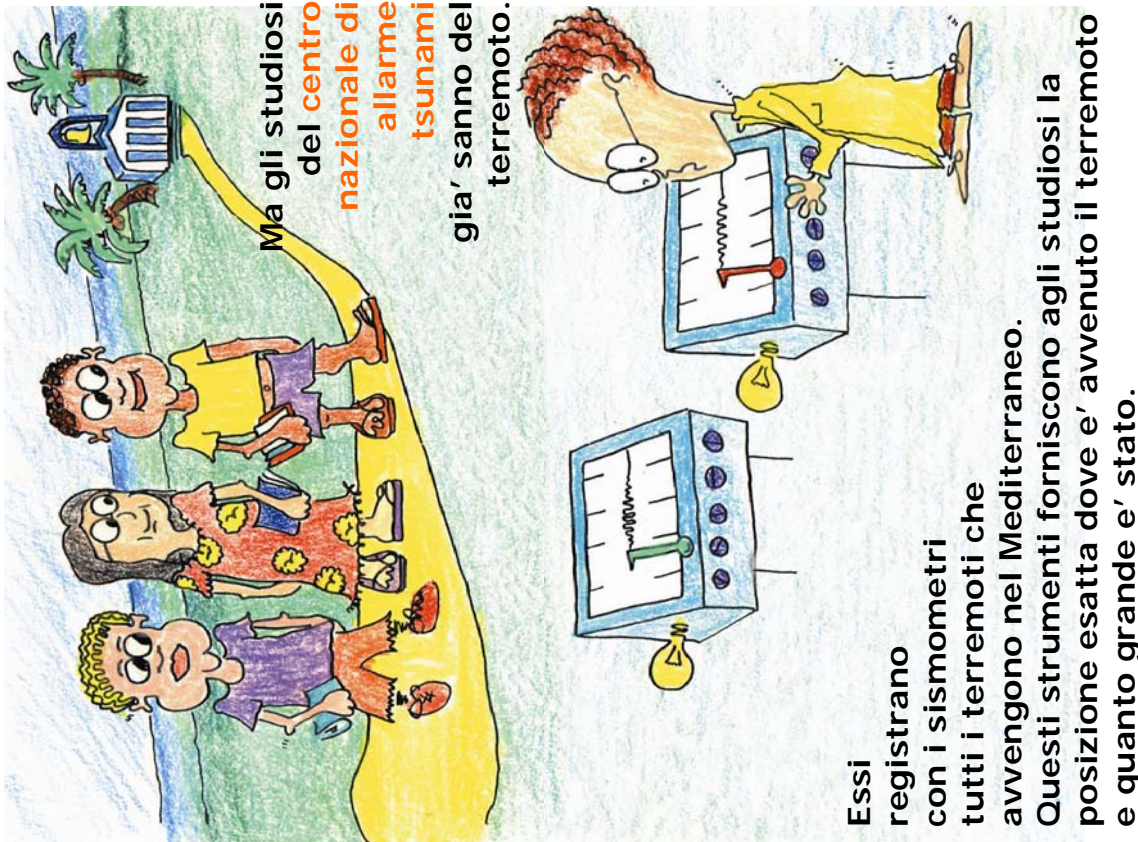
La nave da crociera non puo' attraccare al porto ma rimarra' in acque profonde dove sara' al sicuro.

Nell'Isola d'Elba la colazione e' finita e adulti e bambini stanno uscendo da casa, non sanno ancora niente del terremoto avvenuto vicino alla Sicilia.



La guardia costiera i diportisti e i pescherecci rimangono al largo dove le acque sono piu' profonde di 400 m per non essere danneggiate dalle onde di tsunami.

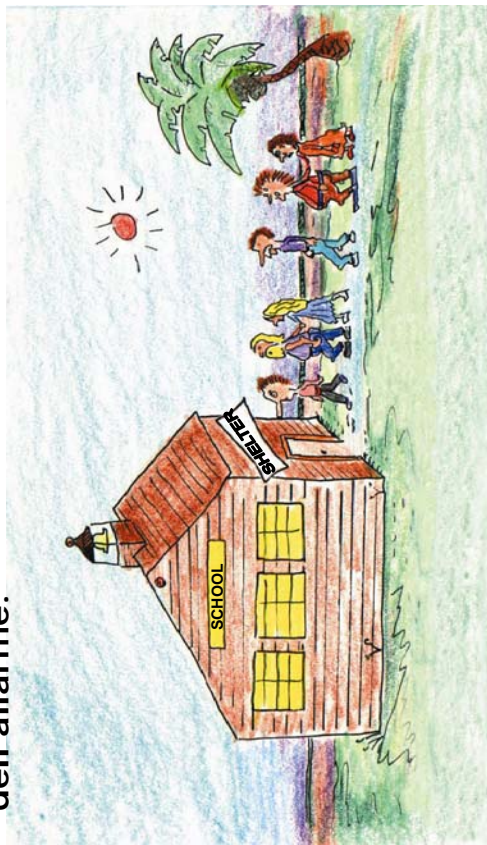
Le imbarcazioni non rientreranno fino a che la protezione civile non emettera' il segnale di "CESSATO ALLARME".



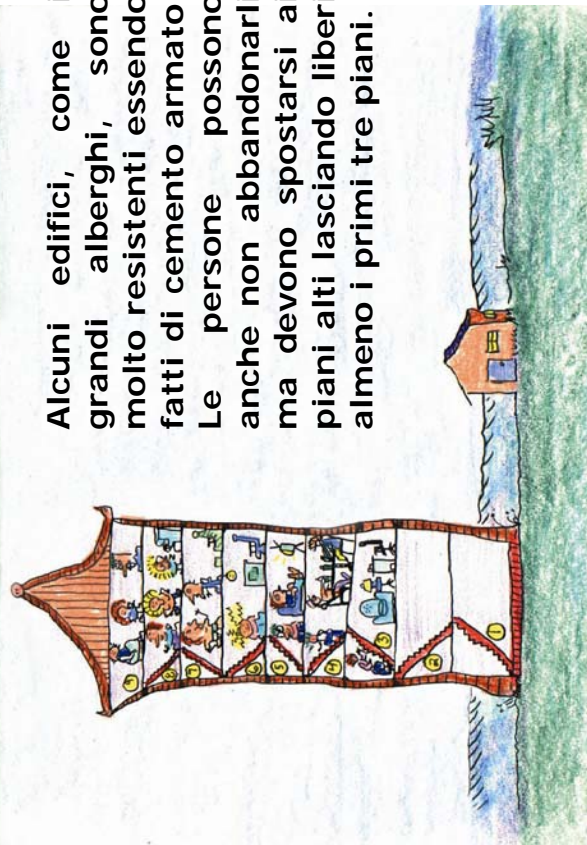
Ma gli studiosi del centro nazionale di allarme **tsunami** già sanno del terremoto.

Essi registrano con i sismometri tutti i terremoti che avvengono nel Mediterraneo. Questi strumenti forniscono agli studiosi la posizione esatta dove e' avvenuto il terremoto e quanto grande e' stato.

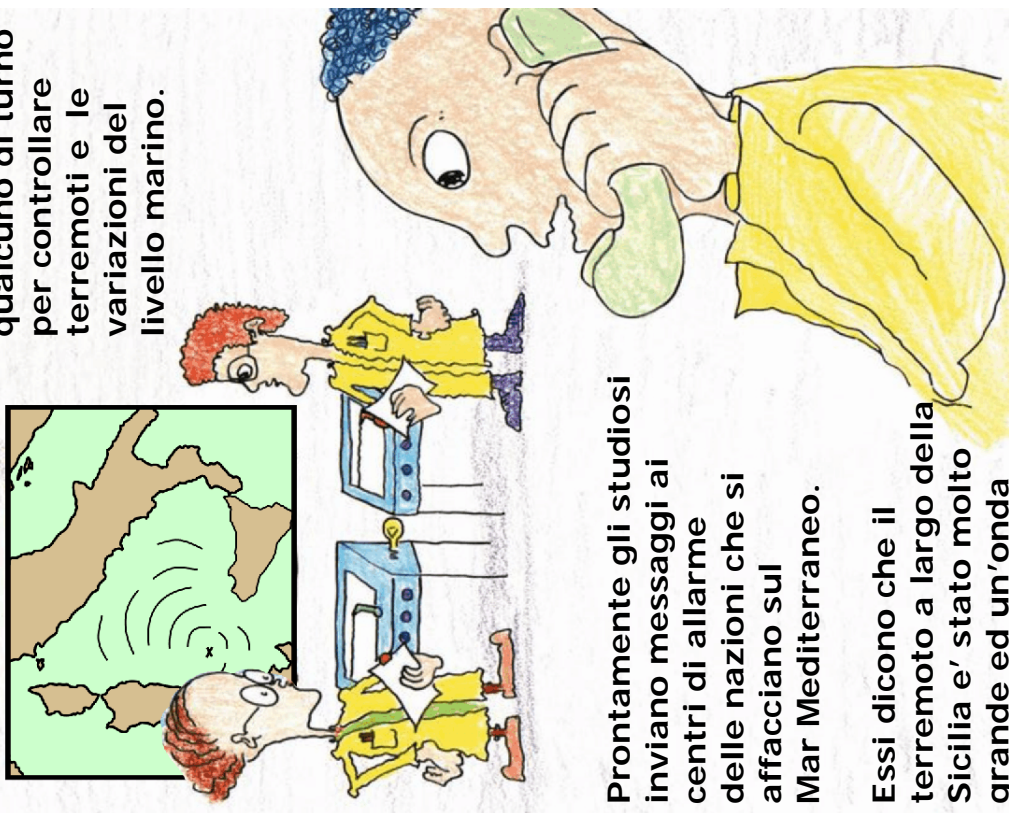
La popolazione si sposta dalle zone di inondazione verso le aree sicure o verso i rifugi. Le scuole lontane dalle aree pericolose possono essere usate come ripari dove ognuno puo' andare ed attendere la fine dell'allarme.



Alcuni edifici, come i grandi alberghi, sono molto resistenti essendo fatti di cemento armato. Le persone possono anche non abbandonarli ma devono spostarsi ai piani alti lasciando liberi almeno i primi tre piani.



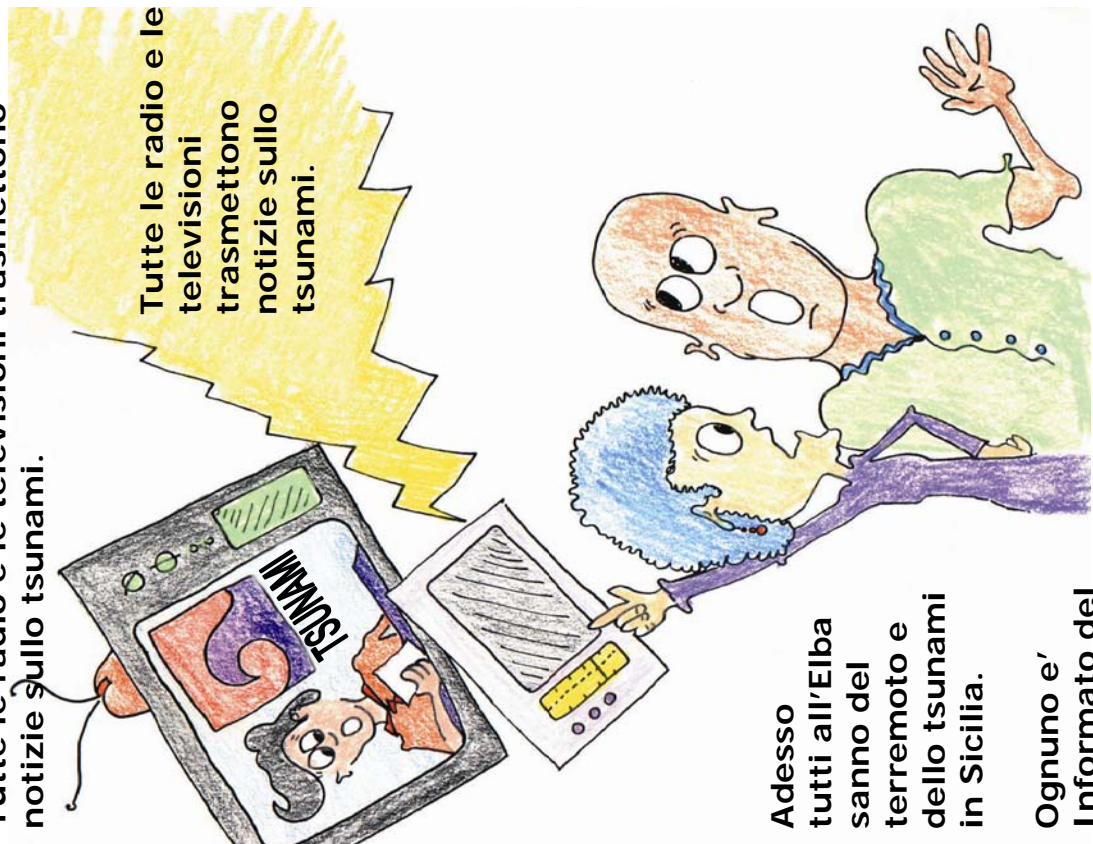
Gli studiosi del centro lavorano tutti i giorni 24 ore su 24, in modo che ci sia sempre qualcuno di turno per controllare terremoti e le variazioni del livello marino.



Prontamente gli studiosi inviano messaggi ai centri di allarme delle nazioni che si affacciano sul Mar Mediterraneo.

Essi dicono che il terremoto a largo della Sicilia e' stato molto grande ed un'onda di tsunami sta attraversando il Tirreno in tutte le direzioni.

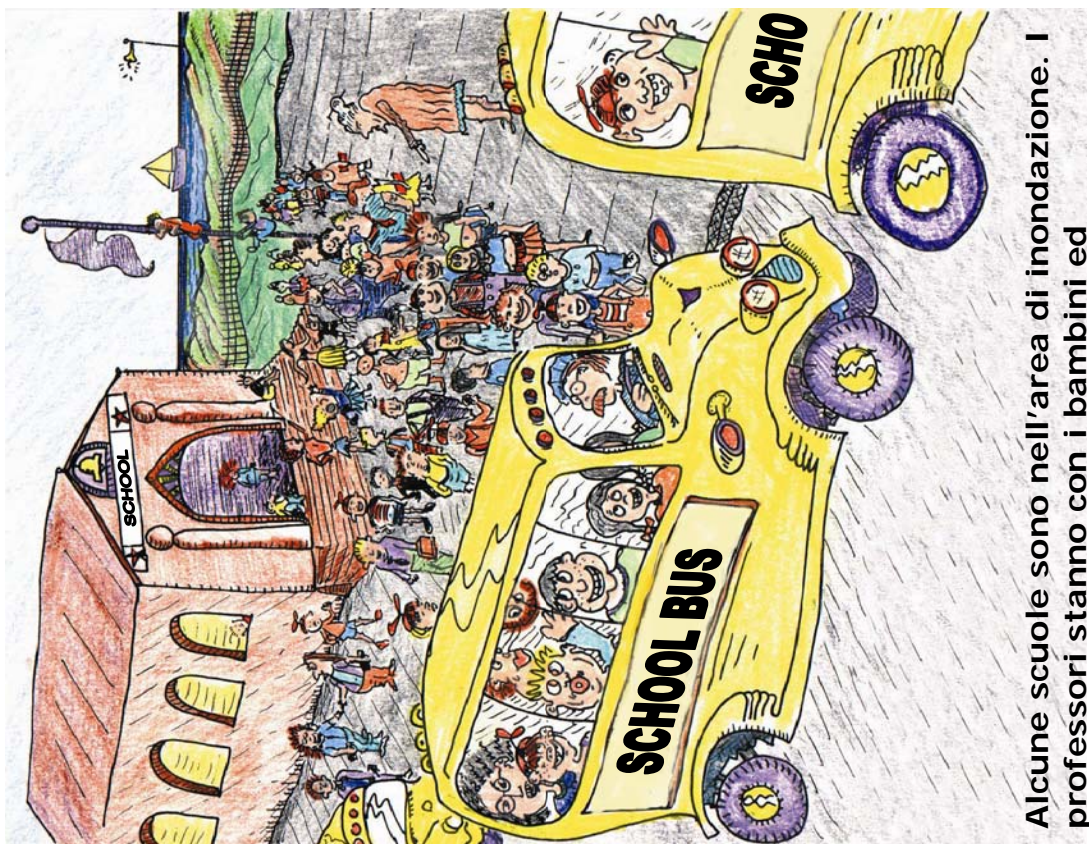
Gli studiosi del **centro di allarme tsunami** emettono un allarme tsunami. La protezione civile si prepara a fronteggiare l'emergenza. Tutte le radio e le televisioni trasmettono notizie sullo tsunami.



Adesso tutti all'Elba sanno del terremoto e dello tsunami in Sicilia.

Ognuno e' informato del fatto che uno tsunami sta arrivando all'Elba.

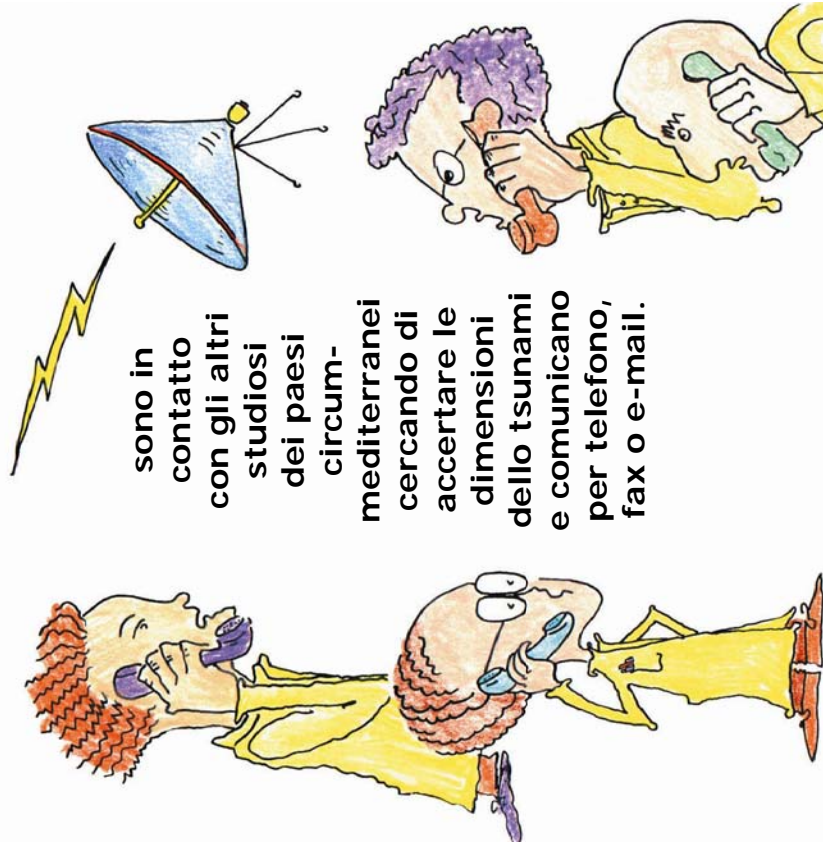
9



Alcune scuole sono nell'area di inondazione. I professori stanno con i bambini ed abbandonano le scuole a piedi o con gli autobus verso le zone sicure lontane dalla zona di inondazione. Aspetteranno la' con i bambini fino a che il pericolo non sia cessato. Dopo i genitori andranno a prendere i bambini.

20

Durante la sorveglianza tsunami gli studiosi del **centro allarme tsunami**

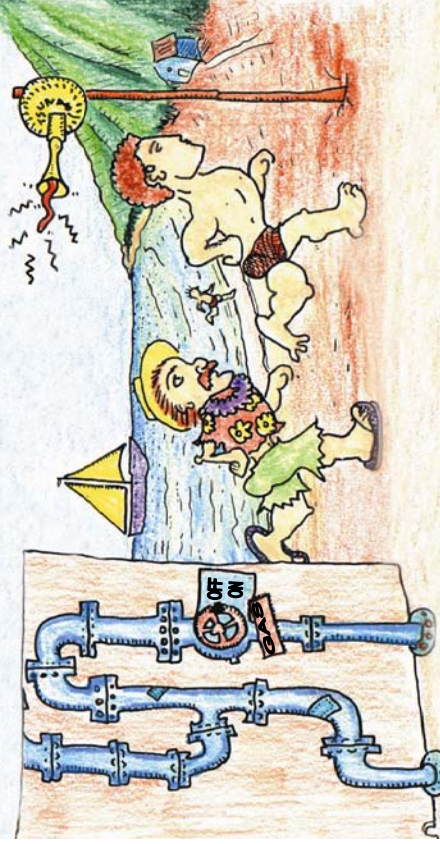


Gli studiosi chiedono informazioni sull'altezza del livello del mare e controllano con i loro strumenti per vedere se registrano un grande tsunami e se il livello del mare sta crescendo o diminuendo. Vogliono sapere se le onde di tsunami sono state avvistate in altre aree come Calabria, Campania, Corsica, Tunisia.

Le spiagge e le aree al di sotto del livello del mare lungo la costa che possono essere sommersse rientrano nella zona di inondazione tsunami.

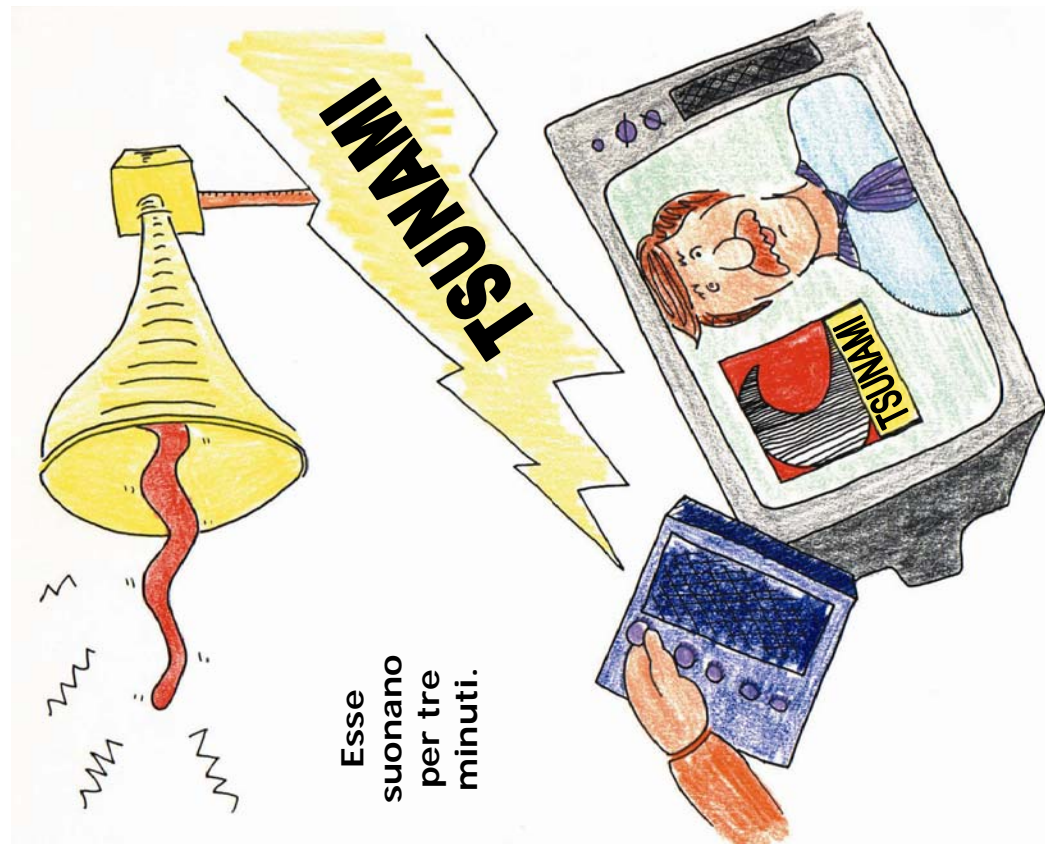


Questi sono i luoghi in cui si puo' abbattere lo tsunami ed causare danni e inondazioni.



I bagnanti e le persone in vacanza lasciano le spiagge. Le persone che vivono nelle zone di inondazione devono evacuare le loro case. Esse chiudono i rubinetti dell'acqua, del gas e staccano la corrente. Il personale degli alberghi aiuta gli ospiti ad evadere le stanze. Anche i negozi e gli uffici delle zone di inondazione devono essere evacuati.

Alle 8.00 suonano le sirene in tutta l'isola d'Elba .



Esse suonano per tre minuti.

In tutta l'isola la popolazione accende radio e televisione per ascoltare le ultime notizie ed imparare cosa fare.

Adesso gli studiosi hanno molte informazioni, sanno che uno tsunami sta attraversando il Tirreno.

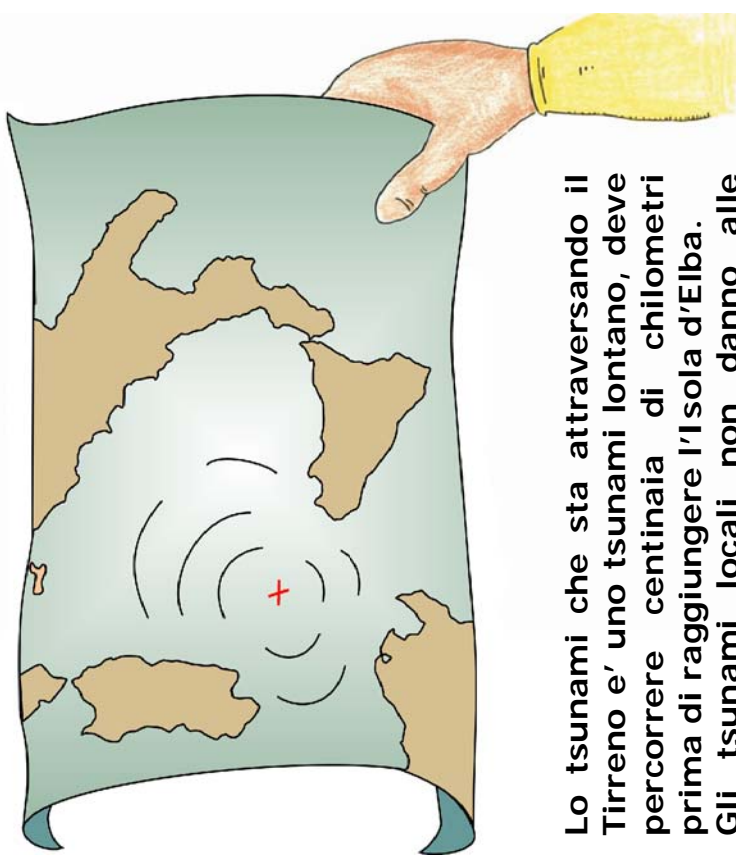
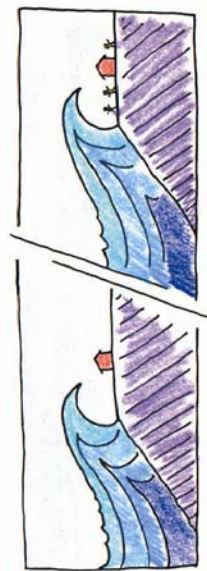
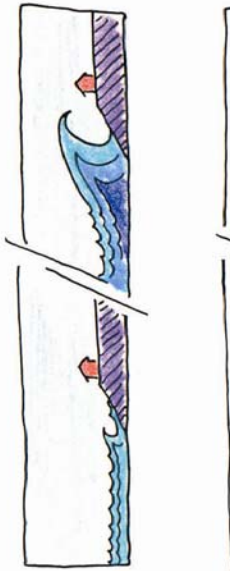
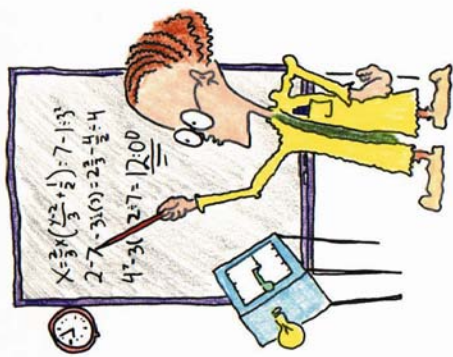


Devono avisare tutti e lanciano un ALLARME TSUNAMI.

Lo tsunami che ha danneggiato la Sicilia e' stato un evento locale perche' e' avvenuto nello stesso luogo del terremoto e subito dopo che la terra aveva iniziato a tremare.

Le onde potrebbero essere piccole o gigantesche.

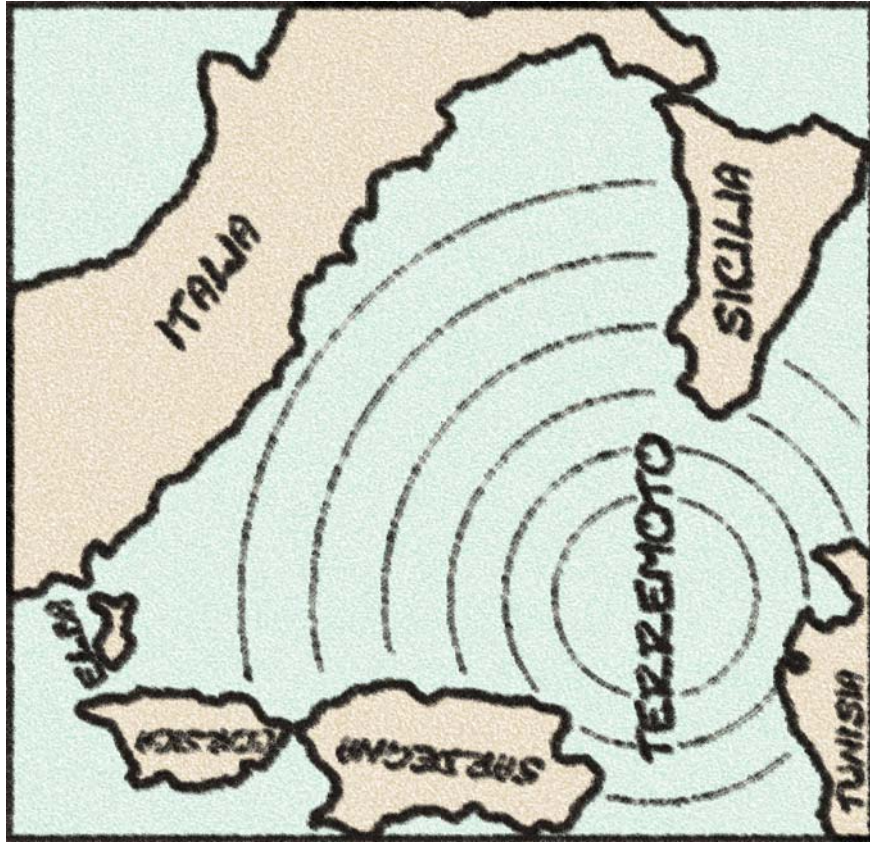
Possono essere innocue o oppure essere delle onde assassine. La popolazione deve essere preparata al peggio e sperare per il meglio.



Lo tsunami che sta attraversando il Tirreno e' uno tsunami lontano, deve percorrere centinaia di chilometri prima di raggiungere l'Isola d'Elba. Gli tsunami locali non danno alle persone molto tempo per raggiungere luoghi sicuri. Gli tsunami lontani daranno alle persone che vivono all'Elba almeno un ora per cercare rifugio nei luoghi sopraelevati. Gli studiosi hanno calcolato che arrivera' verso le 8.45.

Questo perche' un'onda di tsunami puo' divenire molto pericolosa. Una piccola onda di 30 cm di altezza in mare aperto puo' crescere e diventare un mostro di 30 m di altezza quando spazza la costa.

La velocita' delle onde di tsunami dipende dalla profondita' dell'acqua. In acque molto profonde, le onde viaggiano veloci come un aeroplano, anche piu' di 800 km/h.



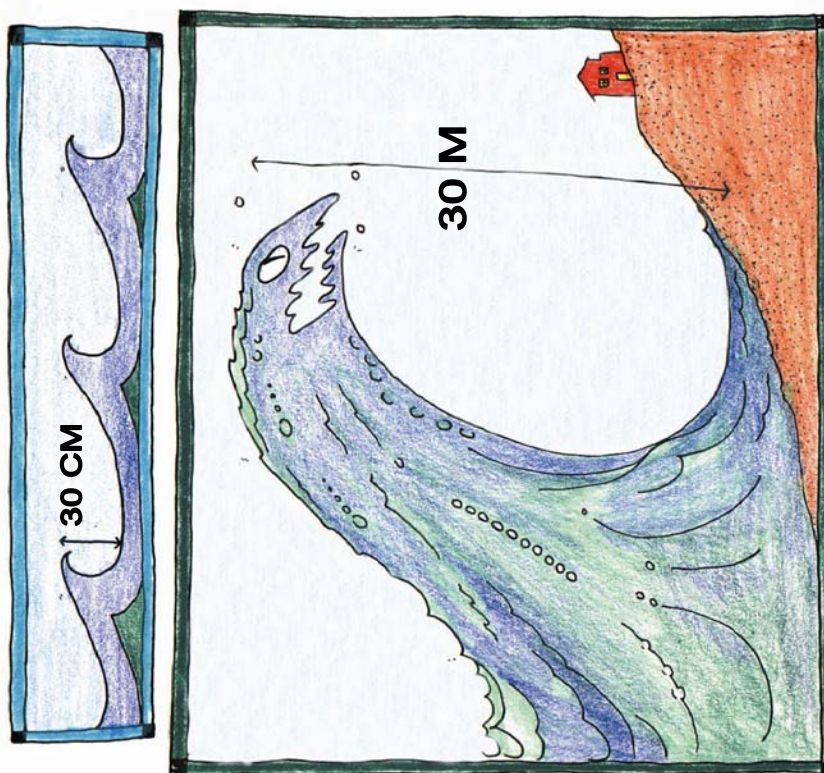
Lo tsunami non puo' essere visto o sentito dalle navi in mare aperto. Il capitano della nave da crociera ha udito dello tsunami via radio, ma

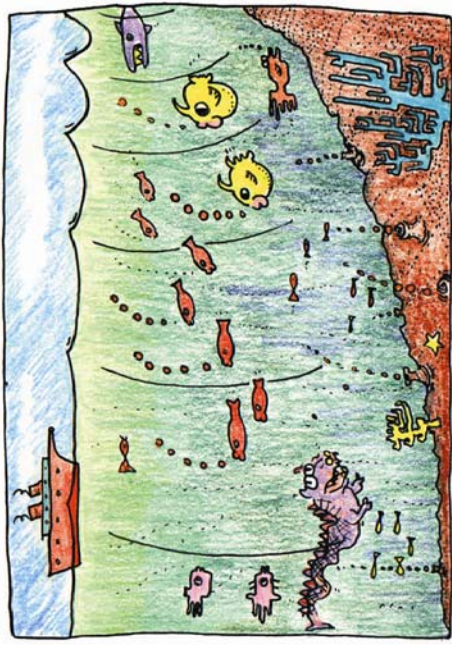
Nessuno a bordo della nave puo' sentire le onde che passano sotto. Lo tsunami non puo' essere visto dagli aeroplani.

13

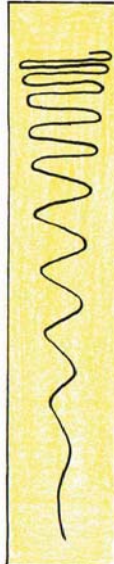
Lo Tsunami che si sta dirigendo verso l'Elba e' formato da una serie di onde lunghe. Uno tsunami e' costituito da molte onde singole che possono colpire la costa per ore.

16

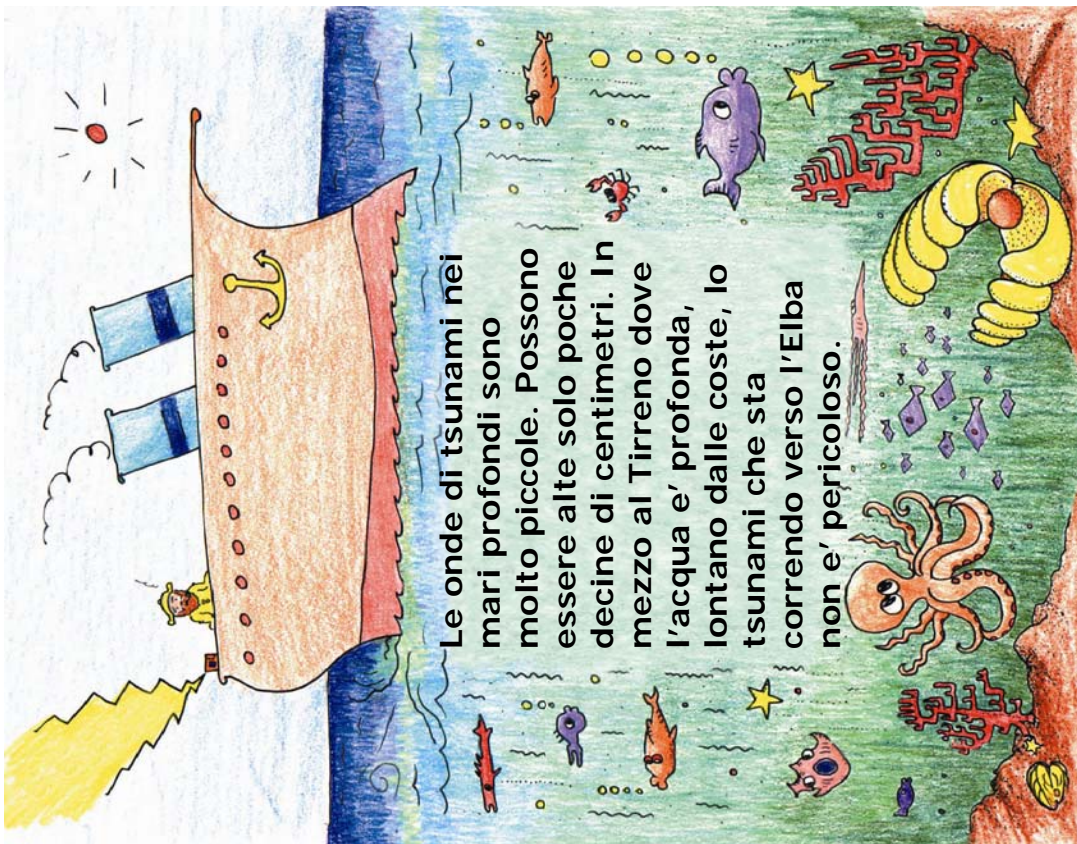




Su un fondo di 10 metri un'onda di tsunami viaggia a 40 km/h, velocita' bassa ma sicuramente piu' alta di quanto possa correre una persona.



Sebbene la prima onda rallenta quando arriva in acqua bassa, la seconda e' ancora lontana e sta viaggiando piu' velocemente e la raggiunge. Il risultato e' che la distanza tra le onde non rimane quella iniziale ma diminuisce. Le onde si raggruppano. Questo "spiaccicarsi" insieme fa sì che le onde divengano piu' alte.



Le onde di tsunami nei mari profondi sono molto piccole. Possono essere alte solo poche decine di centimetri. In mezzo al Tirreno dove l'acqua e' profonda, lontano dalle coste, lo tsunami che sta correndo verso l'Elba non e' pericoloso.

Ma come lo tsunami si avvicina alle coste diventa pericoloso. Le onde rallentano quando la profondita' diminuisce.